universität
wien

DISSERTATION

Titel der Dissertation

Nekhoroshev Stability in the Elliptic Restricted Three Body Problem.
The 1:1 Resonance in the Sun-Jupiter System

angestrebter akademischer Grad

Doktor der Naturwissenschaften (Dr. rer.nat.)

Verfasserin / Verfasser:	Mag. Christoph Lhotka
Matrikel-Nummer:	9947176
Dissertationsgebiet (lt. Studienblatt):	A 091 413
Betreuerin / Betreuer:	Univ.-Prof. Dr. Rudolf Dvorak,
	Univ.-Prof. Dr. Christos Efthymiopoulos

Wien, am 24. Dezember 2008

Contents

1. Introduction

1.1. Historical remarks on the problem of stability of our Solar system

The question of the stability of the N-body problem dates back to the 18th century (see the historical comments of Moser (1973), the introduction of Abraham & Marsden (1978) and Lichtenberg & Lieberman (1992, Section 1.1)). The first scientific investigations can be traced back to Laplace (1798-1825), Lagrange (1788), Poisson (1808, 1809) and Dirichlet (1805-1858), who all together analyzed the problem by means of series expansions. Although they all claimed, that the Solar system is stable on short time scales, the important question of the long-time stability could not be answered by these early perturbative techniques.

The work of Hamilton and Liouville in the mid 19th century, stimulated the development of the Hamiltonian formalism. The canonical approach lies at the foundation of most of our modern treatment of classical mechanics, but it also opens the door to the modern formulations of quantum physics and general relativity. The "modern" version of the stability problem was first formulated by the letters of Weierstrass (published in Act. Math.. 35, 1911, pp.29-65). In his notes, he claimed to possess formal series expansions (in a letter to S. Kovalevski) but was unable to show the convergence of these series, containing very large numbers produced by the small denominators in the series terms. Since he hoped to overcome this difficulty (Dirichlet made a similar remark to Kronecker in 1858, that he also found such solutions; but he died before writing his proof) he suggested the problem to Mittag-Leffler as a prize question sponsored by King Oscar, the Swedish king. Bruns (1887) stated that no other tool than series expansions could resolve the problem. The prize was awarded to H. Poincaré (1890), who actually did not solve the problem, but suggested, that the series expansions of former colleagues diverge. To this end the preliminary results of Haretu (1878) and Poincaré (1892) where justified in the work of Poincaré (1893), where he proved that the three body problem does not possess any integrals aside the ten known ones. This would imply the non-existence of quasi-periodic solutions in the system, which was in contradiction to Weierstrass expectations, based on his formal series expansions. Since the simplest model of our Solar system is the three-body problem, which is indeed also connected to the interest in understanding the general features of dynamical systems, the question of the stability of our own Solar system seemed to be answered: the problem, which was pointed out by Poincaré, was, that even a simple stable system, like the two-body problem, could be destabilized by a small influence of an additional third disturbing body. He and Von Zeipel (1916) devised the perturbative methods to treat integrable and therefore stable systems, and showed the behavior of these systems on short-time scales. With their work they introduced for the first time the geometric concepts into analytical mechanics (which was in contrast to the approaches of Laplace and Lagrange).

Nowadays, this period could be regarded as the starting point for a modern topological treatment of symplectic manifolds.

The secular perturbation theory, accounting for resonant interactions between more than one degrees of freedom, was formalized in the early days of quantum mechanics (Born 1927). Since the general theory of relativity (Einstein, 1917) and the theory of quantum mechanics (beginning of 20th century) were at the center of the concerns of physicist at that time, the question of the stability of the Solar system was somewhat left to the margin. Nevertheless Birkhoff (1927) proved Poincaré´s conjecture, that an even number of stable and unstable fixed points must exist in generic nonlinear systems, in which there is a rational frequency ratio between two degrees of freedom. The higher order resonances change the topology of the phase space, leading to the formation of island chains on an increasingly finer and finer scale. Although the work of Poincaré and Birkhoff indicated the exceeding complexity of the phase space, Siegel (1942) showed, via Diophantine conditions, the possibility that the formal series, describing quasiperiodic solutions may converge. At the international Mathematical Congress of 1954 (Amsterdam) Kolmogorov announced his theorem proving that indeed quasiperiodic solutions exist in Hamiltonian dynamical systems, which are confined on invariant tori of the phases space. The detailed proof of Kolmogorov´s theorem, under different restrictions, was given by Arnold (1963) and by Moser (1962) in the case of symplectic mappings. The Kolmogorov-Arnold-Moser theorem (KAM) states, that a large measure of invariant tori survive under the perturbation of an integrable Hamiltonian system. With the KAM theorem, the question of the stability of the Solar system opened again, and it was shown that the motion in the phase space is not necessarily ergodic, although the motion near the separatrix of each resonance is chaotic. For weakly perturbed systems the KAM tori penetrate the chaotic domains and the variations of the actions within any separatrix layer are exponentially small.

The first results on the exponentially stability in weakly perturbed systems can be traced back to Moser (1955) and Littlewood (1959ab) and they are at the core of the so called Nekhoroshev stability estimates. A short historical treatment on this topic is also made Section 1.2.. These results rely on analytical theories based on formal integrals of motion, which date back to Whittaker (1916, 1937), Cherry (1924) and Birkhoff (1927). Although the series giving the third integral are in general divergent (Siegel 1956) it was shown (Contopoulos 1960, 1963, Gustavson 1966) that the truncated third integral series is a better conserved quantity, when going to higher orders. In fact, with the application of the third integral to galactic dynamics Contopoulos (1960) showed, that the dynamical systems are neither completely integrable nor ergodic, which was in contradiction with the prevailing opinion of that time. As a basic model for illustrating the transitions from regular to stochastic motion (which was later replaced by the term chaotic motion) Hénon-Heiles (1964) introduced a simplified nonlinear Hamiltonian system simulating the behavior of the orbits in the central parts of the Galaxy. With the aid of computer experiments, numerical and analytical theories evolved in the upcoming years to determine the critical value of the perturbation at which the transition from order to a large degree of chaos. Inspired by the old question of the stability of the Solar system, Chaos theory evolved and gave

new insights into different fields of modern physics. Contopoulos (1966), Rosenbluth (1966) and Chirikov (1969) gave an understanding of the transition between chaotic and regular motion as a result of resonance overlapping in phase space. The question of ergodicity of simple dynamical systems, like the Sinai billiard (Sinai 1963) could be established but only for idealized cases. Arnold (1963) showed that for systems with more than two degrees of freedom the chaotic layers are interconnected to form a web of resonances that is dense in the phase space. For initial conditions on this web, chaotic motion is driven along the layers leading to global diffusion not constrained by the KAM curves. This mechanism, nowadays called Arnold diffusion exists down to the limit of infinitesimal perturbations from integrable systems and can be fast enough to bring a system into an unstable state. The lack of integrals of motion in higher dimensional systems, on the one hand, and the possibility of chaotic motion, on the other hand, challenged again the problem of the stability of N-body systems. The ultimate question of the stability of the Solar system remains today still partly unanswered.

1.2. KAM theorem and the concept of exponential stability

Moser (1955) and Littlewood (1959a,b) examined the question of the stability of motions around elliptic equilibria. The model of interest was the Lagrange configuration in Celestial mechanics. This model served as the basis for many other exponential stability estimates from that date on and will also be the application of interest in this thesis. After an initial boost, the subject of exponential stability was overshadowed in the 60´s and 70s by the investigation of KAM stability: the persistence of invariant tori in generic Hamiltonian systems, found by Kolmogorov (1954), Moser (1962, 1967) and Arnold (1963ab), interrupted former research on exponential stability, which was revived by Nekhoroshev (1971, 1977, 1979). The mathematical rigour of his analysis on the one hand and the generality of the results to arbitrary Hamiltonian systems on the other hand, are main reasons, why a compendium of results on exponential stability in the literature have been collectively called the "Nekhoroshev stability theorem".

Consider a Hamiltonian system in action-angle variable form:

$$H = H(J, \phi) = H_0(J) + \epsilon H_1(J, \phi), \tag{1}$$

where $J = (J_1, \ldots, J_d)$ are the action and $\phi = (\phi_1, \ldots, \phi_d)$ are the angle variables in d degrees of freedom. The parameter ϵ will be considered small. For $\epsilon = 0$, the motions are confined on d-dimensional tori. Nekhoroshev (1977) stated a stability theorem for Hamiltonian of the form (1). The theorem referred to the definition of the stability time $T(\epsilon)$ such that:

$$\forall \, t \in [0, T(\epsilon)] : \, |J(t) - J(0)| < \alpha(\epsilon), \tag{2}$$

where $J(0) = (J_1(0), \ldots, J_d(0))$ are the initial conditions of an orbit in the action space and $\alpha(\epsilon)$ is a small quantity. The question is, to determine an optimal results for the form of the functions $T(\epsilon)$ and

$\alpha(\epsilon)$ in the case, when ϵ is small. The J in the unperturbed system are first integrals of motion. The question of stability is linked to the determination of the rate of change of J along the solutions of the perturbed system. After a time $T = 1/\epsilon$, the values of the action variables in generic systems of the form (1) differ only slightly ($O(\epsilon)$) from the initial values $J(0)$. However, beyond the time $T = 1/\epsilon$ the following questions are posed:

i) Are there perpetually stable solutions, meaning that $|J(t) - J(0)| < \alpha(\epsilon)$ for all real t, where $\alpha(\epsilon)$ tends to zero as $\epsilon \to 0$? If yes, what is the measure of these solutions in the phase space of the system?

ii) For solutions which are not perpetually stable, how long can the time of stability $T(\epsilon)$ be taken so that $J(t)$ is proved to remain close to $J(0)$?

In the integrable case the motion is foliated on d-dimensional tori $\mathbb{T}^d$. The angles evolve in time linearly, the basic frequencies ω of the system being defined by $\partial H / \partial J(0)$. The functions α, T of the stability theorem (2) should therefore satisfy:

$$\lim_{\epsilon \to 0} T(\epsilon) = \infty,$$

$$\lim_{\epsilon \to 0} \alpha(\epsilon) = 0. \tag{3}$$

In the perturbed case, the KAM theorem asserts that:

"If an unperturbed system is non degenerate, then for sufficiently small conservative hamiltonian perturbations, most non-resonant invariant tori do not vanish, but are only slightly deformed, so that in the phase space of the perturbed system, too, there are invariant tori densely filled with phase curves winding around them conditionally periodically, with a number of independent frequencies equal to the number of degrees of freedom. These invariant tori form a majority in the sense that the measure of the complement of their union is small when the perturbation is small...." (Arnold 1978).

At the core of Kolmogorov´s proof (1954), are the following considerations (Arnold 1978):

i) the non resonant set of frequencies ω of the surviving tori is fixed so that the frequencies are: 1) incommensurable and 2) satisfy no resonance condition of low order of the harmonics K. The latter property is expressed via the so called Diophantine conditions, namely $\forall \gamma > d - 1$ there exist a positive constant K such that $|\omega \cdot k| > K |k|^{-\gamma}$ for all integer vectors $k \neq 0$. By this condition it can be shown that the measure of the set of vectors ω, lying in a fixed bounded region, for which the Diophantine condition is violated, is small when K is small. The motion on all other tori should be conditionally-periodic with exactly the same frequencies as in the unperturbed system.

ii) To find the initial conditions leading to conditionally periodic motion, instead of using the usual series expansion in powers of the perturbation parameter, Kolmogorov developed a super convergent method, similar to Newton´s method of tangents. For the *Kolmogorov normal form* to be convergent the necessary condition is, that the unperturbed hamiltonian function H_0 is analytic and nondegenerate, and that the perturbing part of the Hamiltonian H_1 is analytic in a complexified domain of the actions and the angles. On the other hand, as demonstrated by Giorgilli & Locatelli (1998), the superconvergent method is actually not necessary to demonstrate the convergence of the Kolmogorov series.

For weakly perturbed systems of 2 degrees of freedom the KAM tori isolate the thin chaotic layers of different resonances from each other. This is not true in higher dimensional systems. Arnold (1963) showed that in such systems the chaotic layers are interconnected to form a web of resonances, while simple topological arguments yield that the KAM-tori can not guarantee stability. The mechanism, called nowadays Arnold diffusion exists also for infinitesimally small perturbations. A question directly related to the Nekhoroshev theorem is: how fast can Arnold diffusion bring a system into an unstable state?

The main result due to Nekhoroshev (1977) is a stability theorem under the form of equation (2) which i) is valid in systems of any numbers of degrees of freedom and ii) does not depend on the particular initial conditions in the phase space, like in the KAM case. Nekhoroshev´s result is that in open domains of the phase space the functions α, T in (2) are of the form:

$$\alpha(\epsilon) = \epsilon_0 \, \epsilon^a,$$

$$T(\epsilon) = t_0 \, e^{\left(\frac{\epsilon_0}{\epsilon}\right)^b}, \tag{4}$$

i.e., the stability time is exponentially long in $1/\epsilon$. The stability theorem is fulfilled for all initial conditions close to $J(0)$ below a threshold ϵ_0 and the stability time depends only on the parameters a, b, t_0, which are strongly connected to the geometry and dimensionality of the system. Although former studies (Moser 1955, Littlewood 1959ab) already indicated that nearly integrable dynamical systems exhibit exponential stability, the proof by Nekhoroshev 20 years later, and in particular the so called geometrical part of the proof demonstrated that it is a global stability theorem and not a local one, i.e. valid only near elliptic equilibria.

The Nekhoroshev theorem is at the core of the results presented in this thesis. The model of the investigation is the original one, due to Littlewood 1959b: the restricted three body problem. The application to the Lagrangian configuration follows the line of development of earlier works. The main new result is the derivation of physically interesting Nekhoroshev estimates for the long term stability of Trojan motion in the frame work of the elliptic restricted three body problem. A particular

astronomical application regards the long time behavior of Trojan type motion in (exo-)planetary systems. The mathematical and computer-algebraic interest is in the construction of symplectic mappings, and of Nekhoroshev estimates based on them. This was only possible by specialized computer algebra approaches.

1.3. Literature on (Nekhoroshev) stability of Trojan asteroids

The dynamics of the Trojans around Jupiter is a subject of interest to the scientific community since the discovery of the first Trojan in 1906 (Achilles by Max Wolf, Heidelberg). The observation proved the existence of asteroids around the Lagrangian fixed points predicted by Lagrange himself. Besides other analytical approaches than Nekhoroshev estimates (see e.g. Hagel, 1995) various numerical simulations have been undertaken to understand the stability problem around the equilateral fixed points of our Solar system. First numerical estimations of the stability regions around these point were made by Rabe (1967) in the framework of the restricted three body problem. Érdi studied the motion of the Trojans in many papers (starting with 1988, 1997). The former also gives a detailed reference list to earlier work on this topic. Numerical methods were used by Milani (1993, 1994) to show that also real Trojans are in fact on chaotic orbits, extensive numerical simulations were undertaken by Levison et al. (1997) showing that Trojans perform slow dispersion on giga years time scales. We must not forget to mention the work of Beaugé & Roig (2001), Pilat-Lohinger et al. 1999, Dvorak & Tsiganis 2000, Tsiganis et al. 2000, to name a few, concerned with the existence of chaotic orbits in the system. Mitchenko et al. 2001 studied the effect of planetary migration on it, Nesvorny & Dones (2002) analyzed the possibility of Trojan motion around the other planets of our Solar system. The effect of inclination on the stability of motion of Trojan asteroids was investigated e.g. by Dvorak & Schwarz 2005 or Robutel or Gabern & Jorba 2005. Recent work, e.g. on the inclination problem was done by Dvorak et al. 2008, the resonant structure of the problem was analyzed by Robutel & Gabern 2006 or Robutel & Bodossian 2008. A new field on the existence of Trojan planets in extra-solar planetary systems evolved in the recent years, detailed studies were performed e.g. by Schwarz et al. 2007 or Schwarz et al. 2008.

Comparing the analytical methods and results used in earlier works on the Nekhoroshev stability of the Trojan asteroids, different approaches and also different kinds of models are identified on which the analysis was based. Littlewood (1959ab) proved the exponential stability of the Lagrangian configuration (for the first time) using approximate integrals of the equations of motion. On the other hand, a number of authors (Simó (1989), Giorgilli et al. (1989), Celletti & Giorgilli (1991), Giorgilli & Skokos (1997), Benettin, Fassó & Guzzo (1998) but also Skokos & Dokoumetzidis (2001), Efthymiopoulos & Sándor (2005)) gave explicit estimates of the *region* around the Lagrangian points L_4, L_5, within which the stability is ensured for the life-time of the Solar system. Such estimates are

based on the calculation of the size of the *remainder* of a normal form construction. Efthymiopoulos (2005a, 2005b) constructed estimates based also on a direct calculation of the *formal integrals* without the use of *normal forms*, rather estimating the influence of the remainder directly. A novel approach in recent studies has been the use of symplectic mapping models for the analysis of the exponential stability of the Trojan configuration (Efthymiopoulos 2005, Efthymiopoulos & Sándor 2005).

The above cited works deal with the simplified circular model of the restricted three body problem. The 3-dimensional case was used as a basis for the analysis by Giorgilli et al. (1989), Celletti & Giorgilli (1991), Benettin, Fassó & Guzzo (1998) and Skokos & Dokoumetzidis (2001). Littlewood (1959ab), Giorgilli et al. (1989) and Benettin, Fassó & Guzzo (1998) gave a detailed mass study of the mass-ratio of the primaries beyond the application of the Sun-Jupiter case (e.g. Giorgilli et al. 1989 and Benettin, Fassó & Guzzo 1998 up to Routh´s mass or Celletti & Ferrara (1996) for the Earth-Moon system). Differences between the resonant and non-resonant treatment of the normal form where investigated in Efthymiopoulos (2005b) and Efthymiopoulos & Sándor (2005).

To summarize, the exponential stability of the Trojan motion within the framework of the restricted three body problem was shown either i) by direct construction of integrals of the equations of motion, ii) by normal form construction and estimation of the remainder in the case of Hamiltonian flows and iii) by normal form construction for symplectic mappings.

1.4. Goal and thesis outline

The goal of this thesis is to show the presence of Nekhoroshev stability also in the elliptic restricted three body problem. To this end I want to show, that there exists a relevant Nekhoroshev stable regime around the elliptic fixed points of the problem and that there are real (observed) asteroids included in this domain for a Nekhoroshev-time T equal to the age of the Solar system in the Sun-Jupiter case. While all former studies on Nekhoroshev theory are based on the circular modelization of the system, the present thesis extends former results to the elliptic model.

The outline of the thesis is as follows: an outline of Nekhoroshev theorem is given in Chapter 2. While Section 2.1. states the theorem, Section 2.2. and Section 2.3. looks inside the main parts of the proof given in the cited literature.

The restricted problem of three bodies is the main subject of Chapter 3. It covers the different kinds of formulations of the problem, used by the cited authors, to derive Nekhoroshev stability estimates in the restricted problem. The Chapter starts with the dimensional force function and ends up in the formulation of the problem in terms of Delaunay variables.

The model for Trojan-type motion in the restricted problem is subject of Chapter 4. The Lagrangian configuration is introduced in Section 4.1., useful expansions of various quantities in term of Bessel

functions are given in Section 4.2. They serve as the basis to derive the perturbing function of the 1:1 resonance in modified Delaunay variables, given in Section 4.3.

The stability estimates presented in this thesis are based on the theory of normal forms of symplectic mapping, i.e. by estimating the magnitude of the non normal form parts of it. The symplectic mapping approach to Hamiltonian systems is subject of Chapter 5. The connection between the formulation of dynamical systems in terms of continuous flows and discrete mappings is discussed in Section 5.1. the method of construction, the Hadjidemetriou method, developed in Section 5.2. The symplectic mapping model of the Trojan configuration is derived in Section 5.3. the application to the Sun-Jupiter case is presented in Section 5.4.

The normal form theory of symplectic mappings is developed in Chapter 6. The general approach to normal forms of symplectic mappings in $\mathbb{R}^{2m}$ is presented in Section 6.1., the application to the Sun-Jupiter case is demonstrated in Section 6.2. .

The core results are presented in Chapter 7, Section 7.1. introduces the reader to approximate integrals and the remainder function on which the stability theorem is based. The results are applied in Section 7.2. to the Trojan group of asteroids of our Solar system and the main physical results are put together with a discussion of it in Section 7.3.

Chapter 2 is based on the original paper Nekhoroshev (1977), the book of Morbidelli (2002) and lecture notes of Giorgilli (Pisa, 2002). Useful figures, to understand the geometrical part of the theorem were produced on the basis of them. Chapter 3 is adopted to our needs from the book of Szebehely (1967). The basis for Section 4.1. and 4.2. can be found in the book of Stumpff (1959). The book is written in German, basic series expansions, described in English, can also be found in other books on perturbation techniques of Celestial mechanics (e.g. Brumberg 1995). The mapping approach of Chapter 5 is partly based on the book of Lichtenberg & Lieberman (1992), the original paper due to Hadjidemetriou (1991) and a previous approach due to Sándor & Érdi (2003). The results, presented in Chapter 6 and 7 are based on the paper by Efthymiopoulos & Sándor (2005) and are also partly published in Monthly Notices of the Royal Astronomical Society in Lhotka et al. (2008).

2. An Outline of Nekhoroshev Theory

2.1. The theorem

Proofs on the initial formulation of the theorem, which can be found in Nekhoroshev (1977, 1979) are given in Benettin, Galgani & Giorgilli (1985). Extensions of this theorem were found in the case of isochronous systems with elliptic equilibria by Giorgilli (1988) or isochronous symplectic mappings with elliptic fixed points (Bazanni, Marmi & Turchetti 1990).

The theorem was further generalized by Guzzo, Fassó & Benetin (1998) and Fassó, Guzzo & Benetin (1998) in non-isochronous formulations to systems with elliptic equilibria. Other versions of the theorem, together with their proofs, are based on specific classes of dynamical systems, i.e. done by Benetin & Galavotti (1986), Giorgilli, Delshams, Fontich, Galgani & Simó (1989), Giorgilli & Zehnder (1992), Lochak (1992) and Pöshel (1993). From the mid $90\,s$ the theorem was extended to more general dynamical systems or connected to KAM-theorem by Morbidelli & Giorgilli (1995), Delshams & Guiterrez (1995) and Niedermann (2000).

The extended theorems in the case of systems with elliptic equilibria essentially replace the small parameter ϵ (Equation 2 in Chapter 1, in short 2;1) by the distance ρ from the equilibrium (or fixed point) and the theorems assert stability for orbits librating around the equilibria, at a distance ρ in phase space, for times exponentially long in $1/\rho$. A modern version of the theorem, which is also at the basis of the approach of this thesis is given by:

Nekhoroshev theorem (isochronous version)

$$|\rho(t) - \rho(0)| \le \rho(0)^\alpha \ \forall \ T = O\left(e^{\left(\frac{\rho_*}{\rho}\right)^b}\right),$$

where a, b are exponents depending on the number of degrees of freedom and the constant ρ_* is a maximum distance up to which the Nekhoroshev regime applies. Estimates for a, b were given in isochronous systems with diophantine frequencies by Giorgilli (1988, $b = 1/d$) and were further improved by Efthymiopoulos, Giorgilli & Contopoulos (2004, $b = 2/d$).
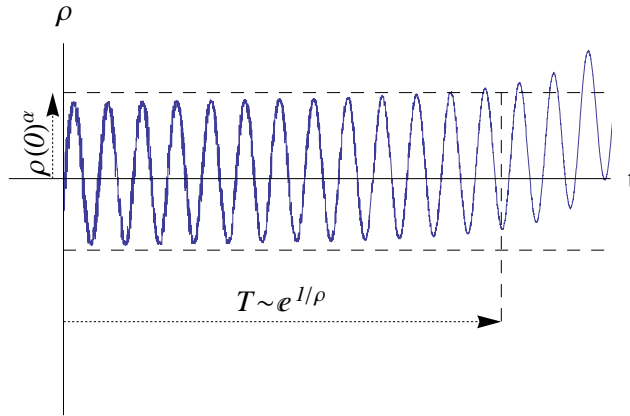
Figure 1. Nekhoroshev time and distance in phase space. After exponentially long times an orbit leaves the initial distance $\rho(0)^{\alpha}$.

Figure 1 sketches the influence of the theorem on the conservation of the actions. The variation of $\rho(t)$ is of order $\rho(0)^{\alpha}$ for exponentially long times in ρ^{-1}.

The original proof of Nekhoroshev theorem is divided into the analytical and geometrical part. In the former one the Hamiltonian is brought into normal form in a local domain of the action space using the method of Lie transform. By estimating the size of the remainder terms a local stability lemma follows. The second step is to construct a covering of the action domain by local subdomains, where the local stability lemma applies. By this construction the global stability lemma follows. Let us provide a formal outline of these ideas.

2.2. Analytical part

At the core of the analytical part of the theorem is a normal form construction for the Hamiltonian. The aim is to make a canonical transformation from old to new action-angle variables such that in the new variables the Hamiltonian dynamics is as simple as possible. This transformation is done by the method of the Birkhoff normal form construction, it is based on the method of Lie-transformations. We briefly discuss the formals aspects and definition of Lie-transform in Hamiltonian flows, as well as the issue of small divisors, which arise in the Birkhoff series.

Consider a nearly integrable Hamiltonian system of the form:

$$H = H_0 + \epsilon H_1,$$

$$\frac{d J_i}{d t} = -\frac{\partial H}{\partial \phi_i} = 0 + \epsilon \frac{\partial H_1}{\partial \phi_i},$$

$$\frac{d \phi_j}{d t} = \frac{\partial H}{\partial J_i} = \omega_i(J) + \epsilon \frac{\partial H_1}{\partial J_i}, \tag{1}$$

where $H = H(J, \phi)$ is in action-angle form, $J = (J_1, …, J_d)$ are the actions and $\phi = (\phi_1, …, \phi_d)$ are the angles respectively. Note, that in the integrable approximation ($\epsilon \to 0$) of system (1), the actions reduce to constants $J_i = J_{i0}$ and the angles $\phi_i = \phi_i(t) = \alpha_i(J)\,t + \phi_{i0}$ are linear evolving in time ($i = 1, …, d$). Assume, that H_1 can be expanded into a convergent Fourier series:

$$H_1 = \sum_{k \in \mathbb{K}} h_k(J)\, e^{i k \phi}, \tag{2}$$

where $k = (k_1, …, k_d)$ is an integer vector, $\mathbb{K}$ is an index set and the order of k is given by $K = |k_1| + … + |k_d|$. Our aim is to transform the Hamiltonian into normal form. A Hamiltonian normal form is defined by:

$$H^{(r)} = Z^{(r)}(J) + O(\epsilon)^{(r+1)} \tag{3}$$

in the non resonant case and by:

$$H^{(r)} = Z^{(r)}(J, \phi_R) + O(\epsilon)^{r+1} \tag{4}$$

in the resonant one, where ϕ_R is a q-dimensional vector $\phi_R = (\phi_{R,1}, …, \phi_{R,q})$ in the q-fold resonant case. The aim is, roughly speaking, to transform the system (1) so, that the perturbations act beyond the order r in the small parameter ϵ. To separate the two different cases (3) and (4) we define the resonant module $M = \{k : |\omega \cdot k| = 0\}$. Here $\omega = (\omega_1, …, \omega_d)$ defines the fundamental set of frequencies. In the integrable approximation of (1) the frequencies are given by $\omega = \nabla_J \cdot H_0(J)$. For any fixed module M the normal form constructed as above is valid in a small open domain of the action space, which contains the points J^* satisfying $\omega(J^*) = \omega$. A resonance condition according to M in this notation is given by:

$$\omega_1 k_1 + … + \omega_d k_d = 0. \tag{5}$$

By the use of M we are interested in eliminating from the transformed Hamiltonian harmonics not belonging to M up to the order $r + 1$ in the perturbing parameter ϵ. The transformation from (1) to (3) or (4) needs to be canonical, to preserve the symplectic structure of the system. For this reason we are looking for a generating function W to transform H to $H^{(r)}$ up to order r.

2.2.1. Definition of the Lie-operator

Sophus Lie (see Gröbner 1967) showed that every canonical transformation can be done using Lie-transforms. Defining the Lie-derivative by means of the Poisson-bracket of any function with a *generating function W*:

$$l_W = \{\cdot, W\}, \tag{6}$$

the Lie-operator is defined as the exponential of the Lie-derivative, i.e.:

$$L_W = e^{l_W}. \tag{7}$$

The Lie-operator is therefore in series representation given by:

$$L_W = \sum_{l=0}^{\infty} \frac{1}{l!} \, l_W{}^{(l)}. \tag{8}$$

The notation $l_W{}^{(l)}$ in (8) is defined as:

$$l_W{}^{(0)} = i\,d$$

$$l_W{}^{(l)} = l_W{}^{(l-1)} \circ l_W = \{\{\dots\{\cdot, W\}\dots, W\}, W\}, \tag{9}$$

i.e. by iterated application of (6), where $i\,d$ is the identity operator. Basic properties of the Lie-operator are the following (f_1, f_2 being functions of (J, ϕ), c being constant):

$$(i): \quad L_W(f_1 + f_2) = L_W f_1 + L_W f_2,$$

$$(ii): \quad L_W(f_1 \cdot f_2) = (L_W f_1) \cdot f_2 + f_1 \cdot (L_W f_2),$$

$$(iii): \quad L_W c = 0.$$

Thus, the Lie-operator L_W has the same properties, like the differential operator $d/d\,t$ (and in fact it is a generalization of it, see Gröbner 1967). To prove that the action of the Lie-operator (8) is indeed a canonical transformation, let $X(J, \phi)$ be any analytic function and define the Hamiltonian flow under X given by:

$$\frac{d\,J_i}{d\,t} = -\frac{\partial X}{\partial \phi_i},$$

$$\frac{d\,\phi}{d\,t} = \frac{\partial X}{\partial J_i}, \tag{10}$$

where $i = 1, \dots, d$. The time flow can be replaced by:

$$(iv): \quad \frac{d}{d\,t} \equiv \{\cdot, X\} = l_X,$$

which is simply shown by:

$$\frac{d\,f}{d\,t} = \frac{\partial f}{\partial \phi_i} \frac{\partial \phi_i}{\partial t} + \frac{\partial f}{\partial J_i} \frac{\partial J_i}{\partial t} = \frac{\partial f}{\partial \phi_i} \frac{\partial X}{\partial J_i} - \frac{\partial f}{\partial J_i} \frac{\partial X}{\partial \phi_i} = \{f, X\}. \tag{11}$$

On the other hand the solution of (10) in terms of Taylor series, centered around t_0, is given by:

$$J_i(t) = J_i(t_0) + \left(\frac{d\,J_i}{d\,t}\right)_{t_0} (t - t_0) + \frac{1}{2}\left(\frac{d^2\,J_i}{d\,t^2}\right)_{t_0} + \dots,$$

$$\phi_i(t) = \phi_i(t_0) + \left(\frac{d\,\phi_i}{d\,t}\right)_{t_0} (t - t_0) + \frac{1}{2}\left(\frac{d^2\,\phi_i}{d\,t^2}\right)_{t_0} + \dots. \tag{12}$$

Using property (iv) and by comparing (12) with (8) we can conclude that the time development itself is equivalent to:

$$J_i(t) = \left(e^{t\, l_X} J_i\right)_{t_0},$$

$$\varphi_i(t) = \left(e^{t\, l_X} \phi_i\right)_{t_0}, \tag{13}$$

where $i = 1, \ldots, d$. But the transformation $(\varphi_0, J_0) \to (\varphi(t), J(t))$ is canonical for any time t, setting $t = 1$ in (13) it follows, that the operator $L_X = e^{l_X}$ is canonical (Arnold, 1978).

By this property, the Lie-operator can be used to approximate the solution of the system, by using (8) for finite order n. Using property *(iv)* the Lie operator has been used in N-body simulations to perform numerical integration (Hanselmeier & Dvorak 1984, Delva 1984, *www.univie.ac.at/adg*).

2.2.2. The homological equation

Let us consider our original problem, to transform (1) into a form (3) or (4). The transformation is carried out through a composition of canonical transformations $(J_0, \varphi_0) \to (J_1, \varphi_1) \to \ldots \to (J_r, \varphi_r)$ such that at the rth step the non normalized part of the Hamiltonian is pushed to the order $O(\epsilon)^{r+1}$. Let us consider in detail the first step: the transformation needs a generating function W_1 to be canonical. Due to the definition of the Lie-operator the transformation from the set of old variables $\left(J^{(0)}, \phi^{(0)}\right)$ to a set of new ones $\left(J^{(1)}, \phi^{(1)}\right)$ can now be easily implemented by:

$$J^{(0)} = e^{\epsilon\, l_{W_1}} J^{(1)},$$

$$\phi^{(0)} = e^{\epsilon\, l_{W_1}} \phi^{(1)}. \tag{14}$$

Note that, while the Lie-operator formally acts as the generator of a time flow, in reality it acts as the generator of the canonical transformation with respect to the flow under W_1 for a "time" ϵ. This paradigm shift is at the core of the Lie-transformation method (Rand 1994). Another property of the Lie-operator is, that for arbitrary functions $f = f(J, \phi)$:

$$(v): \quad f(L_W J, L_W \phi) = L_W f(J, \phi), \tag{15}$$

thus, the order of the application of L_{W_r} and f on the variables (J, ϕ) can be interchanged (Gröbner, 1967, ´Vertauschungssatz´). Let us apply (14) to our original Hamiltonian H in (1). We get:

$$H^{(1)}\left(J^{(1)}, \phi^{(1)}\right) = H^{(0)}\left(J^{(0)}\left(J^{(1)}, \phi^{(1)}\right), \phi^{(0)}\left(J^{(1)}, \phi^{(1)}\right)\right). \tag{16}$$

Using property *(v)* the transformation (16) can be brought into the form:

$$H^{(1)} = H^{(1)}\left(J^{(1)}, \phi^{(1)}\right) = L_{W_1} H^{(0)} \tag{17}$$

which is by use of (8):

$$H^{(1)} = \left(1 + \epsilon\, l_{W_1} + \frac{1}{2}\, \epsilon^2\, l_{W_1}{}^{(2)} + \frac{1}{6}\, \epsilon^3\, l_{W_1}{}^{(3)} + \ldots\right)\left(H_0{}^{(0)} + \epsilon\, H_1{}^{(0)}\right) \tag{18}$$

Note, that $H_0{}^{(1)} = H_0{}^{(0)}$, i.e. we are dealing with a near-identity or contact transformation. At this point we have to specify, which terms of the Hamiltonian perturbation $\epsilon\,H_1{}^{(0)}$ should be canceled out by W_1 from (18) in order that the new Hamiltonian $H_1{}^{(1)}$ has the form (3) or (4) up to order $r = 1$. In lack of knowledge of the specific form of H_1 a natural choice would be to collect terms a) being of first order of smallness in ϵ and b) not belonging to the resonant module M defined above. From the algorithmic point of view, a more efficient choice takes care of the exponential decay of the coefficients of the Fourier series expansion of (2) which is due to the analyticity condition satisfied by $H_1{}^{(1)}$ (see Giorgilli 2002): introducing a new book keeping variable λ and organizing the Fourier terms of $H_1{}^{(1)}$ in powers of λ according to the order of the harmonics K of each term $e^{i \cdot k \cdot \varphi}$. The new book-keeping takes care of the *real* magnitude of terms, which is defined by the Fourier theorem rather than their formal size in powers of ϵ (Efthymiopoulos 2008). We will not go into further detail on this two different approaches, but only stress their common point, which is to collect the contributions of first order of smallness not belonging to the resonant module, denoted by $\hat{H}_1$. The cancelation is achieved by defining W_1 so as to satisfy the equation:

$$l_{W_1} H_0{}^{(0)} + \hat{H}_1 = 0. \tag{19}$$

Equation (19) is called the *homological equation*. By use of the definition of l_W in (6) the equation (19) is equivalent to the form:

$$\left\{ H_0{}^{(0)}, W_1 \right\} + \hat{H}_1 = 0 \tag{20}$$

and by implementing the Poisson brackets, we get:

$$-\frac{\partial H_0{}^{(0)}}{\partial J_i} \frac{\partial W_1}{\partial \phi_i} + \hat{H}_1 = 0. \tag{21}$$

Writing $\hat{H}_1$ according to:

$$\hat{H}_1 = \sum_{k \in \mathbb{K}} \hat{h}_k(J)\, e^{i k \phi}, \tag{22}$$

where $\hat{h}_k$ marks terms in (2) being of suitable magnitude (see discussion above), a suitable generating function must also take the form:

$$W_1 = \sum_{k \in \mathbb{K}} w_{1,k}(J)\, e^{i k \phi}. \tag{23}$$

Implementing the derivatives in (21) yield:

$$\omega_i(J) \frac{\partial}{\partial \phi_i} \sum_{k \in \mathbb{K},\, k \notin M} w_{1,k}(J)\, e^{i k \cdot \phi} = \sum_{k \in \mathbb{K},\, k \notin M} \hat{h}_k(J)\, e^{i k \cdot \phi} \tag{24}$$

and comparing coefficients we finally get:

$$w_k(J) = \frac{\hat{h}_k(J)}{i(k_1\,\omega_1(J) + \ldots + k_d\,\omega_d(J))}, \; \forall\, k \in \mathbb{K}, \, k \notin M, \tag{25}$$

where $k = (k_1, \ldots, k_d)$.

This completes one iteration step of the so called Lie-transformation method. In the same way we may eliminate terms of second order to get $H^{(2)}$ and in general terms of order r to get $H^{(r)}$. The recursive formulae for the r-th Lie-transformation read:

$$J^{(r-1)} = e^{\epsilon\,l_{W_r}}\,J^{(r)},$$

$$\phi^{(r-1)} = e^{\epsilon\,l_{W_r}}\,\phi^{(r)}, \tag{26}$$

and

$$H^{(r)} = L_{W_r}\,H^{(r-1)}, \tag{27}$$

where W_r satisfy the homological equations:

$$l_{W_r}\,H_0^{(r)} + \hat{H}_1^{(r-1)} = 0 \tag{28}$$

for $r = 1, 2, \ldots$. The iteration of the procedure will produce terms in *normal form* up to order r (terms being invariant to the application of the Lie-transformation of order greater than r) and terms being not in normal form of order $r + 1$, i.e. (3):

$$H^{(r)} = Z^{(r)}(J) + R^{(r+1)}(J, \phi), \tag{29}$$

in the nonresonant case, and (4):

$$H^{(r)} = Z^{(r)}(J, \phi_R) + R^{(r+1)}(J, \phi) \tag{30}$$

in the resonant case. The quantity $R^{(r+1)}$ is called the *remainder* of the Hamiltonian *normal form* and it is of order $O(\epsilon)^{r+1}$. For generic Hamiltonian systems it will be itself of the form (2), i.e.

$$R^{(r+1)}(J, \phi) = \sum_{k\in\mathbb{K}} h_{r+1,k}(J)\,e^{i\,k\,\phi} \tag{31}$$

which is an analytic function provided that the Lie-transformation is convergent at every step.

Before we proceed to estimate the influence of $R^{(r+1)}$ on the general dynamics some special care should be taken as regards equation (25). By the definition of the resonant module M it becomes clear, why we excluded resonant terms, i.e. of the form (5) in the normal form construction: the series expansion would diverge due to the largeness of the coefficients of the resonant terms, stemming from the denominators of (25). But this is not the only problem. At any stage of the normalization scheme there is also a possibility of the denominator to vanish exactly, at values of J, where:

$$k_1\,\omega_1(J) + \ldots + k_d\,\omega_d(J) = 0. \tag{32}$$

The point is, that any open domain in the action space, small what so ever, is densely crossed by an infinity of resonant manifolds defined by equations of the form (32). Therefore, assuming that H_1 contains all the harmonics $e^{i\cdot k\cdot\varphi}$ with vectors k fulfilling equation (32) the construction as described so

far cannot be defined in any open domain of the phase space. This fact prevents in general the integrability of the system (Poincaré 1892).

In the Nekhoroshev theorem, this problem is dealt with by considering only a *finite set of harmonics* to be removed from the Hamiltonian at every step. For finite order K, the normal form obtained by this construction will always be valid in some local open domain of the system, defined so as to exclude only low order resonant manifolds of the form (32). This is accomplished by changing the definition of the resonant module. Namely one has:

$$M = \{k : |\omega \cdot \kappa| = 0 \ \bigvee \ K > K_c\}. \tag{33}$$

The truncation order K_c in Fourier space plays an important role in the derivation of the estimates of exponential stability. In fact an optimal choice (see Morbidelli 2002) yields that $K_c \simeq \epsilon^{-1}$. The remainder contains terms of size $exp(-K_c \cdot \sigma) \simeq exp(\epsilon^{-1}\sigma)$, where σ is the size of the analyticity domain of the Hamiltonian in the space of complexified angles. It follows that the remainder is exponential small in ϵ^{-1}.

The restriction of the normal form to be valid only in a local domain is the reason, why the analytical part only states a local stability theorem to the system: it is based on the normal form construction of this form, calculated by means of (25).

2.2.3. Approximate integrals

Assume that we achieved to normalize the Hamiltonian up to order r, i.e. $H^{(r)}$. To derive a stability estimate we are interested in bounding the effect of the remainder $R^{(r+1)}$ on the dynamics induced by the normal form $Z^{(r)}$. For this reason we will construct approximate integrals from the normal form $Z^{(r)}$ and the sequence of generating functions $\{W_1, \ldots, W_r\}$ and look on the influence of the remainder on them. Denoting by $F_0(J^{(r)}, \phi^{(r)})$ a function which is in involution with the normal form $Z^{(r)}$, i.e. $\{F_0, Z^{(r)}\} = 0$, the function F_0 is an approximate integral of motion. Calculating the Poisson bracket of F_0 with the full Hamiltonian, i.e. $\{F_0, H^{(r)}\}$ will therefore result in that the time derivative $d F_0 / d t$ is a quantity of order $r + 1$, depending only on the remainder $R^{(r+1)}$ of $H^{(r)}$. Now, any function defined by:

$$F_0 = \lambda \cdot J, \quad \forall \lambda \neq 0, \ \lambda \perp k \in M \tag{34}$$

is a first integral of $Z^{(r)}$, since, by writing the normal form as

$$Z^{(r)} = \sum_{k \in M} z_k(J^{(r)}) \, e^{i \cdot k \cdot \phi} \tag{35}$$

one has:

$$\{F_0, Z^{(r)}\} = -i \sum_{k \in M} k \cdot \lambda \, z_k(J^{(r)}) \, e^{i \cdot k \cdot \phi} = 0, \tag{36}$$

if $\lambda \perp k \in M$. We conclude that there exist $d - \dim(M)$ first integrals $(F_0, \ldots, F_{d-\dim(M)})$ for $Z^{(r)}$, which

are independent and in involution. Choosing $d - \dim(M)$ independent real vectors $\lambda \perp k \in M$ and computing:

$$\{F_0, H^{(r)}\} = \{Z^{(r)} + R^{(r)}\} = \{F_0, R^{(r+1)}\} \tag{37}$$

results in an estimate on the time variation of the approximate integral according to:

$$\left| \dot{F}_j\left(J^{(r)}, \phi^{(r)}\right) \right| \leq l_W \| \{F_j, R^{(r+1)}\} \| \tag{38}$$

where $\| \cdot \|$ is a suitable norm in the space of Fourier functions. In summary the time variation of approximate integrals F_j can be calculated by means of (37) and from a suitable norm of $\| R^{(r+1)} \|$. It follows that the speed of motion in actions space can be given an upperbound, given essentially by:

$$\| J_i(0) - J_i(t) \| \leq \| \{F_j, R^{(r+1)}\} \| \cdot t. \tag{39}$$

Finally, equation (39) results in a stability estimate of the type (2;1). Namely, if we set $\| J_i(0) - J_i(t) \| \leq \alpha(\epsilon)$ we find via equation (39) a stability time $T(\epsilon)$ given in terms of the remainder $R^{(r+1)}$:

$$T(\epsilon) \sim \frac{\alpha(\epsilon)}{\| R^{(r+1)} \|}. \tag{40}$$

The result $K_c \simeq \epsilon^{-1}$ leading to estimates $\| R^{(r_{\text{opt}})} \| \simeq$ can be reached in principle by upperbounding the effect of the sequence of generating functions $W_1, \ldots, W_r$ on the series expansion terms, namely, the influence of (25) on the coefficients w_k. Since small denominators in (25) will affect the size of the coefficients, the knowledge of the number theoretical properties of (5) and (32) plays a major role to identify leading contributions to the growth of the series terms in the course of the normalization process. Even if exactly resonant terms are not normalized by virtue of the choice of the resonant module M, nearby resonances, i.e. where $k \cdot \omega(J) \simeq 0$, will act on the size of all the coefficients. The effect of small divisors will accumulate for larger r and in the end will render the formal integrals obtained by the normal form construction divergent (see eg. Efthymiopoulos et al. 2004 for a numerical demonstration of this procedure). Thus the optimal order of normalization of $H^{(r)}$ and thus $R^{(r+1)}$ will also optimize the stability estimate, by minimizing $\| R^{(r+1)} \|$ in (39) or (40).
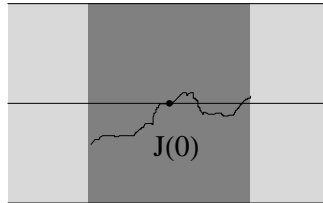
Figure 2.: Local stability theorem. An orbit starting at $J(0)$ leaves a local domain (dark gray) along the plane of fast drift.

Figure 2 illustrates the local stability estimate. The orbit starting at the point $J(0)$ remains in a small

neighbourhood (dark gray) of a plane of "fast drift", until it leaves the local domain, after a time estimated by (40).

2.3. Geometric part

The aim of the geometric part is to identify domains in the action space, where the local stability theorem applies. For this reason one defines a "geography of resonances" in the action space (see e.g. Morbidelli & Guzzo 1997 or Morbidelli 2002 for an instructive introduction). If one can define a covering $\mathfrak{W}$ of local domains in action space, where the local theorem holds one proves, that the theorem holds globally.

In principle two dangerous situations have to be avoided: i) resonance overlapping and ii) fast diffusion channels. The former is connected to the value of the perturbation ϵ, that should be sufficiently small. The latter is connected to the geometric form of the hypersurfaces of constant energy, which are determined by the steepness conditions of the Hamiltonian. We now outline the main features of the geometric part of the theorem and discuss the way how these are connected to the mechanism of the interaction of resonances.

2.3.1. Single resonance dynamics

The local stability estimate of the previous section was developed in resonant domains, defined by the resonant module M, i.e.

$$M = \{\, |k| = 0,\ \omega \cdot k = 0 \ \bigvee\ k > K_c\}. \tag{41}$$

To understand, how the definition of M influences the underlying dynamics of the system, we discuss first the backbone of single resonance dynamics: the pendulum Hamiltonian. The normal form construction of the previous section leads to such types of Hamiltonian as follows.

The general resonance condition according to (5) is given by:

$$\omega \cdot k = \omega_1 \, k_1 + \ldots + \omega_d \, k_d = 0, \tag{42}$$

where $K = |k_1| + \ldots + |k_d|$ is called the order of the resonance. If the resonance condition $\omega \cdot k$ has no integer solution other than the zero vector $k = 0$, the frequencies are called non-resonant and the corresponding motion under the normal form alone is periodic. The corresponding normal form is called a nonresonant Birkhoff normal form, the resonant module being $M = \{\, |k| = 0\}$. On the other hand, if we find $d - 1$ linearly independent integer vectors $k_1, \ldots, k_{d-1}$ satisfying $\omega \cdot k$ the motion under the normal is said to be completely resonant. In this case it is possible to express $d - 1$ angles as periodic functions of one single frequency - connected to one resonant angle ϕ_R in (4) - and thus one

single closed curve will define the orbit, which lies on a so called resonant torus. The intermediate case, where k_1, ..., k_m integer vectors satisfy some resonance condition and therefore m angles are expressed by the other $d - m$ ones the frequencies, is called a resonance of multiplicity m. The motion is separable in two independent motions, one taking place on the torus defined by the values of the actions conjugated to m resonant angles, and the other on the torus defined by the remaining $d - m$ action-angle variables. The former motion is periodic, while the latter is quasiperiodic (see Arnold 1963).

In single resonance domains the motion is dominated by only one main resonance ω_R of multiplicity $m = 1$. The vector k_R denotes the minimal nonzero integer vector related to the main resonance, i.e. the vector of minimal order such, that $k_R \cdot \omega(J) = 0$. The resonant angle is defined by:

$$\varphi_R = k_R \cdot \varphi, \tag{43}$$

while its conjugate action is:

$$J_R = m_R \cdot J \tag{44}$$

where m_R is any integer vector satisfying $m_R \cdot k_R = 0$. Constructing the resonant normal form with respect to the resonant module M results in a decomposition of the transformed Hamiltonian of the form: $H = Z_{\mathrm{nr}} + Z_r + R$, where Z_{nr} depends on a subset of the actions say $(J_2, ..., J_d)$ not containing the action J_R, and Z_R contains all the actions say $(J_R, J_2, ..., J_d)$ but only the resonant angle φ_R, and the remainder R consist of higher order harmonics containing all the variables. In a first analysis let us neglect the remainder terms defined by R. The simplified Hamiltonian results in the form

$$H = Z_{\mathrm{nr}}(J_2, ..., J_d) + Z_r(J_R, J_2, ..., J_d, \varphi_R). \tag{45}$$

Since the angles conjugated to the actions J_2, ..., J_d are cyclic, these actions are integrals of motion. Furthermore, since the Hamiltonian Z_r depends on one pair (J_R, φ_R), this Hamiltonian is also integrable. For any fixed value of the constants J_2, ..., J_d, the evolution of the motion takes place effectively on a reduced phase space defined by the (J_R, φ_R)-plane. The orbit evolves along level curves defined by a constant energy $Z_r = h$, the remaining actions acting only as parameters. If we expand the single resonance Hamiltonian around the exactly resonant value J^* in the action-space J (where $k_R \omega_R(J^*) = 0$) and fix the parameters J_2, ..., J_d to the values J_2^*, ..., J_d^*, the resonant Hamiltonian $\hat{Z}_r$ reduces to the form:

$$\hat{Z}_r = f_1(J^* \mid J_R)\,\hat{I}_1 + \frac{f_2(J^* \mid J_R)}{2!}\,\hat{I}_1^{\,2} + H_F(J^* \mid J_R, \varphi_R) + ..., \tag{46}$$

where we defined $\hat{I} = J_R - J^*$, and we neglected higher order terms in the Taylor series expansion of order $O(J^2)$. The functions f_1, f_2 are coefficients stemming from the series expansion and thus only depend on the parameters J^*. From the resonance condition $k_R \cdot \omega_R(J^*) = 0$ and Hamilton´s equation $\dot{\varphi}_R = -d\,H_{\mathrm{res}}/d\,J_R$ the function f_1 is equal to zero since it is also equal to the time derivative

$\dot{\varphi}_R = d\,\omega_R/d\,t = 0$. By expanding H_F into a Fourier series with respect to φ_R and retaining only the main term (dropping the constant term, since it does not influence the dynamics) the resulting approximating Hamiltonian reduces to the form of the simple pendulum Hamiltonian:

$$H_p = \frac{\beta}{2}\,\hat{I_R}^2 + \gamma\cos(\varphi_R), \tag{47}$$

where $\hat{I}_R = J_R - C_*$ and β, C_* and γ are constants, determined by the constant values of the actions $J_2{}^*, \ldots, J_d{}^*$.

We conclude that in a domain of the action space where a single resonant dynamics holds, the phase portrait of generic nearly integrable Hamiltonian systems of the form (1) can be locally approximated by the simple pendulum dynamics. The deformation of the invariant curves of the pendulum phase structure is given by higher order terms of the Fourier / Taylor series of H_1 on the one hand and by the influence of the remainder R on the system in general on the other hand. The phase portrait of the backbone of dynamics is given in Figure 3.
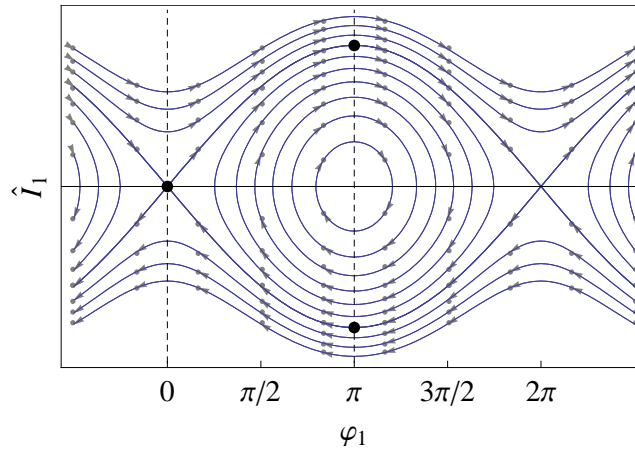
Figure 3. The pendulum Hamiltonian; backbone of single resonance dynamics.

The dynamics of the pendulum Hamiltonian is governed by an elliptic stable fixed point at $(J_R, \varphi_R = \pi)$ and one hyperbolic unstable fixed point at $(J_R, \varphi_R = 0)$. The two equilibrium points are surrounded by invariant curves separated by the separatrix, defined for the energy level $h = \gamma$. Motion (φ_R) above/below the separatrix circulates with positive/negative derivative from $(0, 2\pi)$, while its frequency monotonically increases with the distance from the separatrix. Inside the separatrix the angle φ_R librates around the elliptic fixed point $\varphi_R = \pi$, the motion taking place on closed invariant curves. The frequency is $\sqrt{\beta\gamma} = \sqrt{\beta h}$ very close to the equilibrium point, and it tends to zero as we approach the separatrix. On the separatrix itself it takes an infinite time for the trajectories to reach asymptotically the unstable equilibrium point. The separatrix half-width (counted from $\hat{I}_R$) is

$2\sqrt{\gamma/\beta}$. Therefore the minimum size of the domain for which the resonant construction is valid is $4\sqrt{\gamma/\beta}$ in the J_R direction. The half width of the resonance in the unperturbed frequency space is equal to the time derivative $\dot{\varphi}_R$ at the apex of the separatrix, namely $2\sqrt{\beta\gamma}$.
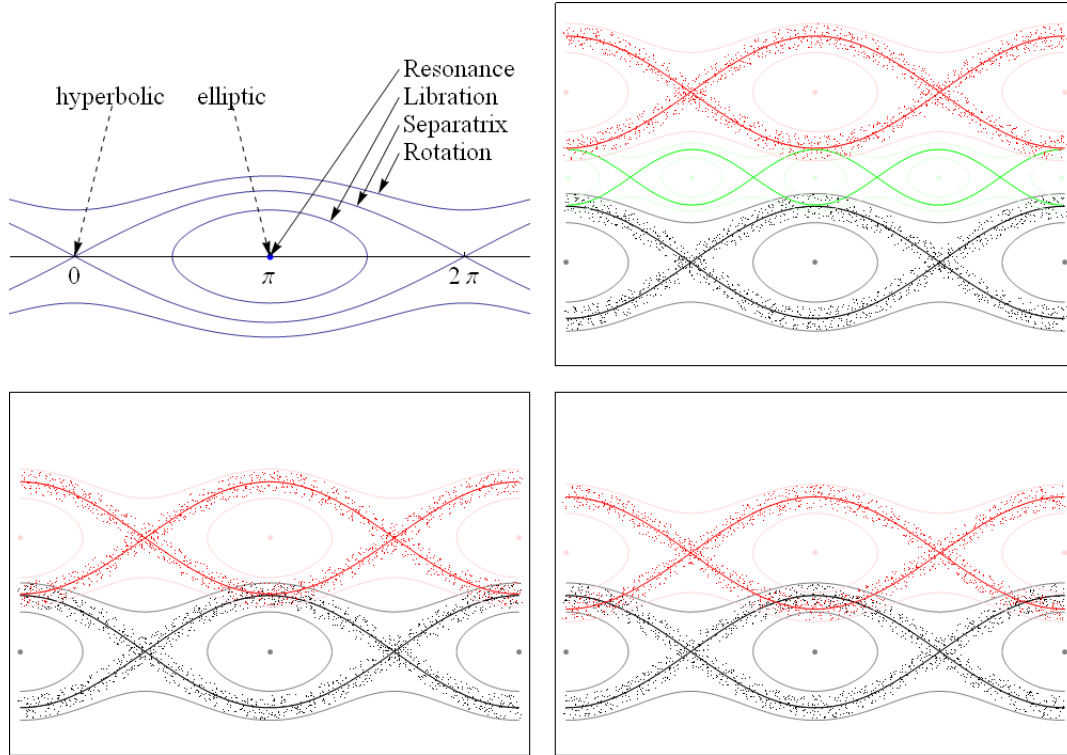
Figure 4. The black and red resonances are well separated (upper right), exchange is possible through chaotic interaction (lower left), resonance overlapping (lower right).

The single resonance model is only valid if the resonances are well separated in the phase space (Chirikov 1979). Contopoulos (1966) used this criterion to quantitatively estimate the threshold value of ϵ, that corresponds to the disappearance of KAM tori and to the global transition to chaos. The separation of resonances in action space is a difficult matter and depends on the number of frequencies taken into account. The different possible states of the system are illustrated schematically in Figure 4. In the upper right frame the red and black resonances are well separated, but their separatrices touch with higher order resonances (i.e. green). Very thin chaotic layers may be present in this situation, but we expect that still many KAM tori exist between the red and black one, such that the chaotic regions are locally confined. Homoclinic intersections of the unstable and stable manifolds are present, but they affect mostly the dynamics of the parent resonance. In the lower left frame the black and red resonances are separated, but interaction may occur due to the thin chaotic layers around the red and black separatrices (red and black dots). In the lower right frame separatrix crossing occurs and the isolation of the red and black resonance breaks. Heteroclinic intersections between the unstable and

stable manifolds of both resonances affect the stability of the system. The lack of KAM tori to separate the thin chaotic regions around each separatrix, results in that global chaos is introduced into the system. While in the upper right and lower left frame of Figure 4, the local stability estimate may apply, it does not so in a situation like in the lower right frame. To define the regions in action space without heteroclinic intersections it is necessary to study the manifolds emanating from the unstable orbits of different resonances and check wether they are isolated or not.

2.3.2. Geography of resonances

The geography of resonances can now be visualized with the help of a concrete example (a more formal and mathematical rigorous approach can be found e.g. in Giorgilli´s lecture notes 2002, Morbidelli 2002, or in the original proof of Nekhoroshev 1977). Let us consider the Hamiltonian introduced in Froeschlé et al. (2000):

$$H = \frac{J_1^2}{2} + \frac{J_2^2}{2} + J_3 + \frac{\epsilon}{\cos(\phi_1) + \cos(\phi_2) + \cos(\phi_3) + 4}. \tag{48}$$

The Hamiltonian perturbation can be expanded into Fourier series, resulting in a Hamiltonian of the form (1). This particular example has the advantage of being simple enough although an infinite number of harmonics are present in the series expansion. The geometry of the flow in hypersurfaces of constant energy is given in Figure 5, and projections of it in Figures 6 and 7. In Figure 5 the generic motion of the system is confined to lie on the surface defined by $H = h \pm O(\epsilon)$, meaning that while in the integrable approximation perpendicular motion to the hyperplane is not allowed it is only of order $O(\epsilon)$ in the full problem. In addition, the motion is also bounded by the separatrix of the local approximation in terms of the pendulum Hamiltonian: while motion induced by Z_r may be fast perpendicular to the resonant plane, which is called the *plane of fast drift*, it can neither enter the non resonance domain nor drift along the resonant plane itself. Thus the motion along the resonant planes (indicated by the arrows in Figure 5, 6, 7 respectively) can therefore only emerge from the action of the remainder R on the dynamics of the system. But since the local stability theorem applies it follows, that it is exponentially small in ϵ, i.e. its presence of diffusion along the resonant planes is only on very (exponentially) long time scales.
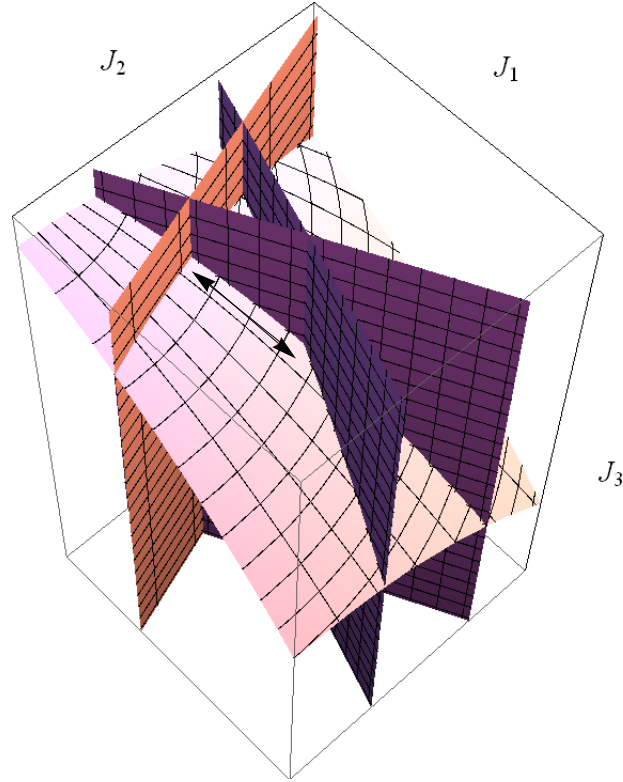
Figure 5.: Geometry of the Froeschlé Hamiltonian. Motion is restricted to the surface defined by the Hamiltonian. Motion along the plane of fast drift (arrow).

Figures 6, 7 show the projection of the model to the plane of the actions (J_1, J_2) for different values of the parameter ϵ. In Figure 6 or 7 we distinguish the so-called web of resonances or Arnold´s web. The figures were produced by considering a finite number of harmonics in the expansion up to the order $K = 6$. From the unperturbed part of equation (48) we have $\omega_1 = J_1$, $\omega_2 = J_2$ and $\omega_3 = 1$. Dark lines indicate exact resonance conditions of the form $J_1 k_1 + J_2 k_2 + k_3 = 0$ up to the order 5, and gray lines up to the order 6 respectively. The widths of the resonant lines in Figures 6 and 7 follows the estimate (Efthymiopoulos, 2008):

$$\Delta I \sim \frac{1}{2} \sqrt{\left| \epsilon h_{0,0,k_3} \right|} \, ,$$

$$\Delta I \sim \sqrt{\left| \epsilon h_{k_1,k_2,k_3} \right|} \, \frac{k_1^2 + k_2^2}{k_1^2 k_2^2} , \tag{49}$$

where h_{k_1,k_2,k_3} is the coefficient of the term $exp(\varphi_1 k_1 + \varphi_2 k_2 + \varphi_3 k_3)$ in the fourier development of equation (48). The parameter ϵ is therefore responsible for the changes of the widths in Figures 6, 7. Far from resonance junctions, every resonant line in Figure 6 yields a single resonant dynamics given by a local Hamiltonian of the form (47), the pendulum Hamiltonian. A Poincaré section condition $\varphi_R = 0$ (dashed line, black points in Figure 3) yield points around each of the central resonant lines in Figure 6, 7. On the other hand a section condition falling on the elliptic fixed point of Figure 3 (dashed

line, 2 black points) results into two resonant lines in Figures 6, 7 parallel to the central line. Since the widths of resonant lines in Figure 6 & 7 depend on the small parameter ϵ, dangerous resonant interactions of the type indicated already in Figure 4 may occur. Figures 6, 7 have to be compared to (Froschlé et al, 2000, 2002), where the web of resonances was found by numerical integration and using the FLI chaos indicator. The Arnold´s web serves as the "landscape", on which the "geography" of resonances is defined. The aim is to define a critical value for ϵ_0 below which it is possible to exclude resonance overlapping, i.e. the lower right frame of Figure 4. The critical value ϵ_0 marks the onset of the so-called Nekhoroshev regime. It should be stressed that some degree of overlapping of the resonances is always present in the action space, since any small domain is crossed by an infinity of resonances. However, the non-overlapping criterion, from which follows the value of ϵ_0, refers only to the finite number of resonances satisfying $K < K_c$. This reveals, again, the key role played in the Nekhoroshev theorem by the choice to truncate the normalization of the Hamiltonian up to a finite order K_c in the Fourier space. In fact, only under such a choice it is possible to construct a full covering of the action space by domains defined through different resonant modules M, so as to ensure that an exponentially long estimate of the stability holds globally, i.e. for all initial conditions in an open set of the action space.
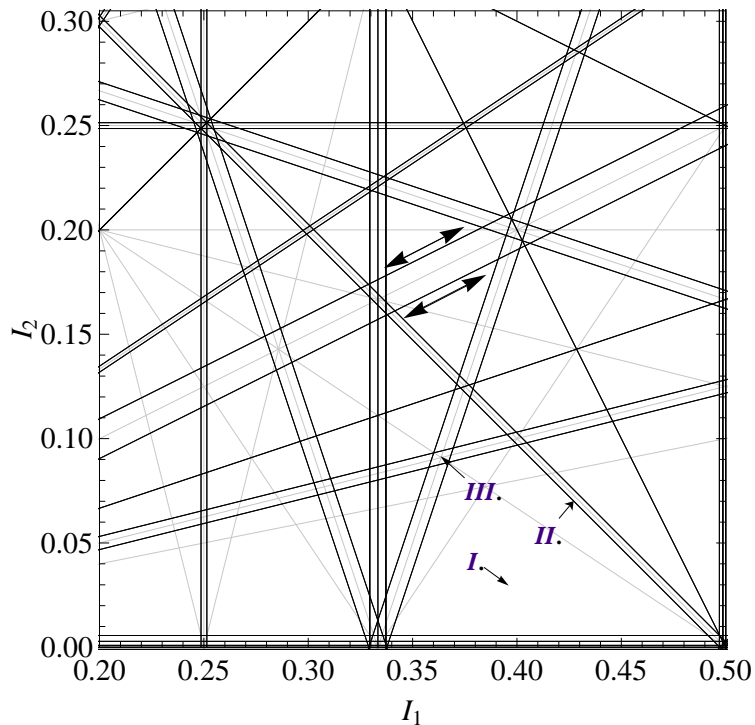
Figure 6.: Arnold Web for ϵ =0.003. No resonance domains, single resonance domains and double resonance domains; compare with Figure 5. I, no, II single, III double resonance domains.

Neglecting the exponential remainder each initial condition is confined to lie within one of the resonance domains. The action can change at most by a quantity equal to the width of the resonant

domains in the fast drift direction, which is proportional to $1/K_c$. Let us define the following sets in action space:

$\times$ *no resonance domains*, as the set of points being far enough away from all resonant surface up to order K (*I.*, in Figure 6)

$\times$ *single resonance domains*, characterized by the presence of only resonant surface of order smaller than K (*II.* in Figure 6)

$\times$ *double resonance domains*, centered around the crossing of two single resonant surfaces of order smaller than K (*III.* in Figure 6)

In the non resonant domains (*I.* in Figure 6), one can eliminate all the harmonics of the perturbation up to order K and the behavior is governed by a normal form of type (3). The actions are constants of motion, the local stability theorem guarantees that motion along the resonant planes is exponentially small. In the single resonance domains (*II.* in Figure 6) all but one harmonics can be eliminated again and the behavior can be modeled by means of a normal form of the form (4). Although the actions are no longer constants of motion, they can only move along the *fast drift direction*. Since the Hamiltonian is steep (or convex) the fast drift direction is transversal to all the resonant surfaces. In addition, the motion is not allowed to enter the non resonant domains, since the actions inside the domains of type *I.* of Figure 6 are constant again. It follows, that the motion is restricted to single resonant domains and the diffusion is bounded again by the exponentially small remainder. In the double resonance domains (*III.* in Figure 6) the normal form Hamiltonian has two independent resonant terms k_1, k_2 of order smaller than order K_c and the motion on the action plane can take place in any direction of the plane spanned by k_1 and k_2. Again the convexity condition prevents the actions to enter the single or no resonance domains, since in the former motion is confined along the fast drift direction and in the latter action would become constant again. The motion therefore is confined to be close to the double resonance region spanned by k_1 and k_2. As a conclusion it is possible to render the local stability theorem of the analytical part global, provided that it is possible to construct a covering of the action space by means of domains in which one of the mentioned different types of resonant dynamics holds. This is possible if $\epsilon < \epsilon_0$.
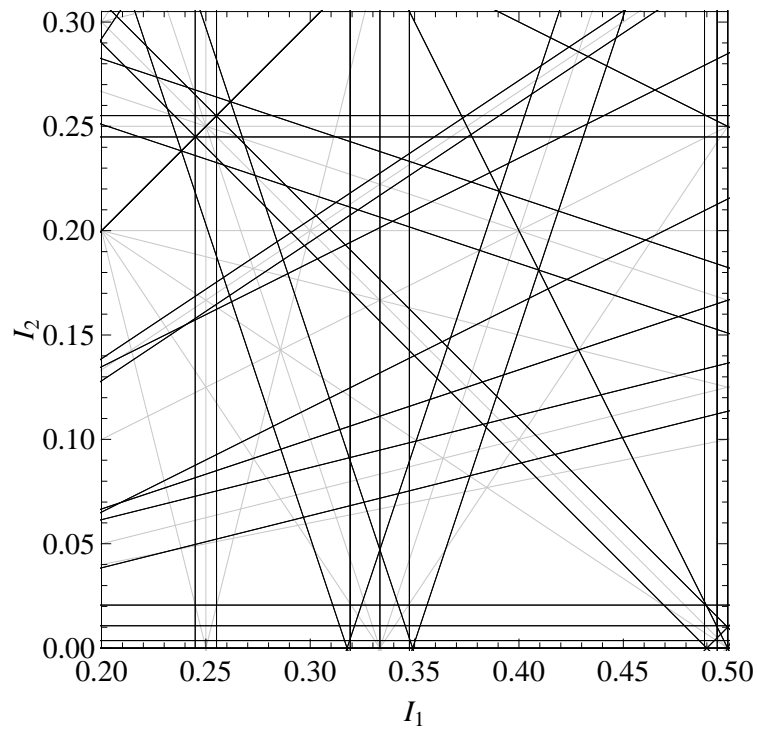
Figure 7.: Arnold Web for ε=0.04. Resonance overlapping introduces large scale chaos. Compare to Figure 6.

The opposite situation is indicated in Figure 7. With increasing ϵ the widths of the resonant zones increase too and open fast diffusion channels from one resonance to another. It is not possible to define resonant domains without overlapping with other resonances of the same order (below K_c) and the diffusion in action space is free to pass from one resonance to another. Resonance overlapping dominates the evolution of the actions, a situation also indicated in Figure 4 (lower right). A schematic representation of the diffusion in the resonance overlap regime is given in Figure 8. When there is no resonance overlap, the system is said to be in the *Nekhoroshev regime*. See figure 9 schematic.
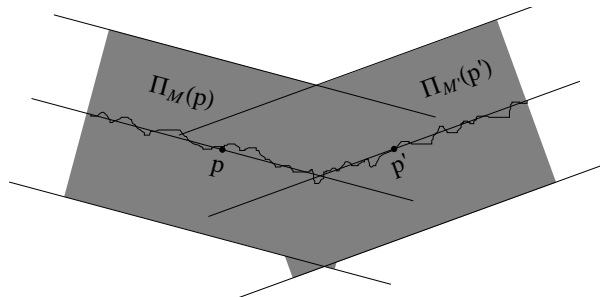
Figure 8.: Unsafe region due to resonance overlapping of same multiplicity. The resonant planes Π_M of different resonances of same multiplicity intersect. Orbits are free to drift from one resonance to another.
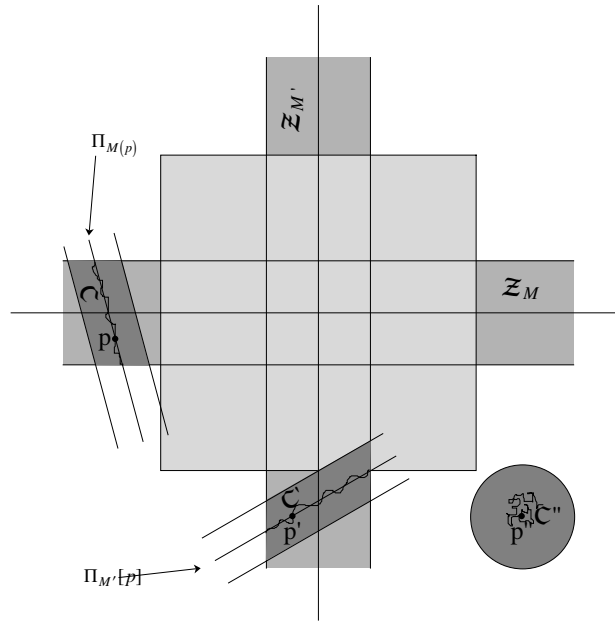
Figure 9.: No resonance domain C´´ (I in Figure 6), single resonance domain C´ and *C* (II in Figure 6). Diffusion is exponentially slow. The stability theorem applies.

2.3.3. Fast diffusion channels

Finally, another dangerous situation, connected to the violation of steepness condition is illustrated in Figure 10. In the absence of convexity, the resonant plane $\Pi_{M,\delta}(J)$ may become tangent to the resonant manifold Σ_M implying, that $J \in \Sigma_M$ and $\Pi_{M,\delta}(J)$ lie very close to each other. The opening of a diffusion channel inside a zone, where the near tangency occurs cannot be prevented and large scale chaos may appear. The necessary condition that the resonant manifold Σ_M and the resonant plane $\Pi_{M,\delta}(J)$ are transversal to each other, or at least have a tangency of only a finite order, is guaranteed by the convexity condition of the Hamiltonian. In the original formulation due to Nekhoroshev this condition refers to steep functions. The stronger condition is convexity. It ensures, that the resonant manifold and the resonant plane are transversal to each other. An easy example given in Arnold´s book (1978), refers to the Hamiltonian:

$$H(J, \phi) = \frac{1}{2}\left(J_1{}^2 - J_2{}^2\right) + \epsilon \sin(\phi_1 - \phi_2), \tag{50}$$

which is neither steep nor convex. Since the orbit, defined by the solution

$$\phi_1(t) = -\epsilon^2 \frac{t}{2}, \quad \phi_2(t) = -\epsilon^2 \frac{t}{2}$$

$$J_1(t) = -\epsilon\, t, \quad J_2(t) = \epsilon\, t, \tag{51}$$

lies on the resonant manifold

$$k_1 J_1 + k_2 J_2 = 0$$

for $k_1 = k_2 = 1$, it coincides with the plane of fast drift at any of its points. Convexity of the Hamiltonian excludes such dangerous situations.
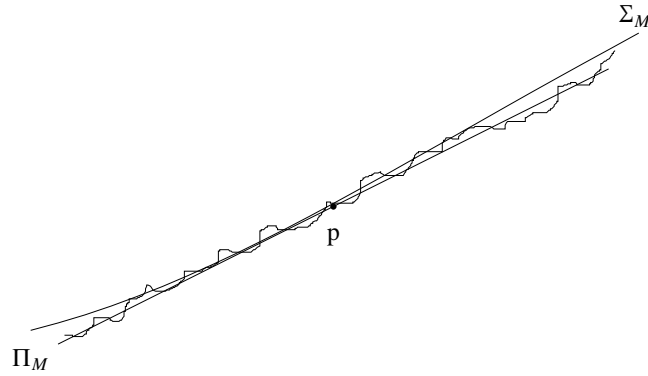
Figure 10.: Unsafe region due to fast diffusion channels. The resonant plane Π_M is nearly tangent to the resonant manifold Σ_M.

3. The Restricted Three Body Problem

In the (general) three body problem (GTBP) three bodies with arbitrary mass (m_1, m_2, m_3) attract each other according to the Newtonian law of gravity. The question is to specify their subsequent motion if the bodies are given arbitrary initial conditions. Let us denote by the restricted three body problem (RTBP) the same problem as the GTBP but with one mass being much smaller than the other two masses ($m_3 << m_1$, m_2). It follows that there is no influence of the third body (m_3) on the first and second body (called primaries), which are therefore moving around their common barycentre in Keplerian motion in a plane. Mathematically speaking $m_3 = 0$. In the circular restricted three body problem (CRTBP) the primaries m_1 and m_2 are moving on circular orbits. In the elliptic restricted three body problem (ERTBP) the primaries are moving on elliptic Keplerian orbits. We may restrict the motion of the third body m_3 to lie on the invariant plane of motion of the primary bodies or not. The former one is called the planar, the latter is called the spatial restricted problem:

GTBP   : m_1, m_2, $m_3 \neq 0$

planar CRTBP : m_1, m_2 on circular orbit, $m_3 = 0$, moving in the plane of the primaries.

spatial CRTBP : m_1, m_2 on circular orbit, $m_3 = 0$, moving in $3D$ space.

planar ERTBP : m_1, m_2 on elliptic orbit, $m_3 = 0$, moving in the plane of the primaries.

spatial ERTBP : m_1, m_2 on elliptic orbit, $m_3 = 0$, moving in $3D$ space.

The historical restricted three body problem (HRTBP) in our setting is the planar CRTBP; the term ´restricted´ seems to go back to Poincaré (1893) who first called the problem "le probleme restreint"; according to Whittaker´s report (1900, Report on progress of the solution of the problem of three bodies) the HRTBP dates back (in a different formulation) also to Jacobi (1836) but following Szebehely (1967) and Winter (1941) the origin may be even due to Euler (1772).

In this section we want to establish the formalism for the planar and spatial CRTBP, ERTBP. The notation in principle follows the book of Szebehely (1967) while some minor modifications in the notation are done for adapting to our needs. The line of development of the models passes from the force function in dimensional coordinates to the dimensionless formulation of the Lagrangian in fixed Cartesian coordinates. The transformation to a rotating frame is done in the Hamiltonian formulation. The construction of the generating functions can be found e.g. in the book of Szebehely. Other relevant formulations given are by Giorgilli & Skokos 1997 and Skokos & Dokoumetzidis 2001. The first part of this chapter is dedicated to the circular model (planar and spatial one), in which the Hamiltonian is constant. The second part introduces the model and upcoming problems when generalizing to the ERTBP (planar and circular). Since the mathematical formulation of both the CRTBP and the ERTBP

can be established in an equivalent form using a uniformly rotating coordinate framework in the circular case and a pulsating non-uniform rotating coordinate system in the elliptic case, the transformation to polar and Delaunay variables is put together for the two cases at the end of this Chapter. Nevertheless one should always keep in mind that the difference between the circular and elliptic problem is that the potential is time dependent in the latter case. Furthermore, under a proper redefinition of the Hamiltonian the generalized Jacobian constant does not vanish when dealing with the elliptic restricted problem.
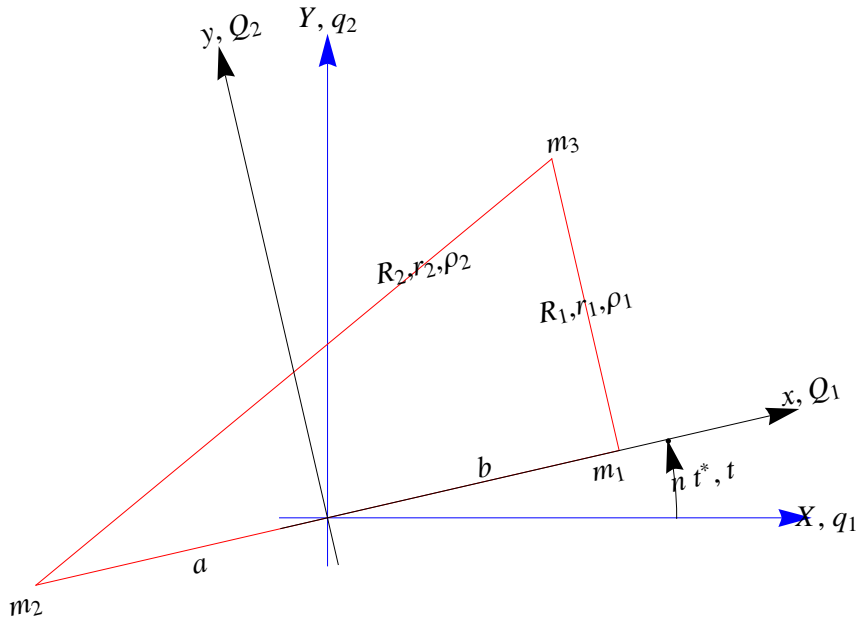
Figure 1: Geometry of the restricted three body problem (arbitrary units); Siderial (blue), synodic (black) reference system. Triangle between m_1, m_2, m_3 (red).

3.1 Planar circular restricted three body problem

3.1.1. Sidereal system

The potential (or in older astronomical literature sometimes called force function) of the restricted problem, in sidereal dimensional coordinates (Figure 1, blue), according to Newton´s law of gravitational attraction is given by:

$$\phi = k^2(m_1 / R_1 + m_2 / R_2), \tag{1}$$

where k is the Gaussian gravitational constant $\left(k \simeq 0.017 \ldots AU^{3/2} M_{sun}^{-1/2} day^{-1}\right)$ and the distances R_1 and R_2 are defined by:

$$R_1{}^2 = (X - X_1)^2 + (Y - Y_1)^2,$$

$$R_2{}^2 = (X - X_2)^2 + (Y - Y_2)^2. \tag{2}$$

Here (X_1, Y_1) and (X_2, Y_2) are the sidereal positions of the masses m_1 and m_2 respectively and the vector (X, Y) is the position of the test body $(m_3 = 0)$. Introducing $a = m_1 \, l / M$, $b = m_2 \, l / M$ as the distances of m_2 and m_1 from the center of mass respectively (l being the mutual distance of the primaries and $M = m_1 + m_2$ being the total mass of the system, Figure 1) the equations of motion in this setting are given by:

$$\frac{d^2 X}{d t^{*2}} = -k^2 \left(m_1 \frac{(X - b \cos n \, t^*)}{R_1{}^3} + m_2 \frac{(X + a \cos n \, t^*)}{R_2{}^3} \right),$$

$$\frac{d^2 Y}{d t^{*2}} = -k^2 \left(m_1 \frac{(Y - b \sin n \, t^*)}{R_1{}^3} + m_2 \frac{(Y + a \sin n \, t^*)}{R_2{}^3} \right), \tag{3}$$

where n is the mean motion, indicating that $n \, t^*$ is the longitude of m_1 and t^* is the dimensional time. By introducing the dimensionless quantities $q_1 = X / l$, $q_2 = Y / l$, $t = n \, t^*$, $\mu_1 = m_1 / M$, $\mu_2 = m_2 / M$ the Lagrangian function of the system takes the form:

$$L = \frac{1}{2} \left(\dot{q}_1{}^2 + \dot{q}_2{}^2 \right) + \phi(q_1, q_2, t) \tag{4}$$

where $\phi = \phi(q_1, q_2, t)$ is the time dependent dimensionless potential of the problem,

$$\phi(q_1, q_2, t) = \frac{\mu_1}{\rho_1} + \frac{\mu_2}{\rho_2}, \tag{5}$$

and ρ_1 and ρ_2 are given in unitless form by:

$$\rho_1{}^2 = (q_1 - \mu_2 \cos t)^2 + (q_2 - \mu_2 \sin t)^2,$$

$$\rho_2{}^2 = (q_1 + \mu_1 \cos t)^2 + (q_2 + \mu_1 \sin t)^2. \tag{6}$$

From the definition of the momenta $p_i = \partial L / \partial \dot{q}_i$, $(i = 1, 2)$ we get the conjugate variables to (q_1, q_2) namely $p_1 = \dot{q}_1$ and $p_2 = \dot{q}_2$. From the definition of the Hamiltonian function $H = p \, q - L$ we find:

$$H = \frac{1}{2} \left(p_1{}^2 + p_2{}^2 \right) - \phi(q_1, q_2, t), \tag{7}$$

which in sidereal coordinates is time dependent through the presence of the time in the distances ρ_1 and ρ_2. Therefore the Hamiltonian in this setting is not a constant of motion. The corresponding canonical equations are given by:

$$\dot{q}_1 = \frac{\partial H}{\partial p_1} = p_1,$$

$$\dot{q}_2 = \frac{\partial H}{\partial p_2} = p_2,$$

$$\dot{p}_1 = -\frac{\partial H}{\partial q_1} = -\left(\mu_1 \frac{(q_1 - \mu_2 \cos t)}{\rho_1{}^3} + \mu_2 \frac{(q_1 + \mu_1 \cos t)}{\rho_2{}^3} \right),$$

$$\dot{p}_2 = -\frac{\partial H}{\partial q_2} = -\left(\mu_1 \frac{(q_2 - \mu_2 \sin t)}{\rho_1{}^3} + \mu_2 \frac{(q_2 + \mu_1 \sin t)}{\rho_2{}^3} \right). \tag{8}$$

3.1.2. Synodic system

To transform the Hamiltonian (7) to a constant of motion we need to introduce a synodic (rotating) coordinate system (Figure 1, black). For this reason we need to fix the location of the primaries and look at the motion of the third body relative to them. In the circular case this is accomplished by choosing a uniformly rotating coordinate system (with respect to the mass m_2).

The transformation to new coordinates follows from a bilinear canonical transformation of the type W_3 with time dependent coefficients of the form

$$W_3(p_1, p_2, Q_1, Q_2, t) = -a_{ij}\, p_i\, Q_j, \tag{9}$$

where the unitary matrix $\left(a_{ij}\right)$ is defined by:

$$\left(a_{ij}\right) = \begin{pmatrix} \cos t & -\sin t \\ \sin t & \cos t \end{pmatrix} \tag{10}$$

and (Q_1, Q_2, P_1, P_2) are the new variables. The transformation via the generating function (9) represents uniform rotation with angular velocity t around the common barycentre resulting in the desired synodic coordinate system. Applying the transformation equations $q_i = -\partial W_3 / \partial p_i$ and $P_i = -\partial W_3 / \partial Q_i$, $(i = 1, 2)$, we get for the transformed Hamiltonian (according to $\tilde{H} = H + \partial W_3 / \partial t$):

$$\tilde{H} = \frac{1}{2} \left(P_1{}^2 + P_2{}^2 \right) + Q_2\, P_1 - Q_1\, P_2 - \tilde{\phi}(Q_1, Q_2) \tag{11}$$

and for the equations connecting the fixed (q_1, q_2) with the rotating (Q_1, Q_2) system $(q_i = a_{ij}\, Q_j)$:

$$q_1 = Q_1 \cos t - Q_2 \sin t,$$

$$q_2 = Q_1 \sin t + Q_2 \cos t. \tag{12}$$

For the conjugate momenta, using the relation $P_i = a_{ji}\, p_j$ we get:

$$P_1 = p_1 \cos t + p_2 \sin t,$$

$$P_2 = p_2 \cos t - p_1 \sin t, \tag{13}$$

(the summation convention is applied to repeated subscripts on the same hand side of the equation) for $i = 1, 2$. To complete the transformation from sidereal (fixed) to synodic (rotating) dimensionless coordinates we need $\tilde{\phi}(Q_1, Q_2)$ in the rotating coordinate frame. For this reason we apply (12) to (6)

and insert (using the identity $cos^2 Q_i + sin^2 Q_i = 1$) in (5) and finally get for $\tilde{\phi}(Q_1, Q_2) \equiv \phi(Q_1, Q_2)$, with distances in the rotating frame defined by

$$\rho_1{}^2 = Q_2{}^2 + (Q_1 - \mu_2)^2,$$

$$\rho_2{}^2 = Q_2{}^2 + (Q_1 + \mu_1)^2. \tag{14}$$

The canonical equations of motion in the new variables read:

$$\dot{Q}_1 = \frac{\partial \tilde{H}}{\partial P_1} = P_1 + Q_2,$$

$$\dot{Q}_2 = \frac{\partial \tilde{H}}{\partial P_2} = P_2 - Q_1,$$

$$\dot{P}_1 = -\frac{\partial \tilde{H}}{\partial Q_1} = P_2 + \frac{\partial \tilde{\phi}}{\partial Q_1} = P_2 - \left(\mu_1 \frac{(Q_1 - \mu_2)}{\rho_1^3} + \mu_2 \frac{(Q_1 + \mu_1)}{\rho_2^3} \right),$$

$$\dot{P}_2 = -\frac{\partial \tilde{H}}{\partial Q_2} = -P_1 + \frac{\partial \tilde{\phi}}{\partial Q_2} = -\left(P_1 + \frac{Q_2 \, \mu_1}{\rho_1^3} + \frac{Q_2 \, \mu_2}{\rho_2^3} \right). \tag{15}$$

The planar CRTBP in this form was used, e.g. by Giorgilli & Skokos (1997).

3.1.3. Newtonian formulation

The Newtonian formulation (Figure 1, black) is found by solving the first two equations in (15) with respect to (P_1, P_2) and substituting in the remaining ones. In the usual notation $(x, y) = (Q_1, Q_2)$, $(\dot{x}, \dot{y}) = (P_1, P_2)$ the equations of motion of the planar CRTBP, in a rotating coordinate frame, are given by:

$$\ddot{x} - 2\,\dot{y} = \frac{\partial \Omega}{\partial x},$$

$$\ddot{y} + 2\,\dot{x} = \frac{\partial \Omega}{\partial y}, \tag{16}$$

where the potential Ω is defined by:

$$\Omega = \mu_1 \left(\frac{r_1^2}{2} + \frac{1}{r_1} \right) + \mu_2 \left(\frac{r_2^2}{2} + \frac{1}{r_2} \right). \tag{17}$$

The formulation in the Newtonian framework is used as a starting point by Littlewood 1959a. Note that he defines the potential slightly differently (as regards the gravitational terms) and puts the terms stemming from the Coriolis force $(\dot{\Omega} \times r)$ on the left hand side of the equations. The distances in (17) are of the form:

$$r_1{}^2 = (x - \mu_2)^2 + y^2,$$

$$r_2{}^2 = (x + \mu_1)^2 + y^2. \tag{18}$$

The Jacobi constant connected to the time-independent formulation of the Hamiltonian in this setting is given by:

$$\dot{x}^2 + \dot{y}^2 = 2\,\Omega - C, \tag{19}$$

where C is the Jacobi constant in the synodic system, which, translated to the sidereal system, results in:

$$\dot{q_1}{}^2 + \dot{q_2}{}^2 = 2\,(q_1\,\dot{q_2} - q_2\,\dot{q_1}) + \frac{2\,\mu_1}{\rho_1} + \frac{2\,\mu_2}{\rho_2} - \overline{C}. \tag{20}$$

Here $C = \overline{C} + \mu_1\,\mu_2$ indicate the Jacobi constant in the rotating and fixed frameworks respectively.
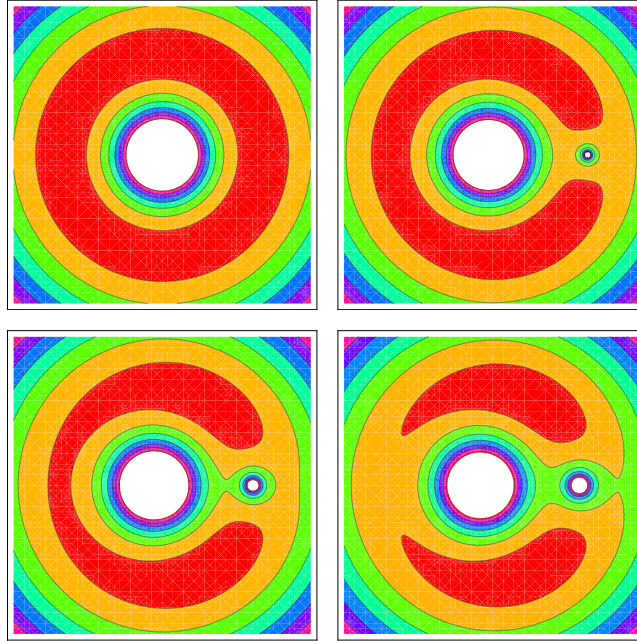
Figure 2: Zero velocity curves in the circular restricted three body problem (x,y)-plane for $\mu_1 = 0.$, 0.04, 0.08, 0.12 (from upper left to lower right).

One can define zero velocity curves in the rotating system by means of (19). For a given value of C, an asteroid cannot escape from within a closed zero velocity curve, since the velocities would become complex outside. This first stability criterion may be generalized to the spatial case (Figure 3) but becomes more complex in the elliptic one. The zero velocity curves defined by different mass ratios of the primaries are given in Figure 2. Four different types of topologies are shown (from upper left to lower right): closed red region ($\mu_1 = 0$), banana shaped red region, separated green regions ($\mu_1 \simeq 0.04$), connected inner and disconnected outer green region ($\mu_1 \simeq 0.08$) and disconnected red, connected green region ($\mu_1 \simeq 0.12$), (compare with Figure 3).

3.2. Spatial circular restricted three body problem

The generalization from the planar to the spatial case of the CRTBP (used by Simó 1989, Giorgilli et al. 1989, Celletti & Giorgilli 1991, Benetin et al. 1998 & Skokos & Dokoumetzidis 2001) is straightforward.

3.2.1. Hamiltonian formulation

The Lagrangian function corresponding to equation (4) is given by:

$$L = \frac{1}{2}\left(\dot{q}_1{}^2 + \dot{q}_2{}^2 + q_3{}^2\right) + \phi(q_1, q_2, q_3, t) \tag{21}$$

and equation (5) generalizes to:

$$\phi(q_1, q_2, q_3, t) = \frac{\mu_1}{\rho_1} + \frac{\mu_2}{\rho_2}, \tag{22}$$

where the distances in the 3D case are defined by (compare with (6)):

$$\rho_1{}^2 = (q_1 - \mu_2 \cos t)^2 + (q_2 - \mu_2 \sin t)^2 + q_3{}^2,$$

$$\rho_2{}^2 = (q_1 + \mu_1 \cos t)^2 + (q_2 + \mu_1 \sin t)^2 + q_3{}^2. \tag{23}$$

As in the planar case, by introducing $p_i = \partial L / \partial \dot{q}_i = \dot{q}_i$, $(i = 1, 2, 3)$, where L is taken from (21), the Hamiltonian in the fixed sidereal coordinate frame reads (compare with (7)):

$$H = \frac{1}{2}\left(p_1{}^2 + p_2{}^2 + p_3{}^2\right) - \phi(q_1, q_2, q_3, t). \tag{24}$$

The relation between the new synodic and old sidereal coordinates and momenta is given by the generating function:

$$W_3(p_1, p_2, p_3, Q_1, Q_2, Q_3, t) = -a_{ij}\, p_i\, Q_j, \tag{25}$$

where the matrix $\left(a_{ij}\right)$ of (10) generalizes to:

$$\left(a_{ij}\right) = \begin{pmatrix} \cos t & -\sin t & 0 \\ \sin t & \cos t & 0 \\ 0 & 0 & 1 \end{pmatrix}. \tag{26}$$

The resulting Hamiltonian in the 3D case $\tilde{H} = H + \partial W_3/\partial t$ (note that here H is defined via (24) and W_3 via (25)) is:

$$\tilde{H} = \frac{1}{2}\left(P_1{}^2 + P_2{}^2 + P_3{}^2\right) + Q_2\, P_1 - Q_1\, P_2 - \tilde{\phi}(Q_1, Q_2, Q_3), \tag{27}$$

where the potential $\tilde{\phi}(Q_1, Q_2, Q_3)$ of (25) is given by :

$$\tilde{\phi}(Q_1, Q_2, Q_3) = \frac{\mu_1}{\rho_1} + \frac{\mu_2}{\rho_2} \tag{28}$$

with the distances in the rotating coordinate frame being given by:

$$\rho_1{}^2 = (Q_1 - \mu_2)^2 + Q_2{}^2 + Q_3{}^2, \tag{29}$$

$$\rho_2{}^2 = (Q_1 + \mu_1)^2 + Q_2{}^2 + Q_3{}^2. \tag{30}$$

The canonical equations of motion of the 3D case are the same as equations (15), with the additional equations $\dot{Q}_3 = P_3$ and $\dot{P}_3 = \partial\tilde{\phi}/\partial Q_3$.

3.2.2. Newtonian formulation

To get the equations of motion in the Newtonian formulation, we follow the same line of calculations as in the 2 D case. Using the set of variables (x, y, z) we get:

$$\ddot{x} - 2\,\dot{y} = \partial\Omega/\partial x,$$

$$\ddot{y} + 2\,\dot{x} = \partial\Omega/\partial y,$$

$$\ddot{z} = \partial\Omega/\partial z, \tag{31}$$

where the potential Ω in the 3D case is given by:

$$\Omega = \frac{1}{2}\left(x^2 + y^2\right) + \frac{\mu_1}{r_1} + \frac{\mu_2}{r_2} + \frac{1}{2}\,\mu_2\,\mu_1. \tag{32}$$

Here, the distances in 3D-space are generalized to:

$$r_1{}^2 = (x - \mu_2)^2 + y^2 + z^2,$$

$$r_2{}^2 = (x + \mu_1)^2 + y^2 + z^2. \tag{33}$$

The Jacobi integral is obtained by multiplying equations (31) by $\dot{x}, \dot{y}, \dot{z}$ respectively, adding the results and integrating with respect to time:

$$\dot{x}^2 + \dot{y}^2 + \dot{z}^2 = 2\,\Omega(x, y, z) - C. \tag{34}$$

The parameter C is called again the Jacobi constant.

Figure 3: Zero velocity curves in the spatial CRTBP for $\mu_1 = 0.14$. Compare colors with lower left of Figure 2.
$C = 10, 5, 2.7, 1.5, .5, 1.1$ (inner to outer).

The zero velocity curves of the spatial restricted problem are shown in Figure 3, which should be compared with Figure 2: the connected (middle orange) region corresponds to the connected orange region in Figure 2 (lower left), the disconnected (inner pink, blue) to the inner pink/blue circle regions. It is also possible to identify the inner and outer green regions of Figure 2 and 3 respectively, while the magenta region in Figure 3 is not visible in Figure 2.

3.3. Elliptic restricted three body problem

While in the circular case the introduction of a uniformly rotating coordinate frame simplifies the form and therefore the analysis of the problem, the elliptic restricted three body problem is of much greater complexity. The main reasons are, on the one hand the generalized motion of the primaries and on the other hand, the fact, that the Hamiltonian becomes time-dependent. The problem has been analyzed to a smaller extent than the circular problem (e.g. Waldvogel 1973, Bennett 1965, Danby 1964, Deprit & Rom 1970 or Érdi 1977). The problem can be reduced to a mathematically similar form as the circular problem by use of a non uniformly rotating and pulsating coordinate reference frame. Setting i) the $(O\,x\,y)$-plane to be the plane of the orbits of the two primaries and ii) the unit of length to the mutual distance between the primaries, the system can again be brought into a form where the positions of the

primaries are fixed and the motion of the third body can be analyzed relative to the fixed primary locations. However contrary to the circular case, the equations of motion are non longer autonomous.

3.3.1. Planar

The mathematical realization is done by introducing the unit length to be the distance between the primaries in Keplerian motion:

$$r = \frac{a(1 - e^2)}{1 + e \cos E}, \tag{35}$$

and using the true anomaly E instead of the time t as the basis for introducing dimensional coordinates. In (35) a is the semi-major axis and e is the value of the eccentricity of the conic section of the motion, which will be restricted in our case to be elliptic or circular ($e < 1$). While the definition takes care of the variable length of the distance between the two primaries, the use of the true anomaly introduces the non uniformly rotating reference frame. The angular motion of the primaries, with variable angular velocity E, is defined by:

$$d E = \frac{k(m_1 + m_2)^{1/2}}{a^{3/2}(1 - e^2)^{3/2}} (1 + \cos E)^2 \, d t^*, \tag{36}$$

Using the definition of the unit length (35), equation (36) takes the form:

$$\frac{d E}{d t^*} r^2 = \left(a(1 - e)^2 k^2 (m_1 + m_2)\right)^{1/2}. \tag{37}$$

It is convenient to write the equations of motion in the fixed coordinate system (compare with (3)) using complex variable notation, before introducing the transformation to the non-uniformly rotating and pulsating coordinate system. Using the identities $X_1 = b \cos n t^*$, $Y_1 = b \sin n t^*$ and $X_2 = -a \cos n t^*$, $Y_2 = -a \sin n t^*$ the equation of motion of the massless test body in complex form $Z = X + i Y$ becomes:

$$\frac{d^2 Z}{d t^{*2}} = -m_1 k^2 \frac{Z - Z_1}{R_1^3} - m_2 k^2 \frac{Z - Z_2}{R_2^3}, \tag{38}$$

where for $i = 1, 2$ the complex variables are $Z_i = X_i + i Y_i$ and the distances R_i are given by

$$R_1 = |Z - Z_1|,$$

$$R_2 = |Z - Z_2|. \tag{39}$$

The rotation in the complex plane is defined via $Z = z e^{i E}$, where $z = \tilde{x} + i \tilde{y}$ is the new dependent variable in the rotating coordinate frame. Substituting to equation (38) yields the equation of motion in the rotating dimensional reference system:

$$\frac{d^2 z}{d t^{*2}} + 2 i \frac{d E}{d t^*} \frac{d z}{d t^*} = -k^2 \left(m_1 \frac{z - z_1}{R_1^{\,3}} + m_2 \frac{z - z_2}{R_2^{\,3}} \right) + z \left(\left(\frac{d E}{d t^*} \right)^2 - i \frac{d^2 E}{d t^{*2}} \right). \tag{40}$$

Using the complex positions (z_1, z_2) the primaries are located on the real axis of the $(\tilde{x}, \tilde{y})$-plane

$$z_1 = \tilde{x}_1 = \frac{p_1}{1 + e \cos E},$$

$$z_2 = \tilde{x}_2 = -\frac{p_2}{1 + e \cos E}, \tag{41}$$

where p_1, p_2 are positive and $p_1 / p_2 = a_1 / a_2 = m_2 / m_1$. The distances R_i, $i = 1, 2$ from the primary bodies in the rotating frame are given by:

$$R_1^{\,2} = |Z - Z_1| = |z - \tilde{x}_1| = (\tilde{x} - \tilde{x}_1)^2 + \tilde{y}^2,$$

$$R_2^{\,2} = |Z - Z_2| = |z - \tilde{x}_2| = (\tilde{x} - \tilde{x}_2)^2 + \tilde{y}^2. \tag{42}$$

Note, that for $e = 0$ equation (40) reduces to the CRTBP (3), where $E = n t^*$, $p_1 = a_1 = b$ and $p_2 = a_2 = a$. The second transformation to pulsating coordinates is given by introducing non dimensional coordinates $\zeta = z / r = \xi + i \eta$, which, together with equation (35), leads to:

$$\xi = \frac{\tilde{x}(1 + e \cos E)}{a\left(1 - e^2\right)},$$

$$\eta = \frac{\tilde{y}(1 + e \cos E)}{a\left(1 - e^2\right)}. \tag{43}$$

Here $\zeta = (\xi, \eta)$ and the equations of motion in synodic coordinates resume the form:

$$\frac{d^2 \zeta}{d E^2} + 2 i \frac{d \zeta}{d E} = \mathrm{grad}_\zeta\, \omega, \tag{44}$$

where the time dependent potential is given by

$$\omega = \Omega(1 + e \cos E)^{-1}, \tag{45}$$

$$\Omega(\zeta) = \frac{1}{2}\left(\xi^2 + \eta^2\right) + \frac{\mu_1}{r_1} + \frac{\mu_2}{r_2} + \frac{1}{2}\mu_1 \mu_2. \tag{46}$$

The resulting set of equations of motion (separating the real and imaginary part of equation (44)) are:

$$\frac{d^2 \xi}{d E^2} - 2 \frac{d \eta}{d E} = \frac{\partial \omega}{\partial \xi},$$

$$\frac{d^2 \eta}{d E^2} + 2 \frac{d \xi}{d E} = \frac{\partial \omega}{\delta \eta}. \tag{47}$$

It is remarkable that the system of equations (47) is formally equivalent to the one of the circular problem (16). However, despite this formal identity, in the elliptic case the function ω depends on the

coordinates as well as on the independent variable E, which is time-dependent. Therefore the system (47) is non-autonomous.

If we multiply the first equation in (47) with $d\xi/dE$ and the second with $d\eta/dE$ and add them the Jacobi integral in the elliptic case is:

$$\left(\frac{d\xi}{dE}\right)^2 + \left(\frac{d\epsilon}{dE}\right)^2 = 2\int\left(\frac{d\omega}{d\xi} + \frac{d\omega}{d\eta}\right) = 2\omega - 2e\int\frac{\Omega\sin E}{(1 + e\cos E)^2}\, dE - C. \tag{48}$$

If the eccentricity of the primaries is $e = 0$ the integral term in equation (48) vanishes: the eccentric anomaly reduces to the dimensionless time and $\omega = \Omega$ and (48) becomes the Jacobian integral, already known from the circular case. In the elliptic case, however due to the presence of E in the integrand of (48) the Jacobi integral is no longer a constant.

Similar results hold for the Hamiltonian formalism of the ERTBP. Although the potential is time dependent, formally the Hamiltonian coincides with the Hamiltonian of the CRTBP:

$$\tilde{H} = \frac{1}{2}\left(P_1{}^2 + P_2{}^2\right) + Q_2 P_1 - Q_1 P_2 - \tilde{\phi}(Q_1,\ Q_2,\ E). \tag{49}$$

The independent time variable has to be replaced by the eccentric anomaly and the canonical equations are:

$$\frac{dQ_1}{dE} = \frac{\partial\tilde{H}}{\partial P_1} = P_1 + Q_2,$$

$$\frac{dQ_2}{dE} = \frac{\partial\tilde{H}}{\partial P_2} = P_2 - Q_1,$$

and

$$\frac{dP_1}{dE} = -\frac{\partial\tilde{H}}{\partial Q_1} = P_2 + \frac{\partial\tilde{\phi}}{\partial Q_1} = P_2 - \left(\mu_1\frac{(Q_1 - \mu_2)}{\rho_1^3} + \mu_2\frac{(Q_1 + \mu_1)}{\rho_2^3}\right),$$

$$\frac{dP_2}{dE} = -\frac{\partial\tilde{H}}{\partial Q_2} = -P_1 + \frac{\partial\tilde{\phi}}{\partial Q_2} = -\left(P_1 + \frac{Q_2\mu_1}{\rho_1^3} + \frac{Q_2\mu_2}{\rho_2^3}\right). \tag{50}$$

3.3.2. Spatial

For the sake of completeness the equations of motion of the spatial ERTBP (e.g. subject in Érdi 1978, 1981) are given here: the derivation of the problem in the spatial case follows the methods already proposed in the planar case by introducing complex variables. After performing the calculations the equations of motion in the spatial problem read:

$$\xi'' - 2\eta' = \frac{\partial\omega}{\partial\xi},$$

$$\eta'' + 2\,\xi' = \frac{\partial \omega}{\partial \eta},$$

$$\zeta'' + \zeta = \frac{\partial \omega}{\partial \zeta}, \qquad (51)$$

where again

$$\omega = (1 + e \cos E)^{-1}\, \Omega \qquad (52)$$

and the potential Ω is given by

$$\Omega = \frac{1}{2}\left(\xi^2 + \eta^2 + \zeta^2\right) + \frac{\mu_1}{r_1} + \frac{\mu_2}{r_2} + \frac{1}{2}\,\mu_1\,\mu_2. \qquad (53)$$

The distances in the rotating coordinate frame of the spatial ERTBP are given by

$$r_1{}^2 = (\xi - \mu_2)^2 + \eta^2 + \zeta^2,$$

$$r_2{}^2 = (\xi + \mu_1)^2 + \eta^2 + \zeta^2, \qquad (54)$$

where the coordinate ζ is also given in time varying units according to the definition of the distance unit as in (35).

3.4 Useful canonical formulations

3.4.1. Polar coordinates

Polar coordinates are defined as follows: as new coordinates we introduce the radial distance $Q_1{}' = r$ of the asteroid from the barycentre of the system together with the angle $Q_2{}' = \theta$ between r and the connecting line of μ_1 and μ_2. The corresponding momenta are defined by the radial velocity $P_1{}' = \dot{r}$ and the angular momentum $P_2{}' = r^2\,\partial_t(\theta + t)$. The canonical transformation is accomplished using a generating function of the third kind

$$W_3 = Q_1{}'\,(P_1\,cos\,Q_2{}' + P_2\,sin\,Q_2{}') + f(Q_1{}',\,Q_2{}') \qquad (55)$$

in the planar and

$$W_3 = Q_1{}'\,(P_1\,cos\,Q_2{}' + P_2\,sin\,Q_2{}') + P_3\,Q_3{}' + f(Q_1{}',\,Q_2{}',\,Q_3{}') \qquad (56)$$

in the spatial case (extension to cylindrical coordinates). The transformation from old to new variables read:

$$Q_1 = Q_1{}'\,cos\,Q_2{}',$$

$$Q_2 = Q_1 \, ' \sin Q_2 \, ',$$

$$(Q_3 = Q_3 \, ') \tag{57}$$

and from old to new momenta:

$$P_1 \, ' = P_1 \cos Q_2 \, ' + P_2 \sin Q_2 \, ' + \partial f / \partial Q_1 \, ',$$

$$P_2 \, ' = Q_1 \, ' (P_2 \cos Q_2 \, ' - P_1 \sin Q_2 \, ') + \partial f / \partial Q_2 \, ',$$

$$(P_3 \, ' = P_3 + \partial f / \partial Q_3 \, '), \tag{58}$$

where we used again the definitions $Q_i = -\partial W_3 / \partial P_i$ and $P \, '_i = -\partial W_3 / \partial Q \, '_i$, with $i = 1, 2 \, (, 3)$ and f can be any arbitrary function in the new coordinates. The new Hamiltonian is given by $\tilde{H} \, ' = \tilde{H} + \partial W_3 / \partial t$, which yields

$$\tilde{H} \, ' = \frac{1}{2} \left(P_1 \, '^2 + P_2 \, '^2 / Q_1 \, '^2 \right) - P_2 \, ' - \tilde{F} \, ' (Q_1 \, ', Q_2 \, ' \, (, E)) \tag{59}$$

$$\tilde{H} \, ' = \frac{1}{2} \left(P_1 \, '^2 + P_2 \, '^2 / Q_1 \, '^2 \right) - P_2 \, ' - \tilde{F} \, ' (Q_1 \, ', Q_2 \, ', Q_3 \, ' \, (, E)) \tag{60}$$

in the planar and spatial case respectively and if we choose f in (55, 56) to be constant. Note that in Giorgilli & Skokos (1997) the authors expressed the planar problem in polar coordinates and transformed to local coordinates around the Lagrangian point (see Skokos & Dokoumetzidis 2001 for the spatial problem). The canonical equations in polar coordinates are given by:

$$\dot{Q}_1 \, ' = P_1 \, ',$$

$$\dot{Q}_2 \, ' = P_2 \, ' / Q_1 \, ' - 1,$$

$$\dot{P}_1 \, ' = P_2 \, '^2 / Q_1 \, '^3 + \frac{\partial \tilde{F} \, '}{\partial Q_1 \, '},$$

$$\dot{P}_2 \, ' = \frac{\partial \tilde{F} \, '}{\partial Q_2 \, '} \tag{61}$$

and similarly for the conjugated set $(Q_3 \, ', P_3 \, ')$. The potential is

$$\tilde{F} \, ' = \frac{\mu_1}{r_1} + \frac{\mu_2}{r_2} \tag{62}$$

where the distances are given by

$$r_1^2 = Q_1 \, '^2 + \mu_2^2 - 2 \, \mu_2 \, Q_1 \, ' \cos Q_2 \, ',$$

$$r_2^2 = Q_1 \, '^2 + \mu_1^2 + 2 \, \mu_1 \, Q_1 \, ' \cos Q_2 \, '. \tag{63}$$

While Giorgilli & Skokos (1997) introduced the polar coordinates locally (they changed the origin to one of the primaries) our notation allows us to state the problem in global polar coordinates. These are

nevertheless defined relative to the rotating coordinate system, uniformly rotating in the circular and non uniformly rotating and pulsating in the elliptic case.

3.4.2. Delaunay variables

In this section we are interested in the formulation of the problem in Delaunay variables, which are action-angle variables, the actions being constant in the case of the two body problem. Introduced by Delaunay in the 19th century, such variables simplify the notation of the perturbed two body problem as well. Using as the set of new variables the mean anomaly $q_1{}'$ and the longitude of the apsidal line $q_2{}'$, relative to the rotating system and $p_1{}'$, $p_2{}'$ as their conjugate momenta a suitable generating function of the second kind

$$W_2 = Q_2{}' p_2{}' + \int_{p_1{}'}^{Q_1{}'} \frac{1}{\left(p_1{}' - (p_1{}'^2 - p_2{}'^2)^{1/2}\right)} \left(-\frac{p_2{}'^2}{2} + \frac{2}{\xi} - \frac{1}{p_1{}'^2} \right) d\xi \tag{64}$$

connects the old polar with the new Delaunay variables via the relations $q_i{}' = \partial W_2 / \partial p_i{}'$ and $P_i{}' = \partial W_2 / \partial Q_i{}'$, $(i = 1, 2)$:

$$q_1{}' = cos^{-1}\left(\frac{1 - Q_1{}'/p_1{}'^2}{\left(1 - (p_2{}'/p_1{}')^2\right)^{1/2}} \right) - \frac{Q_1{}'}{p_1{}'}\left(-\frac{p_2{}'^2}{Q_1{}'^2} + \frac{2}{Q_1{}'} - \frac{1}{p_1{}'^2} \right),$$

$$q_2{}' = Q_2{}' - cos^{-1}\left(\frac{p_2{}'^2/Q_1{}' - 1}{\left(1 - (p_2{}'/p_1{}')^2\right)^{1/2}} \right),$$

$$P_1{}' = \left(-\frac{p_2{}'^2}{Q_1{}'^2} + \frac{2}{Q_1{}'} - \frac{1}{p_1{}'^2} \right)^{1/2},$$

$$P_2{}' = p_2{}'. \tag{65}$$

The connection between the Delaunay variables and the Keplerian elements is given by:

$$q_1{}' = M \equiv l,$$

$$q_2{}' = \phi - f \equiv g,$$

$$p_1{}' = a^{1/2} \equiv L,$$

$$p_2 = a^{1/2} \sqrt{(1 - e^2)} \equiv G, \tag{66}$$

where M stands for the mean and f for the true anomaly, a for the semi-major axis and e for the eccentricity of an asteroids orbit considered to lie on a temporary Keplerian ellipse. Here the argument of the perihelion $(\phi - f)$ in the rotating system is the angle between a radial vector r pointing to the temporary position of the perihelion of the asteroids orbit and the rotating axis (along the primaries).

For the sake of completeness in 3D an additional pair of Delaunay elements $(h, \text{Ⱶ})$ are defined by the longitude of the node Ω and the inclination i, namely:

$$h \equiv \Omega,$$

$$\text{Ⱶ} = G \cos i. \tag{67}$$

The general Hamiltonian in this setting reduces to the very simple form

$$F = -\frac{1}{2\,L^2} - G + R(L,\, G,\, \text{Ⱶ},\, l,\, g,\, h,\, E), \tag{68}$$

where R is called the ´disturbing function´ in terms of Delaunay variables. The expansion of the disturbing function at the 1:1 resonance will be examined in detail in Chapter 4. The equations of motion in terms of the Delaunay elements are in canonical form:

$$\dot{l} = \frac{\partial F}{\partial L}, \quad \dot{L} = -\frac{\partial F}{\partial l},$$

$$\dot{g} = \frac{\partial F}{\partial G}, \quad \dot{G} = -\frac{\partial F}{\partial g},$$

$$\dot{h} = \frac{\partial F}{\partial H}, \quad \dot{H} = -\frac{\partial F}{\partial h}. \tag{69}$$

For $\mu_1 = 0$ the disturbing function vanishes $(R = 0)$ and the equations of motion become $\dot{l} = 1\big/L^3$, $\dot{g} = -1$ and $\dot{L} = \dot{G} = \dot{H} = 0$, indicating that in the rotating system the apsidal line rotates counterclockwise with unit velocity and the orbital parameters a and e are constant (two body motion).

4. The 1:1 Resonance
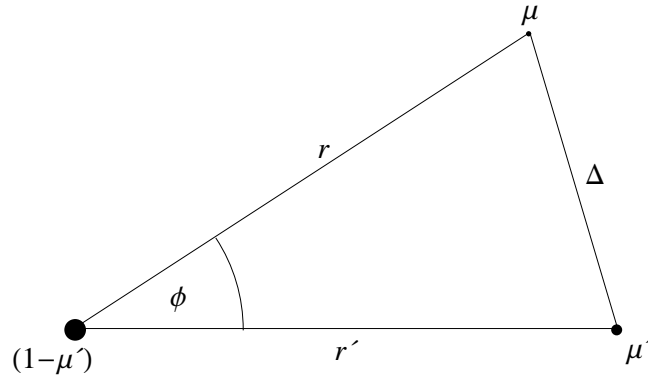
Figure 1: Geometry of the RTBP in heliocentric variables (centered at $\mu_2 = (1 - \mu)$).

4.1. Lagrangian configuration

Besides the case $\mu_1 = 0$ the perturbing function (68;3) creates another interesting equilibrium configuration, called the Lagrangian configuration of the system. To demonstrate it, let us first find the disturbing function in the heliocentric coordinate system. Moving the origin of the reference frame from the center of mass to the larger of the primaries ($\mu_2 = 1 - \mu'$) the force function for the action of the planet with mass $\mu_1 \equiv \mu'$ on the massless body $\mu_3 = m_3 = 0 \equiv \mu$ is written in the form (e.g. Brown & Shook 1964):

$$F = \frac{(1 - \mu')}{r} + \mu'\left(\frac{1}{\Delta} - \frac{r}{r'^2} cos(\phi)\right), \tag{1}$$

where Δ is the distance between the perturbing body and the asteroid, given by:

$$\Delta^2 = r^2 + r'^2 - 2\,r\,r'\,cos(\phi). \tag{2}$$

Here ϕ is the angle between the radius vector r and r' (see Figure 1). Eliminating the angle ϕ between (1) and (2) results, like in the preceding Chapter, to:

$$F = \frac{1}{r} + R, \tag{3}$$

where the disturbing function R in the heliocentric setting becomes:

$$R = \mu'\left(\frac{1}{\Delta} - \frac{1}{r} + \frac{1}{2}\frac{\Delta^2}{r'^3} - \frac{1}{2}\frac{r^2}{r'^3}\right). \tag{4}$$

Here the term $\mu'/2\,r'$ was neglected, since it does not contribute in the equations of motion for μ, which depend only on the derivatives of F with respect to μ'. If we assume that the geometry of the

system is such that the resultant forces are central forces, e.g. the center of force stays in the center of mass of the system, the system may be solved analytically in terms of uncoupled Kepler motions.
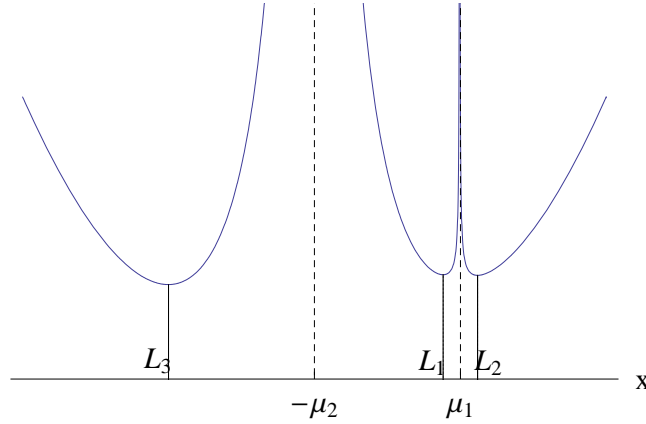
Figure 2: Minima of $\Omega(x,y\equiv0)$ denoting the collateral fixed points of the restricted problem.

This dynamical restriction of the problem was already known to Lagrange, who formulated the right geometrical condition to be fulfilled: the angles between the triangle formed by $(r, r´, \Delta)$ need to be invariants of the system; in other words, if they form an equilateral triangle, all bodies perform uncoupled Keplerian motion. This can be readily seen, if we set $r = r´ = \Delta$ in equation (3) and (4); the force function reduces to the force function of the two body problem. In the Newtonian formulation of the problem in the CRTBP (17;3) planar or (32;3) spatial case, we are looking for extrema of the potential $\Omega = \Omega(r_1, r_2)$ according to the equations:

$$\frac{\partial \Omega}{\partial x} = \frac{\partial \Omega}{\partial r_1} \frac{\partial r_1}{\partial x} + \frac{\partial \Omega}{\partial r_2} \frac{\partial r_2}{\partial x} = 0,$$

$$\frac{\partial \Omega}{\partial y} = \frac{\partial \Omega}{\partial r_1} \frac{\partial r_1}{\partial y} + \frac{\partial \Omega}{\partial r_2} \frac{\partial r_2}{\partial y} = 0, \tag{5}$$

and similarly for $\Omega = \Omega(x, y, z)$ in the spatial case. The derivatives are:

$$\frac{\partial \Omega}{\partial r_1} = \mu_1\left(r_1 - \frac{1}{r_1{}^2}\right), \quad \frac{\partial r_1}{\partial x} = \frac{\mu_1 + x}{r_1}, \quad \frac{\partial r_1}{\partial y} = \frac{y}{r_1},$$

$$\frac{\partial \Omega}{\partial r_2} = \mu_2\left(r_2 - \frac{1}{r_2{}^2}\right), \quad \frac{\partial r_2}{\partial x} = \frac{x - \mu_2}{r_2}, \quad \frac{\partial r_2}{\partial y} = \frac{y}{r_2}. \tag{6}$$

The set of equations (5) are clearly fulfilled if $r_1 = r_2 = 1$, which corresponds to values (x, y) at which the three bodies form a equilateral triangle, with μ_1 and μ_2, being equal to $(1 - \mu´)$ and $\mu´$ respectively.

These points are called equilateral equilibrium points of the restricted problem, namely L_4 and L_5. In addition another set of points could be derived from conditions (5), where r_1, r_2 are not equal to unity:

these solutions are determined by the restriction, that

$$\left\| \begin{pmatrix} \partial r_1 / \partial x & \partial r_2 / \partial y \\ \partial r_1 / \partial y & \partial r_2 / \partial y \end{pmatrix} \right\| = \frac{y(\mu_1 + \mu_2)}{r_1 \, r_2} = \frac{y}{r_1 \, r_2} \tag{7}$$

vanishes identically, which is true only if $y = 0$. Therefore the other extrema of the potential Ω in fact lie all on the x-axis. The corresponding equilibrium points are called colinear equilibrium points of the restricted problem denoted by L_1, L_2 and L_3. The potential along the x-axis (for $\mu = 0.1$) is plotted in Figure 2 and indicates, that there is only one point in between the two primaries (L_1), the other two lying outside μ_2 (L_3) and outside μ_2 (L_2) respectively.

The Lagrangian problem was analyzed in Celestial mechanics for decades. Good reference and literature can be found, e.g. in Érdi (1997) or in the book of Szebehely (1967). The proof, that no other extrema of the potential exist can be found, e.g. in the book of Stumpff (1965) or Marchal (1990). In the latter book it is also shown that the equilateral equilibria (L_4, L_5) are of elliptic type up to Routh´s mass $\left(\mu_R = 1/2 \left(1 - \sqrt{69} / 9 \right) \right)$ or in other words linearly stable motion around them is guaranteed if the mass ratio μ_1 / μ_2 does not exceed 1/27. The colinear fixed points are unstable for all mass rations but nevertheless have their use in space-mission technology (e.g. WMAP observatory, http://map.gsfc.nasa.gov/mission/). Note, that the equilibrium points are also found in the spatial CRTBP and can be generalized to the ERTBP, with the restriction that their position also becomes time dependent and they perform elliptic motion with the same eccentricity like the primaries, since the potential ω is time dependent too.

The geometry of the CRTBP in the Lagrangian configuration is given in Figure 3, indicating the Lagrangian configuration in the CRTBP together with the zero velocity curves already mentioned in Chapter 3, Section 3.1.3.. The Lagrangian configuration is also called 1:1 mean motion resonance (MMR) since one revolution period of the perturbing body is equal to the revolution period of the test body. Although the geometrical setting of the system introduces simple analysis of the motion it will also complicate the analytical treatment of the series expansions, as we will see in upcoming sections, compared to other more general resonance conditions ($p : q$).
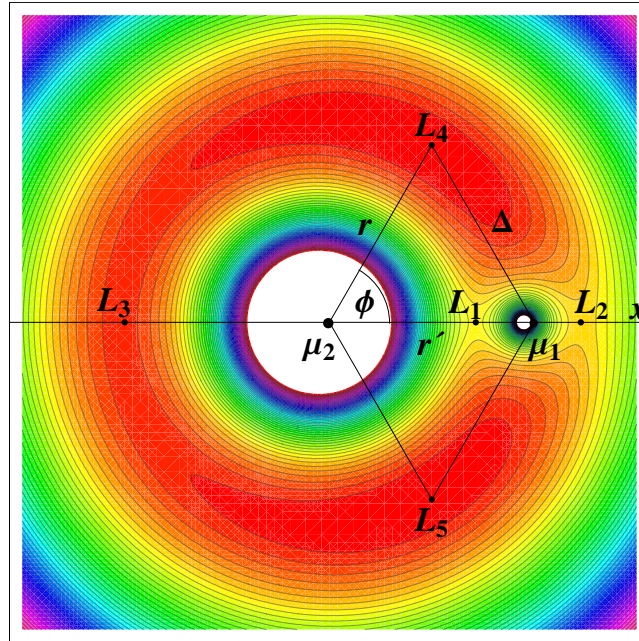
Figure 3: Lagrangian configuration (schematic) of the RTBP; zero velocity curves (left); geometry (right).

We are left in expressing the disturbing function (4) in the 1:1 resonance in terms of Delaunay variables as in Chapter 3, Section 3.4.2. Our aim is to express the problem in terms of (68;3). For this reason we will first express distances in (4) by means of Keplerian orbital elements (a, e, i, ω, Ω, M) and then transform to Delaunay variables similar to (l, g, h, L, G, H) using relations (66;3) and (67;3).

4.2. Disturbing function in terms of Bessel functions

The distance of Keplerian two body motion, in terms of the eccentric anomaly is given by the well known formula:

$$r = a(1 - e \cos E). \tag{8}$$

To express the eccentric anomalies E in terms of the mean anomalies M we make use of Kepler´s equation:

$$M = E - e \sin(E). \tag{9}$$

Since we are interested in powers of r to express the disturbing function (4) we specify trigonometric relations of the form:

$$\cos(n E) = a_0^{(n)} + a_1^{(n)} \cos(M) + a_2^{(n)} \cos(2 M) + \ldots + a_\nu^{(n)} \cos(\nu M) + \ldots,$$

$$\sin(n E) = b_1^{(n)} \sin(M) + b_2^{(n)} \sin(2 M) + \ldots + b_\nu^{(n)} \sin(\nu M) + \ldots, \tag{10}$$

Note that in (9) $E(-M) = -E(M)$, therefore the series representation of the cosine terms consist of

cosine terms, since it is an even function. Similarly, since the sine terms are odd in E and M they consist of sine terms. The Fourier coefficients in (10) are given by the formulae:

$$a_0^{(n)} = \frac{1}{2\pi} \int_0^{2\pi} cos(n E) \, dM,$$

$$a_\nu^{(n)} = \frac{1}{\pi} \int_0^{2\pi} cos(n E) \, cos(\nu M) \, dM,$$

$$b_\nu^{(n)} = \frac{1}{\pi} \int_0^{2\pi} sin(n E) \, sin(\nu M) \, dM. \tag{11}$$

Substituting dM in (11) by the differential of Kepler´s equation (9) $dE(1 - e\cos E)$ the zeroth order coefficient reduces to:

$$a_0^{(n)} = \frac{1}{2\pi} \int_0^{2\pi} cos(n E) \, (1 - e\,cos(E)) \, dE.$$

Since the integral over $(0, 2\pi)$ of the integrand $cos(n E)$ vanishes for all n and

$$\int_0^{2\pi} cos(n E) \, cos(E) \, dE = \begin{cases} 0 & \text{if } n > 1 \\ \pi & \text{if } n = 1 \end{cases},$$

we are left with

$$a_0^{(1)} = -\frac{e}{2}, \quad a_0^{(n>1)} = 0. \tag{12}$$

By partial integration of the remaining $a_\nu^{(n)}$, i.e.

$$a_\nu^{(n)} = \frac{1}{\nu\pi} \int_0^{2\pi} cos(n E) \, \frac{d\,sin(\nu M)}{dM} \, dM =$$

$$= \left(\frac{cos(n E) \, sin(\nu M)}{\nu\pi} \right)_{(0,2\pi)} - \frac{1}{\nu\pi} \int_0^{2\pi} \frac{d\,cos(n E)}{dM} \, sin(\nu M) \, dM,$$

the integral can be written in terms of:

$$a_\nu^{(n)} = \frac{n}{\nu\pi} \int_0^{2\pi} sin(n E) \, sin(\nu M) \, dE.$$

Substituting again M via Kepler´s equation, one is left with:

$$a_\nu^{(n)} = \frac{n}{\nu\pi} \int_0^{2\pi} sin(n E) \, sin(\nu E - \nu e\,sin(E)) \, dE$$

or after trigonometric reduction:

$$a_\nu^{(n)} = \frac{n}{2\nu\pi} \int_0^{2\pi} cos((\nu - n) E - \nu e\,sin(E)) - cos((\nu + n) E - \nu e\,sin(E)) \, dE. \tag{13}$$

Since the integral representation of the Bessel function is of the form:

$$J_n(x) = \frac{1}{2\pi} \int_0^{2\pi} \cos(n\,\varphi - x\sin\varphi)\,d\varphi,$$

the coefficients (13) may be expressed in terms of Bessel-functions of the first kind:

$$a_\nu{}^{(n)} = \frac{n}{\nu}\,(J_{\nu-n}(\nu\,e) - J_{\nu+n}(\nu\,e)). \tag{14}$$

In a similar way the Fourier-coefficients $b_\nu{}^{(n)}$ are expressed by:

$$b_\nu{}^{(n)} = -\frac{1}{\nu\pi} \int_0^{2\pi} \sin(n\,E)\,\frac{d\cos(\nu\,M)}{d\,M}\,d\,M$$

and after partial integration, reduce to :

$$b_\nu{}^{(n)} = \frac{n}{\nu\pi} \int_0^{2\pi} \cos(n\,E)\cos(\nu\,M)\,d\,E = \frac{n}{\nu\pi} \int_0^{2\pi} \cos(n\,E)\cos(\nu\,E - \nu\,e\sin(E))\,d\,E.$$

After reduction of the cosine product in the above equality, the coefficients $b_\nu{}^{(n)}$ are again given in terms of Bessel functions:

$$b_\nu{}^{(n)} = \frac{n}{\nu}\,(J_{\nu-n}(\nu\,e) + J_{\nu+n}(\nu\,e)). \tag{15}$$

For $n > 1$ we therefore get

$$\cos(n\,E) = n\sum_{\nu=1}^{\infty}(J_{\nu-n}(\nu\,e) - J_{\nu+n}(\nu\,e))\,\frac{\cos(\nu\,M)}{\nu},$$

$$\sin(n\,E) = n\sum_{\nu=1}^{\infty}(J_{\nu-n}(\nu\,e) + J_{\nu+n}(\nu\,e))\,\frac{\sin(\nu\,M)}{\nu}. \tag{16}$$

Since for $n = 1$ the constant terms according to (12) do not vanish we need to treat this case separately. Using the properties of Bessel-functions:

$$n\,J_n(x) = \frac{x}{2}\,(J_{n-1}(x) + J_{n+1}(x)),$$

$$\frac{d\,J_n(x)}{d\,x} = \frac{1}{2}\,(J_{n-1}(x) - J_{n+1\,(x)}),$$

we rearrange for $n = 1$ using (12)

$$a_\nu{}^{(1)} = \frac{1}{\nu}\,(J_{\nu-1}(\nu\,e) - J_{\nu+1}(\nu\,e)) = \frac{2}{\nu^2}\,\frac{d\,J_\nu(\nu\,e)}{d\,e},$$

$$b_\nu{}^{(1)} = \frac{1}{\nu}\,(J_{\nu-1}(\nu\,e) + J_{\nu+1}(\nu\,e)) = \frac{2}{\nu\,e}\,J_\nu(\nu\,e).$$

In addition to (16), for $n = 1$, we get:

$$cos(E) = 2 \sum_{\nu=1}^{\infty} \frac{d\,J_\nu(\nu\,e)}{d\,e} \; \frac{cos(\nu\,M)}{\nu^2} - \frac{e}{2},$$

$$sin(E) = \frac{2}{e} \sum_{\nu=1}^{\infty} J_\nu(\nu\,e) \; \frac{sin(\nu\,M)}{\nu}. \tag{17}$$

4.3. Application to the 1:1 resonance

4.3.1. Expansions in terms of mean anomalies

Different kinds of problems, where eccentric anomalies E need to be expressed in terms of mean anomalies, are solved using (16) and (17). In the case of the 1:1 resonance, substituting (16) into (8) we get:

$$\frac{r}{a} = 1 + \frac{1}{2}\,e^2 - 2\,e \sum_{\nu=1}^{\infty} \frac{d\,J_\nu(\nu\,e)}{d\,e} \; \frac{cos(\nu\,M)}{\nu^2}. \tag{18}$$

Since we also need the inverse radius vector r^{-1} in the disturbing function (4) we first write according to Kepler´s equation (9):

$$E - M = e\,sin(E) = 2 \sum_{\nu=1}^{\infty} J_\nu(\nu\,e) \; \frac{sin(\nu\,M)}{\nu}.$$

Differentiating with respect to the mean anomaly M we get:

$$\frac{d\,E}{d\,M} = \frac{1}{1 - e\,cos(E)} = \frac{a}{r}$$

with $a\,/\,r$ being given in terms of Bessel functions:

$$\frac{a}{r} = 1 + 2 \sum_{\nu=1}^{\infty} J_\nu(\nu\,e)\,cos(\nu\,M). \tag{19}$$

In addition powers of the form r^2, r'^{-3} and mixed products of the form $r\,r'$ are part of the disturbing function. Introducing primed variables ($a´$, $e´$, $E´$) to distinguish between quantities concerning μ and $\mu´$ we take care of their different origin, where necessary. The corresponding series expressions in terms of mean anomalies are derived in the following way. The square of the distance r^2 according to (8) is given by the equation:

$$\left(\frac{r}{a}\right)^2 = (1 - e\,cos(E))^2 = 1 - 2\,e\,cos(E) + \frac{e^2}{2}\,(1 + cos(2\,E)), \tag{20}$$

which can be expressed in terms of Bessel functions using (16) and (17). Special care must be taken to find the approximation of Δ. The squares (r^2, r'^2), we have in Δ^2 were already found above, the mixed

product can easily be derived using primed variables for $r´$ in (8) resulting in the identity:

$$\frac{r\,r´}{a\,a´} = 1 - e\cos(E) - e´\cos(E´) + e\,e´\cos(E)\cos(E´). \tag{21}$$

The angle ϕ between r and $r´$ can be easily expressed by true anomalies and the corresponding arguments of the perihelia. Since we are dealing with the planar case the angle is formed by the sum:

$$\phi = f + f´ + \omega + \omega´,$$

where f and $f´$ are the true anomalies of the asteroid and the perturbing planet respectively, ω and $\omega´$ indicate their arguments of the perihelia. The cosine of ϕ after separating the trigonometric terms involving true anomalies in products of their trigonometric arguments takes the form:

$$cos(\phi) = cos(\omega + \omega´)\,(cos(f)\,cos(f´) - sin(f)\,sin(f´)) -$$

$$- sin(\omega + \omega´)\,(cos(f)\,sin(f´) + cos(f´)\,sin(f)). \tag{22}$$

It is therefore enough to express the trigonometric terms of true anomalies $(cos(f),\ sin(f))$ in terms of mean anomalies again using Bessel functions of the first kind. The formula of the conic section gives:

$$cos(f) = \frac{1 - e^2}{e}\frac{a}{r} - \frac{1}{e} \tag{23}$$

and from

$$\frac{d}{dM}\left(\frac{r}{a}\right) = \frac{1}{a}\frac{e\,sin(f)}{\sqrt{a(1 - e^2)}}\sqrt{a^3}$$

we get

$$sin(f) = \frac{\sqrt{1 - e^2}}{e}\frac{d}{dM}\left(\frac{r}{a}\right), \tag{24}$$

since a is a positive quantity. Using the series (19) in (23) and the derivative of (18) with respect to M in (24) we are left with

$$cos(f) = 2\,\frac{1 - e^2}{e}\sum_{\nu=1}^{\infty} J_\nu(\nu\,e)\cos(\nu\,M) - e,$$

$$sin(f) = 2\sqrt{1 - e^2}\sum_{\nu=1}^{\infty}\frac{d\,J_\nu(\nu\,e)}{d\,e}\frac{sin(\nu\,M)}{\nu}. \tag{25}$$

Equations (25) can be readily used to express the cosine of ϕ in (22) in terms of products of simple trigonometric functions in terms of f and $f´$. Up to now all the formulae are exact, with respect to e as long we incorporate all terms of the infinite series. The identities (18) - (12) together with (16), (17) and (25) are convergent series expansions, provided that the eccentricities, occurring in the infinite series (17) and (25) are less than unity. Since all functions are periodic, differentiable and smooth in

their whole domain of definition, their Fourier series expansions are convergent too. Convergence problems begin, when $e \to 1$, although it should be stressed, that the accuracy of the expansions drastically decreases when the eccentricity approaches $e \simeq 0.67 \ldots$. The convergence may be optimized for larger e ($e\,'$), the generalization also to parabolic and hyperbolic motion is possible, we will not treat this case here. The interested reader is referred to the book of Stumpff (1959, p317+). Since in our calculations both, the primaries and the asteroid are assumed to stay in elliptic type motion, we can always assume the eccentricities to remain small. In addition we will use $e\,'$ as a parameter to the system. To get the disturbing function R we are therefore seeking for a multivariate Taylor series in terms of e and $e\,'$. The series expansion of $J_\nu(x)$ with respect to x is maximal of order ν. Therefore it is enough to incorporate all Fourier terms up to order ν in the infinite series (16), (17), (25) to find the correct coefficients of order ν. To keep track of the order in the multivariate expansions we introduce a book keeping variable $\beta \sim e, \ e\,'$, which is good as long as the eccentricities remain of the same order of magnitude.

We only give the Taylor series of the basic terms in R up to first order in the eccentricities here since it suffices to indicate subsequent investigations. The full expansion of the disturbing function up to 7th order is given in the Appendix II. From (18) - (22) we conclude:

$$\frac{r}{a} \simeq 1 - e \cos(M)\,\beta + \ldots, \tag{26}$$

$$\frac{a}{r} \simeq 1 + e\,\cos(M)\,\beta + \ldots, \tag{27}$$

$$\left(\frac{r}{a}\right)^2 \simeq 1 - 2\,e\,\cos(M)\,\beta + \ldots, \tag{28}$$

$$\frac{r\,r\,'}{a\,a\,'} \simeq 1 - (e\cos(M) - e\,'\cos(M\,')) \,\beta + \tag{29}$$

$$\cos(\phi) \simeq \cos(M - M\,' + \omega - \omega') + (-e\,'\cos(M + \omega - \omega) +$$

$$e\cos(2\,M - M\,' + \omega - \omega') - e\cos(M\,' - \omega + \omega'))\,\beta + \ldots \tag{30}$$

We are left to express $r\,'^{-3}$, Δ^2 and Δ^{-1} from R by our derived formulae. The series of $r\,'^{-3}$ with respect to $e\,'$ is given by:

$$\left(\frac{a\,'}{r\,'}\right)^3 = 1 + 3\,\cos(E\,')\,e\,' + \ldots,$$

which after the substitution of (16) and (17) for the eccentric anomalies up to first order yields:

$$\left(\frac{a\,'}{r\,'}\right)^3 \simeq 1 + 3\,e\,'\cos(M\,')\,\beta + \ldots. \tag{31}$$

The combination of (28) (primed and un-primed), (29) as well as (30) is used to get Δ^2:

$$\Delta^2 \simeq a^2 + a'^2 - 2\,a\,a'\cos(M - M' + \omega - \omega') - \left(+2\,a^2\,e\cos(M) + 2\,a'^2\,e'\cos(M') +\right.$$

$$a\,a'\,(3\,e'\cos(M + \omega - \omega') - e'\cos(M - 2\,M' + \omega - \omega') -$$

$$e\cos(2\,M - M' + \omega - \omega') + 3\,e\cos(M' - \omega + \omega')))\,\beta + \dots \tag{32}$$

Finally, the series form of the inverse distance between the asteroid and the perturbing planet Δ^{-1} in R is expressed up to order $O(\beta)$:

$$\Delta^{-1} \simeq \frac{1}{\sqrt{\Delta_0}} + \left(\frac{e\cos(M)\,a^2}{\Delta_0^{3/2}} - \frac{3\,a'\,e'\cos(M + \omega - \omega')\,a}{2\,\Delta_0^{3/2}} +\right.$$

$$+ \frac{a'\,e'\cos(M - 2\,M' + \omega - \omega')\,a}{2\,\Delta_0^{3/2}} + \frac{a'^2\,e'\cos(M')}{\Delta_0^{3/2}} +$$

$$+ \frac{a\,a'\,e\cos(2\,M - M' + \omega - \omega')}{2\,\Delta_0^{3/2}} - \frac{3\,a\,a'\,e\cos(M' - \omega + \omega')}{2\,\Delta_0^{3/2}}\right)\beta + \dots, \tag{33}$$

where we used Δ_0 as an abbreviation for the zeroth order approximation of Δ^2 given in (32). The number of terms clearly increases at higher orders. The disturbing function is given according to (33) - (27) + 1/2 (32)(31) - 1/2(28)(31), and we finally get the disturbing function in Keplerian elements in the form:

$$R = R(a, e, \omega, M, M'; a', e', \omega') = \sum_{\nu=1}^{\nu_{max}} A_\nu(a, e; a', e')\cos(\varphi_\nu(\omega, M, M'; \omega')), \tag{34}$$

where the amplitude terms are polynomial in the eccentricities e and e' and the angles φ_ν are linear combinations of their arguments. Here ν_{max} is equal to the number of all possible trigonometric combinations of the angles consistent with D´Alembert´s rule up to a given order of expansion in the eccentricities. The primed quantities a', e', ω' are parameters of the system. In consistency with our units (unit length between the perturbing body and the central mass) the semi-major axis itself is unity, meaning $a' = 1$. In addition, without loss of generality, we may set the perihelion of the perturbing planet aligned with the axis spanned by the central mass μ_2 and μ_1, resulting in $\omega' = 0$.

4.3.2. Modified Delaunay elements

Introducing mean longitudes via $M = \lambda - \omega$ and $M' = \lambda'$ we may define the critical argument τ of the 1:1 MMR according to $\lambda = \lambda' + \tau$. The series representation of (34) results in:

$$R(a, e, \omega, \tau, \lambda'; e') = \sum_{\nu=1}^{\nu_{max}} A_\nu(a, e; e')\cos(\varphi_\nu(\tau, \omega, \lambda'), \tag{35}$$

where the primed λ' increases linearly in time, defined by the mean motion of the disturbing planet.

The amplitude terms in (35) are either of the form

$$A_\nu = \frac{P_\nu(a, e; a\,', e\,')}{N_\nu \left(a^2 + a\,'^2 - 2\,a\,a\,'\cos(\tau)\right)^{p_\nu/2}} :$$ (36)

or

$$A_\nu = \frac{P_\nu(e, e\,')}{Q_\nu(a, a\,')},$$ (37)

where P_ν, Q_ν are again polynomials in their arguments and N_ν, p_ν are integer numbers. The form depends on the origin of the expansion, namely Δ in the case of (36) and r, $r\,'$ in the case of (37). We already indicated that the 1:1 MMR has to be treated differently than other resonances: while in general resonance conditions $(p:q)$ (not both being unity) of the massless and the perturbing body one may introduce the ratio $\alpha = a/a\,'$ in the case where $a < a\,'$ or $\alpha = a\,'/a$, where $a > a\,'$ as a small parameter, we need to modify the definition of the small parameter in the $1:1$ MMR, since all combinations $(\alpha < 1, \alpha > 1, \alpha = 1)$ may occur during the time evolution of the system. Following Brown and Shook (1964) we introduce the modified ("small") Delaunay element $x = \sqrt{a/a\,'} - 1$ (connected to $L \sim a^{1/2}$ in Chapter 3, Section 3.4.2). In addition we need to modify the Delaunay element $G \sim e$ and τ to form a canonical set of variables to the modified Delaunay elements (τ, ω, x, y) defined by:

$$\tau = \lambda - \lambda\,', \quad x = \sqrt{\frac{a}{a\,'}} - 1,$$

$$\omega, \quad y = \sqrt{\frac{a}{a\,'}} \left(\sqrt{1 - e^2}\right) - 1.$$ (38)

In addition we make use of the fact, that in the $1:1$ MMR the quantity $\cos(\tau)$ remains considerably smaller than unity as long as $|\tau|$ is not very close to zero, which means a close encounter of the massless body with the perturbing one. Since we need to exclude close encounters in our domain of definition (the denominators in (36) would become zero). we limit our study to the Trojan type motion. By expanding (35, i.e. 36) with respect to $\cos(\tau)$ and x we then get:

$$R = R(\tau, \omega, x, y; a\,', e\,') = \sum_{\nu=1}^{\nu_{max}} B_\nu(x, y; a\,', e\,') \cos(\theta_\nu(\tau, \omega, \lambda\,')).$$ (39)

The new coefficients B_ν stem from A_ν and the new angles θ_ν depend again linearly on their arguments. The Hamiltonian in this modified set of Delaunay variables (τ, ω, x, y) in the rotating coordinate system (compare with (68;3)) is of the form:

$$H = H(\tau, \omega, x, y) = -\frac{1}{2\,(1 + x)^2} - (1 + x) - \mu\,' R,$$ (40)

together with the disturbing function R in terms of (τ, ω, x, y) given by (39). The canonical equations of motion in this setting are given by:

$$\frac{d\tau}{dE} = \frac{\partial H}{\partial x} = \frac{1}{(1+x)^3} - 1 + \mu' \frac{\partial R}{\partial x},$$

$$\frac{d\omega}{dE} = \frac{\partial H}{\partial y} = \mu' \frac{\partial R}{\partial y},$$

$$\frac{dx}{dE} = -\frac{\partial H}{\partial \tau} = -\mu' \frac{\partial R}{\partial \tau},$$

$$\frac{dy}{dE} = -\frac{\partial H}{\partial \omega} = -\mu' \frac{\partial R}{\partial \omega}. \tag{41}$$

For $e' = 0$ the problem reduces to the CRTBP $(E = t)$, while for $e' \neq 0$ we are dealing with the ERTBP.

5. The Symplectic Mapping Model
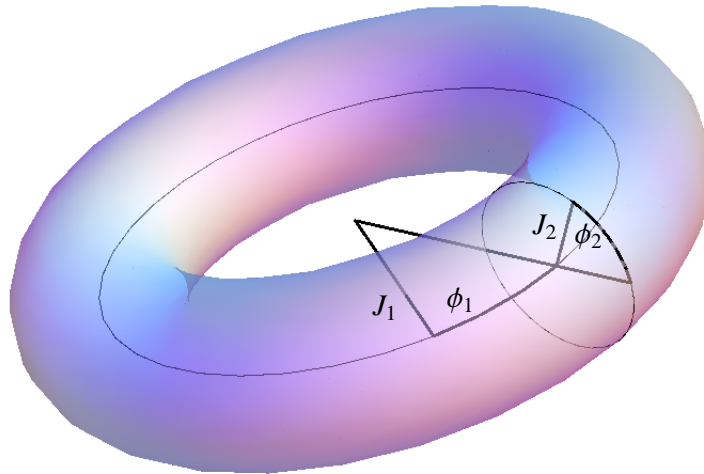
Figure 1.:Motion on the $\mathbb{T}^2$-torus, parametrized by ϕ_1, ϕ_2 with constant actions J_1, J_2.

5.1. Discrete mapping models from continuous flows

The idea of constructing symplectic mapping models for continuous flows is related to the concept of reduced phase space of Hamiltonian systems, leading directly to the concept of surface of sections in continuous flows. If we assume as a basic example a $d > 2$ degrees of freedom autonomous Hamiltonian, in coordinates $(p_1, \ldots, p_d, q_1, \ldots, q_d)$, the energy surface in the phase space has dimensionality $2d - 1$. By projecting out a single generalized coordinate p_d and considering consecutive intersections with the lower dimensional phase space defined by $q_d = const$ we are left with a symplectic mapping, with coordinates $p_1, \ldots, p_{d-1}, q_1, \ldots, q_{d-1}$, defining a surface of section in the reduced phase space with dimension $d_{\text{red}} = 2(d - 1)$, p_d being parameter to the system. Since the Liouville-Arnold theorem applies for conservative systems in general, the volume preserving property also holds for the lower dimensional phase space, therefore if one or more constants of motion in the dynamical system exist, then the intersections of the trajectory with the surface of section will all lie on a unique surface of dimension smaller, than the dimension of the reduced phase space Π_{red}, otherwise the intersections will fill a d_{red}-dimensional volume within this section. In particular, for an autonomous system with two degrees of freedom the phase space is four dimensional. By choosing a constant energy level of H the projection of the trajectory lies on a three dimensional subspace. One

momentum can be expressed by the three other canonical coordinates (*e.g.* $p_2 = p_2(p_1, q_1, q_2)$). By setting $q_2 = const$, any additional constant of motion $I(p_1, p_2, q_1, q_2)$, if it exists, will lie on a unique curve on the reduced phase space of the system, which is of dimensionality 2 (the so-called Poincaré surface of section, Poincaré 1892, 1893). By inspecting the symmetries in the reduced phase space we are able to deduce the existence of additional integrals of motion of the higher dimensional system. By construction the selected surface needs to be transverse to the flow, such that all trajectories starting in the reduced phase space intersect it an infinite number of times. The analysis of the motion on the $(d - 1)$-dimensional subspace helps to understand the geometry of the original phase space.

5.2. Hadjidemetriou´s method

Standard methods to construct mappings from flows and vice versa are based on δ-functions. The theory behind as well as some basic examples can be found, e.g. in Lichtenberg, Lieberman (*Chapter 3*). One of the first mapping models used in Celestial mechanics is due to Hénon-Heiles (1964). The basic idea behind the δ-function approach was due to Chirikov (1979) and introduced to applications of Celestial mechanics by Wisdom (1982). We will not follow this classical approach here but use instead a different one, proposed by Hadjidemetriou (1991), according to which the averaged Hamiltonian with respect to short periodic terms can be used to construct a mapping model to the continuous flow. While the classic approach, based on the use of δ-functions, may violate the Poisson structure of conservative systems (Hadjidemetriou 1996), Hadjidemetriou´s method by construction preserves the symplectic structure of phase space using the averaged Hamiltonian as a generating function for the mapping. Furthermore, one may show that the mapping model has the same fixed points as the original Hamiltonian model and also with the same stability.

Consider a d-degree of freedom nearly integrable Hamiltonian system of the form:

$$H(J, \theta) = H_0(J) + \epsilon H_1(J, \theta), \tag{1}$$

where H_0 denotes the integrable and H_1 the nonintegrable part and ϵ is a small parameter, indicating the strength of the perturbation. Further let H_1 be analytic in (J, θ). Let a pair (J_f, θ_f) be a canonical pair where the angle θ_f is a fast angle with period T significantly shorter than the periods associated with the remaining angles $(\theta_1, \dots \theta_{d-1})$. The motion of the unperturbed system H_0 takes place on an d-dimensional torus $\mathbb{T}^d$ with constant frequencies

$$\omega_j = \omega_j(J) = \frac{\partial H_0}{\partial J_j}, \ \ j = 1, \dots, d. \tag{2}$$

In the integrable approximation of the system the projections onto (J_i, θ_i) of the d-dimensional surface of section defined by $H_0 = h$, $\theta_j = const$ $(\Leftrightarrow J_j = J_{j0}, \theta_j = const)$ defines the twist mapping in the (J_j, θ_j)-plane of the form:

$$J_j{}' \to J_j,$$

$$\theta_j{}' \to \theta_j + \omega_j(J). \tag{3}$$

The connection between the integrable part of the flow H_0 and the twist mapping comes from the fact, that the transformation in phase space $(J, \theta) \to (J', \theta')$ itself is given by:

$$J' = \frac{\partial W}{\partial \theta},$$

$$\theta' = \frac{\partial W}{\partial J'}, \tag{4}$$

where W is the generating function of old and new variables $W(J', \theta)$. Since the generating function of the twist map on the plane (J_j, θ_j) is given by

$$W(J_{j,n+1}, \theta_{j,n}) = J_{j,n+1}\,\theta_{j,n} + \int_0^T \omega_j(J_{n+1})\,dJ_{n+1} \tag{5}$$

the difference equations of the twist mapping projected to (J_j, θ_j) turn out to be:

$$J_{j,n+1} = J_{j,n},$$

$$\theta_{j,n+1} = \theta_{j,n} + 2\pi\,\alpha(J_{n+1}). \tag{6}$$

The mapping in this form is implicit, since the new momentum J_{n+1} appears on the right hand side of the equations.

In the next step we are interested in the effect of the perturbation ϵH_1 on the twist mapping according to the disturbing function of the Hamiltonian when $\epsilon \neq 0$. The main result due to Hadjidemetriou is that the correct phase space topology is approximated by using the averaged Hamiltonian $\tilde{H}$ as a generating function to the system, i.e.:

$$W = J_{n+1}\,\theta_n + T\,\tilde{H}(J_{n+1}, \theta_n), \tag{7}$$

giving the perturbed twist mapping

$$J_n = \frac{\partial W}{\partial \theta_n} \Rightarrow J_n = J_{n+1} + \frac{\partial \tilde{H}}{\partial \theta_n}\,(J_{n+1}, \theta_n),$$

$$\theta_{n+1} = \frac{\partial W}{\partial J_{n+1}} \Rightarrow \theta_{n+1} = \theta_n + \frac{\partial \tilde{H}}{\partial J_{n+1}}\,(J_{n+1}, \theta_n). \tag{8}$$

By averaging over θ_f, we are left with a Hamiltonian $\tilde{H}$ of the same number of degree of freedom but one ignorable coordinate q_f (or from another point of view with a Hamiltonian on the reduced phase

space with an additional parameter J_f). If we now introduce the averaged variable again as the new time variable into the system we obtain a discrete mapping of the dynamical system based on the averaged Hamiltonian of the problem. The discrete time n plays the role of the revolution period of the fast angle q_f at the n-th revolution period. The state of the mapping at the nth step of iteration approximates well the state of the continuous flow at the continuous time $t = n\,T$. In particular, it was shown (Hadjidemetriou 1991) that using (7) as the generating function of the mapping the fixed points and their stability are conserved.

5.3. Application to the Lagrangian configuration

5.3.1. Implicit mapping

Comparing the periods of Trojan-type motion in the case of Sun-Jupiter (Érdi 1997), one finds well separated basic periods. The period of revolution around the Sun is the same like Jupiter (~ 12 yr) due to the 1:1 MMR. The period of libration around the equilateral fixed points is ten time larger ($\sim 145 - 240$ yrs). The period of the free motion of the argument of the perihelion is between 3000 yr and 5600 yr and the proper period of the ascending node is beyond $38\,000$ yr. Since we are interested in the planar approximation of the system we neglect the ascending node and are left with three main periods (~ 12 yr, ~ 150 yr, ~ 3000 yr) governing the system. The fast angle is therefore identified to be the revolution period of Jupiter itself, connected to the orbital longitude λ'. Looking at our Hamiltonian model (40;4) the averaged Hamiltonian therefore becomes:

$$\tilde{H} = -\frac{1}{2\,(1 + x)^2} - (1 + x) - \mu'\,\frac{1}{2\,\pi}\int_0^{2\pi} R(\tau,\,\omega,\,x,\,y,\,\lambda';\,a',\,e')\,\mathrm{d}\lambda', \qquad (9)$$

where the integral of the disturbing function over λ' gives the same terms as the canonical transformation implemented in the original paper of to Hadjidemetriou (1991). In the circular problem ($e' = 0$), it can be readily shown that in all trigonometric arguments of (39;4), the angle λ' can only appear via the combination $\lambda' - \omega$. Thus by averaging the circular problem the argument of the perihelion ω of the asteroid disappears together with the orbital longitude of Jupiter λ' from the averaged Hamiltonian $\tilde{H}$. This implies, that the conjugated variable y becomes an integral of the mapping corresponding to the proper eccentricity, which simply becomes a parameter labelling the 2-dimensional symplectic mapping in the remaining variables (τ, x). On the other hand, in the elliptic case ($e' \neq 0$) there are terms depending on ω in other combinations surviving the averaging process (9). Thus the new mapping is 4-dimensional and the dynamics of the action y (as well as ω) is coupled to the dynamics of the pair (τ, x). This is in fact a consequence of the absence of the Jacobi integral in the elliptic problem. As already mentioned in Chapter 3 it is possible to find an additional integral of

motion in the CRTBP, which is not possible to do in the ERTBP, since the integrand in (48;3) does not vanish. While in the former problem, the additional integral of motion shows up in the time-invariance of y in the mapping approach, in the latter one it does not.

The generating function in the planar elliptic problem turns out to be:

$$W = \tau_n x_{n+1} + \omega_n y_{n+1} - T\left(\frac{1}{2(1+x)^2} + (1+x) + \mu' \tilde{R}(\tau_n, \omega_n, x_{n+1}, y_{n+1}; a', e') \right), \qquad (10)$$

where $\tilde{R}$ is the averaged disturbing function stemming from (9). In units in which the revolution period of Jupiter is $T = 2\pi$, the mapping equations for the massless body are found by applying (8) via

$$\tau_{n+1} = \frac{\partial W}{\partial x_{n+1}} = \tau_n - 2\pi\left(1 - \frac{1}{(1+x_{n+1})^3} + \mu' \frac{\partial \tilde{R}}{\partial x_{n+1}} (\tau_n, \omega_n, x_{n+1}, y_{n+1}; a', e') \right),$$

$$\omega_{n+1} = \frac{\partial W}{\partial y_{n+1}} = \omega_n + \mu' \frac{\partial \tilde{R}}{\partial y_{n+1}} (\tau_n, \omega_n, x_{n+1}, y_{n+1}; a', e'),$$

$$x_n = \frac{\partial W}{\partial \tau_n} = x_{n+1} + \mu' \frac{\partial \tilde{R}}{\partial \tau_n} (\tau_n, \omega_n, x_{n+1}, y_{n+1}; a', e'),$$

$$y_n = \frac{\partial W}{\partial \omega_n} = y_{n+1} + \mu' \frac{\partial \tilde{R}}{\partial \omega_n} (\tau_n, \omega_n, x_{n+1}, y_{n+1}; a', e'). \qquad (11)$$

The mapping is implicit but symplectic by construction. Like in the continuous formulation, the problem reduces to the unperturbed two body Keplerian motion, if $\tilde{R} = 0$ or $\mu' = 0$, which is in agreement with the result already obtained in Chapter 4, Section 4.1 or at the end of Chapter 3, Section 3.4.2.

5.3.2. Fixed points of the mapping

The set of difference equations given by (11) form a set of coupled twist maps of the form (6) in the (τ, x) and (ω, y) planes, where the coupling terms are due to the presence of $\tilde{R}$. The stationary points of the system (corresponding to periodic solutions of the un-averaged system) should satisfy the conditions $\dot{\tau} = \dot{\omega} = \dot{x} = \dot{y} = 0$, i.e.

$$\frac{\partial \tilde{H}}{\partial x} = \frac{\partial \tilde{H}}{\partial y} = \frac{\partial \tilde{H}}{\partial \tau} = \frac{\partial \tilde{H}}{\partial \omega} = 0,$$

the corresponding condition for the period-1 fixed points of the symplectic mapping is given by:

$$(\tau_{n+1}, \omega_{n+1}, x_{n+1}, y_{n+1}) = (\tau_n, \omega_n, x_n \, y_n) = (\tau^*, \omega^*, x^*, y^*),$$

for arbitrary n. The condition for stationary points is:

$$\frac{\partial \tilde{H}}{\partial \tau^*} = \frac{\partial \tilde{H}}{\partial \omega^*} = \frac{\partial \tilde{H}}{\partial x^*} = \frac{\partial \tilde{H}}{\partial y^*} = 0.$$

Therefore the period-1 fixed points of the mapping correspond to the stationary points of the averaged system and thus to periodic solutions of the original system. The theoretical values of the fixed points are given by (Sándor & Érdi 2003):

$$(\tau^*, \omega^*, x^*, y^*) = \left(0, \pm\frac{\pi}{3}, \pm\frac{\pi}{3}, \sqrt{1 - e'^2} - 1\right), \tag{12}$$

corresponding to the equilateral fixed points L_4 and L_5. The colinear fixed point L_3 on the other hand is given by

$$(\tau^*, \omega^*, x^*, y^*) = \left(0, \pi, \pi, \sqrt{1 - e'^2} - 1\right). \tag{13}$$

Note that in our mapping approach we are not able to look for the missing collateral fixed points L_1, L_2 located at $x^* = \tau^* = 0$, since the disturbing function becomes singular at $a/a' = 1$ (see Section 4.3.2). However, this is not a problem as long we limit our analysis to the triangular fixed points L_4 and L_5.

The stability properties of the fixed points of the mapping are found by the eigenvalues of the Jacobian matrix. We denote the variations $\delta\tau_{0|1}$, $\delta\omega_{0|1}$, $\delta x_{0|1}$, $\delta y_{0|1}$ around the fixed point:

$$\tau_{n+j} = \tau^* + \delta\tau_j, \ \omega_{n+j} = \omega^* + \delta\omega_j,$$

$$x_{n+j} = x^* + \delta x_j, \ y_{n+j} = y^* + \delta y_j, \tag{14}$$

where j is meant to be 0 for the old variables $(\tau_n, \omega_n, x_n, y_n)$ and 1 for the new set of variables $(\tau_{n+1}, \omega_{n+1}, x_{n+1}, y_{n+1})$. Plugging (14) in (11) and Taylor expanding around the fixed point $(\tau^*, \omega^*, x^*, y^*)$ up to first order with respect to $(\tau_n, \omega_n, x_{n+1}, y_{n+1})$ gives:

$$\bigcirc_{n+1} - \bigcirc^* = \bigcirc_n - \bigcirc^* + 2\pi\left(\frac{\partial}{\partial\tau_n}\frac{\partial\tilde{H}}{\partial\square_{n+1}}(\tau_n - \tau^*) + \frac{\partial}{\partial\omega_n}\frac{\partial\tilde{H}}{\partial\square_{n+1}}(\omega_n - \omega^*) + \right.$$

$$\left.\frac{\partial}{\partial x_{n+1}}\frac{\partial\tilde{H}}{\partial\square_{n+1}}(x_{n+1} - x^*) + \frac{\partial}{\partial y_{n+1}}\frac{\partial\tilde{H}}{\partial\square_{n+1}}(y_{n+1} - y^*)\right), \tag{15}$$

for $\bigcirc = \tau$, ω and $\square = x$, y or

$$\bigcirc_n - \bigcirc^* = \bigcirc_{n+1} - \bigcirc^* + 2\pi\left(\frac{\partial}{\partial\tau_n}\frac{\partial\tilde{H}}{\partial\square_n}(\tau_n - \tau^*) + \frac{\partial}{\partial\omega_n}\frac{\partial\tilde{H}}{\partial\square_n}(\omega_n - \omega^*) + \right.$$

$$\left.\frac{\partial}{\partial x_{n+1}}\frac{\partial\tilde{H}}{\partial\square_n}(x_{n+1} - x^*) + \frac{\partial}{\partial y_{n+1}}\frac{\partial\tilde{H}}{\partial\square_n}(y_{n+1} - y^*)\right), \tag{16}$$

for $\bigcirc = x$, y and $\square = \tau$, ω. Using (14) together with (15, 16) and collecting terms of same index on the same hand side of the equations results in matrix form:

$$\boldsymbol{B} \cdot (\delta\tau_1, \delta\omega_1, \delta x_1, \delta y_1)^T = \boldsymbol{C} \cdot (\delta\tau_0, \delta\omega_0, \delta x_0, \delta y_0)^T, \tag{17}$$

where $\boldsymbol{B}$, $\boldsymbol{C}$ are 4×4 matrices. Therefore the linearized mapping, centered around the fixed point, reads:

$$(\delta\tau_1,\, \delta\omega_1,\, \delta x_1,\, \delta y_1)^T = \boldsymbol{B}^{-1}\,\boldsymbol{C}\cdot(\delta\tau_0,\, \delta\omega_0,\, \delta x_0,\, \delta y_0)^T. \tag{18}$$

The stability of the fixed point depends on the eigenvalues of $\boldsymbol{B}^{-1}\,\boldsymbol{C} \equiv \boldsymbol{M}$ and since $\boldsymbol{M}$ is symplectic all eigenvalues are either complex conjugate or reciprocal pairs. The eigenvalues of $\boldsymbol{B}^{-1}\,\boldsymbol{C}$ lie on the unit circle if the discriminant $\Delta > 0$ and the modul of $|b_1|$, $|b_2| < 2$. The quantities Δ, b_1, b_2 are defined according to:

$$\Delta = c_3{}^2 - 4\,(c_2 - 2),$$

$$b_{1,2} = \frac{1}{2}\left(\alpha \pm \sqrt{\Delta}\,\right)$$

where c_i, $i = 1, \ldots, 3$ are the coefficients of the characteristic polynomial of $\boldsymbol{B}^{-1}\,\boldsymbol{C}$:

$$\lambda^4 + c_3\,\lambda^3 + c_2\,\lambda^2 + c_3\,\lambda + 1 = 0.$$

The coefficients c_2, c_3 in the Sun-Jupiter case indicate the fixed points to be of elliptic type.

5.4. Mapping model in the Sun - Jupiter - Trojan case

5.4.1. Implicit mapping

In the case of Sun-Jupiter we set in (11) $\mu' = 0.000954\ldots$ and $e' = 0.0487\ldots$ and iterate the mapping in its implicit form. The old variables $(\tau_n, \omega_n, x_n, y_n)$ are used as initial points $(\tau_0, \omega_0, x_0, y_0)$ for the root finding algorithm to solve the mapping (11) with respect to $(\tau_{n+1}, \omega_{n+1}, x_{n+1}, y_{n+1})$. This is done at each step up to given accuracy. Note that in the actual implementation, since the difference system, defined by the mapping is uncoupled with respect to the angles $(\tau_{n+1}, \omega_{n+1})$, it is enough to solve the 2-dimensional system with respect to (x_{n+1}, y_{n+1}) and plug in the solution in the other two equations to get $(\tau_{n+1}, \omega_{n+1})$. The resulting surface of section is a 4-dimensional manifold and cannot be visualized directly. Although we could expect two kinds of twist mapping behavior, the interactions due to the perturbations may introduce complex structure into the system. To get a first visual impression we therefore need to define a suitable section of the Poincaré surface of section, like in Sándor & Érdi (2003). The section condition to find a projection to the (τ, x)-plane is defined according to $\omega_n = \omega_0$, $\omega_{n+1} - \omega_n > 0$. The other projection to the (ω, y)-plane is defined via the section condition $\tau_n = \tau_0$, $\tau_{n+1} - \tau_n > 0 \bigwedge x_n = 0$. The former condition reduces the phase portrait to a 2-dimensional manifold which could be compared to the mapping obtained for the CRTBP. Note, that since we are indeed in the ERTBP and not in the CRTBP, without this section condition the pulsating and nonuniform rotating coordinate system would show up in a pulsating behavior of the phase portrait plots at different `times` n.
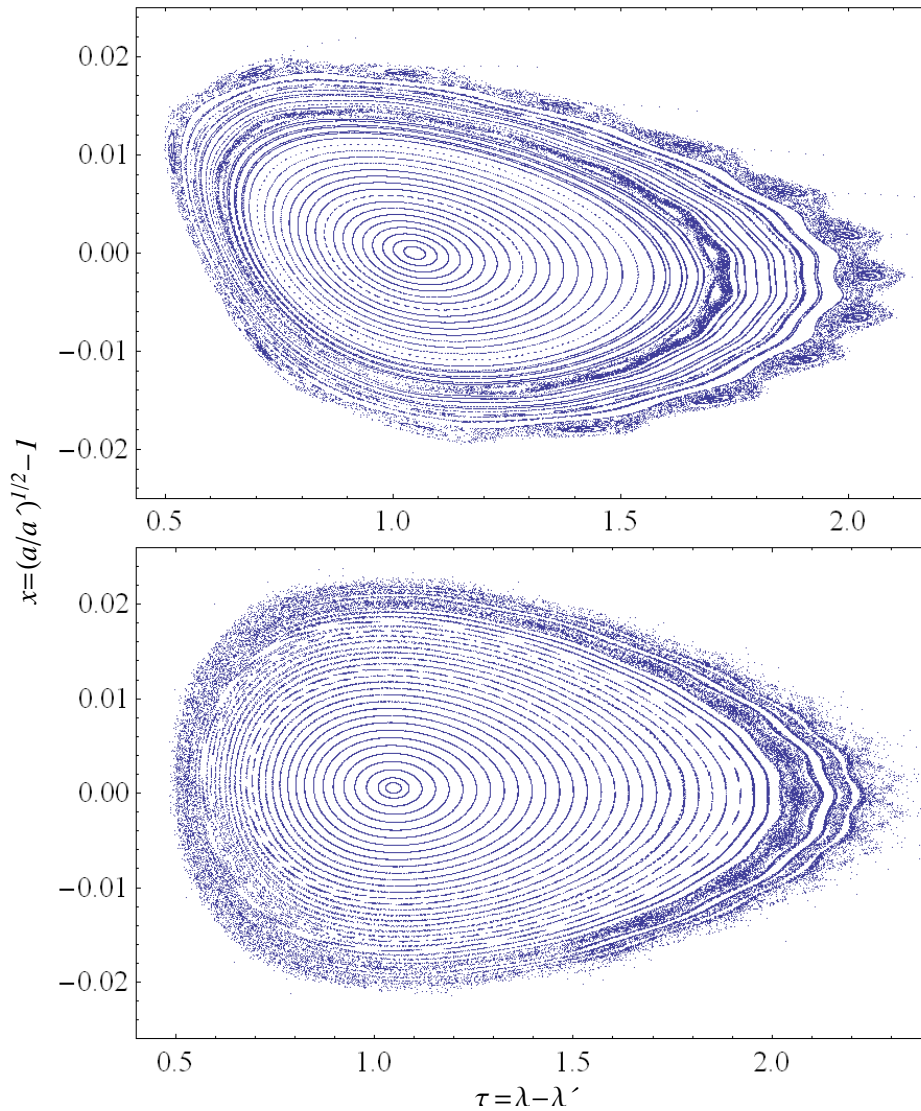
Figure 2a.: Phase portraits for the Trojan case of Jupiter; Hadjidemetriou mapping (upper), continuous flow (lower). Relative orbital longitude τ vs. variation in the semi-major axis x.

The projections on the (τ, x) and (ω, y) plane of the implicit mapping iterations are given in Figure 2a and Figure 2b respectively. While the upper frames in Figure 2a,b show the phase portrait of the implicit mapping model, the lower frames give the mapping obtained by direct numerical integration of the restricted problem. In the continuous formulation the surface of section was again defined by $\lambda' = 0$ and the same initial conditions as in the corresponding mapping figures where used. These compare well from a topological point of view: the angular tilt of the invariant curves in Figure 2a (upper compared to lower frame) corresponds in reality only to a small phase difference in the oscillations $\Delta\theta$ of τ and x and can be explained by the construction due to Hadjidemetriou´s method (Efthymiopoulos & Sándor 2005). Note that the visual impression of the tilt is only due to the very different scale of the axis, the order of $\Delta\theta$ in fact is given by 10^{-2} rad. Figure 2a shows the familiar picture of the dynamics

of the co-orbital motion in the ERTBP, which should be compared to Sándor & Érdi (2003). The regular motion in the (τ, x) planes are rotational and the border of the stability region is marked by high-order resonances creating chains of islands embedded in the chaotic stickiness zone.
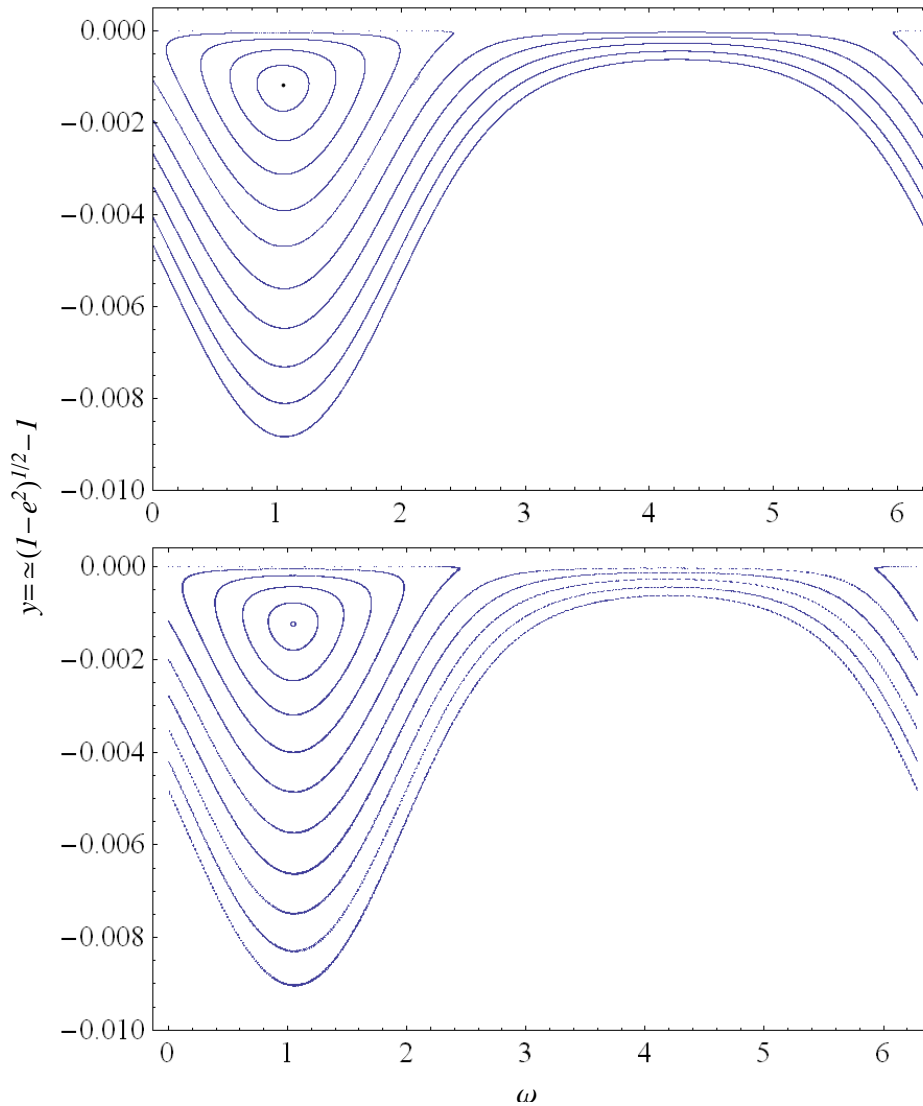
Figure 2b.: Phase portraits for the Trojan case of Jupiter; Hadjidemetriou mapping (upper), continuous flow (lower). Argument of the perihelion ω vs. eccentricities. Librational and rotational regime.

Figure 2b shows the librational and rotational behavior of the system. While in the inner part of the phase space (centered around the fixed point) the asteroid´s perihelion is librating around the fixed point (between two values $0 < \omega_{min} \le \omega \le \omega_{max}$), the perihelion starts rotating in the outer regions ($0 \le \omega \le 2\pi$). In fact the former motions correspond to the ERTBP limit of the motions called "non-paradoxal" by Beaugé & Roig (2001), while the latter motions correspond to the "paradoxal" motions. The reason for this terminology is due to the fact that the difference of the two types of motion on the (ω, y)-plane does not correspond to a separatrix resonant dynamics. In fact, a plot in the Laplace-

Lagrange (h, k)-plane in Figure 3, defined by $h = e\,cos(\omega)$ and $k = e\,cos(\omega)$, shows that all invariant curves are in fact librational around a fixed center. The center is given by the eccentricity of Jupiter and lies $60°$ before and after Jupiter, namely at $(e´\,cos(60°),\ e´sin(60°))$. Note that the radius in the (h, k)-plane e_{free} coincides with the proper eccentricity e_p, i.e. it is an approximate integral of motion, that characterizes together with the other proper elements $D_p = \tau_{\max} - \tau_{\min}$ and $d_p = a_{\max} - a_{\min}$ the motion on a particular invariant torus of the 4-dimensional mapping given by (11).
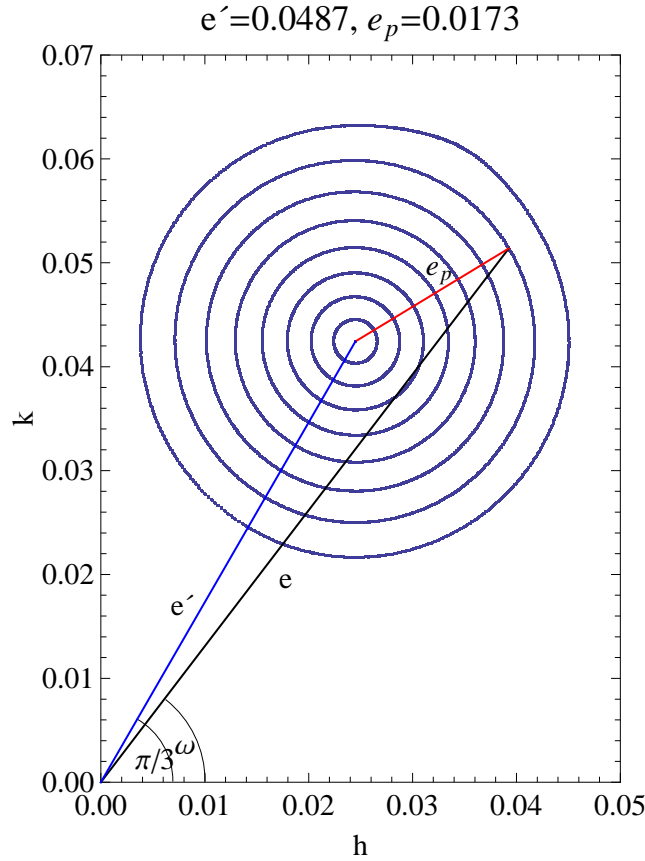
Figure 3.:Laplace-Lagrange plane calculated from the mapping data. The fixed point lies at $(e´\cos(60°),\ e´\sin(60°))$. The forced eccentricity e_p corresponds to an approximate integral of motion.

To validate the use of the mapping model, the relation between the libration amplitudes D_p and d_p was calculated for different invariant curves of Figure 2a and is shown in Figure 4. The relation is almost perfectly linear, and the slope found in the mapping model coincides with the slope given by the theoretical value given by Érdi (1988) based on the continuous formulation of the problem $(1/0.275[rad/AU])$.
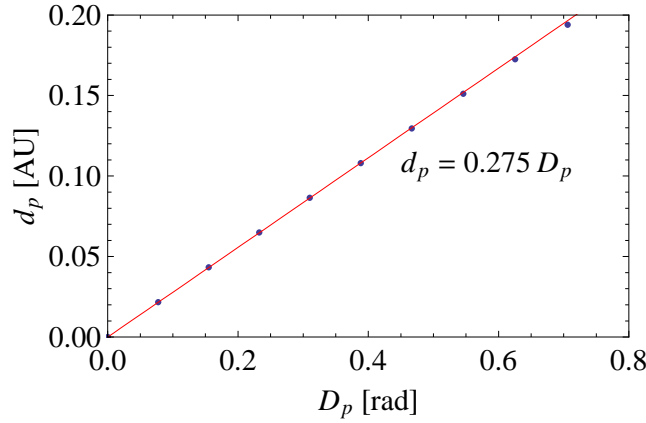
Figure 4.:Relationship between proper elements d_p and D_p calculated from the mapping model in Figure 3 for different invariant curves.

In summary, the mapping model is i) symplectic, ii) reproduces the fixed point and stability of the original flow together with iii) the correct relation-ship of the proper elements of the Hamiltonian model. We therefore conclude, that this mapping yields the precise dynamics of the system and can be used for the construction of Nekhoroshev estimates.

5.4.2. Explicit mapping

To render the implicit mapping (11) explicit we need to expand it with respect to the mapping variables (τ, ω, x, y). Although we may lose the accuracy of the mapping far away from the expansion point, we need to do so, since for the normal form construction in the next chapter we will also need to diagonalize and complexify the mapping in its explicit form. For this reason we expand the generating function of the mapping (10) together with the averaged disturbing function (9) up to sufficiently high order, such that the error in the approximation is bound below machine precision. Since the mapping variables are of order unity or smaller ($0 \leq \tau$, $\omega \leq 2\pi$ and $|x| < 10^{-1}$, $|y| < 10^{-2}$, see Figure 2a,b) the expansion around the fixed point in the case of Jupiter (from 19, with $e\acute{} = .048$):

$$(\tau^*, \omega^*, x^*, y^*)_{\text{Jup}} = (0., 1.0472, 0., -0.001250782228091052) \qquad (19)$$

was truncated at the 16th order. It has to be stressed, that it is preferable to develop the generating function W instead of the mapping equations for two reasons: i) we just need to expand one function W instead of 4 difference equations and ii) the symplectic structure is not violated by the series expansion of the generating function. The approximated generating function W_* is of the multivariate Taylor series form:

$$W_* = \sum_{\{i_j\} \in \mathbb{J}} w_{i_1, i_2, i_3, i_4} \, u_{1n}^{i_1} \, u_{2n}^{i_2} \, v_{1n+1}^{i_3} \, v_{2n+1}^{i_4}, \qquad (20)$$

where the index set $\mathbb{J}$ is defined as the set of all integers (i_1, i_2, i_3, i_4), where $\sum_j i_j \leq 16$. A monomial of

the form:

$$w_{v_1, v_2, v_3, v_4} \, u_{1n}^{i_1} \, u_{2n}^{i_2} \, v_{1n+1}^{i_3} \, v_{2n+1}^{i_4} \tag{21}$$

is said of order r, if $i_1 + i_2 + i_3 + i_4 = r$. From pure number theoretical properties it follows, that the number of monomials of a polynomial of degree r in n variables is given by the binomial:

$$\binom{n+r}{r},$$

which is 4845 in the case of $n = 4$, $r = 16$ and 74 613 in the case $n = 6$, $r = 16$ (needed for the series reversion process of the implicit mapping u_{1n}, u_{2n}, v_{1n}, v_{2n}, v_{1n+1}, v_{2n+1}). Nevertheless the coefficient-arrays of our polynomials will turn out to be relatively sparse as we will see in the proceeding sections. The new variables (u_1, u_2, v_1, v_2) introduced in (21) are the variations of (τ, ω, x, y) with respect to the fixed point $(\tau^*, \omega^*, x^*, y^*)$, namely (similar by 14) they are defined by:

$$u_1 \equiv \tau - \tau^*, \; u_2 = \omega - \omega^*,$$

$$v_1 \equiv x - x^*, \; v_2 = y - y^*. \tag{22}$$

Although the generating function (20) is approximate, the corresponding mapping will be symplectic up to machine precision by construction. Furthermore it can be shown, that after the expansion of W around the fixed points the resulting mapping has the same fixed point at the origin with the same stability as the original fixed point. The resulting mapping from W_* reads:

$$\begin{pmatrix} u_{1n+1} \\ u_{2n+1} \\ v_{1n+1} \\ v_{2n+1} \end{pmatrix} = \boldsymbol{M} \cdot \begin{pmatrix} u_{1n} \\ u_{2n} \\ v_{1n} \\ v_{2n} \end{pmatrix} + \begin{pmatrix} U_1(u_{1n}, u_{2n}, v_{1n+1}, v_{2n+1}) \\ U_2(u_{1n}, u_{2n}, v_{1n+1}, v_{2n+1}) \\ V_1(u_{1n}, u_{2n}, v_{1n+1}, v_{2n+1}) \\ V_2(u_{1n}, u_{2n}, v_{1n+1}, v_{2n+1}) \end{pmatrix}, \tag{23}$$

where $\boldsymbol{M}$ is the linearized part of the mapping (11), solved with respect to the linear part of the new mapping variables $(n + 1)$. It is given by:

$$\boldsymbol{M} = \begin{pmatrix} 724.471 \times 10^{-3} & 1.59277 \times 10^{-3} & -19.0939 & -10.1437 \times 10^{-3} \\ 552.164 \times 10^{-6} & 999.587 \times 10^{-3} & -9.8292 \times 10^{-3} & -8.4445 \\ 13.8281 \times 10^{-3} & -82.7724 \times 10^{-6} & 1.01587 & 0. \\ -81.9979 \times 10^{-6} & 48.9957 \times 10^{-6} & -38.1077 \times 10^{-6} & 1. \end{pmatrix}. \tag{24}$$

The functions $U = (U_1, U_2)$ and $V = (V_1, V_2)$ are again multivariate polynomials of the form

$$\sum_{\{i_j\} \in \mathbb{J}} \bigcirc_{v_1, v_2, v_3, v_4} \, u_{1n}^{i_1} \, u_{2n}^{i_2} \, v_{1n+1}^{i_3} \, v_{2n+1}^{i_4}, \tag{25}$$

where $\bigcirc$ are the real valued coefficients $U_1 \,|\, U_2 \,|\, V_1 \,|\, V_2$ stemming from the multivariate series expansion respectively. The inversion of the series is done by composing monomials containing $(v_{1,n+1}, v_{2,n+1})$ with the linearized solution in $(v_{1,n+1}, v_{2,n+1})$ until all monomials containing terms with v_{1n+1}, v_{2n+1} are pushed to higher orders. After successive steps the multivariate polynomial will be

explicit up to order K, which we set in our calculations to $K = 19$. The resulting explicit mapping is given in matrix form according to:

$$\begin{pmatrix} u_{1n+1} \\ u_{2n+1} \\ v_{1n+1} \\ v_{2n+1} \end{pmatrix} = M \cdot \begin{pmatrix} u_{1n} \\ u_{2n} \\ v_{1n} \\ v_{2n} \end{pmatrix} + \begin{pmatrix} U_1^*(u_{1n}, u_{2n}, v_{1n}, v_{2n}) \\ U_2^*(u_{1n}, u_{2n}, v_{1n}, v_{2n}) \\ V_1^*(u_{1n}, u_{2n}, v_{1n}, v_{2n}) \\ V_2^*(u_{1n}, u_{2n}, v_{1n}, v_{2n}) \end{pmatrix}, \tag{26}$$

where the asteriks in $U^* = (U_1^*, U_2^*)$ and $V^* = (V_1^*, V_2^*)$ indicates, that the monomials are depending on the old variables only, i.e. they are of the form:

$$\bigcirc_{\nu_1, \nu_2, \nu_3, \nu_4} u_{1n}^{i_1} u_{2n}^{i_2} v_{1n}^{i_3} v_{2n}^{i_4} \tag{27}$$

(compare to 23). The full explicit expansion of the mapping consists of $35\,420$ coefficients in the case of $n = 4$, stemming from a multivariate polynomial of dimension $n = 6$, consisting of $708\,400$ monomials. To estimate the error we checked the conservation of the Poisson structure of the explicit mapping, which turned out to be of the order 10^{-10}. This error affects the size of all quantities derived from the mapping (normal form, remainder, estimates) by the same order beyond the truncation order $K = 19$. The basic periods of the system are derived from the eigenvectors $\left(\Lambda_1, \Lambda_2, \overline{\Lambda}_1, \overline{\Lambda}_2\right)$ of the linearized system according to $T_j = 1 \big/ \cos^{-1}\!\left(\text{Re}(\Lambda_j)\right)$ with $j = 1, 2$ and turn out in our case to be $T_1 = 12.1944$ and $T_2 = 310.453$ in revolution periods of Jupiter, which in the present time units is 2π. Translated to physical units we get:

$$T_1 = 144.626 \; yr,$$

$$T_2 = 3681.97 \; yr, \tag{28}$$

which should be compared to the precise theoretical values given by Érdi (1997), namely $T_1 = 147.8 \; yrs$ and $T_2 = 3683.97 \; yrs$. The difference is less than 3 percent. A serious problem regards the radius of convergence of the explicit mapping, centered around the fixed point L_4. After the inversion, it turns out that the radius of convergence is smaller for the explicit mapping than for the implicit mapping. The validity of the explicit mapping is restricted to the librational regime of motion (in Figure 4b). The reason was found in the series reversion process and will not be dealt with in the sequel. Therefore there is still ground to improve the estimates developed in later chapters. We will come back to this point later on in the discussion.

6. Birkhoff Normal Form

Having determined the explicit mapping in the vicinity of the equilateral fixed points L_4, L_5, we can now proceed in implementing the Birkhoff normal form scheme, which is at the core of the analytical apparatus of the Nekhoroshev theory: estimating the size of the remainder of the normal form at the optimal order of truncation yields the estimates of the Nekhoroshev stability of our system (done in Chapter 7). In fact we are looking, like in the Hamiltonian flow (Chapter 2) on the influence of the remainder on the integrable approximation to the system. Integrability in the Hamiltonian system is connected to motion on a torus. The discrete analogon is motion under a twist mapping. The theory on normal forms of Hamiltonian flows was developed in Chapter 2. The construction of normal forms in the case of symplectic mappings is the main subject of the present chapter.

6.1. General Birkhoff normal form algorithm

Let

$$X_{n+1} = A \cdot X_n + G(X_n), \tag{1}$$

be a symplectic mapping of even dimension $d = 2m$, where X is the $2m$ dimensional vector of the mapping variables $(u_1, \ldots, u_m, v_1, \ldots, v_m)$ and A is the linear approximation to the system in matrix form. G is a vector function of the old variables and in principle could be truncated to include all nonlinear couplings up to some finite order N, i.e.:

$$G = G^{(2)} + G^{(3)} + \ldots + G^{(N)}, \tag{2}$$

where the superscript defines the order of the contributions. These are assumed to be in multivariate polynomial form, thus a monomial belongs to class $G^{(r)}$ if it is based on $u_j^{i_j}$, $v_j^{k_j}$ and the sum of the exponents i_j, k_j over $j = 1, \ldots, m$ is r. The symplectic condition for the linear part of the transformation reads:

$$A \cdot J \cdot A^{-1} = J, \tag{3}$$

where J is the skew symmetric matrix of the form:

$$J = \begin{pmatrix} 0_{2m} & 1_{2m} \\ -1_{2m} & 0_{2m} \end{pmatrix}, \tag{4}$$

and 0_{2m}, 1_{2m} are the $2m$ dimensional null and identity matrices respectively. Symplecticity of the full nonlinear mapping implies the Poisson-structure:

$$\{u_i, v_j\} = \delta_{ij},$$

$$\{u_i, u_j\} = \{v_i, v_j\} = 0, \tag{5}$$

where, that $i, \ j \le m$ and δ_{ij} is the Kronecker delta.

6.1.1. Diagonalization and complexification

In the first step we diagonalize and transform the mapping from the set of real variables X to a convenient set of complex variables $Z = (z_1, \ldots, z_m, \bar{z}_1, \ldots, \bar{z}_m)$, which can be achieved by calculating the eigensystem of the transposed matrix A^T. In addition we need to rescale the linear transformation induced by the matrix of eigenvectors, so as to preserve the Poisson structure also in the new variables:

$$\{z_i, \bar{z}_j\} = i\, \delta_{ij},$$

$$\{z_i, z_j\} = \{\bar{z}_i, \bar{z}_j\} = 0, \tag{6}$$

where again $i, \ j \le m$. The transformation B from real to complex variables takes the form:

$$Z = B \cdot X \tag{7}$$

and the resulting mapping in complex coordinates reads:

$$Z_{n+1} = \Omega_\omega \cdot Z_n + F(Z_n). \tag{8}$$

The linearized part Ω_ω is the frequency vector of the unperturbed twist mapping resulting from the complex diagonal form of A, i.e.:

$$\Omega_\omega = \left(e^{i\,\omega_1}, \ldots, e^{i\,\omega_m}, e^{-i\,\omega_1}, \ldots, e^{-i\,\omega_m}\right), \tag{9}$$

where the ω_j are defined via

$$\omega_j = \frac{2\,\pi}{T_j}, \ \ j = 1, \ldots, m, \tag{10}$$

and the periods T_j are the basic periods of the system. They are calculated from the already obtained eigensystem above according to:

$$T_j = \cos^{-1}\!\left(\mathrm{Re}(\Lambda_j)\right), \ \ j = 1, \ldots, m, \tag{11}$$

where $\left(\Lambda_1, \ldots, \Lambda_m, \overline{\Lambda}_1, \ldots, \overline{\Lambda}_m\right)$ are the set of eigenvalues corresponding to the jth eigenvector of the eigensystem (which we already found in the Sun-Jupiter case according to (28;5)).

Like in the real case (1, 2) let us split the function F into contributions of equal order of magnitude:

$$F = F^{(2)} + F^{(3)} + \ldots + F^{(N)}, \tag{12}$$

which in component notation $F = \left(F_1, \ldots, F_m, \overline{F_1}, \ldots, \overline{F_m}\right)$ is given by:

$$F_i = \Omega_{\omega,i}\, z_i + \sum_{\kappa \ge 2}^{N} F_i^{(\kappa)}(z_1, \ldots, z_m, \bar{z}_1, \ldots, \bar{z}_m) \tag{13}$$

and similarly for the complex conjugated part of $\boldsymbol{F}$:

$$\overline{F}_i = \overline{\Omega}_{\omega,i}\,\overline{z}_i + \sum_{\kappa \geq 2}^{N} \overline{F}_i^{(\kappa)}(z_1, \ldots, z_m, \overline{z}_1, \ldots, \overline{z}_m). \tag{14}$$

The goal of the normal form construction is to find a suitable transformation Φ under which the mapping (8) resumes the form of a twist mapping, i.e.:

$$\boldsymbol{\mathcal{Z}}_{n+1} = \boldsymbol{U}(\boldsymbol{\mathcal{Z}}_n) = \Omega_{\omega+\omega'(\zeta,\overline{\zeta})} \cdot \boldsymbol{\mathcal{Z}}_n, \tag{15}$$

where $\boldsymbol{\mathcal{Z}} = \left(\zeta_1, \ldots, \zeta_m, \overline{\zeta}_1, \ldots, \overline{\zeta}_m\right)$ are the new transformed variables and $\boldsymbol{U} = \left(U_1, \ldots, U_m, \overline{U}_1, \ldots, \overline{U}_m\right)$ defines the normal form of it. The vector valued function:

$$\omega'\left(\zeta\,\overline{\zeta}\right) = \left(\omega_1\,'\left(\zeta_1\,\overline{\zeta}_1\right), \ldots, \omega_m\,'\left(\zeta_m\,\overline{\zeta}_m\right)\right)$$

yields the corrections of the fundamental frequencies ω_j. If such a transformation Φ exists and its inverse function Φ^{-1} is defined in the whole domain of the original mapping, including the origin, the mapping is said to be integrable and the exact integrals of the mapping are defined by $I_j = \zeta_j\,\overline{\zeta}_j$ or in old variables:

$$I_j = \Phi_j^{-1}(z_1, \ldots, z_m, \overline{z}_1, \ldots, \overline{z}_m) \cdot \overline{\Phi}_j^{-1}(z_1, \ldots, z_m, \overline{z}_1, \ldots, \overline{z}_m).$$

The level curves $I_j = const$ define $j = 1, \ldots, m$ independent invariant circles in coordinates $\left(\zeta_1, \ldots, \zeta_m, \overline{\zeta}_1, \ldots, \overline{\zeta}_m\right)$ corresponding to invariant curves in the original coordinates $(z_1, \ldots, z_m, \overline{z}_1, \ldots, \overline{z}_m)$ respectively. On the other hand, if the original mapping (8) is not integrable, the form of equation (15) generalizes to:

$$\boldsymbol{\mathcal{Z}}_{n+1} = \boldsymbol{U}(\boldsymbol{\mathcal{Z}}_n) = \Omega_{\omega+\omega'(\zeta,\overline{\zeta})} \cdot \boldsymbol{\mathcal{Z}}_n + \boldsymbol{R}(\boldsymbol{\mathcal{Z}}_n), \tag{16}$$

where $\boldsymbol{R} = \left(R_1, \ldots, R_m, \overline{R}_1, \ldots, \overline{R}_m\right)$ is the vector of the remainder functions. The question arises, if it is possible to minimize $\boldsymbol{R}$ by a finite order transformation. The main result of Nekhoroshev theory is connected to this question and states that by an appropriate transformation Φ, the size of $\boldsymbol{R}$ can be rendered exponentially small in a properly defined domain of the mapping, which is called the Nekhoroshev domain. This guarantees an exponentially long practical stability, i.e. the near-preservation of the integrals I_j of the normal form mapping, defined by $\boldsymbol{U}$, for the orbits of the full mapping.

6.1.2. Solving the homological equation

The normal form construction presented here is based on the algorithm of Servizi et al (1983), see also Bazzani, Marmi & Turchetti (1990) for detailed discussion. Since we are dealing with mappings in

form of multivariate polynomials the unknown functions $\boldsymbol{\Phi}$ and $\boldsymbol{U}$ in component notation $(i = 1, \ldots, m)$ are of the form:

$$\Phi_i = \Phi_i(\boldsymbol{\mathcal{Z}}) = \zeta_i + \sum_{\kappa \geq 2}^{K} \Phi_i^{(\kappa)}\left(\zeta_1, \ldots, \zeta_m, \overline{\zeta}_1, \ldots, \overline{\zeta}_m\right) \tag{17}$$

and

$$U_i = U_i(\boldsymbol{\mathcal{Z}}) = \Omega_{\omega,i}\,\zeta_i + \sum_{\kappa \geq 2}^{K} U_i^{(\kappa)}\left(\zeta_1, \ldots, \zeta_m, \overline{\zeta}_1, \ldots, \overline{\zeta}_m\right). \tag{18}$$

(18) defines a near identity transformation and we therefore already know the first order solutions $U_i^{(1)} = \Omega_{\omega,\iota}\,\zeta_i$ stemming from $\Phi_i^{(1)} = \zeta_i$, $(i = 1, \ldots, m)$. The functions $\Phi_i^{(\kappa)}$ and $U_i^{(\kappa)}$ with $\kappa > 2$ are unknown functions and need to be determined step by step. The homological equation reads:

$$\boldsymbol{\Phi} \circ \boldsymbol{U} = \boldsymbol{F} \circ \boldsymbol{\Phi}, \tag{19}$$

where the small circle denotes polynomial composition. Splitting (19) in terms of the same order, and defining the projection operators:

$$[f]_r = f^{(r)},$$

$$[f]_{<r} = \sum_{k<r} f^{(\kappa)} = f^{(0)} + f^{(1)} + \ldots f^{(r-1)},$$

$$[f]_{\leq r} = \sum_{k \leq r} f^{(\kappa)} = f^{(0)} + f^{(1)} + \ldots + f^{(r)}, \tag{20}$$

acting either on scalar or vector functions f or $\boldsymbol{f}$, the r-th order terms of the homological equation yield:

$$\boldsymbol{\Delta}_\omega[\boldsymbol{\Phi}(\boldsymbol{\mathcal{Z}})]_r + [\boldsymbol{U}(\boldsymbol{\mathcal{Z}})]_r = [\boldsymbol{F}([\boldsymbol{\Phi}(\boldsymbol{\mathcal{Z}})]_{<r})]_r - [\boldsymbol{\Phi}([\boldsymbol{U}(\boldsymbol{\mathcal{Z}})]_{<r})]_r \equiv [\boldsymbol{P}]_r(\boldsymbol{\mathcal{Z}}). \tag{21}$$

In (21) we have defined the linear operator $\boldsymbol{\Delta}_\omega = \left(\Delta_{\omega,1}, \ldots, \Delta_{\omega,m}, \overline{\Delta}_{\omega,1}, \ldots, \overline{\Delta}_{\omega,m}\right)$ according to:

$$\boldsymbol{\Delta}_\omega[\boldsymbol{\Phi}(\boldsymbol{\mathcal{Z}})]_r \equiv [\boldsymbol{\Phi}(\boldsymbol{\Omega}_\omega \cdot \boldsymbol{\mathcal{Z}})]_r - \boldsymbol{\Omega}_\omega \cdot [\boldsymbol{\Phi}(\boldsymbol{\mathcal{Z}})]_r \tag{22}$$

or in component notation $(j = 1, \ldots, m)$:

$$\Delta_{\omega,j}\left[\Phi_j\left(\zeta_1, \ldots, \zeta_m, \overline{\zeta}_1, \ldots, \overline{\zeta}_m\right)\right]_r = \left[\Phi_1\left(\Omega_{\omega,1}\,\zeta_1, \ldots, \Omega_{\omega,m}\,\zeta_m, \overline{\Omega}_{\omega,1}\,\overline{\zeta}_1, \ldots, \overline{\Omega}_{\omega,m}\,\overline{\zeta}_m\right)\right]_r +$$

$$-\Omega_{\omega,j} \cdot \left[\Phi_j\left(\zeta_1, \ldots, \zeta_m, \overline{\zeta}_1, \ldots, \overline{\zeta}_m\right)\right]_r, \tag{23}$$

and similarly for $\overline{\Delta}_\omega$. Equation (21) can be solved recursively to specify the unknown functions $[\boldsymbol{U}]_r$ and $[\boldsymbol{\Phi}]_r$ starting with $[\boldsymbol{U}]_1 = [\boldsymbol{F}]_1$ and $[\boldsymbol{\Phi}_1] = \boldsymbol{\mathcal{Z}}$. The solution at the rth step is found by noting that all quantities appearing on the right-hand side of the equation are already specified by the previous steps, that is $[\boldsymbol{P}]_r$ is a known function at order r. Thus to find the right hand side of equation (21) means to compute the composition of known polynomials and extract the rth order terms. Those which are in normal form can be identified with $[\boldsymbol{U}]_r$, the remaining terms, called $[\boldsymbol{Q}]_r = [\boldsymbol{P}]_r$ - $[\boldsymbol{U}]_r$ are equivalent

to $\Delta_\omega [\Phi]_r$. By inversion of the linear operator (22) we can identify $\Delta_\omega^{-1}[Q]_r$ with $[\Phi]_r$ and thus have solved the equation up to order r.

The definition of monomials being in normal form is based on the condition, that they belong to the kernel of Δ_ω. The action of the inverse operator Δ_ω^{-1} on monomials of the type:

$$\square = a_{\alpha_1,\ldots,\alpha_m,\beta_1,\ldots,\beta_m} \zeta_1^{\alpha_1} \zeta_2^{\alpha_2} \ldots \zeta_m^{\alpha_m} \overline{\zeta}_1^{\beta_1} \overline{\zeta}_2^{\beta_2} \ldots \overline{\zeta}_m^{\beta_m} \tag{24}$$

is defined in component notation by :

$$\Delta_{\omega,i}^{-1}(\square) = a_{\alpha_1,\ldots,\alpha_m,\beta_1,\ldots,\beta_m} \frac{\zeta_1^{\alpha_1} \zeta_2^{\alpha_2} \ldots \zeta_m^{\alpha_m} \overline{\zeta}_1^{\beta_1} \overline{\zeta}_2^{\beta_2} \ldots \overline{\zeta}_m^{\beta_m}}{exp\!\left(i \sum_{k=1}^m (\alpha_k - \beta_k)\,\omega_k\right) - \Omega_{\omega,i}}. \tag{25}$$

Note, that (25) is the discrete analogon to (25;2) of the continuous case. In both equations, small denominators are present. The kernels of the operators in component notation are defined according to $(k, l = 1, 2, \ldots)$:

$$\ker\!\left(\Delta_{\omega,1}\right) = \zeta_1^{k+1} \zeta_2^{l} \ldots \zeta_m^{l} \overline{\zeta}_1^{k} \overline{\zeta}_2^{l} \ldots \overline{\zeta}_m^{l},$$

$$\ker\!\left(\Delta_{\omega,2}\right) = \zeta_1^{l} \zeta_2^{k+1} \ldots \zeta_m^{l} \overline{\zeta}_1^{l} \overline{\zeta}_2^{k} \ldots \overline{\zeta}_m^{l},$$

$$\ldots$$

$$\ker\!\left(\Delta_{\omega,i}\right) = \zeta_1^{l} \zeta_2^{l} \ldots \zeta_i^{k+1} \ldots \zeta_m^{l} \overline{\zeta}_1^{l} \overline{\zeta}_2^{l} \ldots \overline{\zeta}_i^{k} \ldots \overline{\zeta}_m^{l},$$

$$\ldots$$

$$\ker\!\left(\Delta_{\omega,m}\right) = \zeta_1^{l} \zeta_2^{l} \ldots \zeta_m^{k+1} \overline{\zeta}_1^{l} \overline{\zeta}_2^{l} \ldots \overline{\zeta}_m^{k}, \tag{26}$$

and similarly for $\overline{\Delta}_{\omega,i}$ (note a typo in Lhotka et al (2008), where $(\alpha_1 - \alpha_2)$ and $(\beta_1 - \beta_2)$ has to be replaced by $(\alpha_i - \beta_i)$, $i = 1, 2$ in text and *(39)*). The application of (25) on normal form terms of form (26) would lead to zero divisors in (25). This is the reason why such terms are left un-normalized. The definition of the normal form algorithm here is according to the nonresonant construction known also as the Birkhoff form construction.

The definitions of the kernels according to (26) allows one to solve (21) for both, the unknown functions $[U]_r$ and $[\Phi]_r$. The solution in component notation is:

$$[U_i]_r = \left\{\text{terms of } \ker\!\left(\Delta_{\omega,i}\right) \text{ in } [P_i]_r\right\},$$

$$[\Phi_i]_r = \left\{\left[\Delta_{\omega,i}^{-1}(Q_i)\right]_r \equiv \left\{\text{terms of } \mathrm{Rg}\!\left(\Delta_{\omega,i}\right) \text{ in } [P_i]_r\right\}, \tag{27}$$

where $\mathrm{Rg}\!\left(\Delta_{\omega,i}\right)$ denotes the range of the respective operators $\Delta_{\omega,i}$ and $i = 1, 2, \ldots, m$. From the definition of the normal form terms (26) we can conclude that normal form terms exist only for

$$U_i^{(r)} = \overline{U}_i^{(r)} = 0,$$

for r even. On the other hand, the form of the homological equations (21) implies that the equations are still satisfied by the addition of any kernel terms, defined by (26), with arbitrary coefficients in front, to the generating function Φ_i specified through the second of equations (27). Since the transformation to new variables should not violate the Poisson structure of the underlying dynamics, i.e. the symplectic mapping should transform canonically into a symplectic mapping in new variables, we exploit this freedom in order to ensure that the transformation done by Φ_i is symplectic up to order r.

By adding kernel terms with free coefficients of the form ($i = 1, \ldots, m$):

$$[\Phi_i]_r \rightarrow [\Phi_i]_r + \sum_{\alpha_i=\beta_i+1,\, \alpha_j=\beta_j, \sum_\kappa \alpha_\kappa+\beta_\kappa=r} c_{\alpha_1,\ldots,\alpha_m \beta_1,\ldots,\beta_m} \zeta_1^{\alpha_1} \zeta_2^{\alpha_2} \ldots \zeta_m^{\alpha_m} \overline{\zeta}_1^{\beta_1} \overline{\zeta}_2^{\beta_2} \ldots \overline{\zeta}_m^{\beta_m} \qquad (28)$$

to the generating function at order r, the coefficients are specified by the request, that the Poisson structure (6) be preserved up to terms of order $r - 1$, namely:

$$\left\{ [\Phi_i]_r, [\overline{\Phi}_j]_r \right\} = i\, \delta_{i,j}$$

$$\left\{ [\Phi_i]_r, [\Phi_j]_r \right\} = \left\{ [\overline{\Phi}_i]_r, [\overline{\Phi}_j]_r \right\} = 0, \qquad (29)$$

where $i, j = 1, \ldots, m$. The explicit form in the case of the 4 dimensional mapping will be given in the next section. The symplectification of the transformation function completes one step of the normalization procedure. After the rth order of normalization has been accomplished, the $(r + 1)$th order may be obtained by iterating up to the desired number of steps. From this time on, we will denote by $\square^{(r)}$, any quantity at the rth order of normalization, where $\square$ is an arbitrary scalar or vector.

An additional remark: in the previous notation the transformation from old to new variables ($Z \rightarrow \mathcal{Z}$) implies one set of old variables ($z_1, \ldots, z_m, \bar{z}_1, \ldots, \bar{z}_m$) being associated with one set of new variables $\left(\zeta_1, \ldots, \zeta_m, \overline{\zeta}_1, \ldots, \overline{\zeta}_m\right)$. In fact with every step of the transformation a new set of variables is introduced. Thus to be precise in all detail in the notation one would need to incorporate an additional identifier to specify the actual set of variables, i.e. of the form:

$$Z \rightarrow \mathcal{Z}_{(1)} \rightarrow \mathcal{Z}_{(2)} \rightarrow \ldots \rightarrow \mathcal{Z}_{(r)}.$$

However, we avoided this notation for simplicity.

6.2. Normal form construction in the case of Sun-Jupiter

We now give the explicit algorithm of construction of the normal form in the case of 4 dimensional symplectic mappings in this Section and apply it to the ERTBP for the case of Sun-Jupiter.

6.2.1. Complexification and diagonalization

Since the explicit mapping of the Sun-Jupiter-Trojan case (26;5), already found in Chapter 5, is of the

form (1), where

$$A = M, \quad G = (U_1{}^*, U_2{}^*, V_1{}^*, V_2{}^*) \tag{30}$$

and the set of real variables is indeed $X = (u_1, u_2, v_1, v_2)$, we can instantaneously proceed in diagonalizing M and transforming the symplectic mapping into the set of variables $Z \in \mathbb{C}^2$. The matrix B in (7) in the case of Sun-Jupiter-Trojan turns out to be of the form:

$$B = \mathrm{Re}\,(B) + i\,\mathrm{Im}\,(B), \tag{31}$$

where the real and imaginary parts are given by:

$$\mathrm{Re}\,(B) = \begin{pmatrix} 33.5883 \times 10^{-3} & -188.273 \times 10^{-6} & 4.40164 & -9.35407 \times 10^{-3} \\ 43.8972 \times 10^{-6} & 350.249 \times 10^{-6} & 86.6193 \times 10^{-3} & 14.4442 \\ 33.5883 \times 10^{-3} & -188.273 \times 10^{-6} & 4.40164 & -9.35407 \times 10^{-3} \\ 43.8972 \times 10^{-6} & 350.249 \times 10^{-6} & 86.6193 \times 10^{-3} & 14.4442 \end{pmatrix}$$

and

$$\mathrm{Im}(B) = \begin{pmatrix} -113.593 \times 10^{-3} & 681.194 \times 10^{-6} & 0. & -70.4576 \times 10^{-6} \\ -73.7266 \times 10^{-6} & -34.6156 \times 10^{-3} & -21.4709 \times 10^{-6} & 0. \\ 113.593 \times 10^{-3} & -681.194 \times 10^{-6} & 0. & 70.4576 \times 10^{-6} \\ 73.7266 \times 10^{-6} & 34.6156 \times 10^{-3} & 21.4709 \times 10^{-6} & 0. \end{pmatrix}. \tag{32}$$

respectively. The diagonalized linear part in Ω_ω in (8) is given by

$$\Omega_\omega = \left(\Omega_{\omega,1}, \Omega_{\omega,2}, \overline{\Omega}_{\omega,1}, \overline{\Omega}_{\omega,2} \right), \tag{33}$$

where, according to (9):

$$\Omega_{\omega,1} = 870.17 \times 10^{-3} + i\,492.752 \times 10^{-3},$$

$$\Omega_{\omega,2} = 999.795 \times 10^{-3} + i\,20.2374 \times 10^{-3}. \tag{34}$$

The rotation numbers (10) in the Sun-Jupiter-Trojan case are

$$\omega_1 = 0.5152500568840412,$$

$$\omega_2 = 0.02023876973187783, \tag{35}$$

which yield the periods already found in (28;5):

$$T_1 = 12.19443884233018,$$

$$T_2 = 310.4529272489829, \tag{36}$$

The set of eigenvalues $\left(\Lambda_1, \Lambda_2, \overline{\Lambda}_1, \overline{\Lambda}_2 \right)$ and the eigenvectors of the transposed matrix M^T are given by:

$$\Lambda_1 = 999.795 \times 10^{-3} + i\,20.2374 \times 10^{-3},$$

$$\Lambda_2 = 870.170 \times 10^{-3} + i\,492.752 \times 10^{-3}. \tag{37}$$

The matrix of eigenvectors, before rescaling to fit the Poisson structure (6), is given by:

$$
\begin{pmatrix}
-3.03903 \times 10^{-6} & -24.2479 \times 10^{-6} & -5.99671 \times 10^{-3} & -999.979 \times 10^{-3} \\
-3.03903 \times 10^{-6} & -24.2479 \times 10^{-6} & -5.99671 \times 10^{-3} & -999.979 \times 10^{-3} \\
7.62807 \times 10^{-3} & -42.7578 \times 10^{-6} & 999.636 \times 10^{-3} & -2.12436 \times 10^{-3} \\
7.62807 \times 10^{-3} & -42.7578 \times 10^{-6} & 999.636 \times 10^{-3} & -2.12436 \times 10^{-3}
\end{pmatrix},
$$

$$
\begin{pmatrix}
5.104140 \times 10^{-6} & 2.396460 \times 10^{-3} & 1.48644 \times 10^{-6} & 0. \\
-5.10414 \times 10^{-6} & -2.39646 \times 10^{-3} & -1.48644 \times 10^{-6} & 0. \\
-25.7975 \times 10^{-3} & 154.7030 \times 10^{-6} & 0. & -16.0013 \times 10^{-6} \\
25.79750 \times 10^{-3} & -154.703 \times 10^{-6} & 0. & 16.0013 \times 10^{-6}
\end{pmatrix},
\tag{38}
$$

where the former is the real, the latter is the imaginary part of the matrix. The scaling factors to get $\boldsymbol{B}$ were found to be $\delta_1^{-1} = 0.0692306$ and $\delta_2^{-1} = 0.227105$ respectively. The full nonlinear complex mapping (8), together with the nonlinear contributions given in terms of (12) up to order 7 in the mapping variables can be found in the Appendix.

6.2.2. Birkhoff normalization

For the Birkhoff normalization scheme, $\boldsymbol{F}$ together with $\boldsymbol{\Phi}$ and $\boldsymbol{U}$ reduce into the form:

$$
F_1 = F_1(Z) = \Omega_{\omega,1}\, z_1 + \sum_{\kappa \geq 2}^{N} F_1^{(\kappa)}(z_1, z_2, \bar{z}_1, \bar{z}_2),
$$

$$
F_2 = F_2(Z) = \Omega_{\omega,2}\, z_2 + \sum_{\kappa \geq 2}^{N} F_2^{(\kappa)}(z_1, z_2, \bar{z}_1, \bar{z}_2),
\tag{39}
$$

derived from (13) and

$$
\Phi_1 = \Phi_1(Z) = \zeta_1 + \sum_{\kappa \geq 2}^{N} \Phi_1^{(\kappa)}(\zeta_1, \zeta_2, \overline{\zeta}_1, \overline{\zeta}_2),
$$

$$
\Phi_2 = \Phi_2(Z) = \zeta_2 + \sum_{\kappa \geq 2}^{N} \Phi_2^{(\kappa)}(\zeta_1, \zeta_2, \overline{\zeta}_1, \overline{\zeta}_2),
\tag{40}
$$

$$
U_1 = U_1(Z) = \Omega_{\omega,1}\, \zeta_1 + \sum_{\kappa \geq 2}^{N} U_1^{(\kappa)}(\zeta_1, \zeta_1, \overline{\zeta}_1, \overline{\zeta}_2),
$$

$$
U_2 = U_2(Z) = \Omega_{\omega,2}\, \zeta_2 + \sum_{\kappa \geq 2}^{N} U_2^{(\kappa)}(\zeta_1, \zeta_1, \overline{\zeta}_1, \overline{\zeta}_2),
\tag{41}
$$

derived from (17) and (18) respectively. The component notation of the linear operator $\boldsymbol{\Delta}_{\omega}$, according to (23) reduces to:

$$\Delta_{\omega,1}[\Phi_1(Z)]_r = \left[\Phi_1(\Omega_{\omega,1} \cdot Z)\right]_r - \Omega_{\omega,1} \cdot [\Phi_1(Z)]_r,$$

$$\Delta_{\omega,2}[\Phi_2(Z)]_r = \left[\Phi_2(\Omega_{\omega,2} \cdot Z)\right]_r - \Omega_{\omega,2} \cdot [\Phi_2(Z)]_r \tag{42}$$

and the inverse of the operator (from 25) is given by:

$$\Delta_{\omega,1}{}^{-1}(\square) = a_{\alpha_1,\alpha_2,\beta_1,\beta_2} \frac{\zeta_1^{\alpha_1} \zeta_2^{\alpha_2} \overline{\zeta}_1^{\beta_1} \overline{\zeta}_2^{\beta_2}}{exp(i\,(\alpha_1 - \beta_2)\,\omega_1 + (\alpha_2 - \beta_2)\,\omega_2) - exp(i\,\omega_1)},$$

$$\Delta_{\omega,2}{}^{-1}(\square) = a_{\alpha_1,\alpha_2,\beta_1,\beta_2} \frac{\zeta_1^{\alpha_1} \zeta_2^{\alpha_2} \overline{\zeta}_1^{\beta_1} \overline{\zeta}_2^{\beta_2}}{exp(i\,(\alpha_1 - \beta_2)\,\omega_1 + (\alpha_2 - \beta_2)\,\omega_2) - exp(i\,\omega_2)}, \tag{43}$$

together with $\Omega_{\omega,1} = e^{i\,\omega_1}$ and $\Omega_{\omega,2} = e^{i\,\omega_2}$ given in (34). The kernel of the operators Δ_ω in component notation consists, in the 4-dimensional case, of all monomials of the form:

$$\ker(\Delta_{\omega,1}) = \left\{\text{monomials of the form } \zeta_1^{k+1} \zeta_2^{l} \overline{\zeta}_1^{k} \overline{\zeta}_2^{l}\right\},$$

$$\ker(\Delta_{\omega,2}) = \left\{\text{monomials of the form } \zeta_1^{k+1} \zeta_2^{l} \overline{\zeta}_1^{k} \overline{\zeta}_2^{l}\right\}. \tag{44}$$

We follow the steps (27), (28), resulting in:

$$[\Phi_1]_r \to [\Phi_1]_r + \sum_{k,l \geq 0,\, 2\,(k+l)+1=r} c_{1,k+1,l}\, \zeta_1^{k+1} \zeta_2^{l} \overline{\zeta}_1^{k} \overline{\zeta}_2^{l}$$

and

$$[\Phi_2]_r \to [\Phi_2]_r + \sum_{k,l \geq 0,\, 2\,(k+l)+1=r} c_{2,k,l+1}\, \zeta_1^{k} \zeta_2^{l+1} \overline{\zeta}_1^{k} \overline{\zeta}_2^{l}. \tag{45}$$

In the case of the mappings in $\mathbb{C}^2$ the values for the coefficients $c_{1,k+1,l}$ and $c_{2,k,l+1}$ were explicitly found in terms of

$$\operatorname{Re}(c_{1,k+1,l}) = -\operatorname{Re}\left(\operatorname{coeff}\left(P_1, \zeta_1^{k} \zeta_2^{l} \overline{\zeta}_1^{k} \overline{\zeta}_2^{l}\right)\right) \big/ 2\,\kappa,$$

$$\operatorname{Re}(c_{2,k,l+1}) = -\operatorname{Re}\left(\operatorname{coeff}\left(P_2, \zeta_1^{k} \zeta_2^{l} \overline{\zeta}_1^{k} \overline{\zeta}_2^{l}\right)\right) \big/ 2\,\kappa,$$

$$\operatorname{Im}(c_{1,k+1,l}) = \operatorname{Im}\left(\operatorname{coeff}\left(P_3, \zeta_1^{k+1} \zeta_2^{l} \overline{\zeta}_1^{k} \overline{\zeta}_2^{l-1}\right)\right) \big/ l,$$

$$\operatorname{Im}(c_{2,k,l+1}) = 0, \tag{46}$$

where *coeff*(*P, mon*) is the coefficient function, returning the coefficient of monomial *mon* in *P* and P_1, P_2, P_3 are abbreviations for the Poisson brackets from (29) according to:

$$P_1 \equiv \left\{[\Phi_1]_r, [\overline{\Phi}_1]_r\right\} = 1 + O(r-1),$$

$$P_2 \equiv \left\{[\Phi_2]_r, [\overline{\Phi}_2]_r\right\} = 1 + O(r-1),$$

$$P_3 \equiv \{[\Phi_1]_r, [\Phi_2]_r\} = 0 + O(r-1). \tag{47}$$

The normalized mapping U together with the transformating function Φ up to order $r = 25$ can be found in the Appendix. Note that the imaginary part of $c_{2,k,l+1}$ is undetermined and it can be assigned arbitrary values. For simplicity it was set to zero.

6.2.3. Approximate integrals in the case Sun - Jupiter

The effect of the normal form construction in the case of the Sun-Jupiter-Trojan model can be visualized as follows. Iterating the complexified nonlinear mapping (16), normalized up to order r, for one arbitrary orbit started near the fixed point ($d \sim 0.01$), the time-evolution of the corresponding approximate integral of motion can be calculated numerically according to:

$$I_{1,n} = \zeta_{1,n}\,\overline{\zeta}_{1,n},$$

$$I_{2,n} = \zeta_{2,n}\,\overline{\zeta}_{2,n},$$

where n is the discrete time parameter. In the absence of the remainder (15) it is clear, that for all times the quantities $I_{j,n} = I_{j,n+1} = I_j$ are constants ($j = 1, 2$), variation being introduced only by the numerical error in the preservation of the Poisson structure ($err \sim 10^{-10}$, see end of Section 5.4.2). On the other hand the remainder $R\left(\zeta_1, \zeta_2, \overline{\zeta}_1, \overline{\zeta}_2\right)$ in (16) will add some drift, to the values of the approximate integrals, stemming from the real nonlinearity in the system. One expects that the variation of the approximate integrals will decrease with increasing order r up to the optimal order at which the size of the remainder becomes exponentially small. On this basis, a local stability theorem can also be constructed for the discrete case.
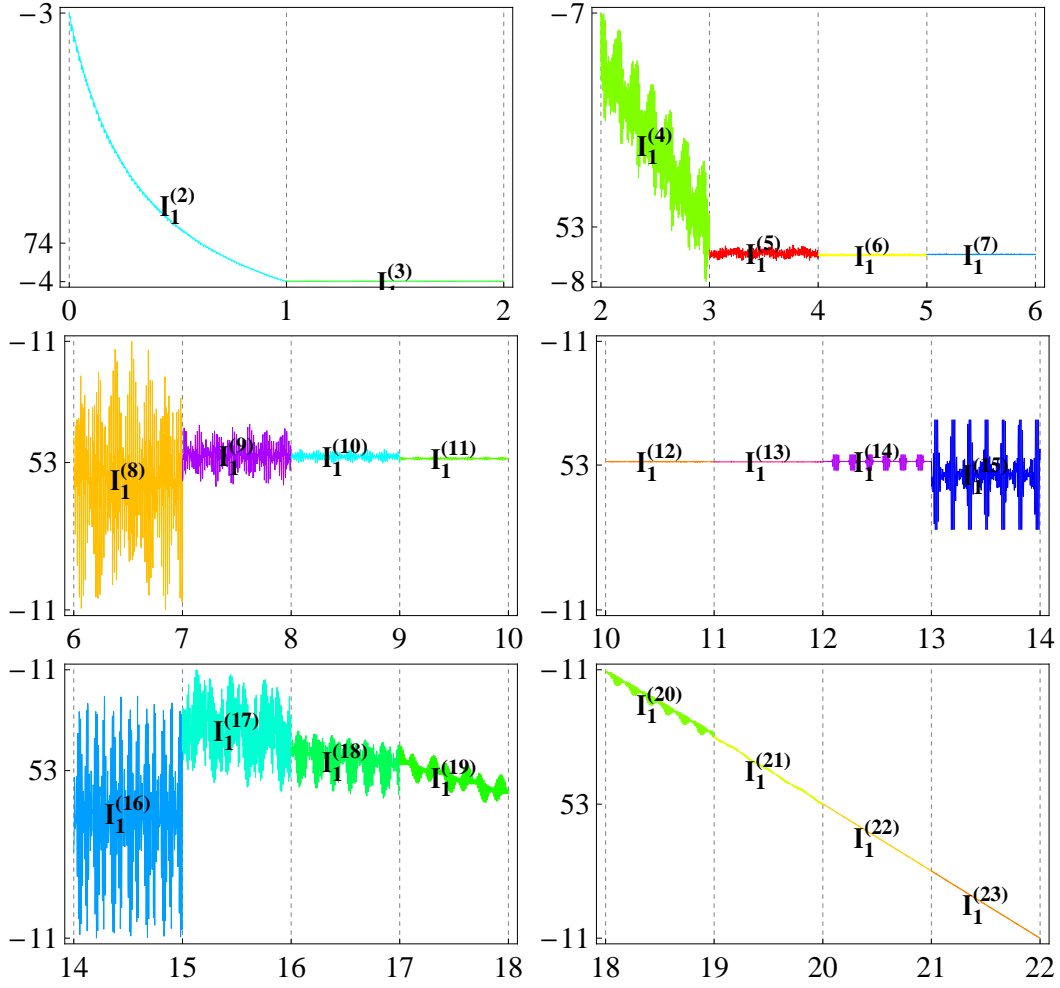
Figure 1.: Evolution in time of the approximate integral I_1; abscissa: time in thousands; ordinate: median in 10^{-6} (middle value), variation in 10^{-y} (logscale upper and lower value). Note the improvement in the successive close ups.

The effect of the normal form construction in the case of Sun-Jupiter-Trojan is shown in Figure 1 and Figure 2. In both figures the complexified mapping (17), normalized up to order r, was iterated for 1000 revolution periods of Jupiter, after which the order of normalization in (16) was increased to $r + 1$ and the orbit was iterated again, using the last state of the system as a new starting point. The figures show the evolution of the approximate integrals with respect to n, given in units of 1000 (revolution periods of Jupiter) on the abscissa. A first inspection clearly indicates that, after some steps, with increasing order of normalization, the approximate integrals $I_{1,2}$ tend to a constant value (given on the ordinate in units of 10^{-6}), while the variation of them decreases (given in units of exponents on the ordinate). In both figures, the best approximation to the integrals is bounded by an error of order 10^{-10} to 10^{-11}, which is in consistency with the error in the preservation of the Poisson structure, due to the finite expansion of the generating function.
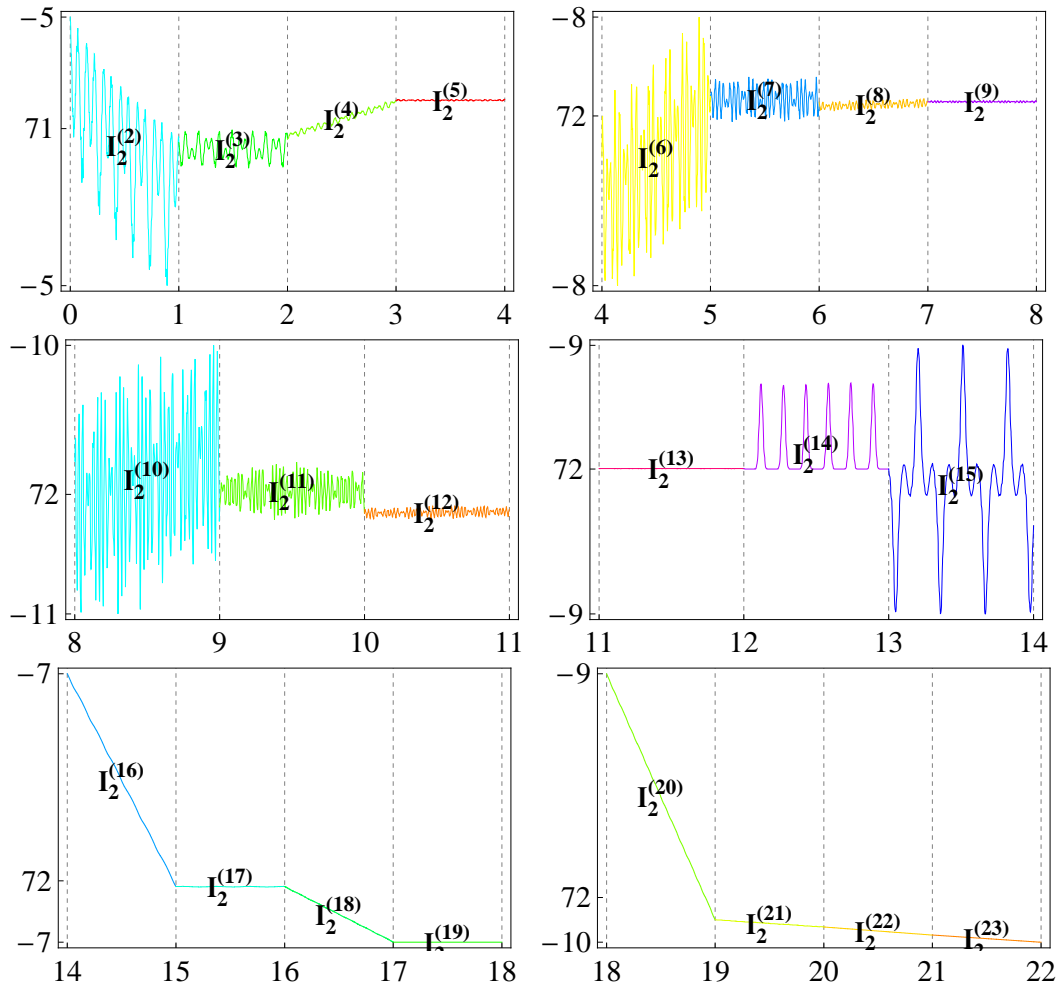
Figure 2.: Evolution in time of the approximate integral I_2. abscissa: time in thousands; ordinate: median in 10^{-6} (middle value), variation in 10^{-y} (logscale upper and lower value). Note the improvement in the successive close ups.

Looking closer in the panels in Figure 1, 2 one also finds a jump in the error of the preservation of the approximate integrals in both figures (Figure 1d-e & Figure 2d): the reason is due to the presence of a small divisor (a_{15}) introduced in the normal form construction (43), showing up at order 16. This behavior will be analyzed in all detail in the end of Chapter 7. We only mention here that it is strongly connected to the generic non-integrability of the system, resulting in the fact, that the normal form construction must fail, when $r \to \infty$. Nevertheless, this time, the normal form recovers again as one can see, when comparing the variations in approximate integrals with increasing order beyond 15. The trends of some of the approximate integrals with respect to time may be explained by two reasons: i) a "real" dynamical trend, introduced by the remainder (i.e. $I_1^{(2)}$ in Figure 1 and $I_2^{(2)}$ in Figure 2) indicating the non-integrability of the system and ii) the non symplecticity of the explicit mapping, due to the finite series reversion (up to order 19); the error in the conservation of the Poisson structure (i.e. $I_1^{(20+)}$, $I_2^{(20+)}$) is present in both figures but bound by the error of approximation.

The actual calculation is based on the non-resonant normal form construction. Nevertheless the frequency of the oscillation of the longitude of the perihelion ω_2 introduces a near resonance, since $\omega_2 \simeq 0$. The smallest divisor up to order 16 is therefore simply ω_2, indicating that the system is nearly resonant. This fact suggests, that an improvement of the present estimates can be obtained by a resonant normal form construction, which was not implemented yet in the Birkhoff normalization scheme. On the other hand, the next small divisor $a_{16} \sim 0.001$ appears at order 16. A modification of the nonresonant construction, in principle follows the idea of Chapter 2: Defining the resonant module M, excluding near resonance terms introducing a_{16} into the series modifies the normal form and takes care of the nearly resonant behavior of the system. However a numerical calculation shows that it does not modify the estimates appreciably.

7. Nekhoroshev Estimates

7.1. Approximate integrals and the remainder function

As already mentioned, the normal form mapping of the preceding chapter $[\boldsymbol{U}]_{\leq r}$ in the new variables becomes a twist mapping (16;6), which by use of the notation (20;6) is of the form:

$$\boldsymbol{\mathcal{Z}}_{n+1} = [\boldsymbol{U}]_{\leq r}(\boldsymbol{\mathcal{Z}}_n) = \boldsymbol{\Omega}_{\omega+\omega'(\zeta,\overline{\zeta})} \cdot \boldsymbol{\mathcal{Z}}_n. \tag{1}$$

The component notation in the m-dimensional case is given by ($j = 1, \ldots, m$):

$$\zeta_{j,n+1} = \left[U_j\right]_{\leq r}\left(\zeta_1, \ldots, \zeta_m, \overline{\zeta}_1, \ldots, \overline{\zeta}_m\right) + e^{i\,\Gamma_j(\zeta_1,\ldots,\zeta_m,\overline{\zeta}_1,\ldots,\overline{\zeta}_m)}\,\zeta_{j,n}, \tag{2}$$

where Γ_j only depends on products of equal powers in the new variables $\zeta_j\,\overline{\zeta}_j$. The mapping (2) is integrable, the exact integrals are defined in terms of

$$I_j = \zeta_j\,\overline{\zeta}_j \tag{3}$$

($j = 1, \ldots, m$). These integrals can be expressed in terms of the old variables, where the transformating function $[\boldsymbol{\Phi}]_{\leq r}$ is invertible in an open domain around the origin. Denoting the inverse by $[\boldsymbol{\Phi}]_{\leq r}^{-1}$, equation (3) transforms to:

$$\boldsymbol{I} = [\boldsymbol{\Phi}]_{\leq r}^{-1}(Z) \cdot [\overline{\boldsymbol{\Phi}}]_{\leq r}^{-1}(Z) \tag{4}$$

which is in component notation:

$$I_j = \left[\Phi_j\right]^{-1}(z_1, \ldots, z_m, \bar{z}_1, \ldots, \bar{z}_m) \cdot [\overline{\Phi}_j]_{\leq r}^{-1}(z_1, \ldots, z_m, \bar{z}_1, \ldots, \bar{z}_m).$$

The level curves, defined by $I_j = const$ ($j = 1, \ldots, m$) define m independent invariant circles in the coordinates Z and $\boldsymbol{\mathcal{Z}}$ respectively. Every orbit is therefore defined by m label values ($I_1, \ldots, I_m$) and lies on an invariant m-torus ($\mathbb{T}^m$) of the normal form mapping, connected to the action-angle variables in the continuous model. If, however, the remainder terms of (16;6) are present, a small drift of the orbits across the invariant tori of the normal form mapping is introduced and may harm the integrability of the system. By upperbounding the cumulative drift induced by the remainder terms of the mapping, the diffusion may be bound for a finite time span T. In the case of the Sun-Jupiter system, T is order of 10^9 revolution periods of Jupiter.

7.1.1. The mapping of radii (action mapping)

The full mapping according to (1) in new variables can also be expressed as

$$\boldsymbol{\mathcal{Z}}_{n+1} = [\boldsymbol{\Phi}]_{\leq r}^{-1} \circ \boldsymbol{F} \circ [\boldsymbol{\Phi}]_{\leq r} (\boldsymbol{\mathcal{Z}}_n) = [\boldsymbol{U}]_{\leq r} (\boldsymbol{\mathcal{Z}}_n) + \boldsymbol{R}^{(r+1)}(\boldsymbol{\mathcal{Z}}_n), \tag{5}$$

which is in component notation ($j = 1, \ldots, m$):

$$\zeta_{j,n+1} = [\Phi_j]_{\leq r} \circ F_j \circ [\Phi_j]_{\leq r} \left(\zeta_1, \ldots, \zeta_m, \overline{\zeta}_1, \ldots, \overline{\zeta}_m\right) =$$

$$[U_j]_{\leq r} \left(\zeta_1, \ldots, \zeta_m, \overline{\zeta}_1, \ldots, \overline{\zeta}_m\right) + R_j^{(r+1)}\left(\zeta_1, \ldots, \zeta_m, \overline{\zeta}_1, \ldots, \overline{\zeta}_m\right). \tag{6}$$

The resulting mapping is symplectic up to order r and the remainder $\boldsymbol{R}^{(r+1)} = \left(R_1^{(r+1)}, \ldots, R_m^{(r+1)}\right)$ at the r-th order of normalization is in principle an infinite series, consisting of all terms of orders beyond r, where these are produced by the terms of the original mapping, defined by $\boldsymbol{F}$. To calculate the drift along the tori we construct the mapping of radii, given by multiplying each of the equations (6) by its complex conjugate. The radii ($j = 1, \ldots, m$),

$$\rho_j = \zeta_j \overline{\zeta}_j, \tag{7}$$

correspond to the drift along the actions, defined by the integrable approximation (3). The mapping of radii is also called the mapping of actions for obvious reasons. Denoting by $\boldsymbol{\rho} = (\rho_1, \ldots, \rho_m)$ it may be written in vector form according to:

$$\boldsymbol{\rho}_{n+1}^2 = \boldsymbol{\rho}_n^2 + \sum_{\kappa=r+2}^{s} \boldsymbol{\mathcal{R}}^{(\kappa,r)}, \tag{8}$$

where $\boldsymbol{\mathcal{R}}^{(\kappa,r)} = \left(\mathcal{R}_1^{(\kappa,r)}, \ldots, \mathcal{R}_m^{(\kappa,r)}\right)$ are the remainder contributions in terms of the radii of order κ, normalized up to order r and s is the order of truncation of the remainder, where $r < s$. In component notation the mapping (8) may be also written in the form:

$$\rho_{j,n+1}^2 = \rho_{j,n}^2 + \sum_{\sum_{i=1}^{m}\alpha_i=r+2}^{s} a_{\alpha_1,\ldots,\alpha_m} \rho_1^{\alpha_1} \rho_2^{\alpha_2} \ldots \rho_m^{\alpha_m}, \tag{9}$$

and since the new variables Z are connected to the actions $\boldsymbol{\rho}$ via ($j = 1, \ldots, m$):

$$\zeta_j = \rho_j \, e^{i\,\phi_j},$$

$$\overline{\zeta}_j = \rho_j \, e^{-i\,\phi_j},$$

the contributions $\mathcal{R}_j$ depend on all $2\,m$ variables too. The domain of convergence of the action-mapping can be estimated by D´Alembert´s criterion implemented to the majorant series of (8) implemented in polar type coordinates. Considering the positive section of a hyperball of dimension m, the space of radii can be seen as a section of a hyperball of dimension m, parametrized by direction angles $\gamma_l \in (0, \pi/2)$, where $l = 1, \ldots, m - 1$. The radii transform into:

$$\rho_j = \rho \, w_j(\gamma_1, \ldots, \gamma_{m-1}), \tag{10}$$

where w_j are just combinations of trigonometric functions, depending on the dimension of the hyperball; i.e. if $m = 3$ the space of radii is (ρ_1, ρ_2, ρ_3) and parametrized by $(\gamma_1, \gamma_2, \rho)$ according to:

$$\rho_1 = \rho \sin(\gamma_1) \cos(\gamma_2),$$

$$\rho_2 = \rho \sin(\gamma_1) \sin(\gamma_2),$$

$$\rho_3 = \rho \cos(\gamma_2),$$

while in the case of $m = 2$ (ρ_1, ρ_2) is parametrized by γ, ρ in polar coordinates (implemented in the Sun-Jupiter case, Section 7.2.1). Note, that since $\rho_j \geq 0$, it is enough to define the range of definitions of γ_j to be $(0, \pi/2)$ for all $j = 1, \ldots, m-1$. This is a modification of the usual convention in parametrizing the hyperball of dimension m. Substituting (10) into (9) we are left with the mapping of radii of the form:

$$\rho_{j,n+1}^2 = \rho_{j,n}^2 + \sum_{\sum_{i=1}^m \alpha_i = r+2}^s a_{\alpha_1,\ldots,\alpha_m} \rho^{\alpha_1+\alpha_2+\ldots+\alpha_m} w_1^{\alpha_1} w_2^{\alpha_2} \ldots w_m^{\alpha_m}, \tag{11}$$

which is majorant to (9), if and only if we choose γ_j in w_j in such a way, that w_j becomes maximal, i.e. of order unity $(j = 1, \ldots, m)$. Note, that this can always be achieved in polar coordinates defined by (10): $\gamma_j = 0$ if $\square(\gamma_j)$ in (10) is of sine type and $\gamma_j = \pi/2$, if $\square(\gamma_j)$ in (10) is of cosine type ($\square$ denoting basic trigonometric functions in w_j). In this case w_j $(j = 1, \ldots, m)$ becomes unity and the majorant mapping reduces to:

$$\rho_{j,n+1}^2 = \rho_{j,n}^2 + \sum_{\sum_{i=1}^m \alpha_i = r+2}^s a_{\alpha_1,\ldots,\alpha_m} \rho^{\alpha_1+\alpha_2+\ldots+\alpha_m}. \tag{12}$$

Note, that in fact, by this construction the mapping (12) will give a specific direction $(\gamma_1^*, \ldots, \gamma_{m-1}^*)$ in action space upperbounding (9) in terms of $\boldsymbol{\rho}$. If the convergence radius of (12) along j is denoted by q_j^{-1} it follows, that the underlying mapping (9) is convergent within q_j^{-1} too. Denoting by $A_{j,\kappa}$ the κth order contributions in (12) with respect to the jth component of $\boldsymbol{\rho} = (\rho_1, \ldots, \rho_m)$, an estimate of the radius of convergence can be given using D´Alembert´s criterion, by:

$$\lim_{s\to\infty} \frac{\left| A_{j,\kappa+1}^{(s)} \right|}{\left| A_{i,\kappa}^{(s)} \right|} < q_j < 1. \tag{13}$$

In practice s will be truncated at a finite order too. Since the radius of convergence according to (13) will also depend on the direction, parametrized by $(\gamma_1, \ldots, \gamma_{m-1})$, estimates will do so too. An example given below (Sun-Jupiter case) will demonstrate this behavior in a real dynamical system.

7.1.2. Diffusion in action space

In the next step we are interested in the maximum distance traveled in the space of radii after N iterations of the mapping. Although it may be possible, that successive drifts in the actions (radii) go along different directions (and in the best case they will cancel out each other, due to opposite

directions), we are looking for an upperbound of the whole drift and are assuming the worst case, in which the drift at each iteration step follows the same direction as the previous one. In other words we are looking for an upperbound of the stability region. We formalize this idea along the lines suggested by Giorgilli & Skokos (1997). The maximum distance ρ_f traveled in the space of radii, starting on an arbitrary torus ρ after N iterations of the mapping (9) can be upper bounded by:

$$\rho_f{}^2 - \rho^2 \leq N \parallel \mathcal{R}^{(r)} \parallel \rho_f{}^r, \tag{14}$$

where r is again the order of normalization of the mapping. Solving with respect to N the inequality transforms into:

$$N \geq \frac{\rho_f{}^2 - \rho^2}{\parallel \mathcal{R}^{(r)} \parallel \rho_f{}^r} \equiv N(\rho, \rho_f), \tag{15}$$

where $N(\rho, \rho_f)$ denotes the number of iterations an orbit needs to drift from an initial torus ρ to a another torus ρ_f. Note that already at this step the number of iterations in inequality (15) will be maximized by minimizing the norm of the remainder $\parallel \mathcal{R}^{(r)} \parallel$, independently of the distance $\rho_f{}^2 - \rho^2$ we are asking for. Let us consider two extreme cases, namely

$$(i) \quad N(\rho, \rho) = 0,$$

$$(ii) \quad \lim_{\rho_f \to \infty} N(\rho, \rho_f) = 0.$$

In the first case (i) the orbit has no time to drift, since the final torus is the initial one , i.e. $\rho_f = \rho$ in (14). In the second case (ii) the estimate of the size of the remainder throughout the whole drift, going from ρ to ρ_f becomes infinite, since we are asking for an upperbound N for the limit $\rho_f \to \infty$. Therefore again the orbit will do it in zero time. The optimal distance of ρ_f is somewhere in between (ρ, ∞), such that it is far away enough from ρ but at the same time as close as possible to it, so that we do not overestimate the remainder seriously. The optimal choice of ρ_f is found by:

$$\frac{d}{d\rho_f} N(\rho, \rho_f) = \frac{d}{d\rho_f} \left(\frac{\rho_f{}^2 - \rho_f}{\parallel \mathcal{R}^{(r)} \parallel \rho_f{}^r} \right) = 0, \tag{16}$$

giving:

$$\frac{1}{\parallel \mathcal{R}^{(r)} \parallel} \left(2\rho_f{}^{1-r} - r\rho_f{}^{-1-r}(\rho_f{}^2 - \rho^2) \right) = 0,$$

or:

$$\rho_f = \rho \sqrt{\frac{r}{r-2}} \; . \tag{17}$$

The time needed for an orbit to drift from ρ to the optimal distance ρ_f, given by (17) is therefore given by inserting (17) into (15), resulting in:

$$N(\rho) = \frac{2}{\|\,\mathfrak{R}^{(r)}\,\|} \, (r-2)^{-1+\frac{r}{2}} \, r^{-r/2} \, \rho^{2-r} \equiv T_{\text{Nek}}. \tag{18}$$

where we defined the Nekhoroshev time T_{Nek} to be the time after N steps of the mapping. Note that in this form $T_{\text{Nek}} = T_{\text{Nek}}(\rho)$ is given by the product of $\|\,\mathfrak{R}^{(r)}\,\|^{-1}$, ρ^2 / ρ^r and $(r-2)^{r/2-1} \, r^{-r/2}$. The upper bound (18) limits the maximum distance ρ up to which an orbit can drift within Nekhoroshev time T_{Nek}. The distance depends on the order of normalization r explicitly and implicitly through the estimate of the norm of the remainder $\|\,\mathfrak{R}^{(r)}\,\|$. It is inversely proportional to the norm of the remainder and directly proportional to $(r-2)^{r/2-1} \, r^{-r/2}$. Solving (18) with respect to ρ one finds the lower bound of the Nekhoroshev stable region within Nekhoroshev time T_{Nek} to be:

$$\rho = 2^{\frac{-1}{2-r}} \left(-(2-r) \left(\frac{r}{r-2} \right)^r \|\,\mathfrak{R}^{(r)}\,\| \, T_{\text{Nek}} \right)^{\frac{1}{2-r}} \tag{19}$$

and since in the space of radii $(\rho_1 \times \rho_2 \times \ldots \times \rho_m)$ the direction ρ was fixed according to the parametrization $(\gamma_1, \ldots, \gamma_{m-1})$ the estimate also depends on the specific direction of diffusion we are looking for. This behavior directly translates into the dependency of the norm of the remainder $\|\,\mathfrak{R}^{(r)}\,\|$ on $(\gamma_1, \ldots, \gamma_{m-1})$. Equation (19) therefore also generalizes to:

$$\rho_{(\gamma_1, \ldots, \gamma_{m-1})} = 2^{\frac{-1}{2-r}} \left(-(2-r) \left(\frac{r}{r-2} \right)^r \|\,\mathfrak{R}^{(r)}\,\|_{(\gamma_1, \ldots, \gamma_{m-1})} \, T_{\text{Nek}} \right)^{\frac{1}{2-r}}, \tag{20}$$

when dealing with a higher dimensional space of radii. As a conclusion, diffusion can be bound, by means of (20), which is an estimate, depending on the normalization order r, the size of the remainder $\|\,\mathfrak{R}^{(r)}\,\|$ and the Nekhoroshev time T_{Nek}. The estimate (20) has to be compared with the isochronous version of Nekhoroshev theorem in Chapter 2. For an optimal estimate, the remainder $\|\,\mathfrak{R}^{(r)}\,\|$ needs to be exponentially small. This happens at an optimal order of truncation $r = r_{\text{opt}}$. The finite bound $\|\,\mathfrak{R}^{(r_{\text{opt}})}\,\|$ gives a finite Nekhoroshev stability time T_{Nek}, which is exponentially long since the optimal remainder is exponentially small.

7.2. Application to Jupiter´s Trojans

In the case of Jupiter´s Trojans we implement the previous estimates in the case $m = 2$. The full normal form and the remainder in terms of the mapping of radii can be found in the Appendix.

7.2.1. Preliminaries

In the case of the Sun-Jupiter-Trojan model the space of radii is 2-dimensional, since

$$\rho_1 = \zeta_1 \, \overline{\zeta}_1,$$

$$\rho_2 = \zeta_2 \, \overline{\zeta}_2 \tag{21}$$

and the mapping of radii (9) therefore reduces to:

$$\rho_{1,n+1}{}^2 = \rho_{1,n}{}^2 + \mathcal{R}_1{}^{(r,s)} = \rho_{1,n}{}^2 + \sum_{i+j=r+2}^{s} a_{i,j}{}^{(r)} \rho_1{}^i \rho_2{}^j,$$

$$\rho_{2,n+1}{}^2 = \rho_{2,n}{}^2 + \mathcal{R}_2{}^{(r,s)} = \rho_{2,n}{}^2 + \sum_{i+j=r+2}^{s} b_{i,j}{}^{(r)} \rho_1{}^i \rho_2{}^j. \tag{22}$$

Denoting by $f_\kappa{}^{(r)}$ the sum over $a_{i,j}{}^{(r)} \rho^i \rho^j$ and by $g_\kappa{}^{(r)}$ the sum over $b_{i,j}{}^{(r)} \rho^i \rho^j$, where $\kappa = i + j$ the mapping also may be written in terms of

$$\rho_{1,n+1}{}^2 = \rho_{1,n}{}^2 + \sum_{\kappa=r+2}^{s} f_\kappa{}^{(r)},$$

$$\rho_{2,n+1}{}^2 = \rho_{2,n}{}^2 + \sum_{\kappa=r+2}^{s} g_\kappa{}^{(r)}, \tag{23}$$

where the functions $f_\kappa{}^{(r)}$, $g_\kappa{}^{(r)}$ depend on all the four variables

$$\zeta_1 = \rho_1 \, e^{i\,\phi_1},$$

$$\zeta_2 = \rho_2 \, e^{i\,\phi_2}, \tag{24}$$

and $\left(\overline{\zeta}_1, \ \overline{\zeta}_2\right)$. The parametrization of the space of radii (10) can be performed using

$$\rho_1 = \rho \cos(\gamma),$$

$$\rho_2 = \rho \sin(\gamma), \tag{25}$$

where γ is the angle defining the direction in the $(\rho_1 \times \rho_2)$ space and since $\rho_1, \rho_2 > 0$, it is defined in the interval $\gamma \in (0, \pi/2)$. By implementing this parametrization in the mapping (23) we get

$$\rho_{1,n+1} = \rho_{1,n}{}^2 + \sum_{i+j=r+2}^{s} a_{i,j}{}^{(r)} \cos^i(\gamma) \sin^j(\gamma) \cdot \rho^{i+j},$$

$$\rho_{2,n+1} = \rho_{2,n}{}^2 + \sum_{i+j=r+2}^{s} b_{i,j}{}^{(r)} \cos^i(\gamma) \sin^j(\gamma) \cdot \rho^{i+j}. \tag{26}$$

The majorant series is defined via $\left|A_\gamma\right|$, $\left|B_\gamma\right|$, which is after definition of A_γ, B_γ according to:

$$A_\gamma^{(r)} = \sum_{i+j=r+2}^{s} \left| a_{i,j}^{(r)} \cos^i(\gamma) \sin^j(\gamma) \right|,$$

$$B_\gamma^{(r)} = \sum_{i+j=r+2}^{s} \left| b_{i,j}^{(r)} \cos^i(\gamma) \sin^j(\gamma) \right| \tag{27}$$

given by

$$\rho_{1,n+1} = \rho_{1,n}^2 + \sum_{\kappa=r+2}^{s} A_\gamma^{(r)} \cdot \rho^\kappa,$$

$$\rho_{2,n+1} = \rho_{2,n}^2 + \sum_{\kappa=r+2}^{s} B_\gamma^{(r)} \cdot \rho^\kappa. \tag{28}$$

The mapping of radii (28) upper-bounds the motion in the action space and can be used to implement the stability estimates. The larger the radius of convergence of the mapping, the larger the distance in phase space we could ask for to be Nekhoroshev stable for a finite Nekhoroshev time T_{Nek}.

7.2.2. Radius of convergence and the remainder function

The convergence of the majorant mapping (28) of (23) is given by:

$$\lim_{r \to \infty} \frac{\left| f_{\kappa+1}^{(r)} \right|}{\left| f_\kappa^{(r)} \right|} < q_1 < 1,$$

$$\lim_{r \to \infty} \frac{\left| g_{\kappa+1}^{(r)} \right|}{\left| g_\kappa^{(r)} \right|} < q_2 < 1, \tag{29}$$

which we need to estimate along different directions γ in order to determine the radius of convergence ρ_γ. For this reason we calculate the ratios (29) by use of the majorant mapping (28) numerically up to sufficiently high orders, where the ratios stabilize. For the original mapping stabilization is found at $r \sim 15$, yielding the convergence radius as:

$$\rho_\gamma < \min\left(\frac{1}{q_{1,\gamma}}, \frac{1}{q_{2,\gamma}} \right), \tag{30}$$

where $q_{1,\gamma}$, $q_{2,\gamma}$ are also defined through:

$$q_{1,\gamma} = \frac{A_\gamma^{(r+1)}}{A_\gamma^{(r)}},$$

$$q_{2,\gamma} = \frac{B_\gamma^{(r+1)}}{B_\gamma^{(r)}}. \tag{31}$$

The norm of the remainders, within the radius of convergence given by (31) can be bound along

different directions γ according to:

$$\| \, \mathcal{R}_1^{(r,s)} \, \|_\lambda = \sum_{\kappa=r+2}^{s} A_\lambda^{(r,\kappa)},$$

$$\| \, \mathcal{R}_2^{(r,s)} \, \|_\lambda = \sum_{\kappa=r+2}^{s} B_\lambda^{(r,\kappa)} \tag{32}$$

and according to our construction it holds true that

$$\| \, \mathcal{R}_1^{(r,s)} \, \| \;\leq\; \| \, \mathcal{R}_1^{(r,s)} \, \|_\lambda,$$

$$\| \, \mathcal{R}_2^{(r,s)} \, \| \;\leq\; \| \, \mathcal{R}_2^{(r,s)} \, \|_\lambda,$$

where $\| \, \mathcal{R}^{(r,s)} \, \| = \left(\| \, \mathcal{R}_1^{(r,s)} \, \|, \, \| \, \mathcal{R}_2^{(r,s)} \, \| \right)$ is the remainder of the original mapping (22, 23) and $\| \, \mathcal{R}^{(r,s)} \, \|_\gamma = \left(\| \, \mathcal{R}_1^{(r,s)} \, \|_\gamma, \, \| \, \mathcal{R}_2^{(r,s)} \, \|_\gamma \right)$ is the remainder due to the majorant mapping of radii, given by (28). In view of (20), we are now able to find the Nekhoroshev stable region for Trojan asteroids in the Sun-Jupiter case in the space of radii $(\rho_1 \times \rho_2)$. In the next step we will transform the convergence region and the estimates of the mapping of radii from the plane of radii to the domain of convergence of the space of proper elements (D_p, e_p). This can be achieved by back transforming the two-torus with $\rho_1 = \rho \cos(\gamma)$ and $\rho_2 = \rho \sin(\gamma)$ to complex variables using the definition:

$$z_1 = \rho_\gamma \cos(\gamma) \, e^{-i \, \varphi_1},$$

$$z_2 = \rho_\gamma \sin(\gamma) \, e^{-i \, \varphi_2} \tag{33}$$

and scan the whole torus $(\varphi_1, \varphi_2) \in [0, 2\pi) \times [0, 2\pi)$ in order to find the maximum and minimum values of the quantities:

$$(\tau, \, \omega, \, x, \, h = e(y)), \tag{34}$$

by means of $\boldsymbol{\Phi^{-1}}$ (18;6, 41;6) and $\boldsymbol{B}^{-1}$ (7;6) or (32;6). This torus is labelled by one pair of values of the proper elements, defined by

$$D_p = (\tau_{\min} - \tau_{\max}) / 2,$$

$$e_p = (h_{\min} - h_{\max}) / 2. \tag{35}$$

7.3. Nekhoroshev estimates in the Sun-Jupiter-Trojan system

Plotting $D_p(\gamma)$ vs. $e_p(\gamma)$ for $0 \leq \gamma < \pi/2$ yields the boundary of the grey-shaded region in Figure 1, which corresponds to the convergence region of the mapping in the space of radii (23), which can be translated to a mapping in the space of proper elements. On the other hand, for any particular direction γ in the space of radii (23), the Nekhoroshev domain of stability region is given by finding, through

(20) with $T_{\text{Nek}} = 10^9$ (revolution periods of Jupiter), the value of the normalization order r, at which one obtains the maximal value of ρ_γ. Back-transforming from the space of radii to the space of proper elements (similar to the convergence region), the stability region in proper element space is given in Figure 1 and bounded by the continuous black line. The numbers in the picture indicate the optimal order of truncation, at which ρ_γ was found in the space of radii. The positions of the observed asteroids in proper element space are shown as points respectively. They are based on a catalogue (http://hamilton.dm.unipi.it/cgi-bin/astdys/astbio), which is based on a variant of Milani´s (1993) calculation of proper elements in the (D_p, e_p)-plane. Most asteroids of the database come with high inclinations, thus the picture is just indicative, since the points are in fact projections to the (D_p, e_p)-plane. Asteroids on inclined orbits are also diffusing chaotically towards higher proper eccentricities as a result of resonant interactions with the Solar system (Robutel, Gabern, Jorba 2005), an effect which we do not take into account in our model. Nevertheless a few real asteroids are within the analytically calculated domain of stability, and most other are outside it by a factor ≤ 3 in the maximum distances in the axes D_p, e_p.

$$T_{\text{Nek}} = 10^9 P_J$$
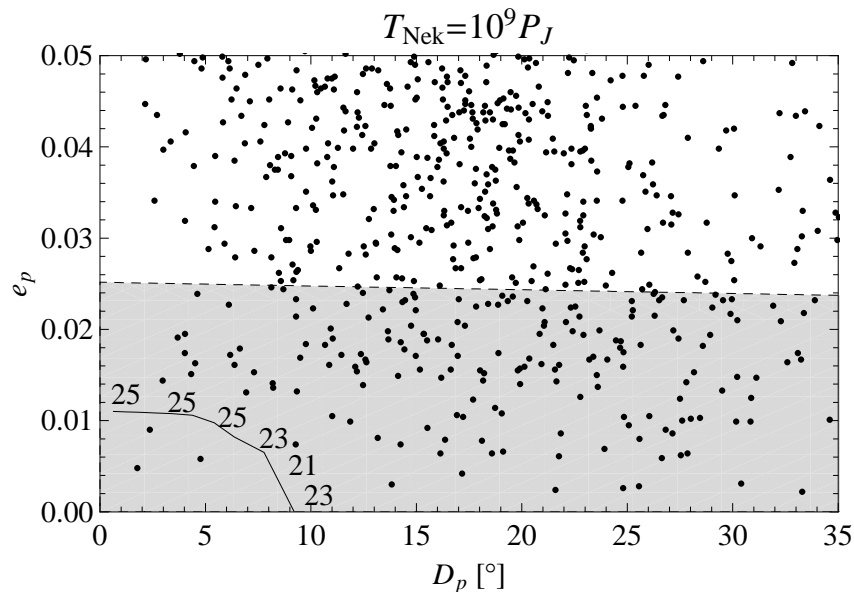
Figure 1.: Nekhoroshev stable asteroids (points) within the age of the Solar system. The mapping converges in the gray shaded region, the stable region is bounded by the thick line. Note the dependency of the region on the optimal order of truncation (21-25+).

The physical interpretation of Figure 1 is the following: The analytically obtained region of Nekhoroshev stability covers $\sim 13\%$ of the convergence domain. In addition, a few asteroids are found within the analytically calculated domain of stability. The stability region is bounded by libration amplitude $D_p < 10°$ and proper eccentricity $e_p < 0.01$. While the maximum value of D_p is close to the value given in Efthymiopoulos & Sándor 2005, the latter seems to be underestimated. The reason is found in the small convergence region of the mapping with respect to proper eccentricities $(e_p < .025)$

and the estimates for e_p could probably be improved by improving the convergence domain of the original explicit mapping.

7.3.1. Analysis of the remainder function

The estimates depend on the size of the remainder function $\mathfrak{R}^{(r)}$, the order of normalization r, the distance in phase space ρ and the direction γ in action space. The influence of the order on the size of the remainder terms, and therefore the optimal order of normalization is given in Figures 2 and 3. In Figure 2 estimates of the size of the remainder as a function of the normalization order r are given for different direction angles $\gamma \in (0°, 18°, \ldots, 90°)$ and different distances in phase space, $\rho_\gamma \in (0.24 \times 10^{-2}, \ldots, 0.017)$. In Figure 3 similar plots are given for different distances in phase space $\rho_\gamma \in (0.75 \times 10^{-2}, \ldots, 0.045)$ by varying the direction angles γ from $0°$ to $90°$ in steps of $18°$. One clearly sees, that for small distances ρ_γ the optimal order of truncation is not reached until $r = 25$. For smaller angles γ the optimal order r lies near 25 and it is shifted to higher orders of normalization for larger values of γ (Figure 2), which is connected to the conclusion given at the end of Section 7.1.1.
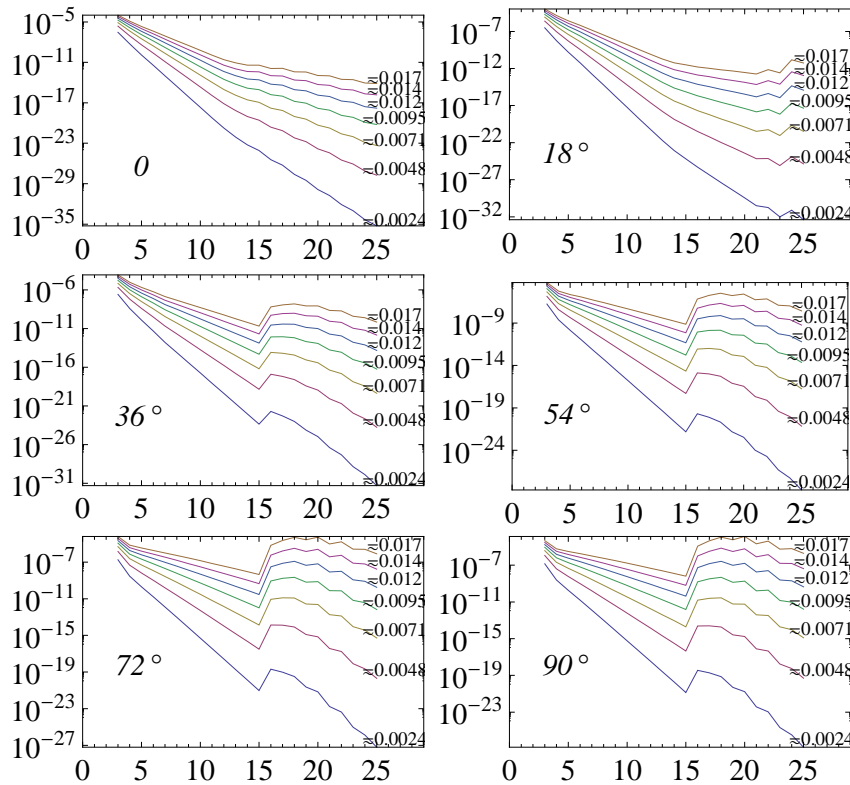
Figure 2.: Dependency of $\| \mathfrak{R} \|_{max}\, \rho_\gamma{}^r$ (ordinate) on the normalization order r (abscissa) and distance ρ.

On the other hand the optimal order of truncation is shifted to smaller values of r when increasing the distance ρ_γ sufficiently (Figure 3). The optimal order of truncation reaches $r = 15$ for very large distances $(\rho_\gamma = 0.045)$ and increases for smaller values of ρ_γ. The influence of the direction angle on the optimal order of normalization is smaller, the optimal order marginally increasing when γ increases. Both figures are given in log-linear scale: while in Figure 2 the ordinate varies up to 30 orders of magnitude with respect to changes in ρ_γ, it varies only up to 10 order of magnitudes when changing γ. Both arguments indicate that a change in ρ_γ dominates the change in the behavior of the remainder, compared to variations in γ.
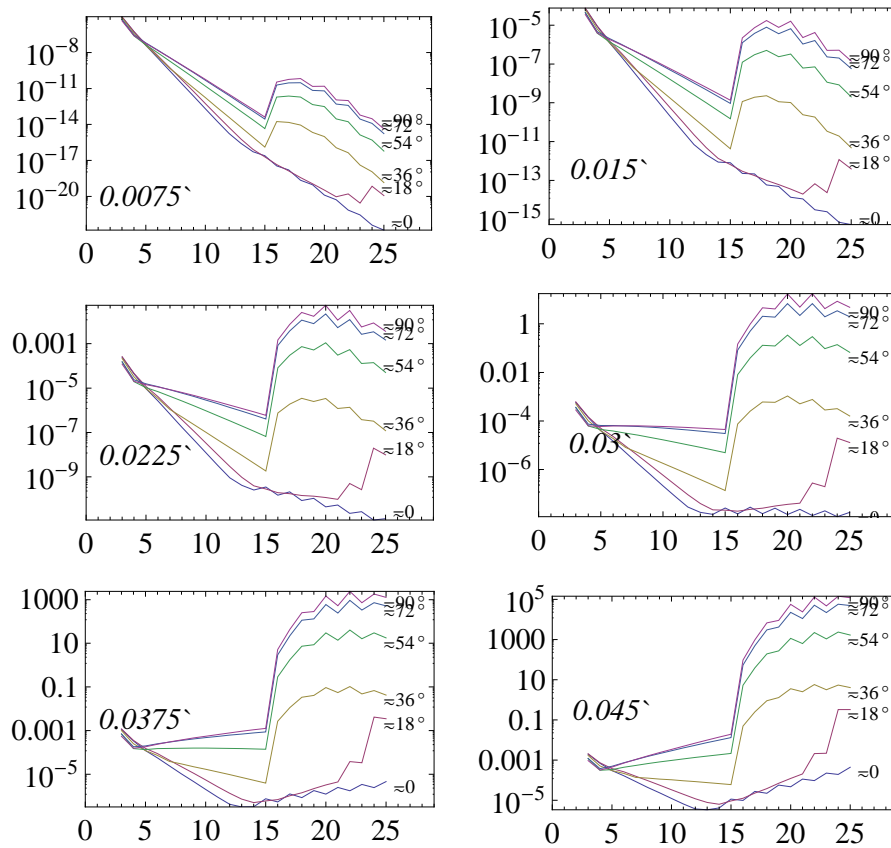
Figure 3.: Dependency of $\| \mathbb{R} \|_{max} \, \rho_\gamma{}^r$ (ordinate) on the normalization order r (abscissa) and direction γ.

An interesting feature, connected to Figures 1, 2 of Chapter 6 shows up when analyzing the series behavior: in both figures 2 and 3 an abrupt change of the remainder function with respect to the normalization order occurs around the normalization order $r = 15$, for sufficiently large direction angles γ. There are two reasons for this behavior: i) the generating function of the mapping was expanded up to order 16 (Chapter 5). Therefore the mapping is symplectic up to order 15. The abrupt change is then partly due to the loss of symplecticity after the order 15. ii) Since the function $\rho_\gamma{}^r$ is smooth with respect to r, its behavior leads also to a change in the gradient of the remainder function

$\| \mathcal{R}^{(r)} \|_{\max}$ with respect to the normalization order r. This can be explained by analyzing the small divisor terms in the normal form construction (25;6, i.e. 43;6). It is done in the next Section.

7.3.2. Small divisors

A small divisor of the normal form construction is defined by looking for integer values α_1, α_2, β_1, β_2, where one of the denominators in (43;6), i.e.

$$\exp(i\,(\alpha_1 - \beta_2)\,\omega_1 + (\alpha_2 - \beta_2)\,\omega_2) - \exp(i\,\omega_1),$$

$$\exp(i\,(\alpha_1 - \beta_2)\,\omega_1 + (\alpha_2 - \beta_2)\,\omega_2) - \exp(i\,\omega_2)$$

becomes very small, i.e. close to zero. The smallness mainly depends on the fundamental periods of the system, namely ω_1 and ω_2 in the Sun-Jupiter system (35;6). Since the order of normalization is connected to the order of truncation in the series, according to $r = \alpha_1 + \alpha_2 + \beta_1 + \beta_2$, the first occurrence of a specific small denominator is determined by the order of normalization. The first dominating small divisors in the Sun-Jupiter case are $a_2 \sim 2.02 \times 10^{-2}$ and $a_3 \sim 4.05 \times 10^{-2}$ respectively. In principle the growth of the series coefficients due to the normal form construction is dominated by those. At a higher normalization order r additional small divisors may occur and are summarized in Table 1. While the left column summarizes the first occurrences of small divisor terms regarding the operator $\Delta_{\omega,1}^{-1}$, the right column does so for $\Delta_{\omega,2}^{-1}$. The order of normalization is given in the first column, the responsible monomial term $\zeta_1^{\alpha_1} \zeta_2^{\alpha_2} \overline{\zeta}_1^{\beta_1} \overline{\zeta}_2^{\beta_2}$ in the second and the order of magnitude in the last column respectively. Both subtables clearly indicate that a new pair of small divisors appear at order 15 and 16 respectively. Since they act at each normalization step from there on, they also affect the growth behavior of the whole series beyond the order 15.

r	α_1	α_2	β_1	β_2	a_r	r	α_1	α_2	β_1	β_2	a_r
15	0	0	11	4	1.92×10^{-2}	15	0	0	12	3	1.92×10^{-2}
16	0	0	11	5	1.01×10^{-3}	16	0	0	12	4	1.01×10^{-3}
25	0	25	0	0	9.28×10^{-3}	25	1	0	0	24	9.28×10^{-3}
33	0	0	23	10	2.02×10^{-3}	33	0	0	24	9	2.02×10^{-3}
59	0	46	13	0	6.68×10^{-4}	59	14	0	0	45	6.68×10^{-4}
66	0	41	25	0	3.41×10^{-4}	66	26	0	0	40	3.41×10^{-4}

Table 1.: Small divisors in the Sun-Jupiter-Trojan model: Δ_1^{-1} (left) and Δ_2^{-1} (right).

The size of a_{15} is comparable to the size of a_2, while the effect of a_{16} is one magnitude larger. Both together dominate the behavior of the series expansions (and therefore also the norm of the remainders in Figure 2 and 3) from this order on, and are thus able to explain the local divergent behavior of the

approximate integrals, already found in Figure 1 & 2 (Chapter 6). In Figure 4 the normalization scheme was ´simulated´ up to order 70 according to a numerical method outlined in Subsection 7.3.3.. It shows the occurrences of the small denominator terms given in Table 1. The dominant denominator is clearly identified a_{16} over a long period of the normalization process and although new small divisors occur at order 25 and 33, the first smaller small divisor appears at order 59, namely $a_{59} \sim 10^{-4}$. After a few normalization steps an additional small divisor occurs, a_{66} governing the size of the series expansions from there on. Although the number of possible small denominators at order r is finite, as long the truncation order itself is finite, the accumulation of small divisor terms spoils the convergence of the series beyond the optimal order of truncation.
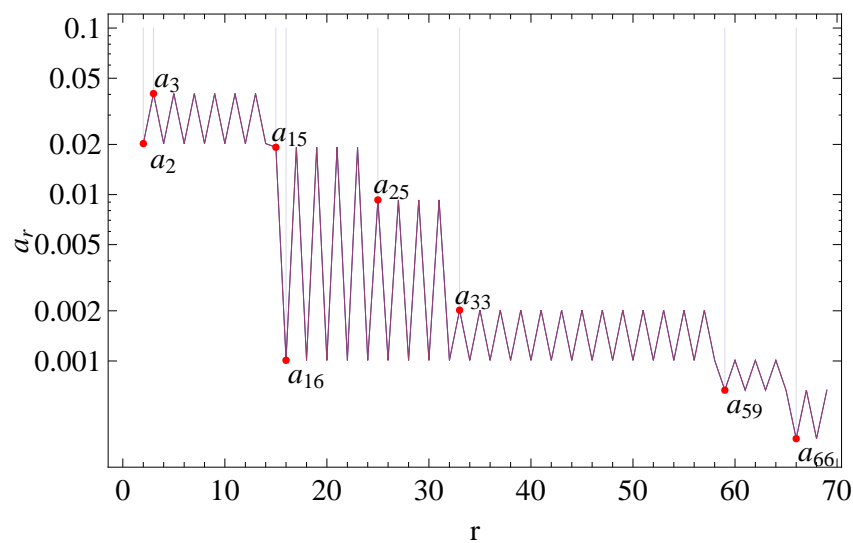
Figure 4.: Small divisors of the Sun-Jupiter system with increasing normalization order.

All figures (Figure 2, 3, 4) therefore already demonstrate the expected behavior of formal series due to the Birkhoff normal form construction. Namely the remainder initially decreases as the order of normalization increases (Figure 2, 3) giving the impression, that the norm of the remainder will tend to zero as $r \to \infty$. This trend is broken due to the accumulation of small divisor terms and even reversed after the optimal order of truncation. The change in the growth of the norm of the remainder function can be attributed to the introduction of new small divisors, which act in the normal form construction by pushing the coefficients of the series expansions to higher and higher orders of magnitude. Indeed with increasing normalization order r the size of the remainder will itself tend to infinity.

Nekhoroshev estimates are therefore optimal at the optimal order of truncation. The estimates in use of (20) are also valid before and beyond, but indeed an underestimation of the stability region. In our attempt we stopped the calculations at the order of normalization $r = 25$, which is at the edge of the optimal order in the normalization scheme for small γ and moderate ρ_γ. On the other hand for larger γ and smaller ρ_γ the optimal order of truncation is beyond our limit, but since the small denominator a_{16}

governs the series expansions up to very high orders ($r \to 60$), the growth behavior of the remainder function will not change significantly. Therefore the order of truncation $r = 25$ seems also to be acceptable, in this case. For larger radii ρ_γ in $\rho_1 \times \rho_2$ phase the optimal order of truncation turns out to be smaller (Figure 3) but the estimates are anyway restricted to lie well within the convergence region of the mapping.

7.3.3. Outlook: pseudo series
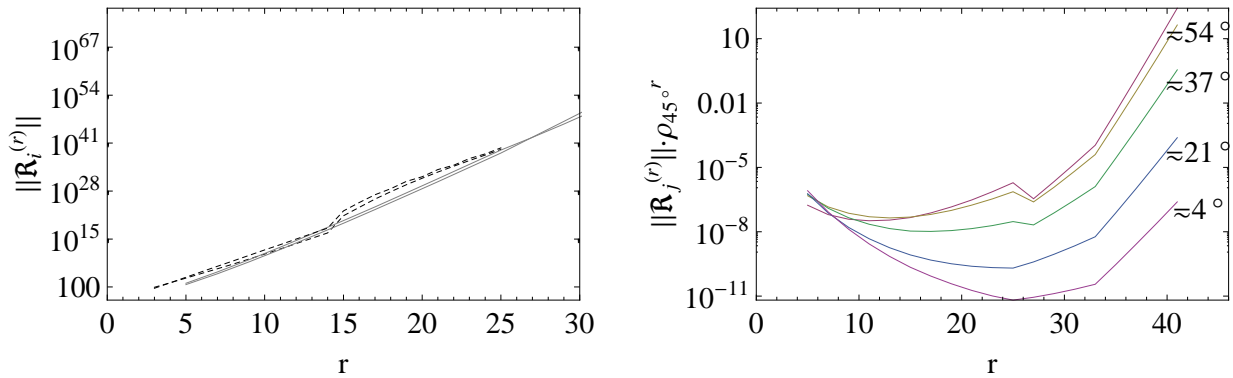
Figure 5.: Non rigorous pseudo-remainder estimate for ρ=0.02 and γ=45°.

A different approach to Nekhoroshev estimates will now be discussed with the help of Figure 5. On the basis of the theory developed by Efthymiopoulos et al. (2004), it is in principle possible to estimate the size of the coefficients of the formal series from the normal form construction itself, without performing the real normalization procedure. The size of the generating function Φ can be proven to be estimated by a detailed analysis of the propagation of small divisors in the various terms of the series (Servizi et al 1983, Efthymiopoulos et al. 2004). The main result is, that the remainder appears as piecewise geometrical, thus the ratio of successive orders is given by:

$$\frac{\| \mathcal{R}^{(r+2)} \|}{\| \mathcal{R}^{(r)} \|} \equiv \lambda_r,$$

is almost constant within fixed intervals of values of r but increases by abrupt steps at particular values of r. In the $2D$ case these values are connected to number-theoretical properties of the fundamental period of the system ω_1. Letting q_n, d_n being the n-th member of the continued fraction sequence of one specific ω_0, the values of abrupt change can be estimated to be equal to $r = q_n + d_n$. The continued fractions sequence regarding the larger period $\omega_1 / 2\pi$ is given by:

$$\left(0, \ \frac{1}{12}, \ \frac{5}{61}, \ \frac{31}{378}, \ \frac{36}{439}, \ \ldots \right),$$

which should be compared to the case of the circular problem, given in Efthymiopoulos & Sándor 2005. Although the difference in the approximation is clearly due the different approximation of the fundamental period in the system ($\omega_0 \simeq 0.0808\ldots$ vs. $\omega_1 \simeq 0.08200$), the first continued fraction approximation is given by $1/12$ in both. Since the normalization procedure starts at order 3, the abrupt change of the quantities, shown in figures (1,2;6 and 2, 3) at order 15 fits well to the predicted value. On the other hand the growth factor in the circular case, was found to be:

$$\lambda_r \simeq \max_{\kappa,\lambda \in \mathbb{N}} \left\{ \frac{A\,|\kappa - \lambda|}{\left| e^{(\kappa - \lambda)\,\omega_0 - 1} \right|} \right\},$$

where κ, λ are integer exponents in the mapping and ω_0 is the fundamental period in the circular case. The fact that the quantity A is constant depends on the size of the nonlinear part of the mapping and was estimated by the authors. In our case of the ERTBP the behavior of the series also depends on the interactions between ρ_1 and ρ_2 and therefore ω_1 and ω_2. This complicates the analysis. A first rough analysis of the influence of (43;6) on arbitrary terms of the form:

$$c_{\alpha_1,\alpha_2,\beta_1,\beta_2}\, \zeta_1^{\alpha_1}\, \zeta_2^{\alpha_2}\, \overline{\zeta}_1^{\beta_1}\, \overline{\zeta}_2^{\beta_2}$$

shows that the following terms could be produced in the normalization procedure at each second step:

$$\lambda_1 \times c_{\alpha_1,\alpha_2,\beta_1,\beta_2}\, \zeta_1^{\alpha_1+1}\, \zeta_2^{\alpha_2}\, \overline{\zeta}_1^{\beta_1+1}\, \overline{\zeta}_2^{\beta_2},$$

$$\lambda_2 \times c_{\alpha_1,\alpha_2,\beta_1,\beta_2}\, \zeta_1^{\alpha_1}\, \zeta_2^{\alpha_2+1}\, \overline{\zeta}_1^{\beta_1}\, \overline{\zeta}_2^{\beta_2+1},$$

$$\lambda_3 \times c_{\alpha_1,\alpha_2,\beta_1,\beta_2}\, \zeta_1^{\alpha_1+1}\, \zeta_2^{\alpha_2}\, \overline{\zeta}_1^{\beta_1+1}\, \overline{\zeta}_2^{\beta_2},$$

$$\lambda_4 \times c_{\alpha_1,\alpha_2,\beta_1,\beta_2}\, \zeta_1^{\alpha_1}\, \zeta_2^{\alpha_2+1}\, \overline{\zeta}_1^{\beta_1}\, \overline{\zeta}_2^{\beta_2+1}.$$

On the other hand, the growth factors λ_i, $(i = 1, \ldots, 4)$ are again strongly connected to the dominating divisor a_r, being small and appearing at order r. Denoting by $u_{11}, u_{12}, u_{21}, u_{22}$ the coefficients of the lowest order normal form terms of monomials of the form $\zeta_1^2 \overline{\zeta}_1$, $\zeta_1 \zeta_2 \overline{\zeta}_1$ and $\zeta_2^2 \overline{\zeta}_2$, $\zeta_1 \zeta_2 \overline{\zeta}_1$ respectively, the growth factors in the case of the ERTBP could be estimated along the direction $\gamma = 45°$ to be:

$$\lambda_1 = e^{i(\alpha_1 - \beta_1)\omega_1 + (\alpha_2 - \beta_2)\omega_2} \frac{\left(\alpha_1 u_{11} e^{-i\omega_1} + \beta_1 \overline{u}_{11} e^{i\omega_1} \right)}{a_r},$$

$$\lambda_2 = e^{i(\alpha_1 - \beta_1)\omega_1 + (\alpha_2 - \beta_2)\omega_2} \frac{\left(\alpha_1 u_{12} e^{-i\omega_1} + \beta_1 \overline{u}_{12} e^{i\omega_1} \right)}{a_r},$$

$$\lambda_3 = e^{i(\alpha_1 - \beta_1)\omega_1 + (\alpha_2 - \beta_2)\omega_2} \frac{\left(\alpha_2 u_{21} e^{-i\omega_2} + \beta_2 \overline{u}_{21} e^{i\omega_2} \right)}{a_r},$$

$$\lambda_4 = e^{i(\alpha_1-\beta_1)\omega_1+(\alpha_2-\beta_2)\omega_2} \frac{\left(\alpha_2\,u_{22}\,e^{-i\,\omega_2} + \beta_1\,\overline{u}_{22}\,e^{i\,\omega_2}\right)}{a_r}.$$

To this end it is possible to predict the size of the coefficients in the normal form by growth factors, instead of actually calculating them. One "just" needs to identify the dominant paths (schematics in Figure 6) of the normalization procedure: starting with a "real" normalized series expansion of order r_0, one could use dominating monomials as a starting point. Implementing the growth factors on the series, a "pseudo" series can be established, and the remainder can be estimated from it, as usual.
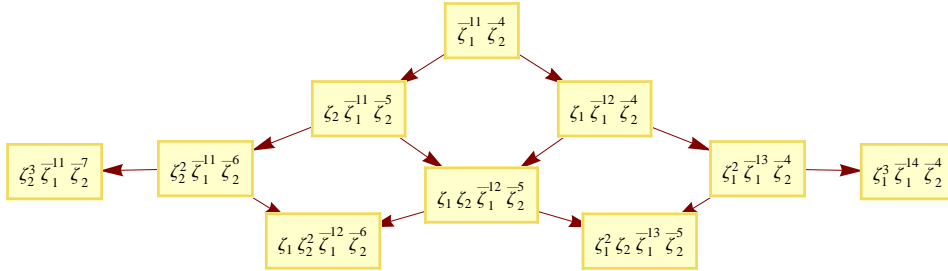
Figure 6.: Schematic example of a dominating path, starting with monomial of form $\overline{\zeta}_1^{\,11}(\overline{\zeta}^4)_2$. Each line indicates one step of Birkhoff normalization.

The growth of the remainder function in $\rho_1 \times \rho_2$ space was found to be in good agreement with respect to directions parametrized by $\gamma = 45\,°$: Preliminary results are presented in Figure 5 (left), where the size of the remainders $\|\mathcal{R}_1^{(r)}\|$ and $\|\mathcal{R}_2^{(r)}\|$ are plotted in dependency of the normalization order r. The norms of the real remainders are given in dashed dark lines, while the norms of the pseudo-remainders are plotted in gray lines. Again we find an abrupt change of the slope of $\mathcal{R}^{(r)}$ around normalization order 15. Although the norm based on the calculation of the pseudo-remainder does not indicate the abrupt change in the slope, it reproduce the slope of the overall dependency on r quite well. In the right frame of Figure 5, the results of the estimation of the pseudo-remainder are used to reproduce the optimal order of truncation at the radius of convergence $\rho_{45°} \simeq 0.2$. Again the optimal order of truncation is found at $r \sim 25$, indicating, that the Nekhoroshev estimates based on estimates of the remainder are valid along this direction. For small variations of the direction angles γ around $45\,°$, the construction of the pseudo-remainder is still valid, while for different direction angles the correspondence between the real and estimates norms brakes. The reason was found in a complex interaction of $\rho_1 \times \rho_2$ space and is subject of future investigations.

8. Summary and Discussion

8.1. English

The question of the long-term stability of our Solar system is still a partly unsolved problem even nowadays. Nevertheless, the treatment of this problem by various scientists (see overview in the Introduction) during the last centuries can be seen as the origin of the modern formulation of science, from which i.e. the KAM or the Nekhoroshev theorem originated in the field of dynamical systems. Based on the results of the latter theorem, the goal of the present thesis is to show the existence of a physically relevant Nekhoroshev stable region around the equilateral fixed points of the elliptic restricted problem for times comparable to the life-time of a planetary system. Since the restricted problem serves as the basic model to describe the motion of asteroids in our own Solar system (their masses can be neglected compared to the masses of the planets) the stability result stated in the restricted problem directly translates into a stability result of motion in our own Solar system. The observation of real asteroids on the one hand and the existence of a Nekhoroshev-type stability region around the Lagrangian equilibrium points, e.g. of Jupiter, shows the possibility of stable motion in our Solar system for the age of itself. It is therefore possible to give a relevant insight into the history of our Solar system by i) observations and the use of a ii) pure mathematical tool, the Nekhoroshev theorem.

Short summary of the thesis:
The KAM and Nekhoroshev theorems are stated in the Introduction, the latter is outlined in detail in Chapter 2. The restricted problem is subject of Chapter 3 which serves as the model to state the stability results in the present thesis for asteroids near the 1:1 mean motion resonance of the planet Jupiter and Trojan asteroids. The mathematical realization, i.e. the disturbing function of the 1:1 commensurability is developed in Chapter 4 and given in the Appendix for arbitrary semi-major axes and eccentricities of the perturbing planet. It can be used for arbitrary configurations of the restricted problem and is therefore also applicable to describe asteroidal motion in exo-planetary systems. Since the stability result is derived on the basis of estimates of the remainder of normal form mappings, the symplectic mapping model for the elliptic restricted problem near the 1:1 resonance is developed in Chapter 5. The normal form theory is derived in Chapter 6 which directly leads to the Nekhoroshev-type stability result given in Chapter 7.

The main conclusions of the present research study:
◆ i) It is possible to show the existence of a relevant Nekhoroshev-type stable region around the equilateral equilibria points of the *elliptic* restricted problem. Real observed asteroids are found within

this region. The present thesis therefore extends previous results based on the *circular* restricted problem.

◆ ii) Since, the operations of series expansion and series reversion of the mapping also limits the domain of convergence of the mapping approach, the stability result is restricted to the librational regime of asteroid motion. It is not possible to state a stability result with the present results for the rotational regime of motion.

◆ iii) Within the domain of convergence of the mapping the size of the coefficients of the formal series expansions depends not only on the normalization order, but also on the direction in phase space, i.e. the variation in the amplitudes of libration and the eccentricity of the test particle. This leads to the concept of directional exponential stability in higher dimensional action space and is part of future investigations.

◆ iv) Analytical formulae are given in Chapter 7 relating the size of stability to the size of the remainder of the normal form along specific directions in action space of the restricted problem. The results are not limited to our Solar system configurations but are also applicable to exo-planetary configurations.

◆ v) In the case of Jupiter´s Trojan asteroids, a domain of stability for the age of the Solar system could be derived by analytical means. It is quite realistic with respect to proper librations of the asteroids but limited with respect to the proper eccentricities due to the limited convergence of the mapping approach. Trojan asteroids in the Sun-Jupiter system are stable for the age of the Solar system for proper eccentricities $e_p < 0.01$ and proper librations $D_p < 10\,^\circ$.

The present study indicates the possibility of long-term stability of asteroids in our Solar system for the age of planetary systems in the framework of the elliptic restricted three body problem. It is the natural generalization of former studies based on the circular restricted problem. Despite this successful generalization, the present research study still neglects the effect of the inclination of the asteroids and the influence of the other planets on the stability region, which is still beyond the cope of a pure analytical treatment nowadays due to the complexity of the calculations. Nevertheless, it is a necessary step for this kind of generalizations of previous results and clearly demonstrates, even at this point, the relevance of a pure mathematical theorem on the behavior of physical systems, like our own Solar system.

8.2. Deutsch

Die Frage nach der Langzeitstabilität unseres Sonnensystems kann nach wie vor nicht völlig beantwortet werden. Die Untersuchung dieser Frage hat dennoch, in den letzten Jahrhunderten, die moderne Formulierung heutiger Wissenschaftsdisziplinen maßgeblich beeinflusst (Hamilton, Lagrange, ...). Wegweisende Entdeckungen, wie das KAM und Nekhoroshev Theorem, im Umfeld des Spezialgebiets Dynamischer Systeme, sind auf diesem Wege entstanden. Basierend auf dem Nekhoroshev Theorem, soll in dieser Arbeit gezeigt werden, das es auch um die equilateralen Gleichgewichtspunkte des elliptischen eingeschränkten Dreikörperproblems einen Nekhoroshev-stabilen Bereich gibt, der für das Zeitalter eines Planetensystems physikalisch relevant ist. Da die Massenverhältnisse in unserem Sonnensystem erlauben, die Massen der Asteroiden im Vergleich zu den Massen der Planeten zu vernachlässigen, ist das eingeschränkte Dreikörperproblem der erste Schritt, die Bewegung der Asteroiden in unserem Sonnensystem zu beschreiben. Aus der Stabilität von Testteilchen im eingeschränkten Dreikörperproblem folgt daher ebenso die Stabilität von Asteroiden in unserem Sonnensystem (in seiner vereinfachten Darstellung). Zusammen mit der Beobachtung von realen Asteroiden um die Lagrangepunkte, z.B. von Jupiter, ist es daher möglich, stabile Bewegung in unserem Sonnensystem für das Zeitalter desselben zu zeigen: Die Beobachtungen, zusammen mit einer rein mathematische Theorie, das Nekhoroshev Theorem, geben Einsicht in die geschichtliche Entwicklung unseres eigenen Sonnensystems.

Kurzdarstellung der Dissertation:

Beide mathematischen Theorien, das KAM und Nekhoroshev Theorem, werden in der Einleitung kurz behandelt, wobei das Nekhoroshev Theorem in Kapitel 2 näher beschrieben wird. Das eingeschränkte Dreikörperproblem liegt den Untersuchungen dieser Arbeit zu Grunde und ist daher Thema von Kapitel 3. Die mathematische Beschreibung der Trojaner-Asteroiden-Bewegung wird in Kapitel 4 hergeleitet, die Störfunktion der Hamiltonfunktion für beliebige System-Parameter findet sich im Anhang II der vorliegenden Arbeit. Da die Angabe des Stabilitätsbereichs auf Abschätzungen der Restglieder von Normalformen von Differenzengleichungen beruht, ist die symplektische Abbildung, welche die Asteroidenbewegung in unserem Sonnensystem beschreibt, Thema von Kapitel 5. Die Theorie von Normalformen von symplektischen Abbildungen wird in Kapitel 6 entwickelt, der Zusammenhang zwischen den Restgliedern dieser Formen und deren Auswirkung auf den Stabilitätsbereich zusammen mit Ergebnissen bzgl. den Jupiter-Trojanern in Kapitel 7 vorgestellt.

Die wichtigsten Resultate der vorliegenden wissenschaftlichen Arbeit:

◆ i) Die Existenz eines relevanten Nekhoroshev stabilen Bereichs um die Lagrangepunkte des *elliptischen* eingeschränkten Dreikörperproblems wurde gezeigt. Reale Asteroiden können in diesem

Bereich beobachtet werden. Das Resultat erweitert somit vorangegangene Studien basierend auf dem *kreisförmigen* Modell des eingeschränkten Dreikörperproblems.

◆ ii) Der Konvergenzbereich der Methode beschränkt sich auf den Phasenraumbereich des Librationsbewegungen von Asteroiden. Die Ursache liegt in der beschränkten Konvergenz der Störreihen. Über Bereiche außerhalb des Konvergenzradius kann anhand der vorliegenden Arbeit keine Aussage bzgl. der Stabilität im Sinne Nekhoroshev getroffen werden.

◆ iii) Die Stabilität folgt direkt aus der Größe der nichtlinearen Anteile. Diese hängt nicht nur von der optimalen Ordnung, sondern auch von der Richtung im Phasenraum ab, in der die Stabilität untersucht wird. Es wurde gezeigt, dass die Stabilität im höher-dimensionalen Wirkungsraum von der Richtung abhängen kann. Diese Erkenntnis ist Bestand zukünftiger Untersuchungen.

◆ iv) Ein analytischer Ausdruck, der die Größe des Stabilitätsbereichs, mit der Nekhoroshev Zeit und der optimalen Richtung verbindet, wurde in Kapitel 7 abgeleitet. Die Anwendbarkeit der Formeln beschränkt sich nicht nur auf unser Sonnensystem, sondern kann auch für extrasolare Planetensysteme verwendet werden.

◆ v) Der Nekhoroshev Bereich im Sonne-Jupiter Fall wurde auf analytischem Wege explizit bestimmt. Die stabile Region stimmt bzgl. der Librationsbewegungen mit den Beobachtungen gut überein. Die Stabilität der Trojaner des Sonne-Jupiter Systems konnte für Exzentrizitäten $e_p < 0.01$ und Librationsbewegungen $D_p < 10\,^\circ$ für das Zeitalter des Sonnensystems gezeigt werden.

Die vorliegende Studie belegt die Möglichkeit der Langzeit-Stabilität von Asteroiden im Sonnensystem für dessen Lebenszeit im Rahmen des elliptisch eingeschränkten Dreikörperproblems. Sie erweitert somit Aussagen vorangegangener Arbeiten, welche auf dem kreisförmigen eingeschränkten Dreikörperproblem basieren. Die (notwendige) Einbindung zusätzlicher Effekte, wie die Inklination der Asteroiden und den Einfluss der anderen Planeten auf die Stabilitätszone stellt den nächsten logischen Schritt einer weiteren Verallgemeinerung dar, die Relevanz einer rein mathematischen Theorie auf reale physikalische Systeme, wie unserem Sonnensystem, kann bereits aus dieser Arbeit abgeleitet werden.

Acknowledgments

Finalizing this thesis would not have been possible without Rudolf Dvorak, who opened the door to science, i.e. the field of Celestial mechanics, for me and Christos Efthymiopoulos equipping myself with all those beautiful ideas of dynamical systems and exponential stability estimates during the stays abroad in Athen or Patras. Both of you are an indispensable part of this thesis. I thank the ADG-group for proof-reading the Chapters and thank Manolis, for scanning and sending the proof-readings back to me. Thank you!

At the bottom of my heart I whish to thank my parents, Bernhard and Magdalena Lhotka for the long term support of my education, and Michaela for her patience with me, when writing the thesis.

Chistoph Lhotka, Vienna 2008

References and Publication List

Publication List

Publications of the author stemming from the research period of the present thesis (see also CV for full publication list):

◇ Lhotka, C., Efthymiopoulos, C., Dvorak, R., 2008: "Nekhoroshev stability at L4 or L5 in the elliptic-restricted three-body problem - application to Trojan asteroids", Mont.Not.Roy.-Astr.Society, 384, 3, 1165-1177.

◇ Lhotka, C.: "Hadjidemetriou´s method revisited", Celest. Mech. Dyn. Astron. (accepted).

◇ Dvorak, R., Lhotka, C., Schwarz, R., 2008: "The dynamics of inclined Neptune Trojans", Celest.Mech.Dyn.Astron., 102, 1-3, 97-110.

◇ Dvorak, R., Schwarz, R., Lhotka, C., 2008: "On the dynamics of Trojan planets in extrasolar planetary systems", Exoplanets: Detection, Formation and Dynamics, IAU Symposium 249, 461-468.

References

◇ Abraham, R., Marsden, E., 1978, 2008: "Foundations of Mechanics", AMS Bookstore.

◇ Arnold, V.I., 1963: "Proof of a theorem of A.N. Kolmogorov on the invariance of quasi-periodic motions under small perturbations of the Hamiltonian", Usp.Mat.Nauk., 18, 91, Russ.Math.Surv. 18, 85.

◇ Arnold, V.I., 1963: "A theorem of Liouville concerning integrable problems od dynamics", Sibirsk.Math.Zh. 4, 471-474.

◇ Arnold, V.I., 1963: "Small denominators and problems of stability of motion in classical and celestial mechanics", Usp.Math.Nauk. 18, N6, 91, Russ.Math.Surv. 18, N6, 85.

◇ Arnold, V.I., 1978: "Mathematical Methods of Classical Mechanics", Springer.

◇ Bazzani A., Giovannozzi M., Servizi G., Todesco E., Turchetti G., 1993: "Resonant normal forms, interpolating Hamiltonians and stability analysis of area preserving maps", Physica D 64, 66-97.

◇ Bazzani A., Marmi S., Turchetti G., 1990: "Nekhoroshev estimate for isochronous non resonant symplectic maps", Celest. Mech. Dyn. Astron. 47, 333-359.

◇ Beaugé, C., Roig, F., 2001: "A Semianalytical Model for the Motion of the Trojan Asteroids: Proper Elements and Families", Icarus 153, 391-415.

◇ Bennett, A., 1965: "Characteristic exponents of the five equilibrium solutions in the ellip-

tic restricted problem", Icarus 1, 177.

◊ Benettin G., Galgani L., Giorgilli A. , 1985: "A proof of Nekhoroshev´s theorem for the stability times in nearly integrable Hamiltonian systems", Celest. Mech. 37, 1-25.

◊ Benettin, G., Gallavotti, G., 1986: "Stability of motions near resonances in quasi-integrable Hamiltonian systems", J. Stat. Phys. 44, 3/4, 293-338.

◊ Benettin G., Fassò F., Guzzo M., 1998: "Nekhoroshev-stability of L4 and L5 in the spatial restricted three-body problem", Regular Chaot. Dyn. 3, 56-72.

◊ Benettin, G., Fassò, F., Guzzo, M., 1999: "Nekhoroshev-stability of L4 and L5 in the spatial restricted problem", IAU 172, Impact of Modern Dynamics in Astronomy, Namur July 1998, 445.

◊ Birkhoff, G.D., 1927: "Dynamical Systems", American Mathematical Society, New York.

◊ Birkhoff, G.D., 1927: "On the periodic motions of dynamical systems", Acta.Math. 50, 359-379.

◊ Born, M., 1927: "The Mechanics of the Atom", Bell. London.

◊ Brown, E.W., Shook, C.A., 1964: "Planetary Theory", Cambridge University Press.

◊ Brumberg, V.A., 1995: "Analytical Techniques of Celestial Mechanics", Springer Verlag.

◊ Bruns, H., 1887: "Berichte de Kgl.Sächs.Ges.d.Wiss. 1, 55", Acta. Math. ix 25.

◊ Celletti A., Giorgilli A., 1991: "On the stability of the lagrangian points in the spatial restricted problem of three bodies", Celest. Mech. Dyn. Astron. 50, 1 31-58.

◊ Celletti, A., Ferrara, L., 1996: "An Application of the Nekhoroshev Theorem to the Restricted Three-Body Problem", Celest. Mech. Dyn. Astron. 64, 3, 261-272.

◊ Cherry, T.M., 1924: "On integrals developable about a singular point of a Hamiltonian system of differential equations", Proc.Cambridge.Phil.Soc. 22, 325-349.

◊ Cherry, T.M., 1924: "On integrals developable about a singular point of a Hamiltonian system of differential equations II", Proc.Cambridge.Phil.Soc. 22, 510-533.

◊ Chirikov, B.V., 1960: "Resonance Processes in magnetic traps", J.Nucl.Energy C 1, 253-260.

◊ Chirikov, B.V., 1979: "A universal instability of many-dimensional oscillator systems", Phys.Rep. 52, 263-379.

◊ Contopoulos, G., 1960: "A third integral of motion in a Galaxy", Z.Astrophy. 49, 273-291.

◊ Contopoulos, G., 1963: "Resonance cases and small divisors in a third integral of motion. I", Astron.J. 68, 763-779.

◊ Contopoulos, G., 1963: "On the existence of a third integral of motion", Astron.J. 68, 1-14.

◊ Contopoulos, G. & Moutsoulas, M., 1965: "Resonance cases and small divisors in a third integral of motion", Astron.J. 70, 817-835.

Contopoulos, G., 1966: "Tables of the Third Integral", Astrophysical Journal Supplement 13, 503-607.

◇ Contopoulos, G., Efthymiopoulos, C., Giorgilli, A., 2003: "Nonconvergence of formal integrals of motion", J.Phys.A:Math.Gen. 36, 8639-8660.

◇ Danby, J.M.A., 1964: "Stability of triangular points in the elliptic restricted problem of three bodies", Astron. J. 68, 159.

◇ Delaunay, C., 1860: "Théorie du mouvement de la lune", Mem. 28; Aca.Sci.France, Paris.

◇ Delshams, A., Gutiérrez, P., 1995: "Effective stability and KAM theory", J.Diff.Equs 128, 415-90.

◇ Delva, M., 1984: "Integration of the elliptic restricted three-body problem with Lie-series", Celest. Mech. 34, 145-154.

◇ Deprit, A., Rom, A., 1970: "Characteristic Exponents at L_4 in the Elliptic Restricted Problem", Astron. & Astrophys. 5, 416-425.

◇ Dvorak, R., Tsiganis, K., 2000: "Why do Trojan ASCs (not) escape?", Celest. Mech. Dyn. Astron. 78, 125-136.

◇ Dvorak, R., Schwarz, R., 2005: "On the stability regions of the Trojan asteroids", Celest. Mech. Dyn. Astron. 92, 19-28.

◇ Dvorak, R., Lhotka, C., Schwarz, R., 2008: "The dynamics of inclined Neptune Trojans", Celest. Mech. Dyn. Astron. 102, 97-110.

◇ Dvorak, R., Schwarz, R., Lhotka, C., 2008: "On the dynamics of Trojan planets in extrasolar planetary systems", IAU Proceedings, Cambridge University Press 3, 461-468.

◇ Efthymiopoulos, C., Giorgilli, A., Contopoulos, G., 2004: "Nonconvergence of formal integrals: II. Improved estimates for the optimal order of truncation", J.Phys.A:Math.Gen. 37, 10831-10858.

◇ Efthymiopoulos, C., 2005: "Nekhoroshev stability estimates for different models of the Trojan asteroids", IAU Proceedings No 197.Dynamics of Populations of Planetary Sytems.

◇ Efthymiopoulos C., 2005: "Formal Integrals and Nekhoroshev Stability in a Mapping Model for the Trojan Asteroids", Celest. Mech. Dyn. Astron. 92, 29-52.

◇ Efthymiopoulos C., Sándor Z., 2005: "Optimized Nekhoroshev stability estimates for the Trojan asteroids with a symplectic mapping model of co-orbital motion", MNRAS 364, 6, 253-271.

◇ Efthymiopoulos C., 2008: "On the connection between the Nekhoroshev theorem and Arnold diffusion", Celest. Mech. Dyn. Astron. 102, 1-3, 49-68.

◇ Einstein, A., 1917: Sitzungsber.Akad.wiss.Preuss. 142.

◇ Érdi, B., 1977: "An asymptotic solution for the Trojan case of the plane elliptic restricted three body problem of three bodies", Celest. Mech. 15, 367-383.

Érdi, B., 1978: "The three-dimensional motion of Trojan asteroids", Celest. Mech. 18, 141-161.

◇ Érdi, B., 1981: "The perturbations of the orbital elements of Trojan asteroids", Celest. Mech. 24, 377-390.

◇ Érdi, B., 1987: "Long periodic perturbations of Trojan asteroids", Celest. Mech. 43, 1-4, 303-308.

◇ Érdi B., 1996: "The Trojan Problem", Celest. Mech. Dyn. Astron. 65, 149-164.

◇ Euler, L., 1772: "Theoria Motuum Lunae", Typis Academia Imperialis Scientarium, Petropoli.

◇ Fassó F., Guzzo M., Benettin G., 1998 : "Nekhoroshev-stability of elliptic equilibria of Hamiltonian systems", Commun. Math. Phys. 197, 347.

◇ Ferraz-Mello, S., 2007: "Canonical Perturbation Theories: Degenerate Systems and Resonance", Springer.

◇ Ferraz-Mello, S., 1996: "A symplectic mapping approach to the study of the stochasticity in asteroidal resonances", Celest. Mech. Dyn. Astron. 64, 4, 421-437.

◇ Froeschlé, C., Guzzo, M., Lega, E., 2000: "Graphical Evolution of the Arnold Web: From order to Chaos", Science 289, 2108-2110.

◇ Giorgilli, A., 2002: "Notes on Exponential Stability of Hamiltonian Systems", Centro di Ricerca Mathematica Ennio De Giorgi.

◇ Giorgilli, A., 1979: "A computer program for integrals of motion", Comput.Phys.Commun. 16, 331-343.

◇ Giorgilli A., 1988: "Rigorous results on the power expansion for the integrals of a hamiltonian system near a equilibrium point", Ann. Inst. H. Poincaré 48, 423-439.

◇ Giorgilli A., Delshams A., Fontich E., Galgani L., Simó C., 1989: "Effective stability for a Hamiltonian system near an elliptic equilibrium point, with an application to the restricted three body problem", J.Diff.Equ. 77, 167-198.

◇ Giorgilli, A., Galgani, L., 1978: "Formal integrals for an autonomous Hamiltonian system near an equilibrium point", Celestial Mechanics 17, 267-280.

◇ Giorgilli A., Skokos Ch., 1997: "On the stability of the Trojan asteroids.", A&A 317, 254-261.

◇ Giorgilli, A., Zehnder, E. , 1992: "Exponential stability for time dependent potentials", ZAMP 43.

◇ Goldstein, H., Poole, C., Safko, J., 2002: "Classical Mechanics", Addison Wesely.

◇ Gröbner, W., 1967: "Die Lie-Reihen und Ihre Anwendungen", Mathematische Monographien, Begonnen von Wilhem Blaschke, VEB Deutscher Verlag der Wissenschaften.

◇ Gustavson, F.G., 1966: "On constructing formal integrals of a Hamiltonian system near an

equilibrium point", Astron.J. 71, 670-686.

◇ Guzzo M., Fassó F., Benettin G., 1998: "On the Stability of Elliptic Equilibria", Math. Phys. Electron. J. 4, 1.

◇ Guzzo M., Lega E. and Froeschlé C., 2002: "On the numerical detection of the effective stability of chaotic motions in quasi-integrable systems", Physica D 163, Issues 1-2, 1-25.

◇ Hadjidemetriou, J.D., 1991: "Mapping models for Hamiltonian systems with application to resonant asteroid motion", NATO Advanced Study Institute on Predictability, Stability, and Chaos in N-Body Dynamical Systems, 157-175.

◇ Hadjidemetriou, J.D., 1992: "The elliptic restricted problem at the 3:1 resonance", Celest. Mech. Dyn. Astron. 53, 151-183.

◇ Hadjidemetriou, J.D., 1993: "Long Term evolution of asteroids near a resonance", Celest. Mech. Dyn. Astron. 57, 96-96.

◇ Hadjidemetriou, J.D., 1991: "Roy A.E. Predictability, Stability and Chaos in N-body Dynamical Systems", Plenum Press, New York.

◇ Hadjidemetriou, J.D., 1996: "Symplectic Mappings", IAU Symposium 172, Paris, France, p 255.

◇ Hagel, J., Lhotka, C., 2005: "A High order perturbation analysis of the Sitnikov problem", Celest. Mech. Dyn. Astron. 93, 1, 201-228.

◇ Hagel, J., 1995: "Analytical Investigation of Non-Linear Stability of the Lagrangian Point L_4 Around the Commensurability 1:2", Celest. Mech. Dyn. Astron. 63, 2, 205-225.

◇ Hanselmeier, A., Dvorak, R., 1984: "Numerical integration with Lie-series", Astron.Astrophys. 132, 203-207.

◇ Haretu, S.C., 1878: "Thesis, Fac. de Sciences", Paris.

◇ Hénon, M., Heiles, C., 1964: "The applicability of the third integral of motion: Some numerical experiments", Astronomical Journal 69, 73.

◇ Jacobi, C.G.J., 1836: "Sur le mouvement d´un point et sur un cas particulier du problème des trois corps", Compt. Rend. 3, 59.

◇ Kolmogorov, A.N., 1954: "Preservation of conditionally periodic movements with small change in the Hamiltonian function", Dokl.Akad.Nauk.USSR 98, 527.

◇ Kolmogorov, A.N., 1957: "Théorie générale des systémes dynamiques et mécanique classique.", Proc.Int.Conf. of Math.Amsterdam.

◇ Kuypers, F., 1997: "Klassische Mechanik", Wiley-VCH.

◇ Lagrange, J.L., 1788: "Mécanique analytique", Paris.

◇ Laplace, P.S., 1798-1825: "Traité de mécanique céleste", Paris.

◇ Lega, E., Guzzo, M., Froeschlé, C., 2002: "Detection of Arnold Diffusion in Hamiltonian Systems", Physica D: Nonlinear Phenomena 182, 3-4, 179-187.

◇ Levison, H., Shoemaker, E.M., Nature, 385, 42: "The dispersal of the Trojan swarm", Nature 385, 42-44.

◇ Lhotka, C., Dvorak, R., 2006: "A new determination of the fundamental frequencies in our solar system", Publications of Astronomy, Eötvös University, Vol.18. 33-46.

◇ Lhotka, C., Efthymiopoulos, C., Dvorak, R., 2008: "Nekhoroshev stability at L4 or L5 in the elliptic-restricted three-body problem - application to Trojan asteroids", Mont.Not.Roy.-Astr.Society 384, 3, 1165-1177.

◇ Lhotka, C., 2004: "Störungsanalyse des Sitnikov Problems für hohe Ordnungen unter Verwendung automatisierter Herleitungsmethoden in *Mathematica*", Univ. Vienna. Institute for Astronomy.

◇ Lichtenberg, J., Lieberman, M., 1983: "Regular and Stochastic Motion", Springer Verlag.

◇ Littlewood, J.E., 1959: "On the equilateral configuration in the restricted problem of three bodies", Proc.London.Math.Soc. 9, 343.

◇ Littlewood, J.E., 1959: "The Lagrange configuration in celestial mechanics", Proc.London.-Math.Soc. 9, 525.

◇ Lochak, P., 1992: "Canonical Perturbation Theory via simultaneous approximations", Usp.Math.Nauk. 47, 59-140.

◇ Lochak, P., Neistadt, A.I., 1991: "Stability of nearly integrable convex Hamiltonian systems over exponentially long times", Proc. 1991, Conf. on Dyn. Systems, Boston, Birkhäuser.

◇ Marchal, Ch., 1990: "The Three Body Problem", Elsevier Science Publishers B.V.

◇ Milani, A., 1993: "The Trojan asteroid belt:proper elements, stability, chaos and families", Celest. Mech. Dyn. Astron. 57, 59-94.

◇ Milani, A., 1994: "The dynamics of Trojan asteroids", IAU Symp. 160, Asteroids, Comets, Meteors 160, 159.

◇ Mitchenko, T., Beaugé, C., Roig, F., 2001:, Astron. Journ. 122, 3485.

◇ Morbidelli, A., Guzzo, M. 1997: "The Nekhoroshev Theorem and the Asteroid Belt Dynamical System", Proceedings of the 4th Alexander von Humboldt Colloquium, Kluwer 1997, p107.

◇ Morbidelli, A., 2002: "Modern Celestial Mechanics: Aspects of Solar System Dynamics", Taylor & Francis.

◇ Morbidelli, A., Giorgilli, A., 1995: "On a connection between KAM and Nekhoroshev´s theorems", Physica D: Nonlinear Phenomena 86, 3, 514-516.

◇ Moser, J., 1973: "Stable and Random Motion in Dynamical Systems", Princeton Univer-

sity Press.

◇ Moser, J., 1962: "On invariant Curves of Area Preserving Mappings on an Annulus", Nachr.Akad.Wiss.Göttingen.Math.Phys.K1.p1.

◇ Moser, J., 1967: "Convergent series expansions for quasi-periodic motions", Math.Ann. 169, 136-176.

◇ Moser, J., 1955: "Stabilitätsverhalten kanonischer Differentialgleichungssysteme", Nachr.-Akad.Wiss.Göttingen.Math.Phys. K1 IIa, 6, 87-120.

◇ Moser, J., 1967: "Convergent series expansions for quasi-periodic motions", Math.Ann. 169, 136-176.

◇ Nekhoroshev, N.N., 1971: "Behavior of Hamiltonian systems close to integrable", Funct.-Anal.Appl. 5, 338-339.

◇ Nekhoroshev, N.N., 1977: "Exponential estimates of the stability time of near-integrable Hamiltonian systems", Russ.Math.Surv. 32, 1.

◇ Nekhoroshev, N.N., 1979: "Exponential estimates of the stability time of near-integrable Hamiltonian systems 2", Trudy Sem.Petrovos. 5, 5.

◇ Nesvorny, D., Dones, L., 2002: Icarus 160, 271-288.

◇ Niederman, L., 2000: "Exponential stability for small perturbations of steep integrable Hamiltonian systems", Mathematical Physics Preprint Archive 2000, http://www.ma.utexas.edu/mp.

◇ Palacián, J.F., Yanguas, P., 2006: "From the circular to the spatial elliptic restricted three-body problem", Celest. Mech. Dyn. Astron. 95, 1-4, 81-99.

◇ Pilat-Lohinger, E., Dvorak, R., Burger, Ch., 1999: "Trojans in stable chaotic motion", Celest. Mech. Dyn. Astron. 73, 117-126.

◇ Poincaré, H., 1890: "Sur le problème de trois corps et les équations de la dynamique", Acta. Math. 13, 1-271.

◇ Poincaré, H., 1892: "Les méthodes nouvelles de la mécanique céleste, vol.1", Gauthier-Villars, Paris.

◇ Poincaré, H., 1893: "Les méthodes nouvelles de la mécanique céleste, vol.2", Gauthier-Vilars, Paris.

◇ Poisson, S.D., 1808: "Sur les inégalités des moyens mouvements des planétes", Academy of Science.

◇ Pöshel, J., 1993: "Nekhoroshev´s estimates for quasi-convex Hamiltonian systems", Math.Z. 213, 187.

◇ Rabe, E., 1967: "Third-order stability of the long-period Trojan librations", Astron. Journ. 72, 10.

◇ Rand, R. H., 1994: "Topics in nonlinear dynamics with computer algerbra", Computation

and Education:Mathematics, Science and Engineering.

◇ Robutel, P., Gabern, F., Jorba, A., 2005: "The observed Trojans and the global dynamics around the Lagrangian points of the Sun-Jupiter system", Celest. Mech. Dyn. Astron. 92, 53-69.

◇ Robutel, P., Gabern, F., 2006: "The resonant structure of Jupiter´s Trojan asteroids - I. Long-term stability and diffusion", Monthly Notices od the Royal Astronomical Society 372, 4, 1463-1482.

◇ Robutel, P., Bodossian, F., 2008: "The resonant structure of Jupiter´s Trojan asteroids-II. What happens for different configurations of the planetary system", (in press).

◇ Schwarz, R., Dvorak, R., Süli, Á., Érdi, B. 2007: "Survey of the stability region of hypothet ical habitable Trojan planets", A&A 474, 3, 1023-1029.

◇ Schwarz, R., Dvorak, R., Pilat-Lohinger, E., Süli, Á., Érdi, B. 2007: "Trojan planets in HD 108874?", Astron. Astroph. 462, 3, 1165-1170.

◇ Schwarz, R., Süli, Á, Dvorak, R., Pilat-Lohinger, E. 2008: "Stability of Trojan planets in multiplanetary systems", Celest. Mech. Dyn. Astron. (submitted).

◇ Sándor, Z., Érdi, B., 2003: "Symplectic mapping model for Trojan-type motion in the elliptic restricted three-body problem", Celest. Mech. Dyn. Astron. 86, 301-319.

◇ Sándor, Z., Érdi, B., Murray, C., 2002: "Symplectic Mappings of Co-orbital Motion in the Restricted Problem of Three Bodies", Celest. Mech. Dyn. Astron. 84, 4, 355-268.

◇ Servizi G., Turchetti G., Benettin G., Giorgilli A., 1983: "Resonances and asymptotic behaviour of Birkhoff series", Phys. Lett. A 95, 11-14.

◇ Siegel, C.L., 1941: "On the integrals of canonical systems", Ann.Math. 42, 806-822.

◇ Siegel, C.L., 1956: "Vorlesungen über Himmelsmechanik", Springer Verlag.

◇ Simó, C., 1989: "Estabilitat de sistemes hamiltonians", Memorias de la Real Academia de Ciencias y Artes de Barcelona 48, 303-339.

◇ Sinai, Ya.G., 1963: Sov.Math.Dokl. 4, 1818.

◇ Skokos Ch., Dokoumetzidis A., 2001: "Effective stability of the Trojan asteroids", A&A 367, 729-736.

◇ Stumpff, K., 1959: "Himmelsmechanik, I", VEB Deutscher Verlag der Wissenschaften.

◇ Stumpff, K., 1965: "Himmelsmechanik, II", VEB Deutscher Verlag der Wissenschaften.

◇ Szebehely, V., 1967: "Theory of Orbits", Academic Press.

◇ Tsiganis, K., Dvorak, R., Pilat-Lohinger, E., 2000: "Thersites: a jumping Trojan ?", Astron. Astroph. 354, 1091-1100.

◇ Tsiganis, K., Varvoglis, H., Dvorak, R., 2005: "Chaotic diffusion and effective stability of Jupiter Trojans", Celest. Mech. Dyn. Astron. 92, 71-87.

Von Zeipel, H., 1916: Ark.Astron.Mat.Fys. 11.

◇ Waldvogel, J. 1973: "The rectilinear restricted problem of three bodies", Celestial Mechanics 8, 189-198.

◇ Weierstrass, K.T.W., 1911: "Über das Problem der Störungen in der Astronomie", 1880-1881.

◇ Whittaker, E.T., 1916: "On the adelphic integral of the differential equations of dynamics", Proc.Roy.Soc.Edinburgh. 37, 95-109.

◇ Whittaker, E.T., 1937: "A Treatise on the Analytical Dynamics of Particles and Rigid Bodies", 4th Ed. Cambridge Univ.Press.

◇ Winter, A., 1941: "Analytical Foundations of Celestial Mechanics", Princeton University Press, New Jersey.

◇ Wisdom, J., 1982: "The origin of the Kirkwood gaps - A mapping for asteroidal motion near the 3/1 commensurability", Astronomical Journal 87, 577-593.

◇ Wisdom, J., 1983: "Chaotic behavior and the origin of the 3/1 Kirkwood gap", Icarus 56, 51-74.

Appendix I: List of Figures & Tables

Chapter 1

–

Chapter 2

Chapter 3

Chapter 4

Chapter 5

Appendix II: Formulae

The complete set of formulae, derived in this thesis would fill another 100 pages (depending on the representation). The expressions given here are meant to be i) anchor points to rederive the calculations and ii) examples complementing the formal treatment in the Chapters. The lightbulb at the beginning of each proceeding section refers to the origin of the expressions, i.e. the Chapter, Section and equation number. The content of this Appendix is:

page IV   II.I. Disturbing function in the 1:1 resonance

Derived and used in Chapter 4, 5. As a result it can be used for different parameters $e´$ and $a´$ of the perturbing planet. The series are sorted with respect to increasing order in the trigonometric arguments.

page XIV   II.II. Explicit mapping

Derived and used in Chapter 5, 6. Based on the approximate disturbing function it covers the librational regime of asteroids of the Sun-Jupiter case.

page XXI   II.III. Normal form mapping

Derived and used Chapter 6, 7. The normal form defines the approximate integrals used in Chapter 7 to derive the stability estimates.

page XXV   II.IV. Remainder function

Derived in Chapter 7. The remainder is at the basis of the Nekhoroshev stable region, derived for the Sun-Jupiter configuration in 1:1 resonance.

II.I. Disturbing function in the 1:1 resonance

💡 Chapter, 4, 5, Section 4.3.2.

The disturbing function of the 1:1 MMR in the case of Sun-Jupiter was derived in Chapter 4, i.e. by means of (34;4), (35;4), (39;4). It is part of the generating function, derived in Chapter 5, i.e. through (9;5), (10;5).

The following notation is introduced:

$\omega' \equiv 0$,

$\Delta_*^{\ k} \equiv \Delta_0^{-k/2}$

$\Delta_0 = (a^2 + a'^2 - 2\, a\, a'\cos(\tau))$

The terms are sorted according to their trigonometric argument with increasing order $|k_1| + |k_2|$:

◆ $\left(\dfrac{1155}{256} a'^{12} e^{-6} \Delta_*^{13} + \dfrac{1155}{256} a^{12} e^6 \Delta_*^{13} - \dfrac{2205}{256} a^{10} e^6 \Delta_*^{11} + \right.$

$\dfrac{1225}{256} a^8 e^6 \Delta_*^9 - \dfrac{175}{256} a^6 e^6 \Delta_*^7 + a'^{10}\left(a^2\left(\dfrac{31185\, e^{-6}}{512} + \dfrac{51975\, e^2\, e^{-4}}{512} \right)\Delta_*^{13} - \dfrac{2205}{256} e^{-6} \Delta_*^{11} \right) + a^{-8}\left(a^4\left(\dfrac{301455\, e^{-6}}{2048} + \right.\right.$

$\dfrac{966735\, e^2\, e^{-4}}{1024} + \dfrac{613305\, e^4\, e^{-2}}{2048} \right)\Delta_*^{13} + a^2\left(-\dfrac{15435\, e^{-6}}{256} - \dfrac{10395\, e^2\, e^{-4}}{64} \right)\Delta_*^{11} + \dfrac{1225}{256} e^{-6} \Delta_*^9 \right) + a^{-2}\left(a^{10}\left(\dfrac{31185\, e^6}{512} + \dfrac{51975\, e^{-2}\, e^4}{512} \right) \right.$

$\Delta_*^{13} + a^8\left(-\dfrac{15435\, e^6}{256} - \dfrac{10395\, e^{-2}\, e^4}{64} \right)\Delta_*^{11} + a^6\left(\dfrac{3115\, e^6}{256} + \dfrac{36435\, e^{-2}\, e^4}{512} + \dfrac{105\, e^{-4}\, e^2}{512} \right)\Delta_*^9 + a^4\left(-\dfrac{75\, e^6}{512} - \dfrac{1725\, e^{-2}\, e^4}{256} - \dfrac{75\, e^{-4}\, e^2}{512} \right)$

$\Delta_*^7 + a^2\left(\dfrac{29\, e^{-6}}{768} - \dfrac{3\, e^2\, e^{-4}}{256} - \dfrac{3\, e^4\, e^{-2}}{256} + \dfrac{29\, e^6}{768} \right)\Delta_*^5 \right) + a^{-6}\left(a^6\left(\dfrac{444675\, e^{-6}}{4096} + \dfrac{6330555\, e^2\, e^{-4}}{4096} + \dfrac{6330555\, e^4\, e^{-2}}{4096} + \dfrac{444675\, e^6}{4096} \right) \right.$

$\Delta_*^{13} + a^4\left(-\dfrac{120015\, e^{-6}}{2048} - \dfrac{743715\, e^2\, e^{-4}}{1024} - \dfrac{673785\, e^4\, e^{-2}}{2048} \right)\Delta_*^{11} + a^2\left(\dfrac{3115\, e^{-6}}{256} + \dfrac{36435\, e^2\, e^{-4}}{512} + \dfrac{105\, e^4\, e^{-2}}{512} \right)\Delta_*^9 - \dfrac{175}{256} e^{-6} \Delta_*^7 \right) +$

$a^{-4}\left(a^8\left(\dfrac{301455\, e^6}{2048} + \dfrac{966735\, e^{-2}\, e^4}{1024} + \dfrac{613305\, e^{-4}\, e^2}{2048} \right)\Delta_*^{13} + a^6\left(-\dfrac{120015\, e^6}{2048} - \dfrac{743715\, e^{-2}\, e^4}{1024} - \dfrac{673785\, e^{-4}\, e^2}{2048} \right)\Delta_*^{11} + a^4\left(-\dfrac{315\, e^6}{2048} + \right.\right.$

$\dfrac{167265\, e^2\, e^4}{2048} + \dfrac{167265\, e^4\, e^{-2}}{2048} - \dfrac{315\, e^6}{2048} \right)\Delta_*^9 + a^2\left(-\dfrac{75\, e^{-6}}{512} - \dfrac{1725\, e^2\, e^4}{256} - \dfrac{75\, e^4\, e^{-2}}{512} \right)\Delta_*^7 \right) \right) \beta^6 + \left(\dfrac{105}{64} a^{-8} e^4 \Delta_*^9 + \dfrac{105}{64} a^8 e^4 \right.$

$\Delta_*^9 - \dfrac{75}{32} a^6 e^4 \Delta_*^7 + \dfrac{45}{64} a^4 e^4 \Delta_*^5 + a^{-6}\left(a^2\left(\dfrac{735\, e^4}{64} + \dfrac{525\, e^2\, e^2}{32} \right)\Delta_*^9 - \dfrac{75}{32} e^4 \Delta_*^7 \right) + a^{-2}\left(a^6\left(\dfrac{735\, e^4}{64} + \dfrac{525\, e^{-2}\, e^2}{32} \right)\Delta_*^9 + a^4\left(-\dfrac{375\, e^4}{64} - \right.\right.$

$\dfrac{555\, e^{-2}\, e^2}{32} \right)\Delta_*^7 + a^2\left(\dfrac{3\, e^4}{128} + 3\, e^2\, e^{-2} + \dfrac{3\, e^4}{128} \right)\Delta_*^5 \right) + a^{-4}\left(a^4\left(\dfrac{6195\, e^4}{512} + \dfrac{8715\, e^2\, e^2}{128} + \dfrac{6195\, e^4}{512} \right)\Delta_*^9 + a^2\left(-\dfrac{375\, e^4}{64} - \dfrac{555\, e^2\, e^2}{32} \right) \right.$

$\Delta_*^7 + \dfrac{45}{64} e^4 \Delta_*^5 \right)\right) \beta^4 + \left(\dfrac{3}{4} a^{-4} e^{-2} \Delta_*^5 + \dfrac{3}{4} a^4 e^2 \Delta_*^5 - \dfrac{3}{4} a^2 e^2 \Delta_*^3 + a^{-2}\left(a^2\left(\dfrac{15\, e^2}{8} + \dfrac{15\, e^2}{8} \right)\Delta_*^5 - \dfrac{3}{4} e^{-2} \Delta_*^3 \right) \right) \beta^2 + \Delta_* + \dfrac{1}{2\, a'} - \dfrac{1}{a}$

◆ $\cos(\omega)\left(\left(-\dfrac{10395}{256} e^{-5} a\, e\, a'^{11} + a^3\left(-\dfrac{218295\, e\, e^{-5}}{512} - \dfrac{343035\, e^3\, e^{-3}}{1024} \right)a'^9 + a^5\left(-\dfrac{1632015\, e\, e^{-5}}{2048} - \right.\right.\right.$

$\dfrac{4272345\, e^3\, e^{-3}}{2048} - \dfrac{717255\, e^5\, e'}{2048} \right)a'^7 + a^7\left(-\dfrac{717255\, e\, e^{-5}}{2048} - \dfrac{4272345\, e^3\, e^{-3}}{2048} - \dfrac{1632015\, e^5\, e'}{2048} \right)a'^5 + a^9\left(-\dfrac{218295\, e'\, e^5}{512} - \right.$

$$\left.\frac{343035\,e^{\prime 3}\,e^3}{1024}\right)a^{\prime 3}-\frac{10395}{256}\,e^{\prime}a^{\prime 11}\,e^5\,a^{\prime}\right)\beta^6\,\Delta_*^{13}+\left(\frac{19845}{256}\,e^{\prime 5}\,a\,e\,a^{\prime 9}+a^3\left(\frac{218295\,e\,e^{\prime 5}}{512}+\frac{509355\,e^3\,e^{\prime 3}}{1024}\right)a^{\prime 7}+a^5\left(\frac{681345\,e\,e^{\prime 5}}{2048}+\right.\right.$$

$$\left.\frac{3219615\,e^3\,e^{\prime 3}}{2048}+\frac{681345\,e^5\,e^{\prime}}{2048}\right)a^{\prime 5}+a^7\left(\frac{218295\,e^{\prime}e^5}{512}+\frac{509355\,e^{\prime 3}\,e^3}{1024}\right)a^{\prime 3}+\frac{19845}{256}\,e^{\prime}a^9\,e^5\,a^{\prime}\right)\beta^6\,\Delta_*^{11}+\left(\left(-\frac{11025}{256}\,e^{\prime 5}\,a\,e\,a^{\prime 7}+\right.\right.$$

$$a^3\left(-\frac{86835\,e\,e^{\prime 5}}{1024}-\frac{202755\,e^3\,e^{\prime 3}}{1024}+\frac{245\,e^5\,e^{\prime}}{1024}\right)a^{\prime 5}+a^5\left(\frac{245\,e\,e^{\prime 5}}{1024}-\frac{202755\,e^3\,e^{\prime 3}}{1024}-\frac{86835\,e^5\,e^{\prime}}{1024}\right)a^{\prime 3}-\frac{11025}{256}\,e^{\prime}a^7\,e^5\,a^{\prime}\right)$$

$$\beta^6+\left(-\frac{315}{32}\,e^{\prime 3}\,a\,e\,a^{\prime 7}+a^3\left(-\frac{6195\,e\,e^{\prime 3}}{128}-\frac{3465\,e^3\,e^{\prime}}{128}\right)a^{\prime 5}+a^5\left(-\frac{3465\,e\,e^{\prime 3}}{128}-\frac{6195\,e^3\,e^{\prime}}{128}\right)a^{\prime 3}-\frac{315}{32}\,e^{\prime}a^7\,e^3\,a^{\prime}\right)\beta^4\right)\Delta_*^9+\left(\left(\frac{1575}{256}\right.\right.$$

$$a^{\prime 5}\,a\,e\,e^{\prime 5}+\frac{1575}{256}\,a^{\prime}a^5\,e^5\,e^{\prime}+a^3\,a^{\prime 3}\left(\frac{5\,e\,e^{\prime 5}}{32}+\frac{7665\,e^3\,e^{\prime 3}}{512}+\frac{5\,e^5\,e^{\prime}}{32}\right)\right)\beta^6+\left(\frac{225}{16}\,e^{\prime 3}\,a\,e\,a^{\prime 5}+a^3\left(\frac{1635\,e\,e^{\prime 3}}{64}+\frac{1635\,e^3\,e^{\prime}}{64}\right)\right.$$

$$a^{\prime 3}+\frac{225}{16}\,e^{\prime}a^5\,e^3\,a^{\prime}\right)\beta^4\right)\Delta_*^7+\left(\left(-\frac{135}{32}\,a^{\prime 3}\,a\,e\,e^{\prime 3}-\frac{135}{32}\,a^{\prime}a^3\,e^3\,e^{\prime}\right)\beta^4+\left(-\frac{9}{4}\,e^{\prime}a\,e\,a^{\prime 3}-\frac{9}{4}\,e^{\prime}a^3\,e\,a^{\prime}\right)\beta^2\right)\Delta_*^5+\frac{9}{4}\,a^{\prime}e^{\prime}a\,e\,\beta^2\,\Delta_*^3\right)$$

◆ $\cos(\tau)\left(\left(-\frac{3465}{128}\,e^{\prime 6}\,a\,a^{\prime 11}+\right.\right.$

$$a^3\left(-\frac{31185\,e^{\prime 6}}{256}-\frac{93555\,e^2\,e^{\prime 4}}{256}\right)a^{\prime 9}+a^5\left(-\frac{100485\,e^{\prime 6}}{1024}-\frac{654885\,e^2\,e^{\prime 4}}{512}-\frac{592515\,e^4\,e^{\prime 2}}{1024}\right)a^{\prime 7}+a^7\left(-\frac{100485\,e^6}{1024}-\frac{654885\,e^{\prime 2}\,e^4}{512}-\right.$$

$$\left.\frac{592515\,e^{\prime 4}\,e^2}{1024}\right)a^{\prime 5}+a^9\left(-\frac{31185\,e^6}{256}-\frac{93555\,e^{\prime 2}\,e^4}{256}\right)a^{\prime 3}-\frac{3465}{128}\,a^{11}\,e^6\,a^{\prime}\right)\beta^6\,\Delta_*^{13}+\left(a\left(\frac{4095\,e^{\prime 6}}{128}-\frac{945\,e^{\prime 4}\,e^2}{128}\right)a^{\prime 9}+a^3\right.$$

$$\left(\frac{4725\,e^{\prime 6}}{128}+\frac{68985\,e^2\,e^{\prime 4}}{256}-\frac{16065\,e^4\,e^{\prime 2}}{256}\right)a^{\prime 7}+a^5\left(-\frac{40635\,e^{\prime 6}}{1024}+\frac{106785\,e^2\,e^{\prime 4}}{1024}+\frac{106785\,e^4\,e^{\prime 2}}{1024}-\frac{40635\,e^6}{1024}\right)a^{\prime 5}+a^7\left(\frac{4725\,e^6}{128}+\right.$$

$$\left.\frac{68985\,e^{\prime 2}\,e^4}{256}-\frac{16065\,e^{\prime 4}\,e^2}{256}\right)a^{\prime 3}+a^9\left(\frac{4095\,e^6}{128}-\frac{945\,e^{\prime 2}\,e^4}{128}\right)a^{\prime}\right)\beta^6\,\Delta_*^{11}+\left(\left(a\left(\frac{735\,e^{\prime 4}\,e^2}{64}-\frac{735\,e^{\prime 6}}{128}\right)a^{\prime 7}+a^3\left(\frac{7105\,e^{\prime 6}}{512}+\right.\right.\right.$$

$$\left.\frac{1365\,e^2\,e^{\prime 4}}{128}+\frac{31185\,e^4\,e^{\prime 2}}{512}\right)a^{\prime 5}+a^5\left(\frac{7105\,e^6}{512}+\frac{1365\,e^{\prime 2}\,e^4}{128}+\frac{31185\,e^{\prime 4}\,e^2}{512}\right)a^{\prime 3}+a^7\left(\frac{735\,e^{\prime 2}\,e^4}{64}-\frac{735\,e^6}{128}\right)a^{\prime}\right)\beta^6+\left(-\frac{105}{16}\right.$$

$$e^{\prime 4}\,a\,a^{\prime 7}+a^3\left(-\frac{735\,e^{\prime 4}}{64}-\frac{1155\,e^2\,e^{\prime 2}}{32}\right)a^{\prime 5}+a^5\left(-\frac{735\,e^4}{64}-\frac{1155\,e^{\prime 2}\,e^2}{32}\right)a^{\prime 3}-\frac{105}{16}\,a^7\,e^4\,a^{\prime}\right)\beta^4\right)\Delta_*^9+\left(\left(a\left(-\frac{365\,e^{\prime 6}}{256}-\frac{465\,e^2\,e^{\prime 4}}{128}-\right.\right.\right.$$

$$\left.\frac{15\,e^4\,e^{\prime 2}}{256}\right)a^{\prime 5}+a^3\left(\frac{165\,e^{\prime 6}}{1024}-\frac{1515\,e^2\,e^{\prime 4}}{1024}-\frac{1515\,e^4\,e^{\prime 2}}{1024}+\frac{165\,e^6}{1024}\right)a^{\prime 3}+a^5\left(-\frac{365\,e^6}{256}-\frac{465\,e^{\prime 2}\,e^4}{128}-\frac{15\,e^{\prime 4}\,e^2}{256}\right)a^{\prime}\right)\beta^6+\left(a\right.$$

$$\left(\frac{15\,e^{\prime 4}}{4}-\frac{15\,e^{\prime 2}\,e^2}{8}\right)a^{\prime 5}+a^3\left(-\frac{255\,e^{\prime 4}}{64}+\frac{15\,e^2\,e^{\prime 2}}{4}-\frac{255\,e^4}{64}\right)a^{\prime 3}+a^5\left(\frac{15\,e^4}{4}-\frac{15\,e^{\prime 2}\,e^2}{8}\right)a^{\prime}\right)\beta^4\right)\Delta_*^7+\left(\left(a\left(\frac{15\,e^{\prime 6}}{256}-\frac{15\,e^2\,e^{\prime 4}}{32}+\right.\right.\right.$$

$$\left.\frac{15\,e^4\,e^{\prime 2}}{256}\right)a^{\prime 3}+a^3\left(\frac{15\,e^6}{256}-\frac{15\,e^{\prime 2}\,e^4}{32}+\frac{15\,e^{\prime 4}\,e^2}{256}\right)a^{\prime}\right)\beta^6+\left(a\left(\frac{15\,e^{\prime 4}}{16}+\frac{15\,e^2\,e^{\prime 2}}{8}\right)a^{\prime 3}+a^3\left(\frac{15\,e^4}{16}+\frac{15\,e^{\prime 2}\,e^2}{8}\right)a^{\prime}\right)\beta^4+$$

$$\left(-\frac{3}{2}\,e^{\prime 2}\,a\,a^{\prime 3}-\frac{3}{2}\,a^3\,e^2\,a^{\prime}\right)\beta^2\right)\Delta_*^5+\left(a^{\prime}a\left(-\frac{29\,e^{\prime 6}}{1152}+\frac{e^2\,e^{\prime 4}}{128}+\frac{e^4\,e^{\prime 2}}{128}-\frac{29\,e^6}{1152}\right)\beta^6+a^{\prime}a\left(-\frac{e^{\prime 4}}{64}+\frac{e^2\,e^{\prime 2}}{4}-\frac{e^4}{64}\right)\beta^4+a^{\prime}a\left(-\frac{e^{\prime 2}}{2}-\right.\right.$$

$$\left.\frac{e^2}{2}\right)\beta^2\right)\Delta_*^3+\frac{29\,a\,e^6\,\beta^6}{1152\,a^{\prime 2}}-\frac{e^{\prime 2}\,a\,e^4\,\beta^6}{128\,a^{\prime 2}}-\frac{e^{\prime 4}\,a\,e^2\,\beta^6}{128\,a^{\prime 2}}+\frac{29\,e^{\prime 6}\,a\,\beta^6}{1152\,a^{\prime 2}}+\frac{a\,e^4\,\beta^4}{64\,a^{\prime 2}}-\frac{e^{\prime 2}\,a\,e^2\,\beta^4}{4\,a^{\prime 2}}+\frac{e^{\prime 4}\,a\,\beta^4}{64\,a^{\prime 2}}+\frac{a\,e^2\,\beta^2}{2\,a^{\prime 2}}+\frac{e^{\prime 2}\,a\,\beta^2}{2\,a^{\prime 2}}-\frac{a}{a^{\prime 2}}\right)$$

◆ $\cos(2\,\omega)\left(\left(\frac{31185}{512}\,e^{\prime 4}\,a^2\,e^2\,a^{\prime 10}+a^4\left(\frac{10395\,e^2\,e^{\prime 4}}{32}+\frac{93555\,e^4\,e^{\prime 2}}{512}\right)\right.\right.$

$$a^{\prime 8}+a^6\left(\frac{1839915\,e^2\,e^{\prime 4}}{8192}+\frac{1839915\,e^4\,e^{\prime 2}}{8192}\right)a^{\prime 6}+a^8\left(\frac{93555\,e^2\,e^{\prime 4}}{512}+\frac{10395\,e^4\,e^{\prime 2}}{32}\right)a^{\prime 4}+\frac{31185}{512}\,e^2\,a^{10}\,e^{\prime 4}\,a^{\prime 2}\right)\beta^6\,\Delta_*^{13}+$$

$$\left(-\frac{32445}{256}\,e^{\prime 4}\,a^2\,e^2\,a^{\prime 8}+a^4\left(-\frac{235305}{512}\,e^2\,e^{\prime 4}-\frac{74655\,e^4\,e^{\prime 2}}{256}\right)a^{\prime 6}+a^6\left(-\frac{74655\,e^2\,e^{\prime 4}}{256}-\frac{235305\,e^4\,e^{\prime 2}}{512}\right)a^{\prime 4}-\frac{32445}{256}\,e^2\,a^8\,e^{\prime 4}\,a^{\prime 2}\right)$$

$$\beta^6\,\Delta_*^{11}+\left(\left(a^2\left(\frac{19845\,e^{\prime 4}\,e^2}{256}-\frac{35\,e^{\prime 2}\,e^4}{128}\right)a^{\prime 6}+a^4\left(\frac{2205\,e^2\,e^{\prime 4}}{16}+\frac{2205\,e^4\,e^{\prime 2}}{16}\right)a^{\prime 4}+a^6\left(\frac{19845\,e^{\prime 2}\,e^4}{256}-\frac{35\,e^{\prime 4}\,e^2}{128}\right)a^{\prime 2}\right)\beta^6+$$

$$\left(\frac{945}{128}\,e^2\,a^2\,e^2\,a^{\prime 6}+\frac{945}{128}\,e^{\prime 2}\,a^4\,e^2\,a^{\prime 4}+\frac{945}{128}\,e^2\,a^6\,e^{\prime 2}\,a^{\prime 2}\right)\beta^4\right)\Delta_*^9+\left(\left(a^2\left(\frac{25\,e^{\prime 2}\,e^4}{128}-\frac{6275\,e^{\prime 4}\,e^2}{512}\right)a^{\prime 4}+a^4\left(\frac{25\,e^4\,e^{\prime 2}}{128}-\frac{6275\,e^{\prime 2}\,e^4}{512}\right)\right.\right.$$

$$a^{\prime 2}\right)\beta^6+\left(-\frac{1575}{128}\,e^{\prime 2}\,a^2\,e^2\,a^{\prime 4}-\frac{1575}{128}\,e^2\,a^4\,e^{\prime 2}\,a^{\prime 2}\right)\beta^4\right)\Delta_*^7+\left(a^{\prime 2}\,a^2\left(-\frac{1}{128}\,e^2\,e^4-\frac{e^4\,e^{\prime 2}}{128}\right)\beta^6+\frac{597}{128}\,a^{\prime 2}\,e^2\,a^2\,e^2\,\beta^4\right)\Delta_*^5\right)$$

◆ $\cos(\tau+\omega)$

$$\Big[\Big(\frac{72765}{512}e'^5 a^2 e\,a'^{10} + a^4\Big(\frac{86625\,e\,e'^5}{128}+\frac{218295\,e^3 e'^3}{256}\Big)a'^8 + a^6\Big(\frac{5457375\,e\,e'^5}{8192}+\frac{22525965\,e^3 e'^3}{8192}+\frac{5457375\,e^5 e'}{8192}\Big)a'^6 +$$

$$a^8\Big(\frac{86625\,e'e^5}{128}+\frac{218295\,e'^3 e^3}{256}\Big)a'^4 + \frac{72765}{512}e'\,a'^{10}e^5 a^2\Big)\beta^6\Delta_*^{13} + \Big(a^2\Big(\frac{12285\,e'^3 e^3}{512}-\frac{21735\,e'^5 e}{128}\Big)a'^8 + a^4\Big(-\frac{144585\,e\,e'^5}{512} -$$

$$\frac{82215\,e^3 e'^3}{128}+\frac{29295\,e^5 e'}{512}\Big)a'^6 + a^6\Big(\frac{29295\,e\,e'^5}{512}-\frac{82215\,e^3 e'^3}{128}-\frac{144585\,e^5 e'}{512}\Big)a'^4 + a^8\Big(\frac{12285\,e'^3 e^3}{512}-\frac{21735\,e'e^5}{128}\Big)$$

$$a'^2\Big)\beta^6\Delta_*^{11} + \Big(\Big(a^2\Big(\frac{14595\,e'^5 e}{512}-\frac{20475\,e'^3 e^3}{512}\Big)a'^6 + a^4\Big(-\frac{8505\,e\,e'^5}{128}-\frac{20895\,e^3 e'^3}{512}-\frac{8505\,e^5 e'}{128}\Big)a'^4 + a^6\Big(\frac{14595\,e'e^5}{512} -$$

$$\frac{20475\,e'^3 e^3}{512}\Big)a'^2\Big)\beta^6 + \Big(\frac{1575}{64}e'^3 a^2 e\,a'^6 + a^4\Big(\frac{1575\,e\,e'^3}{32}+\frac{1575\,e^3 e'}{32}\Big)a'^4 + \frac{1575}{64}e'\,a'^6 e^3 a^2\Big)\beta^4\Big)\Delta_*^9 + \Big(\Big(a^2\Big(\frac{4665\,e\,e'^5}{512} +$$

$$\frac{7215\,e^3 e'^3}{512}+\frac{25\,e^5 e'}{512}\Big)a'^4 + a^4\Big(\frac{25\,e\,e'^5}{512}+\frac{7215\,e^3 e'^3}{512}+\frac{4665\,e^5 e'}{512}\Big)a'^2\Big)\beta^6 + \Big(a^2\Big(\frac{195\,e'^3 e}{64}-\frac{495\,e'^3 e}{32}\Big)a'^4 + a^4\Big(\frac{195\,e'^3 e}{64} -$$

$$\frac{495\,e'e^3}{32}\Big)a'^2\Big)\beta^4\Big)\Delta_*^7 + \Big(a^2 a^2\Big(-\frac{15\,e\,e'^5}{256}+\frac{507\,e^3 e'^3}{256}-\frac{15\,e^5 e'}{256}\Big)\beta^6 + a^2 a^2\Big(-\frac{117\,e\,e'^3}{32}-\frac{117\,e^3 e'}{32}\Big)\beta^4 + \frac{27}{8}a^2 e'a^2 e\,\beta^2\Big)\Delta_*^5\Big]$$

◆ $\cos(\tau-\omega)$

$$\Big[\Big(\frac{10395}{256}e'^5 a^2 e\,a'^{10} + a^4\Big(\frac{10395\,e'^5 e}{512}-\frac{31185\,e^3 e'^3}{1024}\Big)a'^8 + a^6\Big(-\frac{530145\,e\,e'^5}{2048} -$$

$$\frac{1091475\,e^3 e'^3}{2048}-\frac{530145\,e^5 e'}{2048}\Big)a'^6 + a^8\Big(\frac{10395\,e'e^5}{512}-\frac{31185\,e'^3 e^3}{1024}\Big)a'^4 + \frac{10395}{256}e'\,a'^{10}e^5 a^2\Big)\beta^6\Delta_*^{13} + \Big(a^2\Big(\frac{945\,e'^3 e^3}{64} -$$

$$\frac{5355\,e'^5 e}{128}\Big)a'^8 + a^4\Big(\frac{25515\,e\,e'^5}{512}+\frac{63315\,e^3 e'^3}{1024}+\frac{4725\,e^5 e'}{128}\Big)a'^6 + a^6\Big(\frac{4725\,e\,e'^5}{128}+\frac{63315\,e^3 e'^3}{1024}+\frac{25515\,e^5 e'}{512}\Big)a'^4 +$$

$$a^8\Big(\frac{945\,e'^3 e^3}{64}-\frac{5355\,e'e^5}{128}\Big)a'^2\Big)\beta^6\Delta_*^{11} + \Big(\Big(a^2\Big(\frac{1505\,e'^5 e}{256}-\frac{3255\,e'^3 e^3}{256}\Big)a'^6 + a^4\Big(-\frac{5565\,e\,e'^5}{1024}+\frac{38115\,e^3 e'^3}{1024}-\frac{5565\,e^5 e'}{1024}\Big)a'^4 +$$

$$a^6\Big(\frac{1505\,e'e^5}{256}-\frac{3255\,e'^3 e^3}{256}\Big)a'^2\Big)\beta^6 + \Big(\frac{105}{32}e'^3 a^2 e\,a'^6 + a^4\Big(-\frac{1785\,e\,e'^3}{128}-\frac{1785\,e^3 e'}{128}\Big)a'^4 + \frac{105}{32}e'\,a'^6 e^3 a^2\Big)\beta^4\Big)\Delta_*^9 + \Big(\Big(a^2$$

$$\Big(\frac{95\,e\,e'^5}{256}-\frac{15\,e^3 e'^3}{64}-\frac{55\,e^5 e'}{256}\Big)a'^4 + a^4\Big(-\frac{55\,e\,e'^5}{256}-\frac{15\,e^3 e'^3}{64}+\frac{95\,e^5 e'}{256}\Big)a'^2\Big)\beta^6 + \Big(a^2\Big(\frac{15\,e'^3 e}{8}-\frac{15\,e'^3 e}{32}\Big)a'^4 + a^4\Big(\frac{15\,e'^3 e}{8} -$$

$$\frac{15\,e'e^3}{32}\Big)a'^2\Big)\beta^4\Big)\Delta_*^7 + \Big(a^2 a^2\Big(-\frac{3\,e\,e'^5}{128}-\frac{21\,e^3 e'^3}{128}-\frac{3\,e^5 e'}{128}\Big)\beta^6 + a^2 a^2\Big(-\frac{3\,e\,e'^3}{32}-\frac{3\,e^3 e'}{32}\Big)\beta^4 - \frac{3}{4}a^2 e'a^2 e\,\beta^2\Big)\Delta_*^5\Big]$$

◆ $\cos(2\tau)$

$$\Big[\Big(a^2\Big(\frac{3465\,e'^6}{512}-\frac{31185\,e'^4 e^2}{512}\Big)a'^{10} +$$

$$a^4\Big(-\frac{38115\,e'^6}{512}-\frac{93555\,e^2 e'^4}{256}-\frac{155925\,e^4 e'^2}{512}\Big)a'^8 + a^6\Big(-\frac{1133055\,e'^6}{8192}-\frac{9199575\,e^2 e'^4}{8192}-\frac{9199575\,e^4 e'^2}{8192}-\frac{1133055\,e^6}{8192}\Big)a'^6 +$$

$$a^8\Big(-\frac{38115\,e^6}{512}-\frac{93555\,e'^2 e^4}{256}-\frac{155925\,e^4 e'^2}{512}\Big)a'^4 + a^{10}\Big(\frac{3465\,e^6}{512}-\frac{31185\,e'^2 e^4}{512}\Big)a'^2\Big)\beta^6\Delta_*^{13} + \Big(a^2\Big(\frac{4725\,e'^6}{256}+\frac{29295\,e^2 e'^4}{256}\Big)$$

$$a'^8 + a^4\Big(\frac{45675\,e'^6}{512}+\frac{67095\,e^2 e'^4}{128}+\frac{206955\,e^4 e'^2}{512}\Big)a'^6 + a^6\Big(\frac{45675\,e^6}{512}+\frac{67095\,e'^2 e^4}{128}+\frac{206955\,e^4 e'^2}{512}\Big)a'^4 + a^8\Big(\frac{4725\,e^6}{256} +$$

$$\frac{29295\,e'^2 e^4}{256}\Big)a'^2\Big)\beta^6\Delta_*^{11} + \Big(\Big(a^2\Big(-\frac{1505\,e'^6}{128}-\frac{16065\,e^2 e'^4}{512}+\frac{4935\,e^4 e'^2}{512}\Big)a'^6 + a^4\Big(\frac{5075\,e'^6}{384}+\frac{6615\,e^2 e'^4}{256}+\frac{6615\,e^4 e'^2}{256} +$$

$$\frac{5075\,e^6}{384}\Big)a'^4 + a^6\Big(-\frac{1505\,e^6}{128}-\frac{16065\,e'^2 e^4}{512}+\frac{4935\,e^4 e'^2}{512}\Big)a'^2\Big)\beta^6 + \Big(a^2\Big(-\frac{105\,e'^4}{64}-\frac{315\,e^2 e'^2}{32}\Big)a'^6 + a^4\Big(-\frac{1575\,e'^4}{128} -$$

$$\frac{1155\,e^2 e'^2}{32}-\frac{1575\,e^4}{128}\Big)a'^4 + a^6\Big(-\frac{105\,e^4}{64}-\frac{315\,e'^2 e^2}{32}\Big)a'^2\Big)\beta^4\Big)\Delta_*^9 + \Big(\Big(a^2\Big(-\frac{1225\,e'^6}{512}-\frac{2325\,e^2 e'^4}{128}-\frac{4905\,e^4 e'^2}{512}\Big)a'^4 +$$

$$a^4\Big(-\frac{1225\,e^6}{512}-\frac{2325\,e'^2 e^4}{128}-\frac{4905\,e^4 e'^2}{512}\Big)a'^2\Big)\beta^6 + \Big(a^2\Big(\frac{345\,e'^4}{64}+\frac{375\,e^2 e'^2}{32}\Big)a'^4 + a^4\Big(\frac{345\,e^4}{64}+\frac{375\,e'^2 e^2}{32}\Big)a'^2\Big)\beta^4\Big)\Delta_*^7 + \Big(a^2$$

$$a^2\Big(-\frac{101\,e'^6}{768}-\frac{693\,e^2 e'^4}{256}-\frac{693\,e^4 e'^2}{256}-\frac{101\,e^6}{768}\Big)\beta^6 + a^2 a^2\Big(\frac{141\,e'^4}{128}+\frac{69\,e^2 e'^2}{16}+\frac{141\,e^4}{128}\Big)\beta^4 + a^2 a^2\Big(-\frac{9\,e'^2}{8}-\frac{9\,e^2}{8}\Big)\beta^2\Big)\Delta_*^5\Big]$$

- $\cos(3\omega)\Bigg[\left(-\dfrac{31185\,e'^3\,a^3\,e^3\,a'^9}{1024}+\dfrac{280665\,e'^3\,a^5\,e^3\,a'^7}{4096}+\dfrac{280665\,e'^3\,a^7\,e^3\,a'^5}{4096}-\dfrac{31185\,e'^3\,a^9\,e^3\,a'^3}{1024}\right)\beta^6\,\Delta_*^{13}+\left(\dfrac{76545\,e'^3\,a^3\,e^3\,a'^7}{1024}+\right.$
  $\left.\dfrac{331695\,e'^3\,a^5\,e^3\,a'^5}{4096}+\dfrac{76545\,e'^3\,a^7\,e^3\,a'^3}{1024}\right)\beta^6\,\Delta_*^{11}+\left(-\dfrac{56385\,e'^3\,a^3\,e^3\,a'^5}{1024}-\dfrac{56385\,e'^3\,a^5\,e^3\,a'^3}{1024}\right)\beta^6\,\Delta_*^9+\dfrac{6045}{512}\,a'^3\,e'^3\,a^3\,e^3\,\beta^6\,\Delta_*^7\Bigg]$

- $\cos(\tau+2\omega)\Bigg[\left(-\dfrac{31185}{128}\,e'^4\,a^3\,e^2\,a'^9+a^5\left(-\dfrac{467775}{512}\,e^2\,e'^4-\dfrac{1216215\,e^4\,e'^2}{2048}\right)a'^7+a^7\left(-\dfrac{1216215\,e^2\,e'^4}{2048}-\dfrac{467775\,e^4\,e'^2}{512}\right)\right.$
  $\left. a'^5-\dfrac{31185}{128}\,e'^2\,a^9\,e^4\,a'^3\right)\beta^6\,\Delta_*^{13}+\left(a^3\left(\dfrac{337365\,e'^4\,e^2}{1024}-\dfrac{19845\,e'^2\,e^4}{1024}\right)a'^7+a^5\left(\dfrac{1187865\,e^2\,e'^4}{2048}+\dfrac{1187865\,e^4\,e'^2}{2048}\right)a'^5+$
  $a^7\left(\dfrac{337365\,e'^2\,e^4}{1024}-\dfrac{19845\,e'^4\,e^2}{1024}\right)a'^3\right)\beta^6\,\Delta_*^{11}+\left(\left(a^3\left(\dfrac{38325\,e'^2\,e^4}{1024}-\dfrac{78015\,e'^4\,e^2}{1024}\right)a'^5+a^5\left(\dfrac{38325\,e'^4\,e^2}{1024}-\dfrac{78015\,e'^2\,e^4}{1024}\right)a'^3\right)\beta^6+$
  $\left(-\dfrac{2835}{128}\,e'^2\,a^3\,e^2\,a'^5-\dfrac{2835}{128}\,e'^2\,a^5\,e^2\,a'^3\right)\beta^4\right)\Delta_*^9+\left(a'^3\,a^3\left(-\dfrac{18515\,e^2\,e'^4}{1024}-\dfrac{18515\,e^4\,e'^2}{1024}\right)\beta^6+\dfrac{2565}{128}\,a'^3\,e'^2\,a^3\,e^2\,\beta^4\right)\Delta_*^7\Bigg]$

- $\cos(2\tau+\omega)\Bigg[\left(a^3\left(\dfrac{93555\,e'^3\,e^3}{1024}-\dfrac{51975\,e'^5\,e}{512}\right)a'^9+a^5\left(-\dfrac{218295\,e\,e'^5}{4096}-\dfrac{343035\,e^3\,e'^3}{4096}+\dfrac{654885\,e^5\,e'}{4096}\right)a'^7+a^7\left(\dfrac{654885\,e\,e'^5}{4096}-\right.\right.$
  $\left.\left.\dfrac{343035\,e^3\,e'^3}{4096}-\dfrac{218295\,e^5\,e'}{4096}\right)a'^5+a^9\left(\dfrac{93555\,e'^3\,e^3}{1024}-\dfrac{51975\,e'\,e^5}{512}\right)a'^3\right)\beta^6\,\Delta_*^{13}+\left(a^3\left(-\dfrac{19845\,e\,e'^5}{512}-\dfrac{231525\,e^3\,e'^3}{1024}\right)a'^7+\right.$
  $a^5\left(-\dfrac{1280475\,e\,e'^5}{4096}-\dfrac{2514645\,e^3\,e'^3}{4096}-\dfrac{1280475\,e^5\,e'}{4096}\right)a'^5+a^7\left(-\dfrac{19845\,e'\,e^5}{512}-\dfrac{231525\,e'^3\,e^3}{1024}\right)a'^3\Bigg)\beta^6\,\Delta_*^{11}+\left(\left(a^3\left(\dfrac{69195\,e\,e'^5}{1024}+\right.\right.\right.$
  $\left.\dfrac{99645\,e^3\,e'^3}{1024}-\dfrac{9485\,e^5\,e'}{1024}\right)a'^5+a^5\left(-\dfrac{9485\,e\,e'^5}{1024}+\dfrac{99645\,e^3\,e'^3}{1024}+\dfrac{69195\,e^5\,e'}{1024}\right)a'^3\right)\beta^6+\left(a^3\left(\dfrac{945\,e'\,e^3}{128}-\dfrac{945\,e'^3\,e}{128}\right)a'^5+a^5\right.$
  $\left(\dfrac{945\,e'^3\,e}{128}-\dfrac{945\,e'\,e^3}{128}\right)a'^3\Bigg)\beta^4\Bigg)\Delta_*^9+\left(a'^3\,a^3\left(\dfrac{1515\,e\,e'^5}{128}+\dfrac{19245\,e^3\,e'^3}{512}+\dfrac{1515\,e^5\,e'}{128}\right)\beta^6+a'^3\,a^3\left(-\dfrac{225\,e\,e'^3}{16}-\dfrac{225\,e^3\,e'}{16}\right)\beta^4\right)\Delta_*^7\Bigg]$

- $\cos(3\tau)\Bigg[\left(a^3\left(\dfrac{8085\,e'^6}{256}+\dfrac{31185\,e^2\,e'^4}{256}\right)a'^9+\right.$
  $a^5\left(\dfrac{176715\,e'^6}{2048}+\dfrac{571725\,e^2\,e'^4}{1024}+\dfrac{779625\,e^4\,e'^2}{2048}\right)a'^7+a^7\left(\dfrac{176715\,e^6}{2048}+\dfrac{571725\,e'^2\,e^4}{1024}+\dfrac{779625\,e'^4\,e^2}{2048}\right)a'^5+a^9\left(\dfrac{8085\,e^6}{256}+\right.$
  $\left.\dfrac{31185\,e'^2\,e^4}{256}\right)a'^3\Bigg)\beta^6\,\Delta_*^{13}+\left(a^3\left(-\dfrac{2205\,e'^6}{128}-\dfrac{4725\,e^2\,e'^4}{256}+\dfrac{12285\,e^4\,e'^2}{256}\right)a'^7+a^5\left(\dfrac{97965\,e'^6}{2048}+\dfrac{409185\,e^2\,e'^4}{2048}+\dfrac{409185\,e^4\,e'^2}{2048}+\right.\right.$
  $\left.\dfrac{97965\,e^6}{2048}\right)a'^5+a^7\left(-\dfrac{2205\,e^6}{128}-\dfrac{4725\,e'^2\,e^4}{256}+\dfrac{12285\,e'^4\,e^2}{256}\right)a'^3\Bigg)\beta^6\,\Delta_*^{11}+\left(\left(a^3\left(-\dfrac{8505\,e'^6}{512}-\dfrac{3255\,e^2\,e'^4}{32}-\dfrac{29505\,e^4\,e'^2}{512}\right)\right.\right.$
  $a'^5+a^5\left(-\dfrac{8505\,e^6}{512}-\dfrac{3255\,e'^2\,e^4}{32}-\dfrac{29505\,e'^4\,e^2}{512}\right)a'^3\Bigg)\beta^6+\left(a^3\left(\dfrac{315\,e'^4}{64}+\dfrac{315\,e^2\,e'^2}{32}\right)a'^5+a^5\left(\dfrac{315\,e^4}{64}+\dfrac{315\,e'^2\,e^2}{32}\right)\right.$
  $\left. a'^3\right)\beta^4\Bigg)\Delta_*^9+\left(a'^3\,a^3\left(-\dfrac{3105\,e'^6}{1024}-\dfrac{28545\,e^2\,e'^4}{1024}-\dfrac{28545\,e^4\,e'^2}{1024}-\dfrac{3105\,e^6}{1024}\right)\beta^6+a'^3\,a^3\left(\dfrac{195\,e'^4}{64}+\dfrac{45\,e^2\,e'^2}{4}+\dfrac{195\,e^4}{64}\right)\beta^4\right)\Delta_*^7\Bigg]$

◆ $\cos(\tau - 2\omega)\left(\left(\frac{10395}{128} e'^4 a^3 e^2 a'^9 + a^5\left(\frac{128205\, e^2 e'^4}{256} + \frac{405405\, e^4 e'^2}{1024}\right)a'^7 + \right.\right.$

$a^7\left(\frac{405405\, e^2 e'^4}{1024} + \frac{128205\, e^4 e'^2}{256}\right)a'^5 + \frac{10395}{128} e^2 a^9 e'^4 a'^3\Bigg)\beta^6 \Delta_*^{13} + \left(\frac{315}{256} e'^4 a\, e^2 a'^9 + a^3\left(-\frac{50715\, e^2 e'^4}{1024} - \frac{4725\, e^4 e'^2}{1024}\right)a'^7 + \right.$

$a^5\left(-\frac{142695\, e^2 e'^4}{1024} - \frac{142695\, e^4 e'^2}{1024}\right)a'^5 + a^7\left(-\frac{4725\, e^2 e'^4}{1024} - \frac{50715\, e^4 e'^2}{1024}\right)a'^3 + \frac{315}{256} e^2 a^9 e'^4 a'\Bigg)\beta^6 \Delta_*^{11} + \left(\left(-\frac{245}{128} e'^4 a\, e^2 a'^7 + \right.\right.$

$a^3\left(-\frac{9135\, e^2 e'^4}{1024} - \frac{4095\, e^4 e'^2}{1024}\right)a'^5 + a^5\left(-\frac{4095\, e^2 e'^4}{1024} - \frac{9135\, e^4 e'^2}{1024}\right)a'^3 - \frac{245}{128} e^2 a^7 e'^4 a'\Bigg)\beta^6 + \left(\frac{1575}{128} e^2 a^3 e'^2 a'^5 + \frac{1575}{128}\right.$

$e'^2 a^5 e^2 a'^3\Bigg)\beta^4\Bigg)\Delta_*^9 + \left(\left(a\left(\frac{45\, e^2 e'^4}{64} + \frac{5\, e^4 e'^2}{64}\right)a'^5 + a^3\left(\frac{795\, e^2 e'^4}{1024} + \frac{795\, e^4 e'^2}{1024}\right)a'^3 + a^5\left(\frac{5\, e^2 e'^4}{64} + \frac{45\, e^4 e'^2}{64}\right)a'\right)\beta^6 + \left(\frac{15}{64} e'^2\right.\right.$

$a\, e^2 a'^5 - \frac{315}{128} e'^2 a^3 e^2 a'^3 + \frac{15}{64} e'^2 a^5 e^2 a'\Bigg)\beta^4\Bigg)\Delta_*^7 + \left(\left(a\left(-\frac{5}{256} e^2 e'^4 - \frac{5\, e^4 e'^2}{64}\right)a'^3 + a^3\left(-\frac{5}{64} e^2 e'^4 - \frac{5\, e^4 e'^2}{256}\right)a'\right)\beta^6 + \left(-\frac{15}{64}\right.\right.$

$e'^2 a\, e^2 a'^3 - \frac{15}{64} e'^2 a^3 e^2 a'\Bigg)\beta^4\Bigg)\Delta_*^5 + \left(a'a\left(\frac{e^2 e'^4}{192} + \frac{e^4 e'^2}{192}\right)\beta^6 + \frac{1}{64} a'e'^2 a\, e^2 \beta^4\right)\Delta_*^3 - \frac{e'^2 a\, e^4 \beta^6}{192\, a'^2} - \frac{e'^4 a\, e^2 \beta^6}{192\, a'^2} - \frac{e'^2 a\, e^2 \beta^4}{64\, a'^2}\Bigg)$

◆ $\cos(2\tau - \omega)$

$\left(\left(\frac{3465}{256} e'^5 a\, e\, a'^{11} + a^3\left(\frac{72765\, e\, e'^5}{512} + \frac{197505\, e^3 e'^3}{1024}\right)a'^9 + a^5\left(\frac{987525\, e\, e'^5}{2048} + \frac{2338875\, e^3 e'^3}{2048} + \frac{516285\, e^5 e'}{2048}\right)a'^7 + a^7\right.\right.$

$\left(\frac{516285\, e\, e'^5}{2048} + \frac{2338875\, e^3 e'^3}{2048} + \frac{987525\, e^5 e'}{2048}\right)a'^5 + a^9\left(\frac{72765\, e' e'^5}{512} + \frac{197505\, e^3 e'^3}{1024}\right)a'^3 + \frac{3465}{256} e' a^{11} e^5 a'\Bigg)\beta^6 \Delta_*^{13} + \left(-\frac{5355}{256}\right.$

$e'^5 a\, e\, a'^9 + a^3\left(-\frac{60795\, e\, e'^5}{512} - \frac{199395\, e^3 e'^3}{1024}\right)a'^7 + a^5\left(-\frac{154035\, e\, e'^5}{2048} - \frac{617085\, e^3 e'^3}{2048} - \frac{154035\, e^5 e'}{2048}\right)a'^5 + a^7\left(-\frac{60795\, e' e'^5}{512} - \right.$

$\frac{199395\, e^3 e'^3}{1024}\right)a'^3 - \frac{5355}{256} e' a^9 e^5 a'\Bigg)\beta^6 \Delta_*^{11} + \left(\left(a\left(\frac{1295\, e'^5 e}{256} - \frac{315\, e^3 e'^3}{128}\right)a'^7 + a^3\left(-\frac{6615\, e\, e'^5}{1024} - \frac{22365\, e^3 e'^3}{1024} - \right.\right.\right.$

$\frac{12915\, e^5 e'}{1024}\right)a'^5 + a^5\left(-\frac{12915\, e\, e'^5}{1024} - \frac{22365\, e^3 e'^3}{1024} - \frac{6615\, e^5 e'}{1024}\right)a'^3 + a^7\left(\frac{1295\, e' e'^5}{256} - \frac{315\, e^3 e'^3}{128}\right)a'\Bigg)\beta^6 + \left(\frac{105}{32} e^3 a\, e\, a'^7 + \right.$

$a^3\left(\frac{2625\, e\, e'^3}{128} + \frac{1995\, e^3 e'}{128}\right)a'^5 + a^5\left(\frac{1995\, e\, e'^3}{128} + \frac{2625\, e^3 e'}{128}\right)a'^3 + \frac{105}{32} e' a^7 e^3 a'\Bigg)\beta^4\Bigg)\Delta_*^9 + \left(\left(a\left(\frac{535\, e\, e'^5}{256} + \frac{135\, e^3 e'^3}{64}\right)a'^5 + \right.\right.$

$a^3\left(-\frac{75\, e\, e'^5}{64} - \frac{615\, e^3 e'^3}{512} - \frac{75\, e^5 e'}{64}\right)a'^3 + a^5\left(\frac{535\, e' e'^5}{256} + \frac{135\, e^3 e'^3}{64}\right)a'\Bigg)\beta^6 + \left(-\frac{45}{16} e^3 a\, e\, a'^5 + a^3\left(-\frac{45\, e\, e'^3}{32} - \frac{45\, e^3 e'}{32}\right)\right.$

$a'^3 - \frac{45}{16} e' a^5 e^3 a'\Bigg)\beta^4\Bigg)\Delta_*^7 + \left(\left(a\left(\frac{5\, e\, e'^5}{16} + \frac{99\, e^3 e'^3}{128} + \frac{5\, e^5 e'}{64}\right)a'^3 + a^3\left(\frac{5\, e\, e'^5}{64} + \frac{99\, e^3 e'^3}{128} + \frac{5\, e^5 e'}{16}\right)a'\right)\beta^6 + \left(a\left(-\frac{33\, e\, e'^3}{32} - \right.\right.\right.$

$\frac{9\, e^3 e'}{16}\right)a'^3 + a^3\left(-\frac{9\, e\, e'^3}{16} - \frac{33\, e^3 e'}{32}\right)a'\Bigg)\beta^4 + \left(\frac{3}{4} e' a\, e\, a'^3 + \frac{3}{4} e' a^3 e\, a'\right)\beta^2\Bigg)\Delta_*^5 + \left(a'a\left(\frac{5\, e\, e'^5}{192} + \frac{9\, e^3 e'^3}{64} + \frac{5\, e^5 e'}{192}\right)\beta^6 + a'\right.$

$a\left(-\frac{3\, e\, e'^3}{16} - \frac{3\, e^3 e'}{16}\right)\beta^4 + \frac{1}{4} a'e' a\, e\, \beta^2\Bigg)\Delta_*^3 - \frac{5\, e' a\, e^5 \beta^6}{48\, a'^2} - \frac{9\, e^3 a\, e^3 \beta^6}{16\, a'^2} - \frac{5\, e'^5 a\, e\, \beta^6}{48\, a'^2} + \frac{3\, e' a\, e^3 \beta^4}{4\, a'^2} + \frac{3\, e^3 a\, e\, \beta^4}{4\, a'^2} - \frac{e' a\, e\, \beta^2}{a'^2}\Bigg)$

◆ $\cos(\tau + 3\omega)\left(\left(\frac{280665\, e'^3 a^4 e^3 a'^8}{2048} + \frac{841995\, e'^3 a^6 e^3 a'^6}{4096} + \right.\right.$

$\frac{280665\, e'^3 a^8 e^3 a'^4}{2048}\Bigg)\beta^6 \Delta_*^{13} + \left(-\frac{467775\, e'^3 a^4 e^3 a'^6}{2048} - \frac{467775\, e'^3 a^6 e^3 a'^4}{2048}\right)\beta^6 \Delta_*^{11} + \frac{186795\, a'^4 e'^3 a^4 e^3 \beta^6 \Delta_*^9}{2048}\Bigg)$

◆ $\cos(2\tau + 2\omega)\left(\left(a^4\left(\frac{280665\, e'^4 e^2}{1024} - \frac{93555\, e'^2 e^4}{2048}\right)a'^8 + \right.\right.$

$a^6\left(\frac{1964655\, e^2 e'^4}{4096} + \frac{1964655\, e^4 e'^2}{4096}\right)a'^6 + a^8\left(\frac{280665\, e'^2 e^4}{1024} - \frac{93555\, e^4 e'^2}{2048}\right)a'^4\Bigg)\beta^6 \Delta_*^{13} + \left(a^4\left(\frac{314685\, e'^2 e^4}{2048} - \frac{42525\, e^4 e'^2}{512}\right)\right.$

$a'^6 + a^6\left(\frac{314685\, e^4 e'^2}{2048} - \frac{42525\, e'^2 e^4}{512}\right)a'^4\Bigg)\beta^6 \Delta_*^{11} + \left(a^4 a'^4\left(-\frac{228375\, e^2 e'^4}{2048} - \frac{228375\, e^4 e'^2}{2048}\right)\beta^6 + \frac{8505}{512} a^4 e'^2 a'^4 e^2 \beta^4\right)\Delta_*^9\Bigg)$

◆ $\cos(3\tau + \omega)$

$$\left(\left(a^4\left(-\frac{93555\,e\,e'^5}{1024} - \frac{467775\,e^3\,e'^3}{2048}\right)a'^8 + a^6\left(-\frac{1216215\,e\,e'^5}{4096} - \frac{2900205\,e^3\,e'^3}{4096} - \frac{1216215\,e^5\,e'}{4096}\right)a'^6 + a^8\left(-\frac{93555\,e'\,e^5}{1024} - \frac{467775\,e'^3\,e^3}{2048}\right)a'^4\right)\beta^6\,\Delta_*^{13} + \left(a^4\left(\frac{65205\,e\,e'^5}{512} + \frac{326025\,e^3\,e'^3}{2048} - \frac{31185\,e^5\,e'}{1024}\right)a'^6 + a^6\left(-\frac{31185\,e\,e'^5}{1024} + \frac{326025\,e^3\,e'^3}{2048} + \frac{65205\,e^5\,e'}{512}\right)a'^4\right)\beta^6\,\Delta_*^{11} + \left(a^4\,a'^4\left(\frac{111615\,e\,e'^5}{2048} + \frac{318255\,e^3\,e'^3}{2048} + \frac{111615\,e^5\,e'}{2048}\right)\beta^6 + a^4\,a'^4\left(-\frac{2835\,e\,e'^3}{256} - \frac{2835\,e^3\,e'}{256}\right)\beta^4\right)\Delta_*^9\right)$$

◆ $\cos(4\tau)$

$$\left(\left(a^4\left(-\frac{10395\,e'^6}{2048} + \frac{31185\,e^2\,e'^4}{1024} + \frac{93555\,e^4\,e'^2}{2048}\right)a'^8 + a^6\left(\frac{155925\,e'^6}{4096} + \frac{904365\,e^2\,e'^4}{4096} + \frac{904365\,e^4\,e'^2}{4096} + \frac{155925\,e^6}{4096}\right)a'^6 + a^8\left(-\frac{10395\,e^6}{2048} + \frac{31185\,e'^2\,e^4}{1024} + \frac{93555\,e'^4\,e^2}{2048}\right)a'^4\right)\beta^6\,\Delta_*^{13} + \left(a^4\left(-\frac{60165\,e'^6}{2048} - \frac{178605\,e^2\,e'^4}{1024} - \frac{191835\,e^4\,e'^2}{2048}\right)a'^6 + a^6\left(-\frac{60165\,e^6}{2048} - \frac{178605\,e'^2\,e^4}{1024} - \frac{191835\,e'^4\,e^2}{2048}\right)a'^4\right)\beta^6\,\Delta_*^{11} + \left(a^4\,a'^4\left(-\frac{60095\,e'^6}{6144} - \frac{165585\,e^2\,e'^4}{2048} - \frac{165585\,e^4\,e'^2}{2048} - \frac{60095\,e^6}{6144}\right)\beta^6 + a^4\,a'^4\left(\frac{945\,e'^4}{512} + \frac{945\,e^2\,e'^2}{128} + \frac{945\,e^4}{512}\right)\beta^4\right)\Delta_*^9\right)$$

◆ $\cos(\tau - 3\omega)$

$$\left(\left(-\frac{31185}{256}\,e'^3\,a^4\,e^3\,a'^8 - \frac{1590435\,e'^3\,a^6\,e^3\,a'^6}{8192} - \frac{31185}{256}\,e'^3\,a^8\,e^3\,a'^4\right)\beta^6\,\Delta_*^{13} + \left(-\frac{945}{512}\,e'^3\,a^2\,e^3\,a'^8 + \frac{19845}{256}\,e'^3\,a^4\,e^3\,a'^6 + \frac{19845}{256}\,e'^3\,a^6\,e^3\,a'^4 - \frac{945}{512}\,e'^3\,a^8\,e^3\,a'^2\right)\beta^6\,\Delta_*^{11} + \left(\frac{1365}{512}\,e'^3\,a^2\,e^3\,a'^6 - \frac{4305}{512}\,e'^3\,a^4\,e^3\,a'^4 + \frac{1365}{512}\,e'^3\,a^6\,e^3\,a'^2\right)\beta^6\,\Delta_*^9 + \left(-\frac{515}{512}\,e'^3\,a^2\,e^3\,a'^4 - \frac{515}{512}\,e'^3\,a^4\,e^3\,a'^2\right)\beta^6\,\Delta_*^7 + \frac{47}{768}\,a^2\,e'^3\,a^2\,e^3\,\beta^6\,\Delta_*^5\right)$$

◆ $\cos(2\tau - 2\omega)$

$$\left(\left(-\frac{10395}{256}\,e'^4\,a^2\,e^2\,a'^{10} + a^4\left(-\frac{135135}{512}\,e^2\,e'^4 - \frac{155925\,e^4\,e'^2}{1024}\right)a'^8 + a^6\left(-\frac{550935\,e^2\,e'^4}{2048} - \frac{550935\,e^4\,e'^2}{2048}\right)a'^6 + a^8\left(-\frac{155925\,e^2\,e'^4}{1024} - \frac{135135\,e^4\,e'^2}{512}\right)a'^4 - \frac{10395}{256}\,e^2\,a'^{10}\,e'^4\,a'^2\right)\beta^6\,\Delta_*^{13} + \left(\frac{315}{8}\,e'^4\,a^2\,e^2\,a'^8 + a^4\left(\frac{36855\,e^2\,e'^4}{512} + \frac{42525\,e^4\,e'^2}{1024}\right)a'^6 + a^6\left(\frac{42525\,e^2\,e'^4}{1024} + \frac{36855\,e^4\,e'^2}{512}\right)a'^4 + \frac{315}{8}\,e'^2\,a^8\,e^4\,a'^2\right)\beta^6\,\Delta_*^{11} + \left(\left(a^2\left(\frac{175\,e'^2\,e^4}{64} - \frac{105\,e'^4\,e^2}{64}\right)a'^6 + a^4\left(-\frac{8925\,e^2\,e'^4}{1024} - \frac{8925\,e^4\,e'^2}{1024}\right)a'^4 + a^6\left(\frac{175\,e'^4\,e^2}{64} - \frac{105\,e'^2\,e^4}{64}\right)a'^2\right)\beta^6 + \left(-\frac{315}{64}\,e'^2\,a^2\,e^2\,a'^6 - \frac{1365}{256}\,e'^2\,a^4\,e^2\,a'^4 - \frac{315}{64}\,e'^2\,a^6\,e^2\,a'^2\right)\beta^4\right)\Delta_*^9 + \left(\left(a^2\left(\frac{145\,e'^2\,e^4}{256} + \frac{55\,e^4\,e'^2}{64}\right)a'^4 + a^4\left(\frac{55\,e^2\,e'^4}{64} + \frac{145\,e^4\,e'^2}{256}\right)a'^2\right)\beta^6 + \left(\frac{45}{64}\,e'^2\,a^2\,e^2\,a'^4 + \frac{45}{64}\,e'^2\,a^4\,e^2\,a'^2\right)\beta^4\right)\Delta_*^7 + \left(a^2\,a'^2\left(\frac{9\,e'^2\,e^4}{64} + \frac{9\,e^4\,e'^2}{64}\right)\beta^6 - \frac{3}{64}\,a^2\,e'^2\,a^2\,e^2\,\beta^4\right)\Delta_*^5\right)$$

- $\cos(3\tau - \omega)$

$$\left(\left(\left(-\frac{10395}{512}\,e'^5\,a^2\,e\,a'^{10} + a^4\left(-\frac{10395\,e\,e'^5}{128} - \frac{31185\,e^3\,e'^3}{256}\right)a'^8 + a^6\left(\frac{218295\,e\,e'^5}{8192} + \frac{155925\,e^3\,e'^3}{8192} + \frac{218295\,e^5\,e'}{8192}\right)a'^6 + \right.\right.$$

$$a^8\left(-\frac{10395\,e'\,e^5}{128} - \frac{31185\,e^3\,e^3}{256}\right)a'^4 - \frac{10395}{512}\,e'\,a^{10}\,e^5\,a'^2\right)\beta^6\,\Delta_*^{13} + \left(a^2\left(-\frac{315\,e\,e'^5}{64} - \frac{12285\,e^3\,e'^3}{512}\right)a'^8 + a^4\left(-\frac{51975\,e\,e'^5}{512} - \right.$$

$$\frac{61425\,e^3\,e'^3}{256} - \frac{36855\,e^5\,e'}{512}\right)a'^6 + a^6\left(-\frac{36855\,e\,e'^5}{512} - \frac{61425\,e^3\,e'^3}{256} - \frac{51975\,e^5\,e'}{512}\right)a'^4 + a^8\left(-\frac{315\,e'\,e^5}{64} - \frac{12285\,e^3\,e^3}{512}\right)a'^2\right)\beta^6$$

$$\Delta_*^{11} + \left(\left(a^2\left(\frac{8435\,e\,e'^5}{512} + \frac{10185\,e^3\,e'^3}{512}\right)a'^6 + a^4\left(-\frac{1575\,e\,e'^5}{256} - \frac{1365\,e^3\,e'^3}{512} - \frac{1575\,e^5\,e'}{256}\right)a'^4 + a^6\left(\frac{8435\,e'\,e^5}{512} + \frac{10185\,e^3\,e^3}{512}\right)a'^2\right)$$

$$\beta^6 + \left(-\frac{105}{64}\,e'^3\,a^2\,e\,a'^6 + a^4\left(\frac{105\,e\,e'^3}{32} + \frac{105\,e^3\,e'}{32}\right)a'^4 - \frac{105}{64}\,e'\,a^6\,e^3\,a'^2\right)\beta^4\right)\Delta_*^9 + \left(\left(a^2\left(\frac{3365\,e\,e'^5}{512} + \frac{7845\,e^3\,e'^3}{512} + \right.\right.\right.$$

$$\frac{1505\,e^5\,e'}{512}\right)a'^4 + a^4\left(\frac{1505\,e\,e'^5}{512} + \frac{7845\,e^3\,e'^3}{512} + \frac{3365\,e^5\,e'}{512}\right)a'^2\right)\beta^6 + \left(a^2\left(-\frac{75\,e\,e'^3}{16} - \frac{195\,e^3\,e'}{64}\right)a'^4 + a^4\left(-\frac{195\,e\,e'^3}{64} - \right.$$

$$\frac{75\,e^3\,e'}{16}\right)a'^2\right)\beta^4\right)\Delta_*^7 + \left(a'^2\,a^2\left(\frac{311\,e\,e'^5}{256} + \frac{1029\,e^3\,e'^3}{256} + \frac{311\,e^5\,e'}{256}\right)\beta^6 + a'^2\,a^2\left(-\frac{3\,e\,e'^3}{2} - \frac{3\,e^3\,e'}{2}\right)\beta^4 + \frac{3}{8}\,a'^2\,e'\,a^2\,e\,\beta^2\right)\Delta_*^5\right)$$

- $\cos(2\tau + 3\omega)$ $\left(\left(-\frac{841995\,e'^3\,a^5\,e^3\,a'^7}{4096} - \frac{841995\,e'^3\,a^7\,e^3\,a'^5}{4096}\right)\beta^6\,\Delta_*^{13} + \frac{739935\,a'^5\,e^3\,a^5\,e^3\,\beta^6\,\Delta_*^{11}}{4096}\right)$

- $\cos(3\tau + 2\omega)$ $\left(\left(\frac{280665\,e'^2\,a^5\,e^4\,a'^7}{2048} + \frac{280665\,e'^4\,a^7\,e^2\,a'^5}{2048}\right)\beta^6\,\Delta_*^{13} + a'^5\,a^5\left(-\frac{399735\,e^2\,e'^4}{2048} - \frac{399735\,e^4\,e'^2}{2048}\right)\beta^6\,\Delta_*^{11}\right)$

- $\cos(4\tau + \omega)$ $\left(\left(a^5\left(\frac{280665\,e\,e'^5}{4096} + \frac{280665\,e^3\,e'^3}{4096} - \frac{93555\,e^5\,e'}{4096}\right)a'^7 + \right.\right.$

$$a^7\left(-\frac{93555\,e\,e'^5}{4096} + \frac{280665\,e^3\,e'^3}{4096} + \frac{280665\,e^5\,e'}{4096}\right)a'^5\right)\beta^6\,\Delta_*^{13} + a'^5\,a^5\left(\frac{314685\,e\,e'^5}{4096} + \frac{910035\,e^3\,e'^3}{4096} + \frac{314685\,e^5\,e'}{4096}\right)\beta^6\,\Delta_*^{11}\right)$$

- $\cos(5\tau)$ $\left(\left(a^5\left(-\frac{31185\,e'^6}{2048} - \frac{93555\,e^2\,e'^4}{1024} - \frac{93555\,e^4\,e'^2}{2048}\right)a'^7 + a^7\right.\right.$

$$\left(-\frac{31185\,e^6}{2048} - \frac{93555\,e'^2\,e^4}{1024} - \frac{93555\,e'^4\,e^2}{2048}\right)a'^5\right)\beta^6\,\Delta_*^{13} + a'^5\,a^5\left(-\frac{21735\,e'^6}{2048} - \frac{184275\,e^2\,e'^4}{2048} - \frac{184275\,e^4\,e'^2}{2048} - \frac{21735\,e^6}{2048}\right)\beta^6\,\Delta_*^{11}\right)$$

- $\cos(4\tau - \omega)$

$$\left(\left(\left(a^3\left(-\frac{10395\,e\,e'^5}{512} - \frac{31185\,e^3\,e'^3}{1024}\right)a'^9 + a^5\left(-\frac{509355\,e\,e'^5}{4096} - \frac{1216215\,e^3\,e'^3}{4096} - \frac{301455\,e^5\,e'}{4096}\right)a'^7 + a^7\left(-\frac{301455\,e\,e'^5}{4096} - \right.\right.\right.$$

$$\frac{1216215\,e^3\,e'^3}{4096} - \frac{509355\,e^5\,e'}{4096}\right)a'^5 + a^9\left(-\frac{10395\,e'\,e^5}{512} - \frac{31185\,e'^3\,e^3}{1024}\right)a'^3\right)\beta^6\,\Delta_*^{13} + \left(a^3\left(\frac{16065\,e\,e'^5}{512} + \frac{34965\,e^3\,e'^3}{1024}\right)\right.$$

$$a'^7 + a^5\left(-\frac{69615\,e\,e'^5}{4096} - \frac{61425\,e^3\,e'^3}{4096} - \frac{69615\,e^5\,e'}{4096}\right)a'^5 + a^7\left(\frac{16065\,e'\,e^5}{512} + \frac{34965\,e'^3\,e^3}{1024}\right)a'^3\right)\beta^6\,\Delta_*^{11} + \left(\left(a^3\left(\frac{28455\,e\,e'^5}{1024} + \right.\right.\right.$$

$$\frac{63315\,e^3\,e'^3}{1024} + \frac{13755\,e^5\,e'}{1024}\right)a'^5 + a^5\left(\frac{13755\,e\,e'^5}{1024} + \frac{63315\,e^3\,e'^3}{1024} + \frac{28455\,e^5\,e'}{1024}\right)a'^3\right)\beta^6 + \left(a^3\left(-\frac{525\,e\,e'^3}{128} - \frac{315\,e^3\,e'}{128}\right)a'^5 + a^5\right.$$

$$\left(-\frac{315\,e\,e'^3}{128} - \frac{525\,e^3\,e'}{128}\right)a'^3\right)\beta^4\right)\Delta_*^9 + \left(a'^3\,a^3\left(\frac{925\,e\,e'^5}{128} + \frac{10965\,e^3\,e'^3}{512} + \frac{925\,e^5\,e'}{128}\right)\beta^6 + a'^3\,a^3\left(-\frac{165\,e\,e'^3}{64} - \frac{165\,e^3\,e'}{64}\right)\beta^4\right)\Delta_*^7\right)$$

- $\cos(2\tau - 3\omega)$ $\left(\left(\frac{31185\,e'^3\,a^3\,e^3\,a'^9}{1024} + \right.\right.$

$$\frac{10395\,e'^3\,a^5\,e^3\,a'^7}{2048} + \frac{10395\,e'^3\,a^7\,e^3\,a'^5}{2048} + \frac{31185\,e'^3\,a^9\,e^3\,a'^3}{1024}\right)\beta^6\,\Delta_*^{13} + \left(-\frac{16695\,e'^3\,a^3\,e^3\,a'^7}{1024} - \frac{42525\,e'^3\,a^5\,e^3\,a'^5}{2048} - \right.$$

$$\frac{16695\,e'^3\,a^7\,e^3\,a'^3}{1024}\right)\beta^6\,\Delta_*^{11} + \left(\frac{35}{384}\,e'^3\,a\,e^3\,a'^7 + \frac{5775\,e'^3\,a^3\,e^3\,a'^5}{1024} + \frac{5775\,e'^3\,a^5\,e^3\,a'^3}{1024} + \frac{35}{384}\,e'^3\,a^7\,e^3\,a'\right)\beta^6\,\Delta_*^9 + \left(-\frac{5}{64}\,e'^3\,a\,e^3\right.$$

$$a'^5 + \frac{25}{512}\,e'^3\,a^3\,e^3\,a'^3 - \frac{5}{64}\,e'^3\,a^5\,e^3\,a'\right)\beta^6\,\Delta_*^7 + \left(-\frac{1}{128}\,a'\,e'^3\,a^3\,e^3 - \frac{1}{128}\,a'^3\,e'^3\,a\,e^3\right)\beta^6\,\Delta_*^5 + \frac{1}{576}\,a'\,e'^3\,a\,e^3\,\beta^6\,\Delta_*^3 - \frac{e'^3\,a\,e^3\,\beta^6}{144\,a'^2}\right)$$

◆ $\cos(3\tau - 2\omega)\left(\left(a^5\left(-\dfrac{10395}{64}e^2 e'^4 - \dfrac{135135 e^4 e'^2}{1024}\right)a'^7 + \right.\right.$

$a^7\left(-\dfrac{135135 e^2 e'^4}{1024} - \dfrac{10395 e^4 e'^2}{64}\right)a'^5\right)\beta^6\Delta_*^{13} + \left(\dfrac{945}{256}e'^4 a e^2 a'^9 + a^3\left(\dfrac{55755 e^2 e'^4}{1024} + \dfrac{34965 e^4 e'^2}{1024}\right)a'^7 + a^5\left(\dfrac{62685 e^2 e'^4}{1024} + \right.\right.$

$\dfrac{62685 e^4 e'^2}{1024}\right)a'^5 + a^7\left(\dfrac{34965 e^2 e'^4}{1024} + \dfrac{55755 e^4 e'^2}{1024}\right)a'^3 + \dfrac{945}{256}e^2 a^9 e'^4 a'\right)\beta^6\Delta_*^{11} + \left(\left(-\dfrac{315}{128}e'^4 a e^2 a'^7 + a^3\left(\dfrac{8995 e^2 e'^4}{1024} + \right.\right.\right.$

$\dfrac{9975 e^4 e'^2}{1024}\right)a'^5 + a^5\left(\dfrac{9975 e^2 e'^4}{1024} + \dfrac{8995 e^4 e'^2}{1024}\right)a'^3 - \dfrac{315}{128}e^2 a^7 e'^4 a'\right)\beta^6 + \left(-\dfrac{525}{128}e'^2 a^3 e^2 a'^5 - \dfrac{525}{128}e'^2 a^5 e^2 a'^3\right)\beta^4\right)\Delta_*^9 + $

$\left(\left(a\left(-\dfrac{225}{128}e^2 e'^4 - \dfrac{45 e^4 e'^2}{64}\right)a'^5 + a^3\left(\dfrac{875 e^2 e'^4}{1024} + \dfrac{875 e^4 e'^2}{1024}\right)a'^3 + a^5\left(-\dfrac{45}{64}e^2 e'^4 - \dfrac{225 e^4 e'^2}{128}\right)a'\right)\beta^6 + \left(\dfrac{45}{64}e'^2 a e^2 a'^5 + \dfrac{75}{128}\right.\right.$

$e'^2 a^3 e^2 a'^3 + \dfrac{45}{64}e'^2 a^5 e^2 a'\right)\beta^4\right)\Delta_*^7 + \left(\left(a\left(-\dfrac{153}{256}e^2 e'^4 - \dfrac{27 e^4 e'^2}{64}\right)a'^3 + a^3\left(-\dfrac{27}{64}e^2 e'^4 - \dfrac{153 e^4 e'^2}{256}\right)a'\right)\beta^6 + \left(\dfrac{27}{64}e'^2 a e^2 a'^3 + \right.\right.$

$\dfrac{27}{64}e'^2 a^3 e^2 a'\right)\beta^4\right)\Delta_*^5 + \left(a'a\left(-\dfrac{9}{64}e^2 e'^4 - \dfrac{9 e^4 e'^2}{64}\right)\beta^6 + \dfrac{9}{64}a'e'^2 a e^2\beta^4\right)\Delta_*^3 + \dfrac{81 e'^2 a e^4\beta^6}{64 a'^2} + \dfrac{81 e'^4 a e^2\beta^6}{64 a'^2} - \dfrac{81 e'^2 a e^2\beta^4}{64 a'^2}\right)$

◆ $\cos(5\tau - \omega)\left(\left(a^4\left(\dfrac{17325 e e'^5}{1024} + \dfrac{31185 e^3 e'^3}{2048}\right)a'^8 + a^6\left(-\dfrac{51975 e e'^5}{4096} - \dfrac{72765 e^3 e'^3}{4096} - \dfrac{51975 e^5 e'}{4096}\right)a'^6 + a^8\right.\right.$

$\left(\dfrac{17325 e' e^5}{1024} + \dfrac{31185 e'^3 e^3}{2048}\right)a'^4\right)\beta^6\Delta_*^{13} + \left(a^4\left(\dfrac{315 e e'^5}{8} + \dfrac{174825 e^3 e'^3}{2048} + \dfrac{18585 e^5 e'}{1024}\right)a'^6 + a^6\left(\dfrac{18585 e e'^5}{1024} + \dfrac{174825 e^3 e'^3}{2048} + \right.\right.$

$\dfrac{315 e^5 e'}{8}\right)a'^4\right)\beta^6\Delta_*^{11} + \left(a'^4 a^4\left(\dfrac{30275 e e'^5}{2048} + \dfrac{87675 e^3 e'^3}{2048} + \dfrac{30275 e^5 e'}{2048}\right)\beta^6 + a'^4 a^4\left(-\dfrac{315 e e'^3}{256} - \dfrac{315 e^3 e'}{256}\right)\beta^4\right)\Delta_*^9\right)$

◆ $\cos(3\tau - 3\omega)\left(\left(\dfrac{51975 e'^3 a^4 e^3 a'^8}{1024} + \dfrac{174405 e'^3 a^6 e^3 a'^6}{2048} + \right.\right.$

$\dfrac{51975 e'^3 a^8 e^3 a'^4}{1024}\right)\beta^6\Delta_*^{13} + \left(-\dfrac{315}{64}e'^3 a^2 e^3 a'^8 - \dfrac{9765 e'^3 a^4 e^3 a'^6}{1024} - \dfrac{9765 e'^3 a^6 e^3 a'^4}{1024} - \dfrac{315}{64}e'^3 a^8 e^3 a'^2\right)\beta^6\Delta_*^{11} + \left(-\dfrac{315}{256}\right.$

$e'^3 a^2 e^3 a'^6 + \dfrac{315 e'^3 a^4 e^3 a'^4}{1024} - \dfrac{315}{256}e'^3 a^6 e^3 a'^2\right)\beta^6\Delta_*^9 + \left(-\dfrac{15}{32}e'^3 a^2 e^3 a'^4 - \dfrac{15}{32}e'^3 a^4 e^3 a'^2\right)\beta^6\Delta_*^7 - \dfrac{47}{384}a'^2 e'^3 a^2 e^3\beta^6\Delta_*^5\right)$

◆ $\cos(4\tau - 2\omega)\left(\left(\dfrac{3465}{512}e'^4 a^2 e^2 a'^{10} + a^4\right.\right.$

$\left(\dfrac{10395 e^2 e'^4}{128} + \dfrac{24255 e^4 e'^2}{512}\right)a'^8 + a^6\left(\dfrac{675675 e^2 e'^4}{8192} + \dfrac{675675 e^4 e'^2}{8192}\right)a'^6 + a^8\left(\dfrac{24255 e^2 e'^4}{512} + \dfrac{10395 e^4 e'^2}{128}\right)a'^4 + \dfrac{3465}{512}e^2 a^{10}$

$e^4 a'^2\right)\beta^6\Delta_*^{13} + \left(-\dfrac{945}{256}e'^4 a^2 e^2 a'^8 + a^4\left(\dfrac{21105 e^2 e'^4}{512} + \dfrac{315 e^4 e'^2}{8}\right)a'^6 + a^6\left(\dfrac{315 e^2 e'^4}{8} + \dfrac{21105 e^4 e'^2}{512}\right)a'^4 - \dfrac{945}{256}e^2 a^8 e^4 a'^2\right)$

$\beta^6\Delta_*^{11} + \left(\left(a^2\left(-\dfrac{2835}{256}e^2 e'^4 - \dfrac{735 e^4 e'^2}{128}\right)a'^6 + a^4\left(-\dfrac{385}{128}e^2 e'^4 - \dfrac{385 e^4 e'^2}{128}\right)a'^4 + a^6\left(-\dfrac{735}{128}e^2 e'^4 - \dfrac{2835 e^4 e'^2}{256}\right)a'^2\right)\beta^6 + \left(\dfrac{105}{128}\right.\right.$

$e'^2 a^2 e^2 a'^6 + \dfrac{105}{128}e'^2 a^4 e^2 a'^4 + \dfrac{105}{128}e'^2 a^6 e^2 a'^2\right)\beta^4\right)\Delta_*^9 + \left(\left(a^2\left(-\dfrac{3115}{512}e^2 e'^4 - \dfrac{615 e^4 e'^2}{128}\right)a'^4 + a^4\left(-\dfrac{615}{128}e^2 e'^4 - \dfrac{3115 e^4 e'^2}{512}\right)\right.\right.$

$a'^2\right)\beta^6 + \left(\dfrac{165}{128}e'^2 a^2 e^2 a'^4 + \dfrac{165}{128}e'^2 a^4 e^2 a'^2\right)\beta^4\right)\Delta_*^7 + \left(a'^2 a^2\left(-\dfrac{213}{128}e^2 e'^4 - \dfrac{213 e^4 e'^2}{128}\right)\beta^6 + \dfrac{69}{128}a'^2 e'^2 a^2 e^2\beta^4\right)\Delta_*^5\right)$

◆ $\cos(6\tau)\, a'^6 a^6\left(-\dfrac{31185 e'^6}{8192} - \dfrac{280665 e^2 e'^4}{8192} - \dfrac{280665 e^4 e'^2}{8192} - \dfrac{31185 e^6}{8192}\right)\beta^6\,\Delta_*^{13}$

◆ $\cos(5\tau + \omega)\, a'^6 a^6\left(\dfrac{280665 e e'^5}{8192} + \dfrac{841995 e^3 e'^3}{8192} + \dfrac{280665 e^5 e'}{8192}\right)\beta^6\Delta_*^{13}$

◆ $\cos(4\tau + 2\omega)\, a'^6 a^6\left(-\dfrac{841995 e^2 e'^4}{8192} - \dfrac{841995 e^4 e'^2}{8192}\right)\beta^6\Delta_*^{13}$

◆ $\cos(3\tau + 3\omega) \dfrac{841995\, a'^6\, e'^3\, a^6\, e^3\, \beta^6\, \Delta_*^{13}}{8192}$

◆ $\cos(6\tau - \omega)\left(\left(a^5\left(\dfrac{72765\, e\, e'^5}{4096} + \dfrac{155925\, e^3\, e'^3}{4096} + \dfrac{31185\, e^5\, e'}{4096}\right)a'^7 + \right.\right.$

$a^7\left(\dfrac{31185\, e\, e'^5}{4096} + \dfrac{155925\, e^3\, e'^3}{4096} + \dfrac{72765\, e^5\, e'}{4096}\right)a'^5\right)\beta^6\, \Delta_*^{13} + a'^5\, a^5\left(\dfrac{51345\, e\, e'^5}{4096} + \dfrac{150255\, e^3\, e'^3}{4096} + \dfrac{51345\, e^5\, e'}{4096}\right)\beta^6\, \Delta_*^{11}\right)$

◆ $\cos(5\tau - 2\omega)\left(\left(a^5\left(\dfrac{10395\, e^2\, e'^4}{256} + \dfrac{72765\, e^4\, e'^2}{2048}\right)a'^7 + \right.\right.$

$a^7\left(\dfrac{72765\, e^2\, e'^4}{2048} + \dfrac{10395\, e^4\, e'^2}{256}\right)a'^5\right)\beta^6\, \Delta_*^{13} + \left(a^3\left(-\dfrac{19845\, e^2\, e'^4}{1024} - \dfrac{10395\, e^4\, e'^2}{1024}\right)a'^7 + a^5\left(-\dfrac{22995\, e^2\, e'^4}{2048} - \dfrac{22995\, e^4\, e'^2}{2048}\right)a'^5 + \right.$

$a^7\left(-\dfrac{10395\, e^2\, e'^4}{1024} - \dfrac{19845\, e^4\, e'^2}{1024}\right)a'^3\right)\beta^6\, \Delta_*^{11} + \left(\left(a^3\left(-\dfrac{17605\, e^2\, e'^4}{1024} - \dfrac{13965\, e^4\, e'^2}{1024}\right)a'^5 + a^5\left(-\dfrac{13965\, e^2\, e'^4}{1024} - \dfrac{17605\, e^4\, e'^2}{1024}\right)a'^3\right)\right.$

$\beta^6 + \left(\dfrac{105}{128}\, e^2\, a^3\, e'^2\, a'^5 + \dfrac{105}{128}\, e^2\, a^5\, e'^2\, a'^3\right)\beta^4\right)\Delta_*^9 + \left(a^3\, a'^3\left(-\dfrac{5595\, e^2\, e'^4}{1024} - \dfrac{5595\, e^4\, e'^2}{1024}\right)\beta^6 + \dfrac{75}{128}\, a^3\, e'^2\, a'^3\, e^2\, \beta^4\right)\Delta_*^7\right)$

◆ $\cos(4\tau - 3\omega)\left(\left(-\dfrac{10395\, e'^3\, a^3\, e^3\, a'^9}{1024} - \right.\right.$

$\dfrac{3465\, e'^3\, a^5\, e^3\, a'^7}{2048} - \dfrac{3465\, e'^3\, a^7\, e^3\, a'^5}{2048} - \dfrac{10395\, e'^3\, a^9\, e^3\, a'^3}{1024}\right)\beta^6\, \Delta_*^{13} + \left(-\dfrac{11025\, e'^3\, a^3\, e^3\, a'^7}{1024} - \dfrac{31185\, e'^3\, a^5\, e^3\, a'^5}{2048} - \right.$

$\dfrac{11025\, e'^3\, a^7\, e^3\, a'^3}{1024}\right)\beta^6\, \Delta_*^{11} + \left(\dfrac{35}{48}\, e'^3\, a\, e^3\, a'^7 - \dfrac{2975\, e'^3\, a^3\, e^3\, a'^5}{1024} - \dfrac{2975\, e'^3\, a^5\, e^3\, a'^3}{1024} + \dfrac{35}{48}\, e'^3\, a^7\, e^3\, a'\right)\beta^6\, \Delta_*^9 + \left(\dfrac{5}{8}\, e'^3\right.$

$a\, e^3\, a'^5 - \dfrac{55}{512}\, e'^3\, a^3\, e^3\, a'^3 + \dfrac{5}{8}\, e'^3\, a^5\, e^3\, a'\right)\beta^6\, \Delta_*^7 + \left(\dfrac{5}{16}\, a'\, e'^3\, a^3\, e^3 + \dfrac{5}{16}\, a^3\, e'^3\, a\, e^3\right)\beta^6\, \Delta_*^5 + \dfrac{1}{9}\, a'\, e'^3\, a\, e^3\, \beta^6\, \Delta_*^3 - \dfrac{16\, e'^3\, a\, e^3\, \beta^6}{9\, a'^2}\right)$

◆ $\cos(6\tau - 2\omega)\left(\left(a^4\left(-\dfrac{10395\, e^2\, e'^4}{1024} - \dfrac{10395\, e^4\, e'^2}{2048}\right)a'^8 + \right.\right.$

$a^6\left(-\dfrac{31185\, e^2\, e'^4}{4096} - \dfrac{31185\, e^4\, e'^2}{4096}\right)a'^6 + a^8\left(-\dfrac{10395\, e^2\, e'^4}{2048} - \dfrac{10395\, e^4\, e'^2}{1024}\right)a'^4\right)\beta^6\, \Delta_*^{13} + \left(a^4\left(-\dfrac{4725}{256}\, e^2\, e'^4 - \dfrac{29295\, e^4\, e'^2}{2048}\right)\right.$

$a'^6 + a^6\left(-\dfrac{29295\, e^2\, e'^4}{2048} - \dfrac{4725\, e^4\, e'^2}{256}\right)a'^4\right)\beta^6\, \Delta_*^{11} + \left(a^4\, a'^4\left(-\dfrac{15855\, e^2\, e'^4}{2048} - \dfrac{15855\, e^4\, e'^2}{2048}\right)\beta^6 + \dfrac{105}{512}\, a^4\, e'^2\, a'^4\, e^2\, \beta^4\right)\Delta_*^9\right)$

◆ $\cos(5\tau - 3\omega)\left(\left(-\dfrac{3465}{256}\, e'^3\, a^4\, e^3\, a'^8 - \dfrac{176715\, e'^3\, a^6\, e^3\, a'^6}{8192} - \right.\right.$

$\dfrac{3465}{256}\, e'^3\, a^8\, e^3\, a'^4\right)\beta^6\, \Delta_*^{13} + \left(\dfrac{945}{512}\, e'^3\, a^2\, e^3\, a'^8 - \dfrac{315}{64}\, e'^3\, a^4\, e^3\, a'^6 - \dfrac{315}{64}\, e'^3\, a^6\, e^3\, a'^4 + \dfrac{945}{512}\, e'^3\, a^8\, e^3\, a'^2\right)\beta^6\, \Delta_*^{11} + \left(\dfrac{1505}{512}\, e'^3\right.$

$a^2\, e^3\, a'^6 + \dfrac{3815\, e'^3\, a^4\, e^3\, a'^4}{1536} + \dfrac{1505}{512}\, e'^3\, a^6\, e^3\, a'^2\right)\beta^6\, \Delta_*^9 + \left(\dfrac{975}{512}\, e'^3\, a^2\, e^3\, a'^4 + \dfrac{975}{512}\, e'^3\, a^4\, e^3\, a'^2\right)\beta^6\, \Delta_*^7 + \dfrac{497}{768}\, a^2\, e'^3\, a'^2\, e^3\, \beta^6\, \Delta_*^5\right)$

◆ $\cos(7\tau - \omega)\, a'^6\, a^6\left(\dfrac{31185\, e\, e'^5}{8192} + \dfrac{93555\, e^3\, e'^3}{8192} + \dfrac{31185\, e^5\, e'}{8192}\right)\beta^6\, \Delta_*^{13}$

◆ $\cos(7\tau - 2\omega)\left(\left(a^5\left(-\dfrac{3465}{512}\, e^2\, e'^4 - \right.\right.\right.$

$\dfrac{10395\, e^4\, e'^2}{2048}\right)a'^7 + a^7\left(-\dfrac{10395\, e^2\, e'^4}{2048} - \dfrac{3465\, e^4\, e'^2}{512}\right)a'^5\right)\beta^6\, \Delta_*^{13} + a'^5\, a^5\left(-\dfrac{10395\, e^2\, e'^4}{2048} - \dfrac{10395\, e^4\, e'^2}{2048}\right)\beta^6\, \Delta_*^{11}\right)$

◆ $\cos(6\tau - 3\omega)\left(\left(\dfrac{1155\, e'^3\, a^3\, e^3\, a'^9}{1024} - \dfrac{10395\, e'^3\, a^5\, e^3\, a'^7}{4096} - \dfrac{10395\, e'^3\, a^7\, e^3\, a'^5}{4096} + \dfrac{1155\, e'^3\, a^9\, e^3\, a'^3}{1024}\right)\beta^6\, \Delta_*^{13} + \left(\dfrac{4095\, e'^3\, a^3\, e^3\, a'^7}{1024} + \right.\right.$

$\dfrac{20475\, e'^3\, a^5\, e^3\, a'^5}{4096} + \dfrac{4095\, e'^3\, a^7\, e^3\, a'^3}{1024}\right)\beta^6\, \Delta_*^{11} + \left(\dfrac{3745\, e'^3\, a^3\, e^3\, a'^5}{1024} + \dfrac{3745\, e'^3\, a^5\, e^3\, a'^3}{1024}\right)\beta^6\, \Delta_*^9 + \dfrac{685}{512}\, a^3\, e'^3\, a'^3\, e^3\, \beta^6\, \Delta_*^7\right)$

◆ $\cos(7\tau - 3\omega)\left(\left(\dfrac{3465\, e'^3\, a^4\, e^3\, a'^8}{2048} + \right.\right.$

$\left.\dfrac{10395\, e'^3\, a^6\, e^3\, a'^6}{4096} + \dfrac{3465\, e'^3\, a^8\, e^3\, a'^4}{2048}\right)\beta^6\,\Delta_*^{13} + \left(\dfrac{5985\, e'^3\, a^4\, e^3\, a'^6}{2048} + \dfrac{5985\, e'^3\, a^6\, e^3\, a'^4}{2048}\right)\beta^6\,\Delta_*^{11} + \left.\dfrac{8365\, a'^4\, e'^3\, a^4\, e^3\, \beta^6\,\Delta_*^9}{6144}\right)$

◆ $\cos(8\tau - 2\omega)\, a'^6\, a^6\left(-\dfrac{10395\, e^2\, e'^4}{8192} - \dfrac{10395\, e^4\, e'^2}{8192}\right)\beta^6\,\Delta_*^{13}$

◆ $\cos(8\tau - 3\omega)\left(\left(\dfrac{3465\, e'^3\, a^5\, e^3\, a'^7}{4096} + \dfrac{3465\, e'^3\, a^7\, e^3\, a'^5}{4096}\right)\beta^6\,\Delta_*^{13} + \dfrac{2835\, a'^5\, e'^3\, a^5\, e^3\, \beta^6\,\Delta_*^{11}}{4096}\right)$

◆ $\cos(9\tau - 3\omega)\, \dfrac{1155\, a'^6\, e'^3\, a^6\, e^3\, \beta^6\,\Delta_*^{13}}{8192}$

II.II. Explicit mapping

💡 Chapter 5, 6, Section 5.4.

The explicit mapping, derived in Chapter 6, i.e. in the form (15;6) is given up to 7th order in the mapping variables. It was derived by means of iterative series reversion (Section 5.4.2.). The real form can be reconstructed from it leading to (11;5).

■ II.II.1. $F_1^{(\kappa)}$

◆ $F_1^{(1)} = (0.870169533360692 + 0.4927524563214631\,i)\,z_1$

◆ $F_1^{(2)} = (1.371226070425621 + 0.7019865904020263\,i)\,z_1^2 - (0.01948337574586629 + 0.04667619113389489\,i)\,z_2\,z_1 - (2.614676165190312 + 1.629617436229222\,i)\,z_1\,\bar{z}_1 + (0.0500495184029146 - 0.00730167493516427\,i)\,\bar{z}_2\,z_1 - (0.03618064379809882 - 0.05723327056831234\,i)\,z_2^2 + (1.317008770629897 + 0.7038763157368793\,i)\,\bar{z}_1^2 + (0.03757213633224251 - 0.06971554031126874\,i)\,\bar{z}_2^2 + (0.02331884024591423 + 0.04668979678578943\,i)\,z_2\,\bar{z}_1 - (0.2130644154953522 + 0.1300918835773881\,i)\,z_2\,\bar{z}_2 - (0.04811256229074019 - 0.01114787696209221\,i)\,\bar{z}_1\,\bar{z}_2$

◆ $F_1^{(3)} = (3.702198357347421 - 6.65019267603833\,i)\,z_1^3 - (0.6060399822289254 - 0.2425247310776141\,i)\,z_2\,z_1^2 - (11.0351211318573 - 19.19678490091994\,i)\,\bar{z}_1\,z_1^2 - (0.07704083720746036 + 0.6500335447650077\,i)\,\bar{z}_2\,z_1^2 + (1.203330698332992 + 0.7520349634731888\,i)\,z_2^2\,z_1 + (10.94238675934796 - 18.42334677221183\,i)\,\bar{z}_1^2\,z_1 - (1.265284338743407 + 0.6393112499684074\,i)\,\bar{z}_2^2\,z_1 + (1.176149890262144 - 0.5252830416241154\,i)\,z_2\,\bar{z}_1\,z_1 - (1.428755614387478 - 2.529986796213948\,i)\,z_2\,\bar{z}_2\,z_1 + (0.199756165700369 + 1.263009871829049\,i)\,\bar{z}_1\,\bar{z}_2\,z_1 - (1.69347440356308 + 0.7150921845398489\,i)\,z_2^3 - (3.636931102586162 - 5.959593295441692\,i)\,\bar{z}_1^3 - (1.336910419221685 + 1.327226431731362\,i)\,\bar{z}_2^3 - (0.5754137977610272 - 0.2793435138325123\,i)\,z_2\,\bar{z}_1^2 - (0.9112482863306992 + 2.147908609023459\,i)\,z_2\,\bar{z}_2^2 + (1.322414895411518 + 0.765022519653218\,i)\,\bar{z}_1\,\bar{z}_2^2 - (1.022841254812297 + 0.705454205902162\,i)\,z_2^2\,\bar{z}_1 - (2.030430271207477 + 0.2304139887832361\,i)\,z_2^2\,\bar{z}_2 - (0.1249481454942901 + 0.6181851277503458\,i)\,\bar{z}_1^2\,\bar{z}_2 + (1.556855536321054 - 2.305582519322315\,i)\,z_2\,\bar{z}_1\,\bar{z}_2$

◆ $F_1^{(4)} = (-36.28117923370746 - 20.55060652093868\,i)\,z_1^4 + (2.899515066741232 + 5.459966715298459\,i)\,z_2\,z_1^3 + (140.4119132211359 + 81.99409555082742\,i)\,\bar{z}_1\,z_1^3 - (6.274140424012407 + 0.03297310317745179\,i)\,\bar{z}_2\,z_1^3 + (7.420330712087774 - 11.60974032023177\,i)\,z_2^2\,z_1^2 - (204.8192842208183 + 122.8604198862266\,i)\,\bar{z}_1^2\,z_1^2 - (5.284525040279112 - 11.87116090573378\,i)\,\bar{z}_2^2\,z_1^2 - (8.992719069666087 + 15.99085655591381\,i)\,z_2\,\bar{z}_1\,z_1^2 + (25.52823701871197 + 13.83586692200064\,i)\,z_2\,\bar{z}_2\,z_1^2 + (18.32587673007882 - 0.2328341336457847\,i)\,\bar{z}_1\,\bar{z}_2\,z_1^2 - (5.015009428436764 - 22.07444456232762\,i)\,z_2^3\,z_1 + (133.4880551718053 + 81.9197673912561\,i)\,\bar{z}_1^3\,z_1 - (16.3726431230267 - 15.83510399537384\,i)\,\bar{z}_2^3\,z_1 + (9.286367768690784 + 15.70324260632339\,i)\,z_2\,\bar{z}_1^2\,z_1 - (28.95158594551631 - 8.71404893154371\,i)\,z_2\,\bar{z}_2^2\,z_1 + (12.23510635065575 - 24.11729609201388\,i)\,\bar{z}_1\,\bar{z}_2^2\,z_1 - (14.73821378782083 - 20.5015431273461\,i)\,z_2^2\,\bar{z}_1\,z_1 + (7.793800267922833 + 29.41483667229451\,i)\,z_2^2\,\bar{z}_2\,z_1 - (17.92227042714302 - 0.5968349343999511\,i)\,\bar{z}_1^2\,\bar{z}_2\,z_1 - (48.41447610858743 + 29.7410657464736\,i)\,z_2\,\bar{z}_1\,\bar{z}_2\,z_1 - (22.93261727125236 + 4.378926179232634\,i)\,z_2^4 - (32.79222262096193 + 20.53044014457355\,i)\,\bar{z}_1^4 - (12.02495609531129 + 23.01269896553501\,i)\,\bar{z}_2^4 - (3.191413830480249 + 5.167365053175445\,i)\,z_2\,\bar{z}_1^3 - (50.5424295678792 + 54.92105860167378\,i)\,z_2\,\bar{z}_2^3 + (18.20864982297569 - 11.96658304048294\,i)\,\bar{z}_1\,\bar{z}_2^3 + (7.125879433116444 - 9.06967105877891\,i)\,z_2^2\,\bar{z}_1^2 - (65.08204911354822 + 55.06380245327255\,i)\,z_2^2\,\bar{z}_2^2 - (7.034413628742041 - 12.06340559819943\,i)\,\bar{z}_1^2\,\bar{z}_2^2 + (33.96300370581058 - 2.254885714888939\,i)\,z_2\,\bar{z}_1\,\bar{z}_2^2 + (8.343438048813002 - 20.0807005710995\,i)\,z_2^3\,\bar{z}_1 - (62.52818003543026 + 34.63825807114274\,i)\,z_2^3\,\bar{z}_2 + (5.870206561081335 - 0.3271106588052071\,i)\,\bar{z}_1^3\,\bar{z}_2 + (22.8284352091583 + 15.64830360803655\,i)\,z_2\,\bar{z}_1^2\,\bar{z}_2 - (0.8652052704905859 + 24.23579189596968\,i)\,z_2^2\,\bar{z}_1\,\bar{z}_2$

◆ $F_1^{(5)} = (-112.1450131870067 + 190.0752633267882\,i)\,z_1^5 + (45.04927708650335 - 24.90141431976139\,i)\,z_2\,z_1^4 + (552.8597590023926 - 923.1110121957156\,i)\,z_1\,z_1^4 - (2.370159181504285 - 52.43073014090792\,i)\,z_2\,z_1^4 - (104.071699715881 + 69.14869288457828\,i)\,z_2^2\,z_1^3 - (1092.896562717639 - 1802.864055528455\,i)\,\bar{z}_1^2\,z_1^3 + (105.9292267586898 + 43.44988288189337$

$i) \bar{z}_2^2 z_1^3 - (176.1335987848247 - 101.7248745546424\,i) z_2 \bar{z}_1 z_1^3 + (119.484038255309 - 222.4435944446441\,i) z_2 \bar{z}_2 z_1^3 +$

$(6.049285109038138 - 204.6702274313587\,i) \bar{z}_1 \bar{z}_2 z_1^3 + (222.8903297751101 + 48.32546126075647\,i) z_2^3 z_1^2 + (1083.355159450502 -$

$1770.010316949766\,i) \bar{z}_1^3 z_1^2 + (175.9074893985915 + 155.955609188564\,i) \bar{z}_2^3 z_1^2 + (259.4269448342815 - 156.15040688775$

$i) z_2 \bar{z}_1^2 z_1^2 + (104.4067411143039 + 254.2942015732573\,i) z_2 \bar{z}_2^2 z_1^2 - (322.6566499966986 + 146.7970023052255\,i) \bar{z}_1 \bar{z}_2^2 z_1^2 +$

$(284.3148963692852 + 207.2265463737766\,i) z_2^2 z_1 z_1^2 + (287.0290334761742 - 85.74241227444796\,i) z_2^2 \bar{z}_2 z_1^2 - (3.64966243167018 -$

$300.8523880325855\,i) \bar{z}_1^2 \bar{z}_2 z_1^2 - (376.6590598416656 - 641.5437473815699\,i) z_2 \bar{z}_1 \bar{z}_2 z_1^2 + (49.03023950100422 + 323.5712200126532$

$i) z_2^4 z_1 - (538.7130841136391 - 873.5576898435986\,i) \bar{z}_1^4 z_1 - (302.4206965691108 - 130.3296240455927\,i) \bar{z}_2^4 z_1 -$

$(170.5969709002997 - 106.7156690590157\,i) z_2 \bar{z}_1^3 z_1 - (600.2351724599022 - 624.8898266147512\,i) z_2 \bar{z}_2^3 z_1 - (302.0929171317029 +$

$335.8018817683877\,i) \bar{z}_1 \bar{z}_2^3 z_1 - (258.7842938846516 + 204.1678096205631\,i) z_2^2 \bar{z}_1^2 z_1 - (497.1132643416337 - 902.970819109029$

$i) z_2^2 \bar{z}_2^2 z_1 + (325.8606215021442 + 164.5523193192442\,i) \bar{z}_1^2 \bar{z}_2^2 z_1 - (139.269398979029 + 574.8379073823936\,i) z_2 \bar{z}_1 \bar{z}_2^2 z_1 -$

$(432.3890000210047 + 146.9661410084964\,i) z_2^3 \bar{z}_1 z_1 - (209.5866149272356 - 838.7081397579341\,i) z_2^3 \bar{z}_2 z_1 - (1.344204207570016 +$

$197.3803826292606\,i) \bar{z}_1^3 \bar{z}_2 z_1 + (393.2231609510404 - 616.6434216894575\,i) z_2 \bar{z}_1^2 \bar{z}_2 z_1 - (530.1069228522607 -$

$69.33805013319986\,i) z_2^2 \bar{z}_1 \bar{z}_2 z_1 - (437.4994787459364 + 141.9548726440751\,i) z_2^5 + (107.5379937630958 - 173.3666532098972\,i)$

$\bar{z}_1^5 - (258.6782800376262 + 444.2458089231011\,i) \bar{z}_2^5 + (42.25480622342424 - 27.39237565302497\,i) z_2 \bar{z}_1^4 - (1126.394778306598 +$

$1586.206249629628\,i) z_2 \bar{z}_2^4 + (344.9650713483003 - 43.20050286720749\,i) \bar{z}_1 \bar{z}_2^4 + (78.65002879085549 + 66.31087948955538\,i)$

$z_2^2 \bar{z}_1^3 - (2408.045312223426 + 2446.312870978822\,i) z_2^2 \bar{z}_2^3 + (124.3316701050502 + 173.262066693675\,i) \bar{z}_1^2 \bar{z}_2^3 + (779.685678491318 -$

$364.8252874936239\,i) z_2 \bar{z}_1 \bar{z}_2^3 + (204.8120458889071 + 94.37589265348609\,i) z_2^3 \bar{z}_1^2 - (2662.35481908981 + 2018.943877055291$

$i) z_2^3 \bar{z}_2^2 - (109.1013661705621 + 60.98174244819877\,i) \bar{z}_1^3 \bar{z}_2^2 + (25.05690833712274 + 305.4402086132351\,i) z_2 \bar{z}_1^2 \bar{z}_2^2 +$

$(800.2094659416555 - 593.3881615059685\,i) z_2^2 \bar{z}_1 \bar{z}_2^2 + (32.40101823140348 - 282.2789695897274\,i) z_2^4 \bar{z}_1 - (1593.676944911732 +$

$799.7833109901583\,i) z_2^4 \bar{z}_2 + (1.315878878343561 + 48.76477580135425\,i) \bar{z}_1^4 \bar{z}_2 - (135.8999709657737 - 197.8763354922605$

$i) z_2 \bar{z}_1^3 \bar{z}_2 + (230.814487945046 + 2.615604571485818\,i) z_2^2 \bar{z}_1^2 \bar{z}_2 + (449.5258607474453 - 658.2052779747174\,i) z_2^3 \bar{z}_1 \bar{z}_2$

◆ $F_1^{(6)} = (952.6004267959913 + 596.7878167781123\,i) z_1^6 -$

$(173.8089470253659 + 321.4456485102458\,i) z_2 z_1^5 - (5566.772261995954 + 3488.253961592337\,i) \bar{z}_1 z_1^5 + (371.7617327533642 +$

$26.87424824137332\,i) \bar{z}_2 z_1^5 - (573.660598201242 - 802.3423897785215\,i) z_2^2 z_1^4 + (13631.18317077031 + 8520.28455918821$

$i) \bar{z}_1^2 z_1^4 + (304.3301980716473 - 827.0821786799679\,i) \bar{z}_2^2 z_1^4 + (885.3817360634591 + 1566.432562816978\,i) z_2 \bar{z}_1 z_1^4 -$

$(1583.333754415347 + 858.3714382929372\,i) z_2 \bar{z}_2 z_1^4 - (1813.941815207779 + 101.190367861731\,i) \bar{z}_1 \bar{z}_2 z_1^4 + (423.3671504759949 -$

$1985.12464409862\,i) z_2^3 z_1^3 - (17902.27922873237 + 11136.69916189871\,i) \bar{z}_1^3 z_1^3 + (1355.990394949314 - 1614.44354434639\,i) \bar{z}_2^3 z_1^3 -$

$(1809.429520493292 + 3066.06177800949\,i) z_2 \bar{z}_1^2 z_1^3 + (2111.385054224345 - 920.3372545373387\,i) z_2 \bar{z}_2^2 z_1^3 - (1350.832696997989 -$

$3354.160086414111\,i) \bar{z}_1 \bar{z}_2^2 z_1^3 + (2277.966674808044 - 2957.793774469572\,i) z_2^2 \bar{z}_1 z_1^3 - (840.328753575538 + 2478.365726326116$

$i) z_2^2 \bar{z}_2 z_1^3 + (3555.506788310511 + 134.8449612428256\,i) \bar{z}_1^2 \bar{z}_2 z_1^3 + (6111.88333378333 + 3545.749562575064\,i) z_2 \bar{z}_1 \bar{z}_2$

$z_1^3 + (3144.101754586833 - 592.0059229233962\,i) z_2^4 z_1^2 + (13299.07603081605 + 8218.885004835309\,i) \bar{z}_1^4 z_1^2 + (1602.084833999746 +$

$2756.428836558786\,i) \bar{z}_2^4 z_1^2 + (1854.100556442519 + 3013.417951421548\,i) z_2 \bar{z}_1^3 z_1^2 + (6695.793757244761 + 5319.832898855918$

$i) z_2 \bar{z}_2^3 z_1^2 - (4321.874567768291 - 4365.488708061985\,i) \bar{z}_1 \bar{z}_2^3 z_1^2 - (3369.565940519641 - 4089.822742625001\,i) z_2^2 \bar{z}_1^2 z_1^2 +$

$(9624.93408961107 + 4066.570818906209\,i) z_2^2 \bar{z}_2^2 z_1^2 + (2239.084176455495 - 5091.30311180857\,i) \bar{z}_1^2 \bar{z}_2^2 z_1^2 - (7025.504110706248 -$

$2130.158021704919\,i) z_2 \bar{z}_1 \bar{z}_2^2 z_1^2 - (1747.509752310816 - 5837.794157678899\,i) z_2^3 \bar{z}_1 z_1^2 + (8377.911225667518 + 1315.659608840182$

$i) z_2^3 \bar{z}_2 z_1^2 - (3499.628492533945 + 66.17654742003523\,i) \bar{z}_1^3 \bar{z}_2 z_1^2 - (8864.987545122392 + 5483.448302287936\,i) z_2 \bar{z}_1^2 \bar{z}_2 z_1^2 +$

$(1488.270068722127 + 7088.262159992251\,i) z_2^2 \bar{z}_1 \bar{z}_2 z_1^2 + (292.5337373396933 + 6185.943442674811\,i) z_2^5 z_1 - (5297.782508247688 +$

$3248.30015288977\,i) \bar{z}_1^5 z_1 - (5428.041130615191 - 3110.69856191888\,i) \bar{z}_2^5 z_1 - (952.4189924865316 + 1487.20343640475\,i) z_2 \bar{z}_1^4 z_1 -$

$(17647.02961097291 - 14670.2189573591\,i) z_2 \bar{z}_2^4 z_1 - (2145.254083929289 + 6062.957663346\,i) \bar{z}_1 \bar{z}_2^4 z_1 + (2201.925917498287 -$

$2516.033937893775\,i) z_2^2 \bar{z}_1^3 z_1 - (23159.80770624599 - 32911.44803783632\,i) z_2^2 \bar{z}_2^3 z_1 + (4506.582754707184 - 3874.458531490037$

$i) \bar{z}_1^2 \bar{z}_2^3 z_1 - (10555.18965180744 + 13175.371252883\,i) z_2 \bar{z}_1 \bar{z}_2^3 z_1 + (2198.856479578702 - 5658.685209908314\,i) z_2^3 \bar{z}_1^2 z_1 -$

$(14985.17271243924 - 37300.86918456499\,i) z_2^3 \bar{z}_2^2 z_1 - (1643.528413091337 - 3428.496173670219\,i) \bar{z}_1^3 \bar{z}_2^2 z_1 + (7572.994621186839 -$

$1360.102917634494\,i) z_2 \bar{z}_1^2 \bar{z}_2^2 z_1 - (16370.34726392081 + 12549.33053423822\,i) z_2^2 \bar{z}_1 \bar{z}_2^2 z_1 - (6119.576416847271 +$

$47.83597723132722\,i) z_2^4 \bar{z}_1 z_1 - (2753.116625233637 - 22713.53008716202\,i) z_2^4 \bar{z}_2 z_1 + (1729.732919218356 - 1.837557186425784\,i)$

$\bar{z}_1^4 \bar{z}_2 z_1 + (5728.795568944187 + 3762.111225202644\,i) z_2 \bar{z}_1^3 \bar{z}_2 z_1 - (585.3627967884859 + 6565.530604987566\,i) z_2^2 \bar{z}_1^2 \bar{z}_2 z_1 -$

$(15464.06154665317 + 6221.294471973758\,i) z_2^3 \bar{z}_1 \bar{z}_2 z_1 - (8808.74031834031 + 3326.004747751999\,i) z_2^6 + (883.97524791051 +$

$537.2929500036099\,i) \bar{z}_1^6 - (5090.545905463991 + 9529.812694359676\,i) \bar{z}_2^6 + (196.1758046739394 + 294.8629452759931\,i)$

$z_2 \bar{z}_1^5 - (29496.26074290669 + 45208.42584158829\,i) z_2 \bar{z}_2^5 + (6526.74320920804 - 845.921578553392\,i) \bar{z}_1 \bar{z}_2^5 - (536.7564854143538 -$

$581.4365628141021\,i) z_2^2 \bar{z}_1^4 - (75491.58623730531 + 92345.0450736301\,i) z_2^2 \bar{z}_2^4 + (455.8399427931659 + 3090.923698139294\,i) \bar{z}_1^2 \bar{z}_2^4 +$

$(23325.79456087784 - 5601.306552407927\,i) z_2 \bar{z}_1 \bar{z}_2^4 - (868.0559293826963 - 1813.765644082506\,i) z_2^3 \bar{z}_1^3 - (108515.8566332385 +$

$103298.0555079244\,i)\,z_2^3\,\bar{z}_2^3 - (1538.007518272986 - 1133.572793161025\,i)\,\bar{z}_1^3\,\bar{z}_2^3 + (3451.300093976503 + 7138.001712318725\,i)\,z_2\,\bar{z}_1^2$
$\bar{z}_2^3 + (35490.81200214921 - 17720.39732751558\,i)\,z_2^2\,\bar{z}_1\,\bar{z}_2^3 + (2801.48695737094 + 505.3246914587048\,i)\,z_2^4\,\bar{z}_1^2 - (91295.34144292136 +$
$66109.20231123827\,i)\,z_2^4\,\bar{z}_2^2 + (450.4262064920229 - 864.5305344227253\,i)\,z_1^4\,\bar{z}_2^2 - (2645.299650906987 - 177.8138978120122$
$i)\,z_2\,\bar{z}_1^3\,\bar{z}_2^2 + (6022.853032731652 + 7549.832058932476\,i)\,z_2^2\,\bar{z}_1^2\,\bar{z}_2^2 + (28852.40635491409 - 24189.71651911349\,i)\,z_2^3\,\bar{z}_1$
$\bar{z}_2^2 + (1711.079413420544 - 5103.143237690488\,i)\,z_2^5\,z_1 - (42903.73554525537 + 22925.59245936187\,i)\,z_2^5\,\bar{z}_2 - (343.4307601777096 -$
$7.488153056733425\,i)\,z_2^5\,\bar{z}_2 - (1392.606135878073 + 966.521519745668\,i)\,z_2\,z_1^4\,\bar{z}_2 - (45.65788409229162 - 1980.9601262759$
$i)\,z_2^2\,\bar{z}_1^3\,\bar{z}_2 + (6521.970475735385 + 4346.183325362892\,i)\,z_2^3\,\bar{z}_1^2\,\bar{z}_2 + (10902.32153026759 - 16897.23145270118\,i)\,z_2^4\,\bar{z}_1\,\bar{z}_2$

◆ $F_1^{(7)} = (3149.072255647837 - 4635.934964032738\,i)\,z_1^7 -$
$(2058.458224615344 - 1097.134008651959\,i)\,z_2\,z_1^6 - (21210.04361364009 - 31689.30519749784\,i)\,\bar{z}_1\,z_1^6 + (281.8241140711768 -$
$2376.644384454007\,i)\,\bar{z}_2\,z_1^6 + (5316.890157186999 + 4281.529397232484\,i)\,z_2^2\,z_1^5 + (61398.19277359091 - 93390.23162653384$
$i)\,\bar{z}_1^2\,z_1^5 - (5712.373869419354 + 1814.270194390726\,i)\,\bar{z}_2^2\,z_1^5 + (11998.15591747272 - 6723.795758753223\,i)\,z_2\,\bar{z}_1\,z_1^5 -$
$(5766.63353330369 - 10273.71021911372\,i)\,z_2\,\bar{z}_2\,z_1^5 - (1385.900113441497 - 13898.30838549397\,i)\,\bar{z}_1\,\bar{z}_2\,z_1^5 - (14757.84776268684 +$
$3065.35944273282\,i)\,z_2^3\,z_1^4 - (99065.705741033 - 153811.592784892\,i)\,\bar{z}_1^3\,z_1^4 - (12244.47392328948 + 10032.4036062847\,i)\,\bar{z}_2^3\,z_1^4 -$
$(29257.02201408971 - 17228.97816573683\,i)\,z_2\,\bar{z}_1^2\,z_1^4 - (6464.261566159622 + 15097.16713252074\,i)\,z_2\,\bar{z}_2^2\,z_1^4 + (28883.46192676274 +$
$9921.632465838687\,i)\,\bar{z}_1\,\bar{z}_2^2\,z_1^4 - (24664.17549492347 + 21105.13466584605\,i)\,z_2^2\,\bar{z}_1\,z_1^4 - (18188.14422367407 - 7192.149077569483$
$i)\,z_2^2\,\bar{z}_2\,z_1^4 + (2707.733866859102 - 34016.2417442135\,i)\,\bar{z}_1^2\,\bar{z}_2\,z_1^4 + (29258.40500953106 - 49751.64221587039\,i)\,z_2\,\bar{z}_1$
$\bar{z}_2\,z_1^4 - (5975.912836236237 + 27397.75515647674\,i)\,z_2^4\,z_1^3 + (96263.1814664661 - 152880.3112833329\,i)\,\bar{z}_1^4\,z_1^3 + (23458.88644265544 -$
$14710.43106219242\,i)\,\bar{z}_2^4\,z_1^3 + (38207.86833381158 - 23622.18499027318\,i)\,z_2\,\bar{z}_1^3\,z_1^3 + (43993.90393747272 - 59014.70094743378$
$i)\,z_2\,\bar{z}_2^3\,z_1^3 + (44870.81500380613 + 42114.817727554421\,i)\,\bar{z}_1\,\bar{z}_2^3\,z_1^3 + (45833.94540667772 + 41484.2869892382\,i)\,z_2^2\,\bar{z}_1^2\,z_1^3 +$
$(32166.99168294617 - 86241.53728529061\,i)\,z_2^2\,\bar{z}_2^2\,z_1^3 - (58409.46818605491 + 21680.14080261511\,i)\,\bar{z}_1^2\,\bar{z}_2^2\,z_1^3 + (20778.46049088133 +$
$66252.48516950975\,i)\,z_2\,\bar{z}_1\,\bar{z}_2^2\,z_1^3 + (57994.28796604207 + 16107.17915779478\,i)\,z_2^3\,\bar{z}_1\,z_1^3 + (7925.159954856452 - 72821.58971918897$
$i)\,z_2^3\,\bar{z}_2\,z_1^3 - (2606.80905153164 - 44601.87472699201\,i)\,\bar{z}_1^3\,\bar{z}_2\,z_1^3 - (59430.86834292453 - 96703.72930518405\,i)\,z_2\,\bar{z}_1^2\,\bar{z}_2\,z_1^3 +$
$(69850.71960211016 - 19911.08405590239\,i)\,z_2^2\,\bar{z}_1\,\bar{z}_2\,z_1^3 + (60113.01704058994 - 7835.389500512873\,i)\,z_2^5\,z_1^2 - (56357.42717444222 -$
$91688.54910570232\,i)\,\bar{z}_1^5\,z_1^2 + (36943.78115777198 + 49330.85585709547\,i)\,\bar{z}_2^5\,z_1^2 - (28187.43935082942 - 18273.95053130993$
$i)\,z_2\,z_1^4\,z_1^2 + (165269.6776587986 + 152212.3045698416\,i)\,z_2\,z_2^4\,z_1^2 - (76606.4476439222 - 34310.04582677481\,i)\,\bar{z}_1\,z_2^4\,z_1^2 -$
$(42666.97722059299 + 40655.54015776057\,i)\,z_2\,\bar{z}_1^4\,z_1^2 + (350799.4802592959 + 187305.3053432741\,i)\,z_2^2\,\bar{z}_2^3\,z_1^2 - (61140.79800573714 +$
$65609.06030332898\,i)\,\bar{z}_1^2\,\bar{z}_2^3\,z_1^2 - (158926.3629330345 - 152152.7075457016\,i)\,z_2\,\bar{z}_1\,\bar{z}_2^3\,z_1^2 - (85032.2967297431 +$
$29785.98261021442\,i)\,z_2^3\,\bar{z}_1\,z_1^2 + (382504.9000600936 + 103492.6501215684\,i)\,z_2^3\,\bar{z}_2^2\,z_1^2 + (59058.10941887087 + 23651.96673160645\,i)$
$\bar{z}_1^3\,\bar{z}_2^2\,z_1^2 - (22222.91543474179 + 107083.2766336472\,i)\,z_2\,\bar{z}_1^2\,\bar{z}_2^2\,z_1^2 - (141836.5003818647 - 235048.0738400373\,i)\,z_2^2\,\bar{z}_1\,\bar{z}_2^2\,z_1^2 +$
$(6007.442716818827 + 81521.51586416688\,i)\,z_2^4\,\bar{z}_1\,z_1^2 + (224139.7349417048 + 4362.155680923548\,i)\,z_2^4\,\bar{z}_2\,z_1^2 + (1204.830529272149 -$
$33042.86170105354\,i)\,\bar{z}_1^4\,\bar{z}_2\,z_1^2 + (60415.27146515912 - 94324.71356520383\,i)\,z_2\,\bar{z}_1^3\,\bar{z}_2\,z_1^2 - (98891.9241973041 - 17740.82015734827$
$i)\,z_2^2\,\bar{z}_1^2\,\bar{z}_2\,z_1^2 - (59207.32009800614 - 209267.2489086982\,i)\,z_2^3\,\bar{z}_1\,\bar{z}_2\,z_1^2 + (5523.817073338651 + 128039.2483824716\,i)$
$z_2^6\,z_1 + (18413.9170395828 - 30715.66730319624\,i)\,\bar{z}_1^6\,z_1 - (111401.4654203218 - 66674.604704077727\,i)\,\bar{z}_2^6\,z_1 + (11139.30927424969 -$
$7561.075765407592\,i)\,z_2\,z_1^5\,z_1 - (488168.5704548798 - 404379.5870310922\,i)\,z_2\,\bar{z}_2^5\,z_1 - (47510.42698464574 + 114121.8857022621\,i)$
$\bar{z}_1\,\bar{z}_2^5\,z_1 + (19903.98305210718 + 19871.0703008995\,i)\,z_2^2\,z_1^4\,z_1 - (890026.650427577 - 1.072366562410307\times10^6\,i)\,z_2^2\,\bar{z}_2^4\,z_1 +$
$(80518.658724568 - 23292.62413523112\,i)\,\bar{z}_1^2\,z_2^4\,z_1 - (233634.7784724199 + 387540.7695491761\,i)\,z_2\,z_1\,z_2^4\,z_1 + (55156.65711506445 +$
$23427.73165082647\,i)\,z_2^2\,\bar{z}_1^3\,z_1 - (835111.3468046808 - 1.568036875322472\times10^6\,i)\,z_2^3\,\bar{z}_2^3\,z_1 + (36728.23359509427 +$
$44978.8479526125\,i)\,\bar{z}_1^3\,\bar{z}_2^3\,z_1 + (178702.3586382674 - 121324.9338817016\,i)\,z_2\,z_1^2\,\bar{z}_2^3\,z_1 - (557620.1894224177 +$
$559973.9752889117\,i)\,z_2^2\,\bar{z}_1\,\bar{z}_2^3\,z_1 + (5097.97133594162 - 78231.71315583288\,i)\,z_2^4\,\bar{z}_1^2\,z_1 - (394500.8917017534 -$
$1.33419913198076\times10^6\,i)\,z_2^4\,\bar{z}_2^2\,z_1 - (29860.95182523674 + 12879.12308497718\,i)\,\bar{z}_1^4\,\bar{z}_2^2\,z_1 + (8200.374730005191 +$
$75616.29596149598\,i)\,z_2\,\bar{z}_1^3\,\bar{z}_2^2\,z_1 + (178829.081016404 - 200500.9807777272\,i)\,z_2^2\,\bar{z}_1^2\,\bar{z}_2^2\,z_1 - (661225.3676805884 +$
$418109.6999312937\,i)\,z_2^3\,\bar{z}_1\,\bar{z}_2^2\,z_1 - (116709.237316319 + 15019.21908819138\,i)\,z_2^5\,\bar{z}_1\,z_1 - (66066.95823785529 -$
$627127.5896562831\,i)\,z_2^5\,\bar{z}_2\,z_1 - (181.6343136155338 - 13113.37810740299\,i)\,\bar{z}_1^5\,\bar{z}_2\,z_1 - (30740.79438007373 - 46180.11691444243$
$i)\,z_2\,\bar{z}_1^4\,\bar{z}_2\,z_1 + (61184.26697100323 - 4740.504679001962\,i)\,z_2^2\,\bar{z}_1^3\,\bar{z}_2\,z_1 + (90460.6797510265 - 191553.1130750119$
$i)\,z_2^3\,\bar{z}_1^2\,\bar{z}_2\,z_1 - (414419.1022203964 + 133456.0956443335\,i)\,z_2^4\,\bar{z}_1\,\bar{z}_2\,z_1 - (192196.48021751 + 83176.24040705786\,i)$
$z_2^7 - (2591.187466843369 - 4432.698955126593\,i)\,\bar{z}_1^7 - (109168.6754155818 + 219438.1641081255\,i)\,\bar{z}_2^7 - (1842.415792820005 -$
$1306.990647294577\,i)\,z_2\,\bar{z}_1^6 - (757900.2956391049 + 1.280782242054625\times10^6\,i)\,z_2\,\bar{z}_2^6 + (139587.5468255114 - 6037.475812087592\,i)$
$\bar{z}_1\,\bar{z}_2^6 - (3723.515975897863 + 3875.934015655319\,i)\,z_2^2\,\bar{z}_1^5 - (2.335345120322106\times10^6 + 3.264600967305082\times10^6\,i)\,z_2^2\,\bar{z}_2^5 +$
$(7662.103984721412 + 57753.89575312333\,i)\,\bar{z}_1^2\,\bar{z}_2^5 + (663667.4678007492 - 97522.67738439329\,i)\,z_2\,\bar{z}_1\,\bar{z}_2^5 - (13370.23049525207 +$
$6696.383510253781\,i)\,z_2^3\,\bar{z}_1^4 - (4.115255250844436\times10^6 + 4.694325066685941\times10^6\,i)\,z_2^3\,\bar{z}_2^4 - (27220.53576939688 -$

$4132.453031384477\,i)\,\bar{z}_1^3\,\bar{z}_2^4 + (52177.83311587315 + 205109.9601135406\,i)\,z_2\,\bar{z}_1^2\,\bar{z}_2^4 + (1.357751365747732\times10^6 -$
$411673.4787506969\,i)\,z_2^2\,\bar{z}_1\,\bar{z}_2^4 - (4821.046961750631 - 24419.88474510884\,i)\,z_2^4\,\bar{z}_1^3 - (4.47617083613229\times10^6 +$
$4.10510038139549\times10^6\,i)\,z_2^4\,\bar{z}_2^3 - (8218.157501841139 + 11467.83384919952\,i)\,\bar{z}_1^4\,\bar{z}_2^3 - (63025.59164140862 -$
$29741.06960108254\,i)\,z_2\,\bar{z}_1^3\,\bar{z}_2^3 + (170611.4698845456 + 319525.7411702579\,i)\,z_2^2\,\bar{z}_1^2\,\bar{z}_2^3 + (1.516535218979045\times10^6 -$
$794743.6432735644\,i)\,z_2^3\,\bar{z}_1\,\bar{z}_2^3 + (51027.26620841011 + 18679.7828192563\,i)\,z_2^5\,\bar{z}_1^2 - (2.998531957489848\times10^6 +$
$2.181220787119466\times10^6\,i)\,z_2^5\,\bar{z}_2^2 + (6041.293673521701 + 2800.25589424722\,i)\,\bar{z}_1^5\,\bar{z}_2^2 - (309.3921048283301 +$
$19732.16007040958\,i)\,z_2\,\bar{z}_1^4\,\bar{z}_2^2 - (67828.51520447778 - 53804.67250384609\,i)\,z_2^2\,\bar{z}_1^3\,\bar{z}_2^2 + (237636.4811123662 + 266856.9340941136$
$i)\,z_2^3\,\bar{z}_1^2\,\bar{z}_2^2 + (966825.1106516158 - 815700.2410008031\,i)\,z_2^4\,\bar{z}_1\,\bar{z}_2^2 + (45923.05855762084 - 98814.79202135873\,i)\,z_2^6\,\bar{z}_1 -$
$(1.143963925942474\times10^6 + 649231.1763712855\,i)\,z_2^6\,\bar{z}_2 - (20.04644996193679 + 2177.817066342422\,i)\,\bar{z}_1^6\,\bar{z}_2 + (6264.872026477732 -$
$9080.559418724657\,i)\,z_2\,\bar{z}_1^5\,\bar{z}_2 - (13977.41762269461 + 321.9921851219314\,i)\,z_2^2\,\bar{z}_1^4\,\bar{z}_2 - (38132.33285071128 - 56408.52908117197$
$i)\,z_2^3\,\bar{z}_1^3\,\bar{z}_2 + (166553.8157897645 + 107086.9131066182\,i)\,z_2^4\,\bar{z}_1^2\,\bar{z}_2 + (328553.0908884661 - 438257.1806567265\,i)\,z_2^5\,\bar{z}_1\,\bar{z}_2$

■ II.II.2. $F_2^{(\kappa)}$

◆ $F_2^{(1)} = (0.9997952030905475 + 0.02023738810051618\,i)\,z_2$

◆ $F_2^{(2)} = -0.02193932925093116 + 0.01412771002666203\,i)\,z_1^2 + (0.2496203897735642 - 0.003162962595832208\,i)$
$z_2\,z_1 + (0.04057314255690176 - 0.03020080880174968\,i)\,\bar{z}_1\,z_1 + (0.003824235035699661 + 0.1353666140846914\,i)$
$\bar{z}_2\,z_1 - (0.001213421865078973 - 0.1455805059116234\,i)\,z_2^2 - (0.01852079313490402 - 0.01633259545784685\,i)$
$\bar{z}_1^2 + (7.809581862188754\times10^{-6} + 0.4363878845241665\,i)\,\bar{z}_2^2 - (0.2492879307901039 + 0.01326163208195616\,i)$
$z_2\,\bar{z}_1 - (0.009357407433278423 - 0.2910207265858483\,i)\,z_2\,\bar{z}_2 - (0.0001113555806085825 + 0.1583908948070483\,i)\,\bar{z}_1\,\bar{z}_2$

◆ $F_2^{(3)} = (0.1126448099575112 + 0.1805548562744935\,i)\,z_1^3 - (0.04760095818292598 + 1.451392515230422\,i)$
$z_2\,z_1^2 - (0.3530024015860079 + 0.5208116778740028\,i)\,\bar{z}_1\,z_1^2 + (1.270442008716912 - 0.1354609475376852\,i)\,\bar{z}_2\,z_1^2 +$
$(1.833971306817882 - 1.310854031947808\,i)\,z_2^2\,z_1 + (0.3729701438314642 + 0.5010360180121877\,i)\,\bar{z}_1^2\,z_1 + (5.417047218216617 +$
$0.5286823960334235\,i)\,\bar{z}_2^2\,z_1 - (0.09972213816419995 - 2.913038103485359\,i)\,z_2\,\bar{z}_1\,z_1 + (3.547406223589169 +$
$1.67352893162582\,i)\,z_2\,\bar{z}_2\,z_1 - (2.827483968516755 - 0.1883953816491517\,i)\,\bar{z}_1\,\bar{z}_2\,z_1 - (0.06819825514760738 -$
$5.592018767729273\,i)\,z_2^3 - (0.1326777290695202 + 0.1609973008581332\,i)\,\bar{z}_1^3 - (0.1080368076727457 - 6.959680869314085\,i)\,\bar{z}_2^3 +$
$(0.1471031517325621 - 1.443914585351749\,i)\,z_2\,z_1^2 - (0.3035437015104354 - 16.7695438858668\,i)\,z_2\,\bar{z}_2^2 - (5.381553222923807 +$
$1.378659964324\,i)\,\bar{z}_1\,\bar{z}_2^2 - (1.852509311513431 - 0.6912070199151377\,i)\,z_2^2\,\bar{z}_1 - (0.08735189694351951 - 12.76155161751702$
$i)\,z_2^2\,\bar{z}_2 + (1.55586032219011 - 0.02119789244932857\,i)\,\bar{z}_1^2\,\bar{z}_2 - (3.477726735693164 + 2.908362435551417\,i)\,z_2\,\bar{z}_1\,\bar{z}_2$

◆ $F_2^{(4)} =$
$(1.365128177142607 - 0.6434636163925804\,i)\,z_1^4 - (9.860341838131577 - 0.3454042330535064\,i)\,z_2\,z_1^3 - (5.295335266130175 -$
$2.643725815320209\,i)\,\bar{z}_1\,z_1^3 - (1.699082529674098 + 8.110803364931215\,i)\,\bar{z}_2\,z_1^3 - (13.2698031953423 + 11.58142849910344$
$i)\,z_2^2\,z_1^2 + (7.720034247549895 - 4.107742582850397\,i)\,\bar{z}_1^2\,z_1^2 + (3.179429318830897 - 34.26386217745936\,i)\,\bar{z}_2^2\,z_1^2 +$
$(29.63709069557501 + 0.3530160198551631\,i)\,z_2\,\bar{z}_1\,z_1^2 + (14.1891007804071 - 20.91310024033571\,i)\,z_2\,\bar{z}_2\,z_1^2 + (4.390473479409256 +$
$26.11020382388778\,i)\,\bar{z}_1\,\bar{z}_2\,z_1^2 + (69.53375334067223 - 18.34239643753585\,i)\,z_2^3\,z_1 - (5.016559861162786 - 2.858715511203453$
$i)\,\bar{z}_1^3\,z_1 + (85.89176873923941 + 26.5012520837953\,i)\,\bar{z}_2^3\,z_1 - (29.55998174575717 + 1.780635659789941\,i)\,z_2\,\bar{z}_1^2\,z_1 +$
$(204.511683475663 + 1.044383738327168\,i)\,z_2\,\bar{z}_2^2\,z_1 - (16.7028178877893 - 66.7000055622878\,i)\,\bar{z}_1\,\bar{z}_2^2\,z_1 + (18.86627931115593 +$
$25.04175363484588\,i)\,z_2^2\,\bar{z}_1\,z_1 + (158.3674534831149 - 29.45289770894598\,i)\,z_2^2\,\bar{z}_2\,z_1 - (3.304893544243537 + 27.89966953598986$
$i)\,\bar{z}_1^2\,\bar{z}_2\,z_1 - (43.41582470969642 - 42.47412110617884\,i)\,z_2\,\bar{z}_1\,\bar{z}_2\,z_1 - (0.8957162290035101 - 136.854621750983\,i)$
$z_2^4 + (1.22673900583959 - 0.7510659613754018\,i)\,\bar{z}_1^4 - (4.368753097418479 - 175.9027475168192\,i)\,\bar{z}_2^4 + (9.783344672796801 +$
$1.054566983191129\,i)\,z_2\,\bar{z}_1^3 - (11.05025773127397 - 547.1081293747742\,i)\,z_2\,\bar{z}_2^3 - (84.36877114907286 + 52.87710760086914$
$i)\,\bar{z}_1\,\bar{z}_2^3 - (5.603390325360426 + 12.16825001669465\,i)\,z_2^3\,\bar{z}_1 - (8.186225892992017 - 759.3772122518482\,i)\,z_2^3\,\bar{z}_2 +$
$(13.43085494818493 - 31.08503033169288\,i)\,\bar{z}_1^3\,\bar{z}_2 - (202.7366353098372 + 67.43665447135045\,i)\,z_2\,\bar{z}_1\,\bar{z}_2^2 - (69.59160124503077 +$
$3.837207404116436\,i)\,z_2^3\,\bar{z}_1 - (2.801028537184259 - 506.4048254032073\,i)\,z_2^3\,\bar{z}_2 + (0.6143208119966719 + 9.869630120585654$
$i)\,\bar{z}_1^3\,\bar{z}_2 + (29.19067543848591 - 18.98157633677584\,i)\,z_2\,z_1^2\,\bar{z}_2 - (157.8370945099073 + 33.65114455770132\,i)\,z_2^2\,\bar{z}_1\,\bar{z}_2$

◆ $F_2^{(5)} = (-3.80986511516409 - 9.120156850419514\,i)\,z_1^5 + (2.092133618968774 + 65.32184765706236\,i)\,z_2\,z_1^4 +$
$(19.57481293882461 + 44.26538670536592\,i)\,\bar{z}_1\,z_1^4 - (55.20693343714459 - 15.29946819625608\,i)\,\bar{z}_2\,z_1^4 - (88.8138726094822 -$

$82.02447847240464\,i)\,z_2^2\,z_1^3 - (40.49877253829331 + 86.20559616495922\,i)\,\bar{z}_1^2\,z_1^3 - (250.3797722591814 + 15.01289887123893$

$i)\,\bar{z}_2^2\,z_1^3 + (0.7349838398246504 - 260.4451395670595\,i)\,z_2\,z_1\,z_1^3 - (148.083882036965 + 86.88414790800216\,i)\,z_2\,\bar{z}_2\,z_1^3 +$

$(233.5052660006902 - 56.20541497049689\,i)\,z_1\,\bar{z}_2\,z_1^3 - (198.085635127589 + 410.3155838595347\,i)\,z_2^3\,z_1^2 + (42.15042532608727 +$

$84.22230413482261\,i)\,\bar{z}_1^3\,z_1^2 + (197.2371825819338 - 566.8369729898625\,i)\,\bar{z}_2^3\,z_1^2 - (15.12223863254695 - 389.7035008719093$

$i)\,z_2\,z_1^2\,z_1^2 - (91.43021487538758 + 1239.998706659431\,i)\,z_2\,\bar{z}_2^2\,z_1^2 + (736.826707157376 + 115.6072661717396\,i)\,z_1\,\bar{z}_2^2\,z_1^2 +$

$(286.7294663755225 - 197.4910138487827\,i)\,z_2^2\,\bar{z}_1\,z_1^2 - (364.3612921986422 + 970.0786654518689\,i)\,z_2^2\,\bar{z}_2\,z_1^2 - (369.8705203334965 -$

$74.35854903357098\,i)\,\bar{z}_1^2\,\bar{z}_2\,z_1^2 + (456.0890577231218 + 354.584565511359\,i)\,z_2\,\bar{z}_1\,\bar{z}_2\,z_1^2 + (1695.7153575404 - 697.5893730255923$

$i)\,z_2^4\,z_1 - (22.05435058315011 + 41.28953567932338\,i)\,\bar{z}_1^4\,z_1 + (2162.596290481527 + 346.7969098654269\,i)\,\bar{z}_2^4\,z_1 +$

$(19.43167043608413 - 259.2815932962801\,i)\,z_2\,z_1^3\,z_1 + (6677.133499115829 + 212.0161237095383\,i)\,z_2\,\bar{z}_2^3\,z_1 - (716.8229585973132 -$

$1094.892777650251\,i)\,\bar{z}_1\,\bar{z}_2^3\,z_1 - (291.9694330957726 - 145.2338649294378\,i)\,z_2^2\,z_1^2\,z_1 + (9285.613163779653 - 1305.312124086167$

$i)\,z_2^2\,\bar{z}_2^2\,z_1 - (708.0018379621132 + 185.036681424305\,i)\,z_1^2\,\bar{z}_2^2\,z_1 - (623.3213240231858 - 2512.876312338958\,i)\,z_2\,z_1\,\bar{z}_2^2\,z_1 +$

$(124.708929284344 + 910.2011003726954\,i)\,z_2^3\,\bar{z}_1\,z_1 + (6200.313665072263 - 1692.075432441134\,i)\,z_2^3\,\bar{z}_2\,z_1 + (259.7860786175652 -$

$41.25185462230034\,i)\,\bar{z}_1^3\,\bar{z}_2\,z_1 - (437.9305736585208 + 452.765952763104\,i)\,z_2\,z_1^2\,\bar{z}_2\,z_1 - (40.32963684679578 -$

$2093.138608948398\,i)\,z_2^2\,z_1\,\bar{z}_2\,z_1 + (7.080238054823465 + 3705.784399840547\,i)\,z_2^5 + (4.637761255120817 + 8.127382605075743\,i)$

$\bar{z}_1^5 - (128.0869517986461 - 4304.871109224217\,i)\,\bar{z}_2^5 - (7.136718125468317 - 64.7396329926658\,i)\,z_2\,z_1^4 - (468.837082745775 -$

$18514.36381054579\,i)\,z_2\,\bar{z}_2^4 - (2122.397794113937 + 1179.52050024085\,i)\,\bar{z}_1\,\bar{z}_2^4 + (94.04543602860272 - 31.87419852864817\,i)$

$z_2^2\,z_1^3 - (501.2576690208946 - 33880.47764896119\,i)\,z_2^2\,\bar{z}_2^3 + (516.2786794908859 - 466.0926681044025\,i)\,\bar{z}_1^2\,\bar{z}_2^3 - (6580.3555290761 +$

$3142.78475519106\,i)\,z_2\,z_1\,\bar{z}_2^3 + (74.07651296968973 - 443.3416089597798\,i)\,z_2^3\,z_1^2 - (248.8153623091881 - 33007.52530213765$

$i)\,z_2^3\,\bar{z}_2^2 + (221.6657679767743 + 82.30823514754003\,i)\,z_1^3\,\bar{z}_2^2 + (709.5234097646022 - 1103.565518136857\,i)\,z_2\,z_1^2\,\bar{z}_2^2 -$

$(9223.272935872843 + 2838.551999266233\,i)\,z_2^2\,z_1\,\bar{z}_2^2 - (1704.210441775185 + 36.52089365063776\,i)\,z_2^4\,\bar{z}_1 - (22.59807816830595 -$

$16946.04053167121\,i)\,z_2^4\,\bar{z}_2 - (68.21520829236951 - 7.833441761864712\,i)\,z_1^4\,\bar{z}_2 + (130.0052162297415 + 180.8542980862118$

$i)\,z_2\,\bar{z}_1^3\,\bar{z}_2 + (403.3067560687225 - 957.4899810546536\,i)\,z_2^2\,\bar{z}_1^2\,\bar{z}_2 - (6196.692332102816 + 1071.617520375447\,i)\,z_2^3\,\bar{z}_1\,\bar{z}_2$

◆ $F_2^{(6)} = (-53.28721272483878 + 19.62067909383665\,i)$

$z_1^6 + (379.9208739302135 - 10.40581830249599\,i)\,z_2\,z_1^5 + (309.5023506003686 - 122.036710281754\,i)\,\bar{z}_1\,z_1^5 +$

$(125.6589341289607 + 347.007146094366\,i)\,z_2\,z_1^5 + (562.1623800261984 + 663.5634350047983\,i)\,z_2^2\,z_1^4 - (751.6588169545612 -$

$318.0758639957667\,i)\,\bar{z}_1^2\,z_1^4 - (79.82498386685212 - 1746.977679764426\,i)\,\bar{z}_2^2\,z_1^4 - (1887.776152024317 + 1.231149122840279$

$i)\,z_2\,\bar{z}_1\,z_1^4 - (550.5090131205943 - 1012.815994309817\,i)\,z_2\,\bar{z}_2\,z_1^4 - (598.7161500587196 + 1820.770502900797\,i)\,\bar{z}_1$

$\bar{z}_2\,z_1^4 - (3047.42769174896 - 1244.894966656368\,i)\,z_2^2\,z_1^3 + (977.1949082662879 - 444.3622259818939\,i)\,\bar{z}_1^3\,z_1^3 - (4279.079057448414 +$

$1113.633227983014\,i)\,\bar{z}_2^3\,z_1^3 + (3760.318408198903 + 110.0487918625943\,i)\,z_2\,z_1^2\,z_1^3 - (8929.415843176826 - 548.5399148677132$

$i)\,z_2\,\bar{z}_2^2\,z_1^3 + (823.2594417693127 - 6878.452247271273\,i)\,\bar{z}_1\,\bar{z}_2^2\,z_1^3 - (1883.909561973071 + 2779.572717069974\,i)\,z_2^2\,\bar{z}_1\,z_1^3 -$

$(7249.536419507034 - 2291.369119128269\,i)\,z_2^2\,\bar{z}_2\,z_1^3 + (1123.053671954629 + 3820.581399335272\,i)\,\bar{z}_1^2\,\bar{z}_2\,z_1^3 + (2869.56808752949 -$

$4102.058506808885\,i)\,z_2\,\bar{z}_1\,\bar{z}_2\,z_1^3 - (7295.128134325563 + 9838.797145996654\,i)\,z_2^4\,z_1^2 - (717.3671498273369 - 350.7169227197371$

$i)\,\bar{z}_1^4\,z_1^2 + (1652.941775857593 - 14377.20933893336\,i)\,\bar{z}_2^4\,z_1^2 - (3752.679818578906 + 218.3882247786862\,i)\,z_2\,\bar{z}_1^3\,z_1^2 -$

$(2927.307653364916 + 42014.98505918197\,i)\,z_2\,\bar{z}_2^3\,z_1^2 + (12660.70254774424 + 5507.036734135305\,i)\,\bar{z}_1\,\bar{z}_2^3\,z_1^2 + (2244.304316886827 +$

$4271.928744884403\,i)\,z_2^2\,z_1^2\,z_1^2 - (18182.61127029084 + 55648.81907773615\,i)\,z_2^2\,\bar{z}_2^2\,z_1^2 - (1986.30409312649 - 10081.83588133676$

$i)\,\bar{z}_1^2\,\bar{z}_2^2\,z_1^2 + (27539.33775257437 + 3491.731383397568\,i)\,z_2\,z_1\,\bar{z}_2^2\,z_1^2 + (10081.15789516436 - 2084.675471413291\,i)\,z_2^3\,\bar{z}_1\,z_1^2 -$

$(19311.63621470046 + 35650.73049557144\,i)\,z_2^3\,\bar{z}_2\,z_1^2 - (1032.644109047132 + 4006.825543269355\,i)\,\bar{z}_1^3\,\bar{z}_2\,z_1^2 - (5362.484208853574 -$

$6053.680512573099\,i)\,z_2\,z_1^2\,\bar{z}_2\,z_1^2 + (23559.51108687574 - 2181.048400197642\,i)\,z_2^2\,z_1\,\bar{z}_2\,z_1^2 + (45439.38465349741 -$

$21058.12648897647\,i)\,z_2^5\,z_1 + (281.9951506691051 - 148.1905001602796\,i)\,\bar{z}_1^5\,z_1 + (52691.02665835143 + 5222.53717515714\,i)\,\bar{z}_2^5\,z_1 +$

$(1876.279319609902 + 163.4701406702615\,i)\,z_2\,z_1^4\,z_1 + (225154.8450391003 - 1911.313890442872\,i)\,z_2\,\bar{z}_2^4\,z_1 - (13458.54090492629 -$

$28166.01370347901\,i)\,\bar{z}_1\,\bar{z}_2^4\,z_1 - (1107.838159857808 + 2852.03973276106\,i)\,z_2^2\,\bar{z}_1^3\,z_1 + (411543.7061652645 - 54302.14869562394$

$i)\,z_2^2\,\bar{z}_2^3\,z_1 - (11762.71864504684 + 7670.418676057228\,i)\,\bar{z}_1^2\,\bar{z}_2^3\,z_1 - (29673.42089387198 - 86126.17878583068\,i)\,z_2\,z_1\,\bar{z}_2^3\,z_1 -$

$(10361.69827794807 - 190.7783379419616\,i)\,z_2^3\,\bar{z}_1^2\,z_1 + (400571.6627429918 - 102734.530176082\,i)\,z_2^3\,\bar{z}_2^2\,z_1 + (1800.618956695131 -$

$6514.607368622292\,i)\,\bar{z}_1^3\,\bar{z}_2^2\,z_1 - (26317.68607518332 + 8865.894040648092\,i)\,z_2\,z_1^2\,\bar{z}_2^2\,z_1 - (13760.66505706732 -$

$120607.1872321871\,i)\,z_2^2\,z_1\,\bar{z}_2^2\,z_1 + (5660.625183243737 + 23354.39786240902\,i)\,z_2^4\,\bar{z}_1\,z_1 + (206130.5626585144 -$

$77198.14018784938\,i)\,z_2^4\,\bar{z}_2\,z_1 + (462.9411708137726 + 2099.892418754947\,i)\,\bar{z}_1^4\,\bar{z}_2\,z_1 + (4273.447311749571 - 3843.009991989396$

$i)\,z_2\,\bar{z}_1^3\,\bar{z}_2\,z_1 - (23434.19949065543 + 2990.116587061194\,i)\,z_2^2\,\bar{z}_1^2\,\bar{z}_2\,z_1 + (5198.80211353183 + 81595.80077238426\,i)\,z_2^3$

$\bar{z}_1\,\bar{z}_2\,z_1 + (825.3048483446908 + 99217.99009700005\,i)\,z_2^6 - (46.37923663556279 - 26.17624102910074\,i)\,\bar{z}_1^6 - (4093.210443848799 -$

$111104.7708998313\,i)\,\bar{z}_2^6 - (376.0623497690265 + 43.53976917175885\,i)\,z_2\,\bar{z}_1^5 - (17459.29410299748 - 594776.1262548896\,i)\,z_2\,\bar{z}_2^5 -$

$(51424.54801936122 + 31154.54844142055\,i)\,\bar{z}_1\,\bar{z}_2^5 + (185.3040668560389 + 699.2786425907618\,i)\,z_2^2\,\bar{z}_1^4 - (28018.88991161085 -$

$1.379079571348818 \times 10^6\, i)\, z_2^2\, \bar{z}_2^4 + (11674.13533339656 - 11325.33927490923\, i)\, \bar{z}_1^2\, \bar{z}_2^4 - (220970.7066022785 + 115648.2641387117\, i)\, z_2\, \bar{z}_1\, \bar{z}_2^4 + (3326.309573500978 + 533.8212784327036\, i)\, z_2^5\, \bar{z}_1^3 - (19894.73399686386 - 1.770063506735921 \times 10^6\, i)\, z_2^3\, \bar{z}_2^3 + (3387.334247797892 + 3155.907280875051\, i)\, \bar{z}_1^3\, \bar{z}_2^3 + (32279.49973548401 - 34982.89668377391\, i)\, z_2\, \bar{z}_1^2\, \bar{z}_2^3 - (406811.112837975 + 167499.8347593519\, i)\, z_2^2\, \bar{z}_1\, \bar{z}_2^3 + (1674.431980604828 - 11229.38056198659\, i)\, z_2^4\, \bar{z}_2^2 - (3716.398318429275 - 1.327706000576884 \times 10^6\, i)\, z_2^4\, \bar{z}_2^2 - (557.892664506608 - 1567.493554107312\, i)\, \bar{z}_1^4\, \bar{z}_2^2 + (7717.989321123748 + 4480.533669705435\, i)\, z_2\, \bar{z}_1^3\, \bar{z}_2^2 + (31722.5318145437 - 51786.01310649923\, i)\, z_2^2\, \bar{z}_1^2\, \bar{z}_2^2 - (398980.9570782463 + 114823.4222170126\, i)\, z_2^3\, \bar{z}_1\, \bar{z}_2^2 - (45814.43152512708 + 2493.538168657015\, i)\, z_2^5\, \bar{z}_1 + (2410.160931544448 + 551898.5633995151\, i)\, z_2^5\, \bar{z}_2 - (80.29187933832591 + 439.9295741434651\, i)\, \bar{z}_1^5\, \bar{z}_2 - (1230.149171840629 - 884.8863416936629\, i)\, z_2\, \bar{z}_1^4\, \bar{z}_2 + (7126.757449807181 + 2540.211023795979\, i)\, z_2^2\, \bar{z}_1^3\, \bar{z}_2 + (14125.43011798873 - 37158.98705958242\, i)\, z_2^3\, \bar{z}_1^2\, \bar{z}_2 - (206762.6844055345 + 33779.1679315464\, i)\, z_2^4\, \bar{z}_1\, \bar{z}_2$

◆ $F_2^{(7)} = (83.64408737390178 + 290.0574619582591\, i)\, z_1^7 - (43.43559443737217 + 2126.0712317609\, i)\, z_2\, z_1^6 - (619.7337803689979 + 1954.786698227959\, i)\, \bar{z}_1\, z_1^6 + (2014.781480927104 - 952.131629931276\, i)\, \bar{z}_2\, z_1^6 + (4575.387504398479 - 3628.64457474295\, i)\, z_2^2\, z_1^5 + (1976.171130472751 + 5666.814977585757\, i)\, \bar{z}_1^2\, z_1^5 + (11023.17046809458 + 319.5063574839181\, i)\, \bar{z}_2^2\, z_1^5 - (12.23270735001552 - 12642.57522305934\, i)\, z_2\, \bar{z}_1\, z_1^5 + (6160.473228084133 + 3166.794838176146\, i)\, z_2\, \bar{z}_2\, z_1^5 - (12599.76170568175 - 5564.839164044762\, i)\, \bar{z}_1\, \bar{z}_2\, z_1^5 + (9012.215926813853 + 22493.69793183785\, i)\, z_2^3\, z_1^4 - (3512.518023723479 + 9162.002147931235\, i)\, \bar{z}_1^3\, z_1^4 - (6643.175155733118 - 30523.4454809598\, i)\, \bar{z}_2^3\, z_1^4 + (714.699757418919 - 31417.0927115498\, i)\, z_2\, \bar{z}_1\, z_1^4 + (4767.462138185586 + 62129.12864609378\, i)\, z_2\, \bar{z}_2\, z_1^4 - (54282.05312380492 + 4952.46055647769\, i)\, \bar{z}_1\, \bar{z}_2^2\, z_1^4 - (23682.43887050526 - 15468.82336427138\, i)\, z_2^2\, \bar{z}_1\, z_1^4 + (17150.13741530033 + 52769.19689762125\, i)\, z_2^2\, \bar{z}_2\, z_1^4 + (32853.93269782345 - 13463.74731613414\, i)\, \bar{z}_1^2\, \bar{z}_2\, z_1^4 - (31203.93419768123 + 20388.53123784128\, i)\, z_2\, \bar{z}_1\, \bar{z}_2\, z_1^4 - (74778.13931718652 - 44720.91478373492\, i)\, z_2^4\, z_1^3 + (3755.892245469613 + 8923.860291123128\, i)\, \bar{z}_1^4\, z_1^3 - (109403.2959637758 + 8010.70865799096\, i)\, z_2^4\, z_1^3 - (1871.934357516824 - 41759.3938364254\, i)\, z_2\, \bar{z}_1^3\, z_1^3 - (311275.8393278722 - 22111.54698835874\, i)\, z_2\, \bar{z}_2^3\, z_1^3 + (42588.59842142134 - 120770.8209199879\, i)\, \bar{z}_1\, \bar{z}_2^3\, z_1^3 + (48413.19676663572 - 25463.55035598281\, i)\, z_2^2\, \bar{z}_1^2\, z_1^3 - (408875.6723632055 - 112841.6920438104\, i)\, z_2^2\, \bar{z}_2^2\, z_1^3 + (106548.330595442 + 16528.53194344849\, i)\, \bar{z}_1^2\, \bar{z}_2^2\, z_1^3 + (18144.7229742578 - 252593.092380948\, i)\, z_2\, \bar{z}_1\, \bar{z}_2^2\, z_1^3 - (23813.64761962618 + 95497.59144577864\, i)\, z_2^3\, \bar{z}_1\, z_1^3 - (262069.5354186049 - 119475.5614083777\, i)\, z_2^3\, \bar{z}_2\, z_1^3 - (45720.76823141518 - 17242.96404384041\, i)\, \bar{z}_1^3\, \bar{z}_2\, z_1^3 + (62051.25290181433 + 50235.53513948497\, i)\, z_2\, \bar{z}_1^2\, \bar{z}_2\, z_1^3 - (34361.30519706609 + 221754.1723295659\, i)\, z_2^2\, \bar{z}_1\, \bar{z}_2\, z_1^3 - (219433.043489999 + 251306.6093361899\, i)\, z_2^5\, z_1^2 - (2414.789919405244 + 5237.130214360739\, i)\, \bar{z}_1^5\, z_1^2 - (1667.594135473086 + 355106.7092150292\, i)\, \bar{z}_2^5\, z_1^2 + (2100.399090067842 - 31311.81089294745\, i)\, z_2\, \bar{z}_1^4\, z_1^2 - (218176.5251209737 + 1.427633829654882 \times 10^6\, i)\, z_2\, \bar{z}_2^4\, z_1^2 + (330821.7419092286 + 92530.3436940877\, i)\, \bar{z}_1\, \bar{z}_2^4\, z_1^2 - (48830.07974327527 - 19959.02423905088\, i)\, z_2^2\, \bar{z}_1^3\, z_1^2 - (844444.8694517713 + 2.473832959916086 \times 10^6\, i)\, z_2^2\, \bar{z}_2^3\, z_1^2 - (88408.82713205602 - 174756.0244594812\, i)\, \bar{z}_1^2\, \bar{z}_2^3\, z_1^2 + (979886.5107112944 + 159586.61962986\, i)\, z_2\, \bar{z}_1\, \bar{z}_2^3\, z_1^2 + (14886.06926986529 + 147945.0588084791\, i)\, z_2^3\, \bar{z}_1^2\, z_1^2 - (1.245695124475151 \times 10^6 + 2.286740990685873 \times 10^6\, i)\, z_2^3\, \bar{z}_2^2\, z_1^2 - (104152.9168056533 + 22980.51539437395\, i)\, \bar{z}_1^3\, \bar{z}_2^2\, z_1^2 - (86428.65951621982 - 373445.0878113188\, i)\, z_2\, \bar{z}_1^2\, \bar{z}_2^2\, z_1^2 + (1.346925700664382 \times 10^6 - 34851.79033616533\, i)\, z_2^2\, \bar{z}_1\, \bar{z}_2^2\, z_1^2 + (262727.1912451487 - 82514.73827621773\, i)\, z_2^4\, \bar{z}_1\, z_1^2 - (845925.0380215767 + 1.13955454826914 \times 10^6\, i)\, z_2^4\, \bar{z}_2\, z_1^2 + (35814.01241374293 - 12312.26073246971\, i)\, \bar{z}_1^4\, \bar{z}_2\, z_1^2 - (60428.23513420975 + 59837.15409711911\, i)\, z_2\, \bar{z}_1^3\, \bar{z}_2\, z_1^2 - (5148.489826365119 - 337655.6132466184\, i)\, z_2^2\, \bar{z}_1^2\, \bar{z}_2\, z_1^2 + (901171.9203158641 - 163397.7017662088\, i)\, z_2^3\, \bar{z}_1\, \bar{z}_2\, z_1^2 + (1.202753150714307 \times 10^6 - 631739.4391005157\, i)\, z_2^6\, z_1 + (864.0161107909863 + 1714.930548609126\, i)\, \bar{z}_1^6\, z_1 + (1.353553203208478 \times 10^6 + 53295.77827309529\, i)\, \bar{z}_2^6\, z_1 - (1122.434570818465 - 12557.5210903594\, i)\, z_2\, \bar{z}_1^5\, z_1 + (7.201805018325554 \times 10^6 - 348177.7761270834\, i)\, z_2\, \bar{z}_2^5\, z_1 - (311820.9334343227 - 708972.6340393053\, i)\, \bar{z}_1\, \bar{z}_2^5\, z_1 + (24304.41914015636 - 7272.527161539687\, i)\, z_2^2\, \bar{z}_1^4\, z_1 + (1.665004344384576 \times 10^7 - 2.470440077837727 \times 10^6\, i)\, z_2^2\, \bar{z}_2^4\, z_1 - (304378.9167982383 + 162144.3960830149\, i)\, \bar{z}_1^2\, \bar{z}_2^4\, z_1 - (983385.3734966344 - 2.983139450563304 \times 10^6\, i)\, z_2\, \bar{z}_1\, \bar{z}_2^4\, z_1 + (4353.964912768817 - 98836.7981934411\, i)\, z_2^3\, \bar{z}_1^3\, z_1 + (2.132928343049594 \times 10^7 - 5.410176480737763 \times 10^6\, i)\, z_2^3\, \bar{z}_2^3\, z_1 + (74290.74308773845 - 109164.1722804663\, i)\, \bar{z}_1^3\, \bar{z}_2^3\, z_1 - (918533.165036076 + 400488.8932535503\, i)\, z_2\, \bar{z}_1^2\, \bar{z}_2^3\, z_1 - (980113.3842303595 - 5.464457809794022 \times 10^6\, i)\, z_2^2\, \bar{z}_1\, \bar{z}_2^3\, z_1 - (274358.1031974403 - 18947.64506870945\, i)\, z_2^4\, \bar{z}_1^2\, z_1 + (1.598630289036902 \times 10^7 - 5.718661916503082 \times 10^6\, i)\, z_2^4\, \bar{z}_2^2\, z_1 + (50705.45684121725 + 14581.8311411189\, i)\, \bar{z}_1^4\, \bar{z}_2^2\, z_1 + (95533.2905019866 - 236851.4142545986\, i)\, z_2\, \bar{z}_1^3\, \bar{z}_2^2\, z_1 - (1.312691970312158 \times 10^6 + 306824.6461171093\, i)\, z_2^2\, \bar{z}_1^2\, \bar{z}_2^2\, z_1 - (120380.8640119486 - 5.354664972815532 \times 10^6\, i)\, z_2^3\, \bar{z}_1\, \bar{z}_2^2\, z_1 + (155177.9832310137 + 639181.2471611403\, i)\, z_2^5\, \bar{z}_1\, z_1 + (6.652743023846095 \times 10^6 - 3.004349781035028 \times 10^6\, i)\, z_2^5\, \bar{z}_2\, z_1 - (14971.70998217062 - 4639.318162735666\, i)\, \bar{z}_1^5\, \bar{z}_2\, z_1 + (28778.57898076316 + 34669.69794937759\, i)\, z_2\, \bar{z}_1^4\, \bar{z}_2\, z_1 + (41025.09353562018 - 219950.7165881\, i)\, z_2^2\, \bar{z}_1^3\, \bar{z}_2\, z_1 - (913280.6913344404 + 67769.6268401437\, i)\, z_2^3\, \bar{z}_1^2\, \bar{z}_2\, z_1 + (359942.6021498478 + 2.809948489758765 \times 10^6\, i)\, z_2^4\, \bar{z}_1\, \bar{z}_2\, z_1 + (41926.9113256254 + 2.67709470748605 \times 10^6\, i)\, z_2^7 - (132.6818472053728 + 241.7445097738593\, i)\, \bar{z}_1^7 - (125601.3828252915 -$

$$2.92875251224036 \times 10^6\, i)\, \bar{z}_2^7 + (234.9380538752109 - 2104.460593139071\, i)\, z_2\, \bar{z}_1^6 - (654413.0696609477 - 1.872087203839214 \times 10^7$$

$$i)\, z_2\, \bar{z}_2^6 - (1.312401097841023 \times 10^6 + 853932.4861415006\, i)\, \bar{z}_1\, \bar{z}_2^6 - (4780.516117693688 - 932.3137014160246$$

$$i)\, z_2^2\, \bar{z}_1^5 - (1.34330955769433 \times 10^6 - 5.259084175844097 \times 10^7\, i)\, z_2^2\, \bar{z}_2^5 + (308411.4046871596 - 261498.0724547681$$

$$i)\, \bar{z}_1^2\, \bar{z}_2^5 - (7.026637609531042 \times 10^6 + 4.086055041913429 \times 10^6\, i)\, z_2\, \bar{z}_1\, \bar{z}_2^5 - (4435.494656068623 - 24102.91428164737$$

$$i)\, z_2^3\, \bar{z}_1^4 - (1.344201673389921 \times 10^6 - 8.422556572723623 \times 10^7\, i)\, z_2^3\, \bar{z}_2^4 + (83275.98254093016 + 71819.27993727724\, i)$$

$$\bar{z}_1^3\, \bar{z}_2^4 + (1.184517728771519 \times 10^6 - 1.123531120075142 \times 10^6\, i)\, z_2\, \bar{z}_1^2\, \bar{z}_2^4 - (1.637180474317187 \times 10^7 + 8.034197656217247 \times 10^6\, i)$$

$$z_2^2\, \bar{z}_1\, \bar{z}_2^4 + (86296.47222150961 + 13321.32241191986\, i)\, z_2^4\, \bar{z}_1^3 - (536577.6328042524 - 8.311025167774118 \times 10^7\, i)$$

$$z_2^4\, \bar{z}_2^3 - (21838.07225919552 - 24869.81986093052\, i)\, \bar{z}_1^4\, \bar{z}_2^3 + (250707.3270374737 + 196724.1930462976\, i)\, z_2\, \bar{z}_1^3\, \bar{z}_2^3 +$$

$$(1.805268041933681 \times 10^6 - 2.160887449433845 \times 10^6\, i)\, z_2^2\, \bar{z}_1^2\, \bar{z}_2^3 - (2.114816346163657 \times 10^7 + 8.222181266904347 \times 10^6\, i)\, z_2^3\, \bar{z}_1\, \bar{z}_2^3 +$$

$$(66210.473533216 - 301330.6175309036\, i)\, z_2^5\, \bar{z}_1^2 + (122356.5628028268 + 5.054845293253546 \times 10^7\, i)\, z_2^5\, \bar{z}_2^2 - (9841.792116958253 +$$

$$3501.571388439518\, i)\, \bar{z}_1^5\, \bar{z}_2^2 - (32034.45586485212 - 54491.53165533926\, i)\, z_2\, \bar{z}_1^4\, \bar{z}_2^2 + (375173.8227154319 + 196583.1081955311\, i)$$

$$z_2^2\, \bar{z}_1^3\, \bar{z}_2^2 + (1.3603974991937 \times 10^6 - 2.24918921765156 \times 10^6\, i)\, z_2^3\, \bar{z}_1^2\, \bar{z}_2^2 - (1.598220376283134 \times 10^7 + 4.508206125061251 \times 10^6\, i)$$

$$z_2^4\, \bar{z}_1\, \bar{z}_2^2 - (1.218488345305617 \times 10^6 + 108460.8765970713\, i)\, z_2^6\, \bar{z}_1 + (176645.1363035577 + 1.754052689815114 \times 10^7\, i)$$

$$z_2^6\, \bar{z}_2 + (2609.51152646361 - 718.9253898120566\, i)\, \bar{z}_1^6\, \bar{z}_2 - (5357.965272126289 + 7855.459981125157\, i)\, z_2$$

$$\bar{z}_1^5\, \bar{z}_2 - (18669.45913715022 - 51893.93760870302\, i)\, z_2^2\, \bar{z}_1^4\, \bar{z}_2 + (274124.2453386453 + 90180.46410078433\, i)\, z_2^3\, \bar{z}_1^3\, \bar{z}_2 +$$

$$(489578.3404501648 - 1.255204899224763 \times 10^6\, i)\, z_2^4\, \bar{z}_1^2\, \bar{z}_2 - (6.700753755551565 \times 10^6 + 1.200939503767909 \times 10^6\, i)\, z_2^5\, \bar{z}_1\, \bar{z}_2$$

II.III. Normal form mapping

💡 Chapter 6, 7, Section 6.2, Section 7.2.

The normal form of the mapping model of the Sun-Jupiter system was derived in chapter 6. The form given here is according to (18;6), i.e. (41;6). The mapping is given after diagonalization and complexification. The mapping in $\mathbb{R}^4$ can be reconstructed according to (7;6). The integrable approximation of the mapping of radii (22;7) is calculated via (21;7):

$$\rho_1 = U_1 \cdot \overline{U}_1, \ \rho_2 = U_2 \cdot \overline{U}_2$$

Note, that $U_1^{(\kappa)} = U_2^{(\kappa)} = 0$ for κ even (Section 6.1.2)!

■ II.III.1. U_1

◆ $U_1^{(1)} = (0.870169533360692 + 0.4927524563214631\,i)\,\zeta_1$

◆ $U_1^{(3)} = (3.6546171083044 - 6.453821635951158\,i)\,\zeta_1^2\,\overline{\zeta}_1 - (0.4367732356625151 - 0.771313785372723\,i)\,\zeta_1\,\zeta_2\,\overline{\zeta}_2$

◆ $U_1^{(5)} = (147.2806619443048 - 315.9054061443004\,i)$
$\overline{\zeta}_1^2\,\zeta_1^3 + (33.6995550680424 - 46.16956305305763\,i)\,\zeta_2\,\overline{\zeta}_1\,\overline{\zeta}_2\,\zeta_1^2 + (3.668508271686712 - 7.275604737421741\,i)\,\zeta_2^2\,\overline{\zeta}_2^2\,\zeta_1$

◆ $U_1^{(7)} = (227.9238670475072 - 5632.410232922022\,i)\,\overline{\zeta}_1^3\,\zeta_1^4 + (2072.763334979311 - 3889.973815429828\,i)$
$\zeta_2\,\overline{\zeta}_1^2\,\overline{\zeta}_2\,\zeta_1^3 + (606.0027627965151 - 1090.52184556391\,i)\,\zeta_2^2\,\overline{\zeta}_1\,\overline{\zeta}_2^2\,\zeta_1^2 + (113.1699773688747 - 185.2106659253034\,i)\,\zeta_2^3\,\overline{\zeta}_2^3\,\zeta_1$

◆ $U_1^{(9)} = (119952.5072378412 - 410564.1070613753\,i)$
$\overline{\zeta}_1^4\,\zeta_1^5 - (269235.9655361278 - 378478.0333485194\,i)\,\zeta_2\,\overline{\zeta}_1^3\,\overline{\zeta}_2\,\zeta_1^4 + (11500.60974902951 - 40236.94094236312\,i)$
$\zeta_2^2\,\overline{\zeta}_1^2\,\overline{\zeta}_2^2\,\zeta_1^3 + (18469.26144417725 - 34569.13625983393\,i)\,\zeta_2^3\,\overline{\zeta}_1\,\overline{\zeta}_2^3\,\zeta_1^2 - (6410.350895588956 - 11643.14215663985\,i)\,\zeta_2^4\,\overline{\zeta}_2^4\,\zeta_1$

◆ $U_1^{(11)} = (2.971045363070645\times10^6 - 1.51927782042769\times10^7\,i)\,\overline{\zeta}_1^5\,\zeta_1^6 -$
$(2.344893423179776\times10^6 - 8.18714568522723\times10^6\,i)\,\zeta_2\,\overline{\zeta}_1^4\,\overline{\zeta}_2\,\zeta_1^5 + (3.206069044878364\times10^6 - 8.576467421202682\times10^6\,i)$
$\zeta_2^2\,\overline{\zeta}_1^3\,\overline{\zeta}_2^2\,\zeta_1^4 - (2.0928407312783\times10^6 - 2.810198610562086\times10^6\,i)\,\zeta_2^3\,\overline{\zeta}_1^2\,\overline{\zeta}_2^3\,\zeta_1^3 - (4.695097352122903\times10^6 -$
$8.516057711241841\times10^6\,i)\,\zeta_2^4\,\overline{\zeta}_1\,\overline{\zeta}_2^4\,\zeta_1^2 - (2.831714708871171\times10^6 - 4.970683682115696\times10^6\,i)\,\zeta_2^5\,\overline{\zeta}_2^5\,\zeta_1$

◆ $U_1^{(13)} =$
$(1.634079028298248\times10^8 - 8.409013287376201\times10^8\,i)\,\overline{\zeta}_1^6\,\zeta_1^7 + (3.737544099677136\times10^9 - 6.218206679800825\times10^9\,i)\,\zeta_2\,\overline{\zeta}_1^5\,\overline{\zeta}_2$
$\zeta_1^6 + (2.881486702211762\times10^7 - 2.166605254891796\times10^8\,i)\,\zeta_2^2\,\overline{\zeta}_1^4\,\overline{\zeta}_2^2\,\zeta_1^5 - (5.383473490906677\times10^8 - 9.813111295365295\times10^8\,i)$
$\zeta_2^3\,\overline{\zeta}_1^3\,\overline{\zeta}_2^3\,\zeta_1^4 - (1.215069045986511\times10^9 - 2.28598469753241\times10^9\,i)\,\zeta_2^4\,\overline{\zeta}_1^2\,\overline{\zeta}_2^4\,\zeta_1^3 - (3.561554577732727\times10^9 -$
$6.229339630995239\times10^9\,i)\,\zeta_2^5\,\overline{\zeta}_1\,\overline{\zeta}_2^5\,\zeta_1^2 - (3.284984721880188\times10^9 - 5.853305939691521\times10^9\,i)\,\zeta_2^6\,\overline{\zeta}_2^6\,\zeta_1$

◆ $U_1^{(15)} = (4.275898031737922\times10^{12} - 7.578566542474773\times10^{12}\,i)\,\overline{\zeta}_1^7\,\zeta_1^8 + (1.208153905302991\times10^{13} -$
$2.143790463605147\times10^{13}\,i)\,\zeta_2\,\overline{\zeta}_1^6\,\overline{\zeta}_2\,\zeta_1^7 + (3.211406467975348\times10^{13} - 5.670457974608133\times10^{13}\,i)\,\zeta_2^2\,\overline{\zeta}_1^5\,\overline{\zeta}_2^2\,\zeta_1^6 +$

$(5.708810196512142 \times 10^{14} - 1.008120655090055 \times 10^{15}\, i)\, \zeta_2^3\, \overline{\zeta}_1^4\, \overline{\zeta}_2^3\, \zeta_1^5 + (1.011893841578862 \times 10^{16} - 1.786936839146263 \times 10^{16}\, i)$
$\zeta_2^4\, \overline{\zeta}_1^3\, \overline{\zeta}_2^4\, \zeta_1^4 + (1.838012515522403 \times 10^{17} - 3.245812679915833 \times 10^{17}\, i)\, \zeta_2^5\, \overline{\zeta}_1^2\, \overline{\zeta}_2^5\, \zeta_1^3 + (3.021600555011087 \times 10^{18} -$
$5.335954687339571 \times 10^{18}\, i)\, \zeta_2^6\, \overline{\zeta}_1\, \overline{\zeta}_2^6\, \zeta_1^2 + (3.229289886014312 \times 10^{19} - 5.70272077209762 \times 10^{19}\, i)\, \zeta_2^7\, \overline{\zeta}_2^7\, \zeta_1$

- $U_1^{(17)} = (8.679592471085657 \times 10^{15} - 1.528498604386691 \times 10^{16}\, i)$
  $\overline{\zeta}_1^8\, \zeta_1^9 + (9.353310663513438 \times 10^{15} - 1.651605581767145 \times 10^{16}\, i)\, \zeta_2\, \overline{\zeta}_1^7\, \overline{\zeta}_2\, \zeta_1^8 + (1.021901672348875 \times 10^{16} -$
  $1.463417666489638 \times 10^{16}\, i)\, \zeta_2^2\, \overline{\zeta}_1^6\, \overline{\zeta}_2^2\, \zeta_1^7 + (2.18127788055792 \times 10^{17} - 3.447834401227994 \times 10^{17}\, i)\, \zeta_2^3\, \overline{\zeta}_1^5\, \overline{\zeta}_2^3\, \zeta_1^6 +$
  $(1.030629311371462 \times 10^{19} - 1.774578742443688 \times 10^{19}\, i)\, \zeta_2^4\, \overline{\zeta}_1^4\, \overline{\zeta}_2^4\, \zeta_1^5 + (3.677914449321296 \times 10^{20} - 6.503981138789144 \times 10^{20}\, i)$
  $\zeta_2^5\, \overline{\zeta}_1^3\, \overline{\zeta}_2^5\, \zeta_1^4 + (7.41637348103588 \times 10^{21} - 1.333600115259989 \times 10^{22}\, i)\, \zeta_2^6\, \overline{\zeta}_1^2\, \overline{\zeta}_2^6\, \zeta_1^3 - (8.499213012719778 \times 10^{22} -$
  $1.463030490050339 \times 10^{23}\, i)\, \zeta_2^7\, \overline{\zeta}_1\, \overline{\zeta}_2^7\, \zeta_1^2 - (9.650388924369644 \times 10^{23} - 1.694676586127637 \times 10^{24}\, i)\, \zeta_2^8\, \overline{\zeta}_2^8\, \zeta_1$

- $U_1^{(19)} = (1.510288624105862 \times 10^{18} - 2.711983825958071 \times 10^{18}\, i)\, \overline{\zeta}_1^9\, \zeta_1^{10} - (7.66982661746728 \times 10^{17} - 1.309396071546895 \times 10^{18}\, i)$
  $\zeta_2\, \overline{\zeta}_1^8\, \overline{\zeta}_2\, \zeta_1^9 + (4.963573392053514 \times 10^{18} - 7.607414930670258 \times 10^{18}\, i)\, \zeta_2^2\, \overline{\zeta}_1^7\, \overline{\zeta}_2^2\, \zeta_1^8 - (7.168785290396862 \times 10^{19} -$
  $1.150166751175447 \times 10^{20}\, i)\, \zeta_2^3\, \overline{\zeta}_1^6\, \overline{\zeta}_2^3\, \zeta_1^7 - (2.346348132366417 \times 10^{21} - 3.260387597032162 \times 10^{21}\, i)\, \zeta_2^4\, \overline{\zeta}_1^5\, \overline{\zeta}_2^4\, \zeta_1^6 -$
  $(1.623791062060173 \times 10^{23} - 2.508896007862574 \times 10^{23}\, i)\, \zeta_2^5\, \overline{\zeta}_1^4\, \overline{\zeta}_2^5\, \zeta_1^5 - (2.008639186208575 \times 10^{25} - 3.538830468561769 \times 10^{25}\, i)$
  $\zeta_2^6\, \overline{\zeta}_1^3\, \overline{\zeta}_2^6\, \zeta_1^4 + (3.008749341548426 \times 10^{25} - 4.249676722319035 \times 10^{25}\, i)\, \zeta_2^7\, \overline{\zeta}_1^2\, \overline{\zeta}_2^7\, \zeta_1^3 + (2.374429583322497 \times 10^{27} -$
  $4.172044455334721 \times 10^{27}\, i)\, \zeta_2^8\, \overline{\zeta}_1\, \overline{\zeta}_2^8\, \zeta_1^2 - (7.108846835652774 \times 10^{27} - 1.23270032612648 \times 10^{28}\, i)\, \zeta_2^9\, \overline{\zeta}_2^9\, \zeta_1$

- $U_1^{(21)} = (-2.79423840395444 \times 10^{20} + 4.900486151420649 \times 10^{20}\, i)\, \overline{\zeta}_1^{10}\, \zeta_1^{11} -$
  $(2.844800734438695 \times 10^{20} - 5.606126265540417 \times 10^{20}\, i)\, \zeta_2\, \overline{\zeta}_1^9\, \overline{\zeta}_2\, \zeta_1^{10} + (1.613698142703557 \times 10^{21} - 2.575136978626222 \times 10^{21}\, i)$
  $\zeta_2^2\, \overline{\zeta}_1^8\, \overline{\zeta}_2^2\, \zeta_1^9 - (3.1278875494926 \times 10^{22} - 5.680850211721989 \times 10^{22}\, i)\, \zeta_2^3\, \overline{\zeta}_1^7\, \overline{\zeta}_2^3\, \zeta_1^8 - (3.554866980122412 \times 10^{24} -$
  $6.318178428582637 \times 10^{24}\, i)\, \zeta_2^4\, \overline{\zeta}_1^6\, \overline{\zeta}_2^4\, \zeta_1^7 - (3.445033349075128 \times 10^{26} - 6.398887509217389 \times 10^{26}\, i)\, \zeta_2^5\, \overline{\zeta}_1^5\, \overline{\zeta}_2^5\, \zeta_1^6 +$
  $(1.774786255872778 \times 10^{28} - 3.058169778402861 \times 10^{28}\, i)\, \zeta_2^6\, \overline{\zeta}_1^4\, \overline{\zeta}_2^6\, \zeta_1^5 + (5.670196206918132 \times 10^{28} - 1.095291161616487 \times 10^{29}\, i)$
  $\zeta_2^7\, \overline{\zeta}_1^3\, \overline{\zeta}_2^7\, \zeta_1^4 - (2.473542819345203 \times 10^{30} - 4.310121167857893 \times 10^{30}\, i)\, \zeta_2^8\, \overline{\zeta}_1^2\, \overline{\zeta}_2^8\, \zeta_1^3 + (9.748381770190382 \times 10^{30} -$
  $1.674731882777627 \times 10^{31}\, i)\, \zeta_2^9\, \overline{\zeta}_1\, \overline{\zeta}_2^9\, \zeta_1^2 - (9.177976340461885 \times 10^{30} - 1.553914818299867 \times 10^{31}\, i)\, \zeta_2^{10}\, \overline{\zeta}_2^{10}\, \zeta_1$

- $U_1^{(23)} = (-3.454266025192054 \times 10^{22} +$
  $7.405701039377763 \times 10^{22}\, i)\, \overline{\zeta}_1^{11}\, \zeta_1^{12} - (2.824150635997673 \times 10^{22} - 6.775152976455965 \times 10^{22}\, i)\, \zeta_2\, \overline{\zeta}_1^{10}\, \overline{\zeta}_2\, \zeta_1^{11} +$
  $(1.797375663268221 \times 10^{23} - 2.80961848330659 \times 10^{23}\, i)\, \zeta_2^2\, \overline{\zeta}_1^9\, \overline{\zeta}_2^2\, \zeta_1^{10} + (9.91824594523809 \times 10^{24} - 1.318675290504343 \times 10^{25}\, i)$
  $\zeta_2^3\, \overline{\zeta}_1^8\, \overline{\zeta}_2^3\, \zeta_1^9 + (3.020455255817708 \times 10^{26} - 9.73587449111888 \times 10^{25}\, i)\, \zeta_2^4\, \overline{\zeta}_1^7\, \overline{\zeta}_2^4\, \zeta_1^8 + (4.219703609777554 \times 10^{29} -$
  $7.462585644683929 \times 10^{29}\, i)\, \zeta_2^5\, \overline{\zeta}_1^6\, \overline{\zeta}_2^5\, \zeta_1^7 - (8.6229346464723 \times 10^{30} - 1.445467587192143 \times 10^{31}\, i)\, \zeta_2^6\, \overline{\zeta}_1^5\, \overline{\zeta}_2^6\, \zeta_1^6 -$
  $(7.716039461732535 \times 10^{31} - 1.398369677398347 \times 10^{32}\, i)\, \zeta_2^7\, \overline{\zeta}_1^4\, \overline{\zeta}_2^7\, \zeta_1^5 + (1.582322580976549 \times 10^{33} - 2.72662046252324 \times 10^{33}\, i)$
  $\zeta_2^8\, \overline{\zeta}_1^3\, \overline{\zeta}_2^8\, \zeta_1^4 - (6.517894051571042 \times 10^{33} - 1.105144910310173 \times 10^{34}\, i)\, \zeta_2^9\, \overline{\zeta}_1^2\, \overline{\zeta}_2^9\, \zeta_1^3 + (9.233369821904482 \times 10^{33} -$
  $1.543225696560311 \times 10^{34}\, i)\, \zeta_2^{10}\, \overline{\zeta}_1\, \overline{\zeta}_2^{10}\, \zeta_1^2 - (3.717777533835007 \times 10^{33} - 6.010101904038967 \times 10^{33}\, i)\, \zeta_2^{11}\, \overline{\zeta}_2^{11}\, \zeta_1$

- $U_1^{(25)} = (-7.003405744270526 \times 10^{25} + 1.259043571888496 \times 10^{26}\, i)\, \overline{\zeta}_1^{12}\, \zeta_1^{13} + (4.198634118952993 \times 10^{25} -$
  $7.146830474298998 \times 10^{25}\, i)\, \zeta_2\, \overline{\zeta}_1^{11}\, \overline{\zeta}_2\, \zeta_1^{12} - (2.324469306022222 \times 10^{25} - 3.566465279374746 \times 10^{25}\, i)\, \zeta_2^2\, \overline{\zeta}_1^{10}\, \overline{\zeta}_2^2\, \zeta_1^{11} +$
  $(3.755637377680806 \times 10^{27} - 6.844435407343133 \times 10^{27}\, i)\, \zeta_2^3\, \overline{\zeta}_1^9\, \overline{\zeta}_2^3\, \zeta_1^{10} + (1.998448852181016 \times 10^{30} - 3.741024067020728 \times 10^{30}\, i)$
  $\zeta_2^4\, \overline{\zeta}_1^8\, \overline{\zeta}_2^4\, \zeta_1^9 - (2.446054780462514 \times 10^{32} - 4.213325876550194 \times 10^{32}\, i)\, \zeta_2^5\, \overline{\zeta}_1^7\, \overline{\zeta}_2^5\, \zeta_1^8 + (2.512903293704573 \times 10^{33} -$
  $4.025094319324287 \times 10^{33}\, i)\, \zeta_2^6\, \overline{\zeta}_1^6\, \overline{\zeta}_2^6\, \zeta_1^7 + (5.076246600181306 \times 10^{34} - 8.959243388950134 \times 10^{34}\, i)\, \zeta_2^7\, \overline{\zeta}_1^5\, \overline{\zeta}_2^7\, \zeta_1^6 -$
  $(7.208618798096489 \times 10^{35} - 1.227384986631213 \times 10^{36}\, i)\, \zeta_2^8\, \overline{\zeta}_1^4\, \overline{\zeta}_2^8\, \zeta_1^5 + (2.915277918002478 \times 10^{36} - 4.879896383947164 \times 10^{36}\, i)$
  $\zeta_2^9\, \overline{\zeta}_1^3\, \overline{\zeta}_2^9\, \zeta_1^4 - (4.705104439727929 \times 10^{36} - 7.740501541388316 \times 10^{36}\, i)\, \zeta_2^{10}\, \overline{\zeta}_1^2\, \overline{\zeta}_2^{10}\, \zeta_1^3 + (3.081046929053638 \times 10^{36} -$
  $4.953242864838803 \times 10^{36}\, i)\, \zeta_2^{11}\, \overline{\zeta}_1\, \overline{\zeta}_2^{11}\, \zeta_1^2 - (5.463598549357739 \times 10^{35} - 8.036351959401497 \times 10^{35}\, i)\, \zeta_2^{12}\, \overline{\zeta}_2^{12}\, \zeta_1$

■ II.III.2. U_2

- $U_2^{(1)} = (0.9997952030905475 + 0.02023738810051618\, i)\, \zeta_2$

- $U_2^{(3)} = (0.001438307967395525 - 0.07105727112543825\, i)\, \overline{\zeta}_2\, \zeta_2^2 + (-0.01793831647325128 + 0.8862133102549055\, i)\, \zeta_1\, \overline{\zeta}_1\, \zeta_2$

- $U_2^{(5)} = (0.02582749776665437 - 1.400765478443381\, i)\, \overline{\zeta}_2^2\, \zeta_2^3 +$
  $(0.3923958887605282 - 16.27274370009146\, i)\, \zeta_1\, \overline{\zeta}_1\, \overline{\zeta}_2\, \zeta_2^2 + (0.1817809511190676 - 28.39257878045045\, i)\, \zeta_1^2\, \overline{\zeta}_1^2\, \zeta_2$

- $U_2^{(7)} = -(0.9409276940849999 - 41.56448302687122\, i)\, \overline{\zeta}_2^3\, \zeta_2^4 + (13.24821581767036 - 650.3075274061482\, i)$
  $\zeta_1\, \overline{\zeta}_1\, \overline{\zeta}_2^2\, \zeta_2^3 + (37.7133753079269 - 1249.92673328154\, i)\, \zeta_1^2\, \overline{\zeta}_1^2\, \overline{\zeta}_2\, \zeta_2^2 + (54.72185250698941 - 1459.946476337522\, i)\, \zeta_1^3\, \overline{\zeta}_1^3\, \zeta_2$

- $U_2^{(9)} = -(214.1126419650972 - 10675.0835667431\, i)$
  $\overline{\zeta}_2^4\, \zeta_2^5 - (1181.454663502677 - 53135.61294383878\, i)\, \zeta_1\, \overline{\zeta}_1\, \overline{\zeta}_2^3\, \zeta_2^4 + (1503.82402386999 - 58707.87581557924\, i)$
  $\zeta_1^2\, \overline{\zeta}_1^2\, \overline{\zeta}_2^2\, \zeta_2^3 + (1090.920714618263 - 27090.183882568\, i)\, \zeta_1^3\, \overline{\zeta}_1^3\, \overline{\zeta}_2\, \zeta_2^2 + (-1449.796727746064 + 115687.8348893827\, i)\, \zeta_1^4\, \overline{\zeta}_1^4\, \zeta_2$

- $U_2^{(11)} = -(382940.0530411026 - 1.895950377868603\times10^7\, i)\, \overline{\zeta}_2^5\, \zeta_2^6 - (584001.6099424638 - 2.855921353605305\times10^7\, i)\, \zeta_1\, \overline{\zeta}_1\, \overline{\zeta}_2^4\, \zeta_2^5 -$
  $(456038.2115688027 - 1.944448252269755\times10^7\, i)\, \zeta_1^2\, \overline{\zeta}_1^2\, \overline{\zeta}_2^3\, \zeta_2^4 - (61122.51211467292 - 3.4772097206764\times10^6\, i)\, \zeta_1^3\, \overline{\zeta}_1^3\, \overline{\zeta}_2^2\, \zeta_2^3 +$
  $(64714.15334796216 - 4.532488585950494\times10^6\, i)\, \zeta_1^4\, \overline{\zeta}_1^4\, \overline{\zeta}_2\, \zeta_2^2 + (-176769.5582331664 + 1.616892675250501\times10^6\, i)\, \zeta_1^5\, \overline{\zeta}_1^5\, \zeta_2$

- $U_2^{(13)} =$
  $-(4.36950767069305\times10^8 - 2.158121434393861\times10^{10}\, i)\, \overline{\zeta}_2^6\, \zeta_2^7 - (8.221209303437402\times10^8 - 4.084750391681676\times10^{10}\, i)\, \zeta_1\, \overline{\zeta}_1\, \overline{\zeta}_2^5$
  $\zeta_2^6 - (3.742148207960722\times10^8 - 1.735567586063623\times10^{10}\, i)\, \zeta_1^2\, \overline{\zeta}_1^2\, \overline{\zeta}_2^4\, \zeta_2^5 - (8.702795718252641\times10^7 - 3.448122767440964\times10^9\, i)$
  $\zeta_1^3\, \overline{\zeta}_1^3\, \overline{\zeta}_2^3\, \zeta_2^4 - (2.404497533637502\times10^7 - 8.379160852408345\times10^8\, i)\, \zeta_1^4\, \overline{\zeta}_1^4\, \overline{\zeta}_2^2\, \zeta_2^3 + (5.134794529191457\times10^6 -$
  $8.468897528930426\times10^7\, i)\, \zeta_1^5\, \overline{\zeta}_1^5\, \overline{\zeta}_2\, \zeta_2^2 + (2.524454083150955\times10^7 - 1.208541647953241\times10^9\, i)\, \zeta_1^6\, \overline{\zeta}_1^6\, \zeta_2$

- $U_2^{(15)} = (1.03329773523978\times10^{20} - 5.104839191276652\times10^{21}\, i)\, \overline{\zeta}_2^7\, \zeta_2^8 + (9.283905977468797\times10^{18} -$
  $4.586562560445444\times10^{20}\, i)\, \zeta_1\, \overline{\zeta}_1\, \overline{\zeta}_2^6\, \zeta_2^7 + (3.722922238583539\times10^{17} - 1.839249222051509\times10^{19}\, i)\, \zeta_1^2\, \overline{\zeta}_1^2\, \overline{\zeta}_2^5\, \zeta_2^6 +$
  $(1.258121436682828\times10^{16} - 6.215549113461554\times10^{17}\, i)\, \zeta_1^3\, \overline{\zeta}_1^3\, \overline{\zeta}_2^4\, \zeta_2^5 + (4.155830306528151\times10^{14} - 2.053132180561219\times10^{16}\, i)$
  $\zeta_1^4\, \overline{\zeta}_1^4\, \overline{\zeta}_2^3\, \zeta_2^4 + (1.406671584158221\times10^{13} - 6.94981044501267\times10^{14}\, i)\, \zeta_1^5\, \overline{\zeta}_1^5\, \overline{\zeta}_2^2\, \zeta_2^3 + (4.395987762484166\times10^{11} -$
  $2.171805926144584\times10^{13}\, i)\, \zeta_1^6\, \overline{\zeta}_1^6\, \overline{\zeta}_2\, \zeta_2^2 + (7.24259208215056\times10^{10} - 3.514519337855921\times10^{12}\, i)\, \zeta_1^7\, \overline{\zeta}_1^7\, \zeta_2$

- $U_2^{(17)} = (1.849555152789252\times10^{24} - 9.399650779509293\times10^{25}\, i)$
  $\overline{\zeta}_2^8\, \zeta_2^9 - (3.321449832087814\times10^{23} - 1.572011934089489\times10^{25}\, i)\, \zeta_1\, \overline{\zeta}_1\, \overline{\zeta}_2^7\, \zeta_2^8 - (1.490291213457534\times10^{22} -$
  $6.156124741293047\times10^{23}\, i)\, \zeta_1^2\, \overline{\zeta}_1^2\, \overline{\zeta}_2^6\, \zeta_2^7 + (4.863337447161011\times10^{20} - 3.033980499481236\times10^{22}\, i)\, \zeta_1^3\, \overline{\zeta}_1^3\, \overline{\zeta}_2^5\, \zeta_2^6 +$
  $(1.432783422667513\times10^{19} - 9.790174451896396\times10^{20}\, i)\, \zeta_1^4\, \overline{\zeta}_1^4\, \overline{\zeta}_2^4\, \zeta_2^5 + (1.717200796131567\times10^{17} - 2.027652600004123\times10^{19}\, i)$
  $\zeta_1^5\, \overline{\zeta}_1^5\, \overline{\zeta}_2^3\, \zeta_2^4 - (2.343544271214881\times10^{15} + 4.211170206562405\times10^{17}\, i)\, \zeta_1^6\, \overline{\zeta}_1^6\, \overline{\zeta}_2^2\, \zeta_2^3 - (1.021216204272772\times10^{15} +$
  $1.508406647325889\times10^{16}\, i)\, \zeta_1^7\, \overline{\zeta}_1^7\, \overline{\zeta}_2\, \zeta_2^2 + (-5.413338428796031\times10^{13} - 2.693704193374206\times10^{15}\, i)\, \zeta_1^8\, \overline{\zeta}_1^8\, \zeta_2$

- $U_2^{(19)} = (3.41074674543412\times10^{27} - 2.117942682614908\times10^{29}\, i)\, \overline{\zeta}_2^9\, \zeta_2^{10} - (2.613147757248231\times10^{27} - 1.316546991142139\times10^{29}\, i)$
  $\zeta_1\, \overline{\zeta}_1\, \overline{\zeta}_2^8\, \zeta_2^9 + (3.866260190072042\times10^{26} - 1.883014388200758\times10^{28}\, i)\, \zeta_1^2\, \overline{\zeta}_1^2\, \overline{\zeta}_2^7\, \zeta_2^8 + (6.89045585775991\times10^{24} -$
  $1.768977359388899\times10^{26}\, i)\, \zeta_1^3\, \overline{\zeta}_1^3\, \overline{\zeta}_2^6\, \zeta_2^7 - (1.328730863975397\times10^{24} - 6.077675680610574\times10^{25}\, i)\, \zeta_1^4\, \overline{\zeta}_1^4\, \overline{\zeta}_2^5\, \zeta_2^6 -$
  $(1.107980739308114\times10^{22} - 3.187775524856869\times10^{23}\, i)\, \zeta_1^5\, \overline{\zeta}_1^5\, \overline{\zeta}_2^4\, \zeta_2^5 - (2.097593257773633\times10^{20} - 2.729412601277495\times10^{21}\, i)$
  $\zeta_1^6\, \overline{\zeta}_1^6\, \overline{\zeta}_2^3\, \zeta_2^4 - (9.118077831795012\times10^{18} - 4.254353242993314\times10^{18}\, i)\, \zeta_1^7\, \overline{\zeta}_1^7\, \overline{\zeta}_2^2\, \zeta_2^3 - (1.318106516698827\times10^{18} +$
  $6.468513878324955\times10^{18}\, i)\, \zeta_1^8\, \overline{\zeta}_1^8\, \overline{\zeta}_2\, \zeta_2^2 + (-4.425675952956321\times10^{17} + 8.873474611218464\times10^{16}\, i)\, \zeta_1^9\, \overline{\zeta}_1^9\, \zeta_2$

- $U_2{}^{(21)} = (9.171226004211476 \times 10^{29} - 1.324240271905385 \times 10^{32}\, i)\, \bar{\zeta}_2^{10}\, \zeta_2^{11} -$

$(2.945168871529361 \times 10^{30} - 1.939410543540521 \times 10^{32}\, i)\, \zeta_1\, \bar{\zeta}_1\, \bar{\zeta}_2^{9}\, \zeta_2^{10} + (1.627186413458658 \times 10^{30} - 8.77910260299534 \times 10^{31}\, i)$

$\zeta_1^2\, \bar{\zeta}_1^2\, \bar{\zeta}_2^{8}\, \zeta_2^{9} - (2.593045167564232 \times 10^{29} - 1.292676288736149 \times 10^{31}\, i)\, \zeta_1^3\, \bar{\zeta}_1^3\, \bar{\zeta}_2^{7}\, \zeta_2^{8} + (1.595824069437254 \times 10^{27} -$

$1.675065469199483 \times 10^{29}\, i)\, \zeta_1^4\, \bar{\zeta}_1^4\, \bar{\zeta}_2^{6}\, \zeta_2^{7} + (1.034984101661096 \times 10^{27} - 4.322449468229572 \times 10^{28}\, i)\, \zeta_1^5\, \bar{\zeta}_1^5\, \bar{\zeta}_2^{5}\, \zeta_2^{6} -$

$(1.00718423530293 \times 10^{25} - 5.671866141440631 \times 10^{26}\, i)\, \zeta_1^6\, \bar{\zeta}_1^6\, \bar{\zeta}_2^{4}\, \zeta_2^{5} - (7.991360589956805 \times 10^{22} - 3.50368166886451 \times 10^{24}\, i)$

$\zeta_1^7\, \bar{\zeta}_1^7\, \bar{\zeta}_2^{3}\, \zeta_2^{4} - (2.820754558747539 \times 10^{21} - 5.238783891073432 \times 10^{20}\, i)\, \zeta_1^8\, \bar{\zeta}_1^8\, \bar{\zeta}_2^{2}\, \zeta_2^{3} - (3.288585092980324 \times 10^{20} +$

$1.43884453961433 \times 10^{21}\, i)\, \zeta_1^9\, \bar{\zeta}_1^9\, \bar{\zeta}_2\, \zeta_2^{2} + (-1.754999961914261 \times 10^{20} + 1.11691489656928 \times 10^{20}\, i)\, \zeta_1^{10}\, \bar{\zeta}_1^{10}\, \zeta_2$

- $U_2{}^{(23)} = -(4.144705951023944 \times 10^{32} +$

$2.80458427375955 \times 10^{34}\, i)\, \bar{\zeta}_2^{11}\, \zeta_2^{12} - (5.389649738274323 \times 10^{32} - 9.24174548153584 \times 10^{34}\, i)\, \zeta_1\, \bar{\zeta}_1\, \bar{\zeta}_2^{10}\, \zeta_2^{11} +$

$(1.189654361355738 \times 10^{33} - 9.39259898227713 \times 10^{34}\, i)\, \zeta_1^2\, \bar{\zeta}_1^2\, \bar{\zeta}_2^{9}\, \zeta_2^{10} - (6.589291817160578 \times 10^{32} - 3.890624552398259 \times 10^{34}\, i)$

$\zeta_1^3\, \bar{\zeta}_1^3\, \bar{\zeta}_2^{8}\, \zeta_2^{9} + (1.187275508130774 \times 10^{32} - 6.153718807560169 \times 10^{33}\, i)\, \zeta_1^4\, \bar{\zeta}_1^4\, \bar{\zeta}_2^{7}\, \zeta_2^{8} - (3.508332654537857 \times 10^{30} -$

$1.969218046865654 \times 10^{32}\, i)\, \zeta_1^5\, \bar{\zeta}_1^5\, \bar{\zeta}_2^{6}\, \zeta_2^{7} - (4.391002466502976 \times 10^{29} - 1.766114234016975 \times 10^{31}\, i)\, \zeta_1^6\, \bar{\zeta}_1^6\, \bar{\zeta}_2^{5}\, \zeta_2^{6} +$

$(1.295752927014594 \times 10^{28} - 5.988958353990625 \times 10^{29}\, i)\, \zeta_1^7\, \bar{\zeta}_1^7\, \bar{\zeta}_2^{4}\, \zeta_2^{5} + (1.779474177277355 \times 10^{25} - 2.744898136020664 \times 10^{26}\, i)$

$\zeta_1^8\, \bar{\zeta}_1^8\, \bar{\zeta}_2^{3}\, \zeta_2^{4} - (4.63169724881534 \times 10^{22} + 9.658739846311644 \times 10^{24}\, i)\, \zeta_1^9\, \bar{\zeta}_1^9\, \bar{\zeta}_2^{2}\, \zeta_2^{3} - (5.115539773123686 \times 10^{22} +$

$1.101504432640758 \times 10^{23}\, i)\, \zeta_1^{10}\, \bar{\zeta}_1^{10}\, \bar{\zeta}_2\, \zeta_2^{2} + (-3.098564985943377 \times 10^{22} + 2.055609158507643 \times 10^{22}\, i)\, \zeta_1^{11}\, \bar{\zeta}_1^{11}\, \zeta_2$

- $U_2{}^{(25)} = -(1.475587344070701 \times 10^{35} + 1.913803330465082 \times 10^{36}\, i)\, \bar{\zeta}_2^{12}\, \zeta_2^{13} + (1.551597318177752 \times 10^{35} +$

$1.752838427804375 \times 10^{37}\, i)\, \zeta_1\, \bar{\zeta}_1\, \bar{\zeta}_2^{11}\, \zeta_2^{12} + (9.83878651545924 \times 10^{34} - 3.584293369597244 \times 10^{37}\, i)\, \zeta_1^2\, \bar{\zeta}_1^2\, \bar{\zeta}_2^{10}\, \zeta_2^{11} -$

$(3.252832912067241 \times 10^{35} - 3.19591124542068 \times 10^{37}\, i)\, \zeta_1^3\, \bar{\zeta}_1^3\, \bar{\zeta}_2^{9}\, \zeta_2^{10} + (1.944897151916166 \times 10^{35} - 1.297199128081203 \times 10^{37}\, i)$

$\zeta_1^4\, \bar{\zeta}_1^4\, \bar{\zeta}_2^{8}\, \zeta_2^{9} - (4.059301632344629 \times 10^{34} - 2.232199494102451 \times 10^{36}\, i)\, \zeta_1^5\, \bar{\zeta}_1^5\, \bar{\zeta}_2^{7}\, \zeta_2^{8} + (2.124720302307463 \times 10^{33} -$

$1.09978462430008 \times 10^{35}\, i)\, \zeta_1^6\, \bar{\zeta}_1^6\, \bar{\zeta}_2^{6}\, \zeta_2^{7} + (1.130286394303603 \times 10^{32} - 4.549463427802757 \times 10^{33}\, i)\, \zeta_1^7\, \bar{\zeta}_1^7\, \bar{\zeta}_2^{5}\, \zeta_2^{6} -$

$(6.903526555889309 \times 10^{30} - 3.037598149043002 \times 10^{32}\, i)\, \zeta_1^8\, \bar{\zeta}_1^8\, \bar{\zeta}_2^{4}\, \zeta_2^{5} + (3.021989938216538 \times 10^{28} - 1.752816490896053 \times 10^{30}\, i)$

$\zeta_1^9\, \bar{\zeta}_1^9\, \bar{\zeta}_2^{3}\, \zeta_2^{4} - (3.429372845870374 \times 10^{25} + 2.02352050949818 \times 10^{27}\, i)\, \zeta_1^{10}\, \bar{\zeta}_1^{10}\, \bar{\zeta}_2^{2}\, \zeta_2^{3} - (8.712300872967838 \times 10^{24} -$

$8.994915784576296 \times 10^{24}\, i)\, \zeta_1^{11}\, \bar{\zeta}_1^{11}\, \bar{\zeta}_2\, \zeta_2^{2} + (-3.319500389476047 \times 10^{24} - 5.351976663551477 \times 10^{24}\, i)\, \zeta_1^{12}\, \bar{\zeta}_1^{12}\, \zeta_2$

II.IV. Remainder function

💡 Chapter 7, Section 7.2.

The norm of the remainder series of the mapping of radii (8;7) in the Sun-Jupiter case (22;7) for odd orders ($r = 3 - 25$) (even orders are of same order of magnitude). The dependency on the direction can be reconstructed according to

$$\rho_1 = \zeta_1 \, \overline{\zeta}_1 = \rho \cos(\gamma),$$

$$\rho_2 = \zeta_2 \, \overline{\zeta}_2 = \rho \sin(\gamma)$$

■ II.IV.1. $\| \mathcal{R}_1^{(r,s)} \|_\gamma$

◆ $\| \mathcal{R}_1^{(3,3)} \| = 6.067544969256355 \, \rho_1^3 + 0.2031526280791481 \, \rho_2 \, \rho_1^2 + 0.7930924125165566 \, \rho_2^2 \, \rho_1$

◆ $\| \mathcal{R}_1^{(5,5)} \| = 660.9854974610917 \, \rho_1^5 +$
$893.3345431999121 \, \rho_2 \, \rho_1^4 + 827.5668435116168 \, \rho_2^2 \, \rho_1^3 + 47.45166640448245 \, \rho_2^3 \, \rho_1^2 + 128.8602207908305 \, \rho_2^4 \, \rho_1$

◆ $\| \mathcal{R}_1^{(7,7)} \| = 59937.62496058284 \, \rho_1^7 + 219176.3061002613 \, \rho_2 \, \rho_1^6 + 205718.208962497$
$\rho_2^2 \, \rho_1^5 + 162078.6936470148 \, \rho_2^3 \, \rho_1^4 + 105479.8353469851 \, \rho_2^4 \, \rho_1^3 + 23935.83105309282 \, \rho_2^5 \, \rho_1^2 + 72328.55998600285 \, \rho_2^6 \, \rho_1$

◆ $\| \mathcal{R}_1^{(9,9)} \| = 6.813393944426284 \times 10^6 \, \rho_1^9 + 3.439030598225285 \times 10^7$
$\rho_2 \, \rho_1^8 + 4.863406849262812 \times 10^7 \, \rho_2^2 \, \rho_1^7 + 4.697004084841646 \times 10^7 \, \rho_2^3 \, \rho_1^6 + 3.202523964808095 \times 10^7 \, \rho_2^4 \, \rho_1^5 +$
$2.716194097583456 \times 10^7 \, \rho_2^5 \, \rho_1^4 + 3.424094431472737 \times 10^7 \, \rho_2^6 \, \rho_1^3 + 1.968437075455995 \times 10^7 \, \rho_2^7 \, \rho_1^2 + 4.595190819806927 \times 10^7 \, \rho_2^8 \, \rho_1$

◆ $\| \mathcal{R}_1^{(11,11)} \| =$
$7.78350794220159 \times 10^8 \, \rho_1^{11} + 4.885591034497581 \times 10^9 \, \rho_2 \, \rho_1^{10} + 9.495615508595951 \times 10^9 \, \rho_2^2 \, \rho_1^9 + 1.105417920048005 \times 10^{10} \, \rho_2^3 \, \rho_1^8 +$
$1.075027398820192 \times 10^{10} \, \rho_2^4 \, \rho_1^7 + 9.495342825427193 \times 10^9 \, \rho_2^5 \, \rho_1^6 + 9.783075817440138 \times 10^9 \, \rho_2^6 \, \rho_1^5 + 1.250217881925651 \times 10^{10}$
$\rho_2^7 \, \rho_1^4 + 2.298157084285596 \times 10^{10} \, \rho_2^8 \, \rho_1^3 + 1.645456364196362 \times 10^{10} \, \rho_2^9 \, \rho_1^2 + 3.116749174898388 \times 10^{10} \, \rho_2^{10} \, \rho_1$

◆ $\| \mathcal{R}_1^{(13,13)} \| = 1.249583919044931 \times 10^{11} \, \rho_1^{13} + 7.35454392960342 \times 10^{11} \, \rho_2 \, \rho_1^{12} + 1.749765090679242 \times 10^{12}$
$\rho_2^2 \, \rho_1^{11} + 2.284811732696258 \times 10^{12} \, \rho_2^3 \, \rho_1^{10} + 2.746050700802838 \times 10^{12} \, \rho_2^4 \, \rho_1^9 + 2.42397141128426 \times 10^{12} \, \rho_2^5 \, \rho_1^8 +$
$2.53825128785677 \times 10^{12} \, \rho_2^6 \, \rho_1^7 + 3.702473613297327 \times 10^{12} \, \rho_2^7 \, \rho_1^6 + 6.527059783234685 \times 10^{12} \, \rho_2^8 \, \rho_1^5 + 1.016830722277507 \times 10^{13}$
$\rho_2^9 \, \rho_1^4 + 1.805128747413071 \times 10^{13} \, \rho_2^{10} \, \rho_1^3 + 1.389540634614125 \times 10^{13} \, \rho_2^{11} \, \rho_1^2 + 2.203477051209622 \times 10^{13} \, \rho_2^{12} \, \rho_1$

◆ $\| \mathcal{R}_1^{(15,15)} \| = 1.192874526327742 \times 10^{14} \, \rho_1^{15} +$
$2.580708584663976 \times 10^{14} \, \rho_2 \, \rho_1^{14} + 4.256274005779924 \times 10^{14} \, \rho_2^2 \, \rho_1^{13} + 4.98047377315536 \times 10^{14} \, \rho_2^3 \, \rho_1^{12} + 6.306672974478102 \times 10^{14}$
$\rho_2^4 \, \rho_1^{11} + 6.257195773068062 \times 10^{14} \, \rho_2^5 \, \rho_1^{10} + 6.403051706293906 \times 10^{14} \, \rho_2^6 \, \rho_1^9 + 7.73526994219681 \times 10^{14} \, \rho_2^7 \, \rho_1^8 +$
$1.48558130626056 \times 10^{15} \, \rho_2^8 \, \rho_1^7 + 3.049582218762737 \times 10^{15} \, \rho_2^9 \, \rho_1^6 + 5.764830237353008 \times 10^{15} \, \rho_2^{10} \, \rho_1^5 + 9.40891948947894 \times 10^{15}$
$\rho_2^{11} \, \rho_1^4 + 1.481023516584818 \times 10^{16} \, \rho_2^{12} \, \rho_1^3 + 1.186342088734544 \times 10^{16} \, \rho_2^{13} \, \rho_1^2 + 1.604031297776095 \times 10^{16} \, \rho_2^{14} \, \rho_1$

◆ $\| \mathcal{R}_1^{(17,17)} \| = 1.405803838611058 \times 10^{17} \, \rho_1^{17} + 2.366343239743881 \times 10^{17} \, \rho_2 \, \rho_1^{16} + 3.455389868599391 \times 10^{17} \, \rho_2^2 \, \rho_1^{15} +$
$2.152182348591765 \times 10^{17} \, \rho_2^3 \, \rho_1^{14} + 2.788176219357597 \times 10^{17} \, \rho_2^4 \, \rho_1^{13} + 1.904789246642115 \times 10^{17} \, \rho_2^5 \, \rho_1^{12} + 8.849649255677335 \times 10^{17}$
$\rho_2^6 \, \rho_1^{11} + 9.926119861769206 \times 10^{17} \, \rho_2^7 \, \rho_1^{10} + 1.609960261515904 \times 10^{19} \, \rho_2^8 \, \rho_1^9 + 2.308440789959799 \times 10^{19} \, \rho_2^9 \, \rho_1^8 +$
$3.21556696917892 \times 10^{20} \, \rho_2^{10} \, \rho_1^7 + 4.800977394871314 \times 10^{20} \, \rho_2^{11} \, \rho_1^6 + 5.639142533467146 \times 10^{21} \, \rho_2^{12} \, \rho_1^5 + 9.972285816742162 \times 10^{21}$
$\rho_2^{13} \, \rho_1^4 + 7.048876005552761 \times 10^{22} \, \rho_2^{14} \, \rho_1^3 + 1.138294862168551 \times 10^{23} \, \rho_2^{15} \, \rho_1^2 + 4.342006015334529 \times 10^{23} \, \rho_2^{16} \, \rho_1$

◆ $\| \mathfrak{R}_1^{(19,19)} \| = 1.37662197915433 \times 10^{20} \, \rho_1^{19} + 2.637721772867691 \times 10^{20}$
$\rho_2 \, \rho_1^{18} + 4.537161922612415 \times 10^{20} \, \rho_2^2 \, \rho_1^{17} + 2.62328006126058 \times 10^{20} \, \rho_2^3 \, \rho_1^{16} + 3.835749211635842 \times 10^{20} \, \rho_2^4 \, \rho_1^{15} +$
$2.205151233376422 \times 10^{20} \, \rho_2^5 \, \rho_1^{14} + 5.51408901031919 \times 10^{20} \, \rho_2^6 \, \rho_1^{13} + 2.178305149925885 \times 10^{21} \, \rho_2^7 \, \rho_1^{12} + 2.167887298021244 \times 10^{22}$
$\rho_2^8 \, \rho_1^{11} + 8.317996471707014 \times 10^{22} \, \rho_2^9 \, \rho_1^{10} + 9.078376689579527 \times 10^{23} \, \rho_2^{10} \, \rho_1^9 + 2.199904563910685 \times 10^{24} \, \rho_2^{11} \, \rho_1^8 +$
$2.849044463158056 \times 10^{25} \, \rho_2^{12} \, \rho_1^7 + 4.072067550513621 \times 10^{25} \, \rho_2^{13} \, \rho_1^6 + 2.896881437533926 \times 10^{26} \, \rho_2^{14} \, \rho_1^5 + 3.386208384378846 \times 10^{26}$
$\rho_2^{15} \, \rho_1^4 + 5.16977095767574 \times 10^{27} \, \rho_2^{16} \, \rho_1^3 + 1.227553701709335 \times 10^{27} \, \rho_2^{17} \, \rho_1^2 + 2.953719970420448 \times 10^{27} \, \rho_2^{18} \, \rho_1$

◆ $\| \mathfrak{R}_1^{(21,21)} \| =$
$1.291437747313399 \times 10^{23} \, \rho_1^{21} + 2.77729443633699 \times 10^{23} \, \rho_2 \, \rho_1^{20} + 6.170595343492383 \times 10^{23} \, \rho_2^2 \, \rho_1^{19} + 4.481061731179697 \times 10^{23}$
$\rho_2^3 \, \rho_1^{18} + 1.107268717036203 \times 10^{24} \, \rho_2^4 \, \rho_1^{17} + 9.043614317201981 \times 10^{24} \, \rho_2^5 \, \rho_1^{16} + 3.610203523953384 \times 10^{24} \, \rho_2^6 \, \rho_1^{15} +$
$2.32153757972757 \times 10^{24} \, \rho_2^7 \, \rho_1^{14} + 8.36070577037354 \times 10^{24} \, \rho_2^8 \, \rho_1^{13} + 3.487954721325087 \times 10^{25} \, \rho_2^9 \, \rho_1^{12} + 3.299902001320863 \times 10^{26}$
$\rho_2^{10} \, \rho_1^{11} + 1.4855639699394 \times 10^{27} \, \rho_2^{11} \, \rho_1^{10} + 4.485470045981244 \times 10^{28} \, \rho_2^{12} \, \rho_1^9 + 8.364265502070442 \times 10^{28} \, \rho_2^{13} \, \rho_1^8 +$
$6.340416697494951 \times 10^{29} \, \rho_2^{14} \, \rho_1^7 + 6.875810357687016 \times 10^{29} \, \rho_2^{15} \, \rho_1^6 + 1.028729944279687 \times 10^{31} \, \rho_2^{16} \, \rho_1^5 + 5.107605093653178 \times 10^{30}$
$\rho_2^{17} \, \rho_1^4 + 2.427340264758347 \times 10^{31} \, \rho_2^{18} \, \rho_1^3 + 2.968489637104511 \times 10^{30} \, \rho_2^{19} \, \rho_1^2 + 6.281995911055177 \times 10^{30} \, \rho_2^{20} \, \rho_1$

◆ $\| \mathfrak{R}_1^{(23,23)} \| = 1.193744825074662 \times 10^{26} \, \rho_1^{23} + 2.981323765572293 \times 10^{26} \, \rho_2 \, \rho_1^{22} + 9.046637683829687 \times 10^{26}$
$\rho_2^2 \, \rho_1^{21} + 8.76050672789297 \times 10^{26} \, \rho_2^3 \, \rho_1^{20} + 5.106684679181833 \times 10^{28} \, \rho_2^4 \, \rho_1^{19} + 7.83356914839294 \times 10^{29} \, \rho_2^5 \, \rho_1^{18} +$
$3.213491334812885 \times 10^{29} \, \rho_2^6 \, \rho_1^{17} + 2.35128748905594 \times 10^{29} \, \rho_2^7 \, \rho_1^{16} + 8.214735562530348 \times 10^{28} \, \rho_2^8 \, \rho_1^{15} + 6.699555200362312 \times 10^{28}$
$\rho_2^9 \, \rho_1^{14} + 1.119630566642137 \times 10^{30} \, \rho_2^{10} \, \rho_1^{13} + 3.798735394089479 \times 10^{30} \, \rho_2^{11} \, \rho_1^{12} + 3.292983221487054 \times 10^{31}$
$\rho_2^{12} \, \rho_1^{11} + 8.201681368259995 \times 10^{31} \, \rho_2^{13} \, \rho_1^{10} + 7.02975509197347 \times 10^{32} \, \rho_2^{14} \, \rho_1^9 + 9.7253341143492 \times 10^{32} \, \rho_2^{15} \, \rho_1^8 +$
$9.647460244822484 \times 10^{33} \, \rho_2^{16} \, \rho_1^7 + 8.072609433645651 \times 10^{33} \, \rho_2^{17} \, \rho_1^6 + 3.076011762955811 \times 10^{34} \, \rho_2^{18} \, \rho_1^5 + 1.263325683112151 \times 10^{34}$
$\rho_2^{19} \, \rho_1^4 + 2.672915578988992 \times 10^{34} \, \rho_2^{20} \, \rho_1^3 + 2.401339824817205 \times 10^{33} \, \rho_2^{21} \, \rho_1^2 + 6.074535233443848 \times 10^{33} \, \rho_2^{22} \, \rho_1$

◆ $\| \mathfrak{R}_1^{(25,25)} \| = 1.09201894839391 \times 10^{29} \, \rho_1^{25} + 3.269246255284195 \times 10^{29}$
$\rho_2 \, \rho_1^{24} + 1.356337294759432 \times 10^{30} \, \rho_2^2 \, \rho_1^{23} + 1.818821261708849 \times 10^{30} \, \rho_2^3 \, \rho_1^{22} + 4.056394172010488 \times 10^{33} \, \rho_2^4 \, \rho_1^{21} +$
$7.03063072994163 \times 10^{34} \, \rho_2^5 \, \rho_1^{20} + 3.010303387993029 \times 10^{34} \, \rho_2^6 \, \rho_1^{19} + 2.855405535429123 \times 10^{34} \, \rho_2^7 \, \rho_1^{18} + 1.025860233151016 \times 10^{34}$
$\rho_2^8 \, \rho_1^{17} + 4.393288462963795 \times 10^{33} \, \rho_2^9 \, \rho_1^{16} + 2.191115294435907 \times 10^{33} \, \rho_2^{10} \, \rho_1^{15} + 4.327558332526302 \times 10^{33}$
$\rho_2^{11} \, \rho_1^{14} + 1.455461479174372 \times 10^{34} \, \rho_2^{12} \, \rho_1^{13} + 4.569935528026919 \times 10^{34} \, \rho_2^{13} \, \rho_1^{12} + 4.963663678345839 \times 10^{35}$
$\rho_2^{14} \, \rho_1^{11} + 8.54329926207975 \times 10^{35} \, \rho_2^{15} \, \rho_1^{10} + 5.848812387375207 \times 10^{36} \, \rho_2^{16} \, \rho_1^9 + 6.891758420248563 \times 10^{36} \, \rho_2^{17} \, \rho_1^8 +$
$2.046041227695089 \times 10^{37} \, \rho_2^{18} \, \rho_1^7 + 1.498451949283383 \times 10^{37} \, \rho_2^{19} \, \rho_1^6 + 2.589694108887235 \times 10^{37} \, \rho_2^{20} \, \rho_1^5 + 9.365254207329485 \times 10^{36}$
$\rho_2^{21} \, \rho_1^4 + 1.214977712871328 \times 10^{37} \, \rho_2^{22} \, \rho_1^3 + 1.185311764442144 \times 10^{36} \, \rho_2^{23} \, \rho_1^2 + 4.663574434036739 \times 10^{36} \, \rho_2^{24} \, \rho_1$

■ II.IV.2. $\| \mathfrak{R}_2^{(r,s)} \|_\gamma$

◆ $\| \mathfrak{R}_2^{(3,3)} \| = 1.163946894776521 \, \rho_2^3 + 0.5876231127842281 \, \rho_1 \, \rho_2^2 + 0.2027349765301897 \, \rho_1^2 \, \rho_2$

◆ $\| \mathfrak{R}_2^{(5,5)} \| = 966.8901562605935 \, \rho_2^5 +$
$1000.84944994661 \, \rho_1 \, \rho_2^4 + 410.8653547622711 \, \rho_1^2 \, \rho_2^3 + 157.1191055814907 \, \rho_1^3 \, \rho_2^2 + 55.84592784858629 \, \rho_1^4 \, \rho_2$

◆ $\| \mathfrak{R}_2^{(7,7)} \| = 805686.2648389341 \, \rho_2^7 + 816031.0990634556 \, \rho_1 \, \rho_2^6 + 429356.5864886108$
$\rho_1^2 \, \rho_2^5 + 287234.6702970397 \, \rho_1^3 \, \rho_2^4 + 77574.0686106625 \, \rho_1^4 \, \rho_2^3 + 26808.3522688543 \, \rho_1^5 \, \rho_2^2 + 5840.346848935354 \, \rho_1^6 \, \rho_2$

◆ $\| \mathfrak{R}_2^{(9,9)} \| = 6.711717249365206 \times 10^8 \, \rho_2^9 + 6.738564348702282 \times 10^8$
$\rho_1 \, \rho_2^8 + 4.212016136415594 \times 10^8 \, \rho_1^2 \, \rho_2^7 + 2.958899773737204 \times 10^8 \, \rho_1^3 \, \rho_2^6 + 8.668857065804628 \times 10^7 \, \rho_1^4 \, \rho_2^5 +$
$3.639596242854349 \times 10^7 \, \rho_1^5 \, \rho_2^4 + 1.068305878791899 \times 10^7 \, \rho_1^6 \, \rho_2^3 + 3.934421284696603 \times 10^6 \, \rho_1^7 \, \rho_2^2 + 882319.9661965335 \, \rho_1^8 \, \rho_2$

◆ $\| \mathfrak{R}_2^{(11,11)} \| =$
$5.592873239182805 \times 10^{11} \, \rho_2^{11} + 5.575578226422363 \times 10^{11} \, \rho_1 \, \rho_2^{10} + 4.042055338880091 \times 10^{11} \, \rho_1^2 \, \rho_2^9 + 2.988100232169888 \times 10^{11}$
$\rho_1^3 \, \rho_2^8 + 9.37660781373795 \times 10^{10} \, \rho_1^4 \, \rho_2^7 + 4.120621662441386 \times 10^{10} \, \rho_1^5 \, \rho_2^6 + 1.364533779201369 \times 10^{10} \, \rho_1^6 \, \rho_2^5 +$
$5.909508195571081 \times 10^9 \, \rho_1^7 \, \rho_2^4 + 1.617511206668383 \times 10^9 \, \rho_1^8 \, \rho_2^3 + 5.449467003541929 \times 10^8 \, \rho_1^9 \, \rho_2^2 + 9.976363364225641 \times 10^7 \, \rho_1^{10} \, \rho_2$

◆ $\| \mathfrak{R}_2^{(13,13)} \| = 4.661064162058988 \times 10^{14}\, \rho_2^{13} + 4.616864248322368 \times 10^{14}\, \rho_1\, \rho_2^{12} + 3.830807903191426 \times 10^{14}$
$\rho_1^2\, \rho_2^{11} + 2.931138546348709 \times 10^{14}\, \rho_1^3\, \rho_2^{10} + 1.03367418533115 \times 10^{14}\, \rho_1^4\, \rho_2^9 + 4.978088698839289 \times 10^{13}\, \rho_1^5\, \rho_2^8 +$
$1.683120424827433 \times 10^{13}\, \rho_1^6\, \rho_2^7 + 7.296677755031196 \times 10^{12}\, \rho_1^7\, \rho_2^6 + 2.19209277800467 \times 10^{12}\, \rho_1^8\, \rho_2^5 + 7.74673437380145 \times 10^{11}$
$\rho_1^9\, \rho_2^4 + 2.461337591623659 \times 10^{11}\, \rho_1^{10}\, \rho_2^3 + 8.297051605500658 \times 10^{10}\, \rho_1^{11}\, \rho_2^2 + 1.230692582678724 \times 10^{10}\, \rho_1^{12}\, \rho_2$

◆ $\| \mathfrak{R}_2^{(15,15)} \| = 3.884932341675807 \times 10^{17}\, \rho_2^{15} +$
$3.826360182859123 \times 10^{17}\, \rho_1\, \rho_2^{14} + 3.595785741851012 \times 10^{17}\, \rho_1^2\, \rho_2^{13} + 2.813399848049671 \times 10^{17}\, \rho_1^3\, \rho_2^{12} + 1.120903362952521 \times 10^{17}$
$\rho_1^4\, \rho_2^{11} + 5.889765373361141 \times 10^{16}\, \rho_1^5\, \rho_2^{10} + 2.06082590374634 \times 10^{16}\, \rho_1^6\, \rho_2^9 + 8.619686189784648 \times 10^{15}\, \rho_1^7\, \rho_2^8 +$
$2.839945425227416 \times 10^{15}\, \rho_1^8\, \rho_2^7 + 1.146721450877686 \times 10^{15}\, \rho_1^9\, \rho_2^6 + 3.344218713137113 \times 10^{14}\, \rho_1^{10}\, \rho_2^5 + 1.289599923393471 \times 10^{14}$
$\rho_1^{11}\, \rho_2^4 + 3.755518897296949 \times 10^{13}\, \rho_1^{12}\, \rho_2^3 + 2.005143849652294 \times 10^{13}\, \rho_1^{13}\, \rho_2^2 + 6.781787846640516 \times 10^{12}\, \rho_1^{14}\, \rho_2$

◆ $\| \mathfrak{R}_2^{(17,17)} \| = 1.855780281825191 \times 10^{24}\, \rho_2^{17} + 1.437132703073301 \times 10^{24}\, \rho_1\, \rho_2^{16} + 2.133066417306583 \times 10^{23}\, \rho_1^2\, \rho_2^{15} +$
$8.408716064030813 \times 10^{22}\, \rho_1^3\, \rho_2^{14} + 2.821541704492799 \times 10^{22}\, \rho_1^4\, \rho_2^{13} + 5.169084343423263 \times 10^{21}\, \rho_1^5\, \rho_2^{12} + 1.207033890084717 \times 10^{21}$
$\rho_1^6\, \rho_2^{11} + 2.011964852418651 \times 10^{20}\, \rho_1^7\, \rho_2^{10} + 4.012756259749229 \times 10^{19}\, \rho_1^8\, \rho_2^9 + 5.910615196806119 \times 10^{18}\, \rho_1^9\, \rho_2^8 +$
$1.087523152366079 \times 10^{18}\, \rho_1^{10}\, \rho_2^7 + 2.3085815633282 \times 10^{17}\, \rho_1^{11}\, \rho_2^6 + 5.297411911498192 \times 10^{16}\, \rho_1^{12}\, \rho_2^5 + 4.674051074016941 \times 10^{16}$
$\rho_1^{13}\, \rho_2^4 + 3.43232373187483 \times 10^{16}\, \rho_1^{14}\, \rho_2^3 + 1.628137191843413 \times 10^{16}\, \rho_1^{15}\, \rho_2^2 + 1.003259881607825 \times 10^{16}\, \rho_1^{16}\, \rho_2$

◆ $\| \mathfrak{R}_2^{(19,19)} \| = 7.232339444125665 \times 10^{27}\, \rho_2^{19} + 9.547135566492241 \times 10^{27}$
$\rho_1\, \rho_2^{18} + 4.826558198548479 \times 10^{27}\, \rho_1^2\, \rho_2^{17} + 3.13402840364809 \times 10^{27}\, \rho_1^3\, \rho_2^{16} + 4.304352049551814 \times 10^{26}\, \rho_1^4\, \rho_2^{15} +$
$2.128218790992451 \times 10^{26}\, \rho_1^5\, \rho_2^{14} + 5.04915842967402 \times 10^{25}\, \rho_1^6\, \rho_2^{13} + 5.12681062134098 \times 10^{24}\, \rho_1^7\, \rho_2^{12} + 7.941614684076075 \times 10^{23}$
$\rho_1^8\, \rho_2^{11} + 1.491781343064699 \times 10^{23}\, \rho_1^9\, \rho_2^{10} + 1.790294187690415 \times 10^{22}\, \rho_1^{10}\, \rho_2^9 + 2.657753940591617 \times 10^{21}\, \rho_1^{11}\, \rho_2^8 +$
$3.285860500439996 \times 10^{20}\, \rho_1^{12}\, \rho_2^7 + 1.034468231854947 \times 10^{20}\, \rho_1^{13}\, \rho_2^6 + 7.495057579466818 \times 10^{19}\, \rho_1^{14}\, \rho_2^5 + 5.198632103750061 \times 10^{19}$
$\rho_1^{15}\, \rho_2^4 + 5.2035123836294 \times 10^{19}\, \rho_1^{16}\, \rho_2^3 + 1.562137077328767 \times 10^{19}\, \rho_1^{17}\, \rho_2^2 + 1.047137678593161 \times 10^{19}\, \rho_1^{18}\, \rho_2$

◆ $\| \mathfrak{R}_2^{(21,21)} \| =$
$2.68652624563653 \times 10^{31}\, \rho_2^{21} + 1.936185097025911 \times 10^{31}\, \rho_1\, \rho_2^{20} + 1.688722179296134 \times 10^{31}\, \rho_1^2\, \rho_2^{19} + 1.271661250804644 \times 10^{31}$
$\rho_1^3\, \rho_2^{18} + 5.347287015883034 \times 10^{30}\, \rho_1^4\, \rho_2^{17} + 2.879739631316473 \times 10^{30}\, \rho_1^5\, \rho_2^{16} + 4.389881232247301 \times 10^{29}\, \rho_1^6\, \rho_2^{15} +$
$2.191491310323724 \times 10^{29}\, \rho_1^7\, \rho_2^{14} + 3.952217950361371 \times 10^{28}\, \rho_1^8\, \rho_2^{13} + 5.529857170536881 \times 10^{27}\, \rho_1^9\, \rho_2^{12} + 1.329450522831822 \times 10^{27}$
$\rho_1^{10}\, \rho_2^{11} + 1.231502627323516 \times 10^{26}\, \rho_1^{11}\, \rho_2^{10} + 1.331264112355659 \times 10^{25}\, \rho_1^{12}\, \rho_2^9 + 2.732944705296066 \times 10^{24}\, \rho_1^{13}\, \rho_2^8 +$
$2.015710891420806 \times 10^{24}\, \rho_1^{14}\, \rho_2^7 + 8.2877486922267 \times 10^{23}\, \rho_1^{15}\, \rho_2^6 + 1.874324138763366 \times 10^{24}\, \rho_1^{16}\, \rho_2^5 + 7.309533080703934 \times 10^{22}$
$\rho_1^{17}\, \rho_2^4 + 8.103990315261074 \times 10^{22}\, \rho_1^{18}\, \rho_2^3 + 1.521686104780058 \times 10^{22}\, \rho_1^{19}\, \rho_2^2 + 1.090708855285213 \times 10^{22}\, \rho_1^{20}\, \rho_2$

◆ $\| \mathfrak{R}_2^{(23,23)} \| = 3.096483411043619 \times 10^{34}\, \rho_2^{23} + 2.039594895792996 \times 10^{34}\, \rho_1\, \rho_2^{22} + 3.455322153418525 \times 10^{34}$
$\rho_1^2\, \rho_2^{21} + 1.882294218269946 \times 10^{34}\, \rho_1^3\, \rho_2^{20} + 1.611618675768198 \times 10^{34}\, \rho_1^4\, \rho_2^{19} + 8.811454023765305 \times 10^{33}\, \rho_1^5\, \rho_2^{18} +$
$3.528774663278542 \times 10^{33}\, \rho_1^6\, \rho_2^{17} + 1.674862971687115 \times 10^{33}\, \rho_1^7\, \rho_2^{16} + 3.267592183854049 \times 10^{32}\, \rho_1^8\, \rho_2^{15} + 1.309987137309758 \times 10^{32}$
$\rho_1^9\, \rho_2^{14} + 1.96275062675114 \times 10^{31}\, \rho_1^{10}\, \rho_2^{13} + 4.134713294809157 \times 10^{30}\, \rho_1^{11}\, \rho_2^{12} + 1.147330700772292 \times 10^{30}$
$\rho_1^{12}\, \rho_2^{11} + 1.003750643033879 \times 10^{29}\, \rho_1^{13}\, \rho_2^{10} + 5.218291354035019 \times 10^{28}\, \rho_1^{14}\, \rho_2^9 + 9.028677379013372 \times 10^{28}\, \rho_1^{15}\, \rho_2^8 +$
$1.692963277121078 \times 10^{29}\, \rho_1^{16}\, \rho_2^7 + 6.412757292823847 \times 10^{28}\, \rho_1^{17}\, \rho_2^6 + 1.500441949562256 \times 10^{29}\, \rho_1^{18}\, \rho_2^5 + 1.4663683041741 \times 10^{26}$
$\rho_1^{19}\, \rho_2^4 + 1.346958302094532 \times 10^{26}\, \rho_1^{20}\, \rho_2^3 + 1.581817063249453 \times 10^{25}\, \rho_1^{21}\, \rho_2^2 + 1.121871665156261 \times 10^{25}\, \rho_1^{22}\, \rho_2$

◆ $\| \mathfrak{R}_2^{(25,25)} \| = 3.066385461029748 \times 10^{37}\, \rho_2^{25} +$
$2.990596972417421 \times 10^{37}\, \rho_1\, \rho_2^{24} + 3.383771987343658 \times 10^{37}\, \rho_1^2\, \rho_2^{23} + 1.995958210079233 \times 10^{37}\, \rho_1^3\, \rho_2^{22} + 1.976125875373333 \times 10^{37}$
$\rho_1^4\, \rho_2^{21} + 1.011171904039853 \times 10^{37}\, \rho_1^5\, \rho_2^{20} + 8.72234847645974 \times 10^{36}\, \rho_1^6\, \rho_2^{19} + 4.137114768481591 \times 10^{36}\, \rho_1^7\, \rho_2^{18} +$
$1.81814214181587 \times 10^{36}\, \rho_1^8\, \rho_2^{17} + 7.313467701236144 \times 10^{35}\, \rho_1^9\, \rho_2^{16} + 1.762756752607539 \times 10^{35}\, \rho_1^{10}\, \rho_2^{15} + 5.823730240792398 \times 10^{34}$
$\rho_1^{11}\, \rho_2^{14} + 7.553509534135575 \times 10^{33}\, \rho_1^{12}\, \rho_2^{13} + 2.836886134855179 \times 10^{33}\, \rho_1^{13}\, \rho_2^{12} + 1.415808735972305 \times 10^{33}$
$\rho_1^{14}\, \rho_2^{11} + 2.835091538088612 \times 10^{33}\, \rho_1^{15}\, \rho_2^{10} + 5.914460093738904 \times 10^{33}\, \rho_1^{16}\, \rho_2^9 + 8.598212286000661 \times 10^{33}\, \rho_1^{17}\, \rho_2^8 +$
$1.594574396345958 \times 10^{34}\, \rho_1^{18}\, \rho_2^7 + 5.479638049930263 \times 10^{33}\, \rho_1^{19}\, \rho_2^6 + 1.25607472697997 \times 10^{34}\, \rho_1^{20}\, \rho_2^5 + 4.986389099849952 \times 10^{29}$
$\rho_1^{21}\, \rho_2^4 + 2.368203742378497 \times 10^{29}\, \rho_1^{22}\, \rho_2^3 + 1.765795757739843 \times 10^{28}\, \rho_1^{23}\, \rho_2^2 + 1.150204899930511 \times 10^{28}\, \rho_1^{24}\, \rho_2$

Email: lhotka@astro.univie.ac.at

Lhotka Christoph Heinrich

Born in Vienna on November 23rd, 1978 as son of Bernhard and Magdalena Lhotka

Personal Information:

Title:	Magister reris naturalis (Mag.rer.nat.)
Citizenship:	Austria
Marital status:	Unmarried

Schooling:

1985 – 1988	Elementary school in Greifenburg, Kärnten.
1989 – 1998	Secondary school / High school (AHS), Spittal a.d. Drau.
1994 – 1996	Head boy / President of student´s Council, member of the SGA (democratic institution in Austrian´s school system).
06 / 1998	General qualification for university entrance (AHS Spittal a.d. Drau).

University, Schools (s), Workshops (w), Conferences (c):

10 / 1999	Beginning of studies in Astronomy at the University of Vienna.
09 / 2002	Beginning of studies in Mathematics at the University of Vienna.
03 / 2004 c w	*"6th Alexander von Humboldt Colloquium"*, Bad Hofgastein, Austria, 21.-27., [LOC, Talk].
07 / 2004 c s w	*„Complexity in Science and Society",* Center for Research and Applications of Nonlinear Systems, Patras, Greece, 14.-26., [Poster].
12 / 2004	Final degree in Astronomy – Magister reris naturalis with excellent degree [Thesis].
06 / 2005 w	*"IV. Austrian - Hungarian workshop on Celestial Mechanics",* Eötovös University, Budapest, Hungary 23.-25., [Talk].
09 / 2006 c	*"The Future of Mathematica"*, Uni Zürich, Wolfram Research, Zürich, Switzerland, 06.
09 / 2006 c w	*"Asteroids and Resonances – Open Problems and Perspectives"*, Centre Internationale d´Ateleiers Scientifiques, Observatoire de Paris, Château de Meudon, France, 25.-28., [Talk].
03 / 2007 c	*"A New Era of Mathematica Technology",* University of Vienna, Vienna, Austria, 08.
03 / 2007 s	*"Winter school on Celestial Mechanics"*, Centre National de la Recherche Scientifique (CNRS), Bad Hofgastein, Austria, 25.-31.
04 / 2007 c	*„Wissenschaftliche Jahrestagung ÖGA"*, Institute for Astronomy, University of Vienna, Austria, 13.-14., [Poster].
05 / 2007 w	*"BRITE Workshop"*, University of Vienna, Austria, 22.-23., [Talk].
06 / 2007 c	*"Dynamical Systems – Theory and Application"*, Spoleto, Italy, 24.-28., [Poster].

07 / 2007 s c	"*20th International Conference / Summerschool – Nonlinear Science and Complexity*", Center for Research and Application of Dynamical Systems, Patras, Greece, 19.-29., [Poster].
09 / 2007 s	"*Advanced School on Specific Algebraic Manipulators*", Institut de Mathemàtica, Barcelona, Spain., 3.-7.
12 / 2007 c	"*6th Christmas Symposium on Physics and Nonlinear Dynamics*", Center for Applied Mathematics and Theoretical Physics, Maribor, Slovenia, 13.-15., [Talk].
01 / 2008 w	"*Minutes CEST meeting*" – CNES, ESA, Berlin, Germany, 24.-25.
03 / 2008 c	"*7th Alexander von Humboldt Colloquium*", ADG, University of Vienna, Bad Hofgastein, Austria, 30.3.-5.4. [LOC, Talk].
07 / 2008 c	"*Let´s face Chaos through non linear dynamics*", Center for Applied Mathematics and Theoretical Physics, Maribor, Slovenia, 1.-7.[Talk].
07 / 2008 c	"*Conference on Applications of Computer Algebra*", RISC Institute for Symbolic Computation, Hagenberg, Austria, 27.-30.[Talk].

Job experience:

1994 – 1997	Job in a kiosk (Spittal a.d. Drau, Austria) (10-12 weeks a year).
1998 – 1999	Social casework in a nursing home, social service in the Franziskusheim, Klagenfurt (fulltime).
06 – 09 / 2002	Trainer in the Familienhotel Post, Millstatt am See, Carinthia, Austria.
07 – 09 / 2003	Trainer in the Familienhotel Post, Millstatt am See (organization of sportive and creative events for children and grown-ups).
08 / 2004 – 06 / 2006	Various Jobs at the Institute of Astronomy at the University of Vienna based on Werkverträge (implementation of algorithms for automized analysis of large data sets, time dependent Fourier analysis, data-reduction, statistical analysis, etc...).
05 - 06 / 2005	Evaluation of innovative concepts during the "Ideenwettbewerb 2005" (contest of innovative ideas) of the "Ministerium für Verkehr, Innovation und Technologie" (ministry for traffic, innovation and technology) - member of the expert team at the Austrian Wirtschafts Service.
08 / 2005 – 06 / 2006	Project management at the Austrian Wirtschafts Service (Intelectual Property Organisation). Commercialization, supervision and support of the winners of the Ideenwettbewerb 2005. Evaluation of inventions based on mathematical / technical innovations (patent strategy or not).
07 / 2007 up to now	Research work, employee at the FWF (Austrian Science Foundation) Project P-18930 "Effektive Stabilität der equilateralen Lagrangepunkte".

Working Stays Abroad:

11, 12 / 2006	Research Center for Astronomy and Applied Mathematics, Academy of Athens in collaboration with Christos Efthymiopoulos (2 weeks).
02, 07, 11, 12 / 2007	Resarch Center for Astronomy and Applied Mathematics, Academy of Athens. (5 weeks)
09-11 / 2008	Department of Mathematics, Shanghai Normal University 200234 PR China, collaboration with Prof. Maoan Han (2 months).

Email: lhotka@astro.univie.ac.at

Courses, Lectures (delivered):

"Celestial Mechanics and Exponential Stability" (series of lectures 8 á 2h) at the Shanghai Normal University

"280146 UE Astronomische Rechenmethoden" (astronomical calculation methods, exercise course 5ECTS), Institute for Astronomy, University of Vienna (2008).

Various seminars and courses (1-4 hours) on Mathematica (introductory and advanced), Vienna (Austria), Athens, Patras (Greece).

Scientific Talks:

"A High Order Perturbation Expansion to the Sitnikov Problem by using Mathematica" - at the 6th Alexander von Humboldt Colloquium in Bad Hofgastein, Austria (03 / 2003).

"An introduction to Mathematica - applications to dynamical astronomy" - at the Institute for Astronomy, Vienna, Austria (SS / 2004).

"How your Mathematica is getting faster and faster without loosing generality or functionality" at the Research Center for Astronomy & Applied Mathematics, Academy of Athens, Greece (03 / 2005).

"Chaos in our Solar System - The fundamental frequencies in the dynamics of our planetary system" at the IV. Austrian - Hungarian Workshop, Budapest, Hungary (06 / 2005).

"Nekhoroshev Estimates of Asteroids in the 1:1 resonance" - at the conference on Asteroids and Resonances in Meudon, France (09 / 2006).

"Automated Derivation Methods in the Sitnikov problem – Lindstedt-Series done with Mathematica" at the Research Center for Astronomy & Applied Mathematics, Academy of Athens, Greece (11, 12 / 2006).

"Nekhoroshev Estimates in the 1:1 Resonance of Our Solar System II: Symplectic Mappings in the case of Jupiter" at the Center of Research and Applications of Nonlinear Systems (CRANS), Patras, Greece (02 / 2007).

"Exponential Stability Estimates in the Elliptic Restricted Three Body Problem" – at the 6th Christmas Symposium in Maribor, Slovenia (12 / 2007).

"On the Expansion of the Generating Function in the Mapping Case. Hadjidemetriou´s method revisited" - at the "7th Alexander von Humboldt Colloquium" in Bad Hofgastein, Austria (03 / 2008).

"Exponential Stability Estimates for Trojan Asteroids – Nekhoroshev Theorem meets Celestial Mechanics" - at the Center for Applied Mathematics and Theoretical Physics in Slovenia, Maribor (07 / 2008).

"Nekhoroshev estimates in a symplectic mapping model of the 1:1 resonance of the elliptic restricted three body problem" - at the "Conference on Applications of Computer Algebra" in Hagenberg, Austria (07 / 2008).

"Exponential Stability Estimates in Hamiltonian Systems. Application to Trojan Asteroids" - at the "Center for Nonlinear Science" in Nanjing, China (10 / 2008).

Scientific Publications:

"Störungsanalyse des Sitnikov Problems für hohe Ordnungen unter Verwendung automatisierter Herleitungsmethoden in Mathematica", (Lhotka C.), master thesis, University of Vienna, (2004).

"A High Order Perturbation Analysis of the Sitnikov Problem", (Hagel J., Lhotka C.) – Celestial Mechanics and Dynamical Astronomy, 93, 1-4, 201-228 (2005).

"A new determination of the fundamental frequencies in our Solar System", (Lhotka C, Dvorak R.), Proceedings of the 4th Austrian Hungarian Workshop on Celestial Mechanics, Publications of the Astronomy Department of the Eötvös University Vol 18. 33-46 (2006).

"The Detection Of Planets In The 1:1 Resonance" (Dvorak R., Schneider J., Schwarz R., Lhotka C., Sandor Z.), European Planetary Science Congress 2006, Berlin, Germany , abstract book, page 716 (2006).

"BRITE Orbits – Visibility and Feature Plots", (Lhotka C., Funk B.), Communications in Astroseismology, 152, 51-54 (2008).

"On the dynamics of Trojan planets in extra solar planetary systems", (Dvorak R., Schwarz R., Lhotka C.), Proceedings of the International Astronomical Union, IAU Symposium 249, 461-468 (2008).

"Nekhoroshev stability at L_4 and L_5 in the elliptic restricted three body problem – application to Trojan asteroids" (Lhotka C., Efthymiopoulos C., Dvorak R.), Monthly Notices of the Royal Astronomical Society, 284, 3, 1165-1177 (2008).

"The dynamics of inclined Neptune Trojans", (Dvorak R., Lhotka C., Schwarz R.), Celestial Mechanics and Dynamical Astronomy, 102, 1-3, 97-110 (2008).

Posters:
"A High Order Perturbation Analysis of the Sitnikov Problem by Using Mathematica" - at the summer school and conference in Patras, Greece (07 / 2003).

"The Stability of few Body Systems (The Sitnikov Problem, Our Solar System, Extra solar Systems)", (Funk, Lhotka, Pilat-Lohinger, Dvorak, Schwarz, Gyergyovits) - at the summer school and conference in Maribor, Slovenia (06 / 2005).

"Nekhoroshev Estimates in the 1:1 Resonance of Our Solar System I: Symplectic Mappings in the Elliptic Restricted Three Body Problem" – at Wissenschaftliche Jahrestagung der ÖGA – Wien, Austria (04 / 2007).

"Nekhoroshev Estimates in the Elliptic Restricted Three Body Problem" - at the conference in Spoleto, Italy (06 / 2007) and in the summer school and conference in Patras, Greece (07 / 2007).

Public Outreach:
"Climate Change", (Eggl S., Lhotka C.), creation of an animation video showing astronomical effects of climate change for the "Natural History Museum of Vienna", exhibition since spring 2007.

"Trojaner in unserem Sonnensystem", (Lhotka C.), public talk at the WAA (Wiener Arbeitsgemeinschaft für Astronomie), 4.2. 2008.

Further Education:
„Rechtsschutz von computerimplementierten Erfindungen in Österreich" (intelectual property rights concerning software), Austrian Patent Office, (Fastenbauer, Kögl), Patentamt Wien (2006).

„Proton Europe Vienna Workshop", (intellectual property management), ProTon Europe / Austria Wirtschafts Service, Vienna, Austria (11.05-12.05.2006).

„M101: A First Course in Mathematica", Wolfram Research, Comsol (Schweiz AG), Zürich, Switzerland (2006).